

**LEVEL**

12

A066043

FINAL REPORT ON THE WORK DONE UNDER CONTRACT

N 000 14-77-C-0102

AD A090516

EXCIMER POTENTIAL CURVES

H.S. Taylor

M. Valley

C. Jung

C. Watts

F. Bobrowicz

DTIC  
OCT 7 1980

University of Southern California

Los Angeles, California, 90007

NR 395-570  
Code 421

The views and conclusions contained in this document are those of the authors and should not be interpreted as necessarily representing the official policies, either expressed or implied, of the Defense Advanced Research Projects Agency or the US Government.

DDC FILE COPY

DISTRIBUTION STATEMENT A  
Approved for public release;  
Distribution Unlimited

361554

80 9 10 00

## Summary

↘ The purpose of this project is the development of semi-empirical and theoretical methods of obtaining reasonably accurate potential curves for diatomic excimer systems. These curves are of importance for applications to fluorescence spectra, stimulated emission coefficients, excimer laser development and electron impact excitations. We have been mainly interested in the development of a new effective potential method which obtains potential curves by calculating the energy levels of one atom in the external field of the other atom. In order to be able to compare our new method to other well established methods, we have first done a CI calculation for GaKr and applied the Gordon-Kim method to GaKr. This provided some knowledge of the effect of a Kr atom on another atom which might be used later as input into the effective potential method.

The basic idea of the new method is as follows: In all low lying states of a metal-rare gas system one atom (the rare gas atom which has a high first excitation energy) is asymptotically in its ground state and the various molecular states correspond to the various low lying excited states of the metal atom. Therefore the basic assumption of our method is, that it is possible to calculate the molecular energy levels as the energy levels of a single metal atom in an external field which represents the rare gas atom. This external field which represents the second atom is our effective potential. The general form of this potential can be derived from the many body Greens function. Phenomenological treatments of the many body theory leads to a form with free parameters. Our idea is to determine these parameters by fitting one molecular potential curve, calculated by our new method, to a known curve. We hope that

the effective potential resulting from one particular state describes the effect of the rare gas atom also in other molecular states and even in other molecules, i.e. independently of the type and state of the other atom. The big problem in this new method is, that new types of integrals have occurred, which have not appeared in quantum chemistry before and for which no standard computer programs exist. Therefore, we spent most of the time developing and testing new computer programs. By now the programs seem to work properly but they are still very slow and at the moment we are still testing the whole method on a simple system, on LiHe. We have tried to parametrize the effective potential of the He ground state by fitting the resulting molecular potential for the  $2_{\pi}$  state of HeLi to the known potential curve of this state. Probably we did not use the best fitting strategy so far and therefore we did not get a satisfactory fit of the molecular potential. It seems to be necessary to repeat the fitting procedure with a more efficient strategy, which we consider in the text. The next step in the program, after the fit of the molecular potential curve for one state, is to calculate the molecular potential curves for other states of HeLi using the same effective potential to represent the He atom. The result of this test will show if the whole idea works or not. We are continuing work on this idea even without the support of ARPA-ONR as we believe it to be a valuable new method.

Accession For	
NTIS	<input checked="" type="checkbox"/>
DTIC	<input type="checkbox"/>
USDA	<input type="checkbox"/>
Joint	<input type="checkbox"/>
Publ	<input type="checkbox"/>
Dist	<input type="checkbox"/>
Avail	<input type="checkbox"/>
Dist	<input type="checkbox"/>
or	
Dist	<input type="checkbox"/>
Special	
A	

§1

1.1 Introduction

The general purpose of this project is to continue the development and implementation of semi-empirical and theoretical methods of obtaining reasonably accurate potential curves for diatomic excimer systems.<sup>1</sup> Once the potential curves have been obtained, they can be used to predict fluorescence spectra<sup>2</sup>, and to compute laser gain, stimulated emission coefficients<sup>3</sup> and total cross sections for excitation by electron impact.<sup>4</sup> While highly accurate potential curves are always a goal, our immediate goal is the relatively rapid production of potential curves that are accurate enough to guide experimentalists in choosing or rejecting possible laser systems on the basis of inexpensive theoretical calculations rather than on the basis of expensive and time-consuming experiments.

We are particularly interested in developing methods that in the future would be applicable to excimer systems because of the current emphasis on these systems as candidates for efficient, high-power visible and ultraviolet lasers.<sup>1</sup> The specific systems that motivated this proposal were the group IIA-, IIB- and IIIA-rare gas systems (such as MgXe and TlXe), alkali-group IIB systems and Thallium-group IIB systems. Our immediate goal is to develop a new efficient method to calculate potential curves for non-bonding diatomic systems in which the asymptotic atoms have greatly different ionization potentials (as do most metal-rare gas systems). We will then view the lowest several states of the molecule as roughly represented by a specific state of the metal in the effective "external" field of the high ionization potential (i.e. here a rare gas) atom.

The next step will be to parametrize this potential (and the effective electron potentials that arise therein) using a form suggested by field theory and data from any known molecular state of any metal-rare gas system that goes at large internuclear distance to the ground state of the rare gas. This effective potential will then be used to describe unknown states of the same or different metals by viewing their calculation as one of the metal atom in the field of this potential. If this aim is attained a basis empirical transfer of information from known to unknown systems and states will be achieved with an in principle accompanying simplification in calculations. This in turn would allow us to go to bigger systems.

Although extensive work has been done on calculating potential curves, the currently available methods are inadequate for large systems such as TlXe. While self-consistent field (SCF) and configuration interaction (CI) programs are the most accurate, at this time those computer codes cannot handle molecular systems with  $f$  electrons, such as TlXe.

Now, simplified methods, that are alternatives to CI do exist: The Gordon-Kim<sup>5</sup> (GK) method is available but has not been adequately tested for large systems with open shells. We believe that our method, theoretically is better based than this method, as the reader can judge for himself in later sections, and it takes in such effects as mutual atomic polarization that the GK leaves out.

The most promising method for treating big systems rigorously is the pseudopotential method. The pseudopotential method<sup>6</sup> is currently being extended to large systems.<sup>7,8</sup>

The new method we are developing, the effective potential method, is essentially a means of calculating the potential curves for a diatomic system AB (where A is a closed shell atom) by doing an atomic SCF or CI calculation on B in which A is treated as an external (effective) potential. The effective potential is the sum of the Hartree-Fock potential for A and a polarization potential. The polarization potential consists of a one-particle part describing the polarization of A by an external charged particle and a two-particle part which corrects for the "depolarization" due to the presence of the other electrons and nucleus of B. The parameter of the effective potential will be obtained by using perturbation theory and a known potential curve of AX (X is any atom). If X is not highly polarized, a first order approximation to the effective potential  $U^A$  may be obtained by fitting the parameters to

$$V_{X,e}^A(R) = \int d\tau U^A(R,\tau) \rho_X(\tau)$$

where  $\rho_X$  is the density of atom X and  $V_{X,e}^A$  is the electronic part of the known potential curve for AX. The theory of the effective potential and the perturbation treatment of it are discussed in more detail in §4.

This effective potential method has several advantages over the Gordon-Kim and pseudopotential methods. Because the effective potential allows for polarization of A and the SCF calculation allows for polarization of B, this method should be more accurate than GK. At the same time, LS coupling and relativistic effects can be included as easily in our method: the treatment of LS coupling would be the same and relativistic effects can be included in the core potentials. In comparing our effective potential method to pseudopotential methods, the following points should be noted. Methods which use only a pseudopotential to replace the valence-core inter-

actions do not include polarization of the core. In contrast, our method includes core polarization; consequently, the core-core interaction is correct at large distances so the correct van der Waals interaction will be obtained. Because we take advantage of the fact that there is no real bonding in the systems we are studying, our calculations will be essentially atomic calculations and will include fewer electrons explicitly than a pseudopotential calculation. Use of a semi-empirical potential which is parameterized to molecular data should result in better molecular potential curves than use of semi-empirical potentials parameterized to atomic data. In addition, use of molecular data will allow us to obtain effective potentials for electrons outside of rare gas atoms and for electrons outside of highly charged cores; these are two cases in which parameterization to atomic data would be extremely difficult.

Since the effective potential method is semi-empirical and since the potential parameters will be fit to molecular data, some potential curves are needed. Basically, there are two options available for parameterizing the effective potential of A in order to calculate potential curves for AB: 1) The effective potential for A can be fit to known potential curves for XA (where X is any atom) or 2) The effective potential for A can be fit to whatever ground and excited state curves for AB are known. The second option recognizes the facts that it is easier to obtain ground state curves than excited state curves by other methods and that both are needed to pick possible laser systems. The curves needed for fitting can be obtained by a variety of techniques varying from rigorous CI calculations to analysis of experimental data. As examples of available techniques, consider the following: When experimental band spectra data exist, the quasi-static theory of line shapes could be used to extract potentials.<sup>9</sup> Atomic beam data (such as that supplied by Yuan Lee in Berkeley) could also be used to fit potential forms.<sup>10</sup> The RKR method<sup>11</sup> could be used when, as is rarely the case in excimers, vibrational data exists. For positive-negative ion systems Rittner potentials<sup>12</sup> can be fit to available data. For systems with closed-shell separated atoms and ions or for certain types of open-shell

systems, the Gordon-Kim method<sup>5</sup> can be used to predict short range potentials, and long range corrections can be added to this model. Short range repulsive potentials for closed-shell atoms and ions can also be fitted, correlated and interpolated using: (a) the delta-function model for homonuclear systems<sup>10</sup>; (b) the delta-function and distortion model with combination rules for heteronuclear systems<sup>10</sup>; (c) the related softness parameter methods that require atomic Hartree-Fock charge densities.<sup>13</sup>

Now after listing the advantages of our method we must admit to slow progress and a lack of success in so far completing our objectives due to two problems. The first is that our effective potential leads to new two center (atom-external potential) integrals such as those representing the interaction with the part of the effective potential representing the polarized rare gas (see later sections for details). We have developed methods and programs for treating these integrals but unfortunately the programs are still very consuming of computer time. These integrals have never appeared in quantum chemistry before and we had to develop new methods of doing them. We do not believe our methods are presently optimum. Big savings in computer time can probably be achieved with a few years more efforts ("years" may seem long but not when one considers the thirty or so years it took to reach the state of the art in present molecular programs). Our strategic problem was that it was senseless to develop speedy packages to use in a method that might not work. Hence we used our slow packages and went on to the second problem, that of parametrizing the effective potential. In a sense the problems are linked, in that the trial and error fittings necessary to parametrize are severely limited in application by the computer cost for doing integrals as parameters are varied. The



second problem is therefore a so far less than ideal but perhaps not unacceptable fit of the parameters in the effective potential to the known curves. We will return to this problem in section 4. IV.

Now of the outset of our work we decided that we would like as input from theory some accurate GaKr curves so that we could get on effective potential for Kr to use in InKr or TlKr computations. Hence we split our work in three parts - the first part reviewed in §2 was to do accurate CI calculations on GaKr.

§3 is an application of the Gordon-Kim method to GaKr and a comparison with the results from §2.

The third part was to develop and test our theory in §4. As it turned out the third part is still not able to take advantage of the first part since even for Li-He we have not, because of the above two mentioned problems, achieved success. In any case we will report here our progress omitting the large sections of efforts that lead to even inferior methods of integration and parametrization and reporting only the most promising methods. At the writing of this report we are close to a critical test calculation of LiHe, having achieved what may be a satisfactory (how satisfactory it is future results will show) calculation of the effective Helium potential. Time and personnel changes have prevented us from making this last step which we shall certainly do in the near future even without further support. If we are successful we shall return to the problems of speeding up our integral computation methods and routines. This will prepare the method to move on to bigger systems and get us to where we had hoped to be now, at the end of our contract period. Of course if the calculations are not successful theoretical

reasons need be sought and the promise of the method would be in question. While doing this work Dr. Taylor and Dr. Jung had a discussion about electron scattering in a strong laser field and wrote a paper about this subject. A copy is included in Appendix E. This work was not in the original grant but as many things in science it just happened in discussion. No computing funds from the grant were used for this project.

References for §1

1. For a discussion of excimers and their relation to lasers see A. V. Phelps, JILA Report 110, "Tunable Gas Lasers Using Ground State Dissociation," (1972) and references therein.
2. This requires highly accurate curves as it depends on the derivative with respect to internuclear distance of the difference between the excited and ground state potentials. As such we must consider these as being only semi-quantitative.
3. B. Cheron, R. Scheps and A. Gallagher, J. Chem. Phys. 65, 326 (1976).
4. We shall not discuss the methods of going from potential curves and wave functions to these properties as they are standardly given in textbooks. The quasistatic theory of line broadening is reviewed in JILA Report 110 [1].
5. V. I. Gaydaenko and V. K. Nikulin, Chem. Phys. Letters 7, 360 (1970); V. K. Nikulin, Zh. Tekh. Fiz. 41, 41 (1970) [English transl. Soviet Phys. Tech. Phys. 16, 28 (1971)]; R. G. Gordon and Y. S. Kim, J. Chem. Phys. 56, 3122 (1972); M. J. Clugstor and R. G. Gordon, J. Chem. Phys. 66, 239 (1977).
6. C. F. Melius and W. A. Goddard III, Phys. Rev. A10, 1528 (1970); C. F. Melius, B. D. Olafson and W. A. Goddard III, Chem. Phys. Lett. 28, 457 (1974).
7. Y. S. Lee, W. C. Ermler and K. S. Pitzer, J. Chem. Phys. 67, 5861 (1977).
8. W. R. Wadt, P. J. Hay and L. R. Kahn, J. Chem. Phys. 68, 1752 (1978).
9. R. Scheps, C. Ottinger, G. York and A. Gallagher, J. Chem. Phys. 63, 2581 (1975) and references therein on alkali-rare gas systems.
10. N. A. Sordergaard and E. A. Mason, J. Chem. Phys. 62, 1299 (1974) on rare gas-rare gas systems.
11. J. T. Vanderslice, E. A. Mason, W. G. Maisch and E. R. Lippincott, J. Mol. Spec. 3, 17 (1959); J. Chem. Phys. 32, 515 (1960).
12. E. S. Rittner, J. Chem. Phys. 19, 1030 (1951).
13. T. L. Gilbert, J. Chem. Phys. 63, 4061 (1975).

Electronic States of GaKr : Ab initio calculations of a prototype for  
TlKr

2.1 Introduction

Among the metal-rare gas eximers, the TlXe system is believed to be an excellent candidate for an efficient visible, high power, tunable laser.<sup>1</sup> Since ab initio calculations on this system are beyond the scope of present computer programs, we present here a configuration interaction (CI) calculation on GaKr, which is the largest group IIIB-rare gas system for which CI calculations can be done. We use the calculated GaKr curves to model the potential curves for InKr and TlKr. Although our model does not allow further extrapolation from TlKr to TlXe, it is hoped that these calculations will yield some insight into the properties of the TlXe eximer. In addition, Gallagher<sup>2</sup> has recently raised the possibility of using GaXe as a laser if the Ga can be obtained from dissociation of GaI<sub>3</sub>. Consequently the GaKr curves should also be of intrinsic interest.

In this paper, the CI calculations on GaKr are presented along with the model calculations on InKr and TlKr. These potential curves are used as the basis of a classical calculation of the emission and absorption coefficients for these systems.

## 2.II Details of the calculation

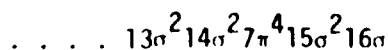
### A. Basis set

The calculations use (14s11p6d) primitive Gaussian bases for gallium and krypton<sup>3</sup> as a starting point. The core orbitals (1s,2s,2p,3s,3p) are singly contracted to the Hartree-Fock atomic orbitals while the valence orbitals (4s and 4p) and the 3d orbitals are each described by two contracted functions(see Table I). The resulting (5s4p2d/5s4p2d) contracted bases are constructed using the general contraction scheme of Raffenetti.<sup>4</sup>

These basis sets are extended to include polarisation by adding two diffuse s functions (5s and 5s') and a diffuse p function (5p) to describe the lowest Rydberg orbitals. The exponents for these orbitals ( $\zeta(5s) = .026$ ,  $\zeta(5s') = .011$ ,  $\zeta(5p) = .01$ ) are obtained from atomic calculations on the excited states of Ga . The final basis set thus consists of a (16s12p6d) primitive basis contracted to [7s5p2d] for Ga and a (14s11p6d) primitive basis contracted to [5s4p2d] for Kr .

### B. SCF calculation

The starting point for the CI calculation is a Hartree-Fock calculation on the  $^2\Sigma^+$  state



The inner core molecular orbitals (twelve  $\sigma$ , twelve  $\pi$  and four  $\delta$ ) are held doubly occupied from this point on and are replaced by the rigorous nonlocal Hartree-Fock potential.

$$V_{\text{core}} = V_N + \sum_{i=\text{core}} (2J_i - K_i)$$

With the core orbitals removed from consideration, it is convenient to renumber the valence orbitals so that the Hartree-Fock configuration is written as

$$1\sigma^2 2\sigma^2 3\sigma^2 4\sigma^2 1\pi^4$$

At large  $R$  the correspondence for the valence orbitals is

$$1\sigma \rightarrow 4s_{\text{Kr}}$$

$$2\sigma \rightarrow 4p_{\text{Kr}}$$

$$3\sigma \rightarrow 4s_{\text{Ga}}$$

$$4\sigma \rightarrow 4p_{\text{Ga}}$$

$$1\pi \rightarrow 4p_{\text{Kr}}$$

In addition to the valence orbitals, nine  $\sigma$ , six  $\pi$  and four  $\delta$  virtual orbitals are used in the CI calculations. The lowest virtual orbitals ( $5\sigma$ ,  $6\sigma$ ,  $7\sigma$ ,  $2\pi$ ,  $3\pi$ ), which correspond to the Ga  $5s$ ,  $5s'$ ,  $4p$  and  $5p$  atomic orbitals for large internuclear separations, are obtained by the improved virtual orbital (IVO) procedure.<sup>5</sup> The IVO orbitals are obtained by removing the electron from the  $4\sigma$  (valence) orbital of the above configuration and calculating the virtual orbitals for the (N-1)-electron Hamiltonian.

#### C. CI calculations

Full polarization CI (POL-CI) calculations<sup>6</sup> which provide a balanced description of all states of the  $4s$ - $4p$  manifold were carried out. A set of reference configurations was chosen (see Table II) to describe the dominant configurations for the  $^2\Sigma^+$  and  $^2\Pi$  states of the molecule and the  $^1\Sigma^+$  state of the ion.

The full POL-CI calculations include all (1+2) electron excitations relative to each reference configuration subject to the restrictions that no more than one electron occupy the Rydberg  $5\sigma$  orbital and no more than one electron occupy any virtual orbital ( $6\sigma$ ,  $2\pi$  etc.). This results in 764 spatial and 2314 spin configurations for the  $^2\Sigma^+$  states, 556 spatial and 1565 spin configurations for the  $^2\Pi$  states and 368 spatial and 558 spin configurations for the  $^1\Sigma$  state. A total of  $15\sigma$ ,  $14\pi$  and  $2\delta$  occupied and virtual orbitals are used in the POL-CI calculations.

The potential energy curves (Fig. 2 and Table III) from the POL-CI calculations generally follow the behavior predicted from these theoretical considerations. These calculations are not, however, designed to treat long-range dispersion forces. Many excitations which contribute to a  $C_6 r^{-6}$  attraction are not included in the wavefunction. For these reasons, one would expect deeper wells in all the potential curves including the two lowest, generally repulsive, states. As predicted, the  $1^2_{\Pi}$  state is less repulsive than the  $1^2_{\Sigma^+}$  state. The bound excited state  $2^2_{\Sigma^+}$  has a minima at 6.36 a.u. about 3.0 eV above the ground state curve, while the minima in the ion curve is at 6.28 a.u. and 5.6 eV above the ground state. The well depths are compared with those obtained by Gallagher<sup>11</sup> in Table IV, and as expected, Gallagher's wells are deeper.

The dipole moments of these states and the transition moments between  $2^2_{\Sigma^+}$  and the lower states have also been calculated and are given in Table V and Figs. 3 and 4.



## B. Electronic states including spin-orbit coupling

A complete treatment of the electronic states of GaKr must include the effects of spin-orbit coupling. The states considered here, which dissociate to the closed-shell ground state of Kr and an open-shell state of Ga or Ga<sup>+</sup> are influenced only by the spin-orbit matrix elements of the open-shell atom.

Following the procedure used previously,<sup>7,8,9,10</sup> we have adopted a simple model for including the effects of spin-orbit coupling on the calculated potential energy curves and wavefunctions. The experimental spin-orbit parameters for the open-shell atom (Ga and later In, Tl) are used to determine the matrix elements of the spin-orbit interaction,  $H_{so}$ , coupling the molecular states at infinite separation and these matrix elements are assumed to be independent of internuclear distance. The resulting spin-orbit matrix  $H_{so}$  is added to the diagonal matrix of electronic energies  $H_{elec}(R) = \delta_{ij}E_i(R)$ :

$$H(R) = H_{elec}(R) + H_{so}$$

and the total matrix  $H$  is then diagonalized at each internuclear distance  $R$ . Thus, in addition to the assumption that the spin-orbit matrix elements do not change as functions of  $R$ , this model assumes that only one-center terms need be included so that only the spin-orbit coupling on Ga is important. We would expect this procedure to provide reasonable results to the extent that the molecular states retain the identity of the atomic

states from which they are formed. The spin-orbit matrices are given in Table VI along with the atomic parameters used in these calculations. The parameter  $\lambda$  is chosen so that the atomic  ${}^2p_{3/2}$  and  ${}^2p_{1/2}$  states have energies of  $+\lambda$  and  $-2\lambda$  respectively.

We shall label the molecular states using the convention of Hund's case (c) where  $\Omega$ , the projection of total angular momentum along the molecular axis, is the only good quantum number.  $\Omega$  is defined as  $\Omega = \Lambda + S_z$ , where  $\Lambda$  and  $S_z$  are the orbital and spin angular momentum projection, respectively. The molecular  ${}^2\Sigma^+$  states have only a  $\Omega = 1/2$  component, while the  ${}^2\Pi$  states yield a  $\Omega = 3/2$  and  $\Omega = 1/2$  state. The states in the  $\Omega$  representation are labeled according to increasing energy by a Roman numeral. So the  $\Omega = 1/2$  states are designated as I 1/2, II 1/2 and the  $\Omega = 3/2$  states are I 3/2, II 3/2.

The coupled states are expressed as follows:

$$\begin{aligned} |I 1/2\rangle &= C_{\Sigma} |1^2\Sigma^+\rangle + C_{\Pi} |1^2\Pi\rangle \\ |II 1/2\rangle &= -C_{\Pi} |1^2\Sigma^+\rangle + C_{\Sigma} |1^2\Pi\rangle \\ |I 3/2\rangle &= |1^2\Pi\rangle \end{aligned}$$

The spin-orbit coefficient  $C_{\Sigma}$  and  $C_{\Pi}$  are given in Table VII. The potential curves and transition moments for GaKr including spin-orbit coupling are given in Table VIII and Figs. 5 and 6.

## 2.IV Extrapolations to InKr and TlKr

The potential curves for InKr and TlKr are modeled on the GaKr curves. The lowest excitation energies and the ionization potentials for the series Ga, In, Tl are given in Table IX. As can be seen, this series does not form a steady progression. In has a lower ionization potential and lower excitation energies than Ga, as expected for a heavier atom. However, Tl has a higher ionization potential and higher excitation energies. This is due in part to the presence of a filled 4f shell in Tl and the larger spin-orbit effects.<sup>12</sup> These effects should be considered when extrapolating the GaKr curves to InKr and TlKr.

To simulate InKr and TlKr, the experimental spin-orbit parameters for In and Tl are used to couple the GaKr curves. The curves are also shifted to give the correct atomic excitation energies at  $R = \infty$  (see Table IX). This procedure should give at best a qualitative description of states of InKr and TlKr, since the non-spin-orbit coupled states are expected to have quantitatively different well depths and equilibrium separations.

The effect of the increasing spin-orbit perturbation in going from Ga to In and Tl is evident in the calculated curves which are given in Figs. 7 and 8. Only the well depths and positions for the  $I 1/2$  and  $II 1/2$  states are affected by the spin-orbit coupling. The other states

are the same as those for GaKr except that they have the correct asymptotic spacing.

The mixing parameters from the spin-orbit coupling calculations for TlKr are also used as the coefficients of the GaKr wave function to estimate the transition moments for this system. The TlKr transition moments are given in Table X and Fig. 9.

## 2.V Absorption and stimulated emission coefficients for possible laser transitions

The interest in the group IIIB-rare gas systems arises from the possibility of their use as visible laser systems. In order to judge their usefulness as lasers it is convenient to calculate the absorption  $k_{\nu}(t)$  and stimulated emission  $g_{\nu}(T)$  coefficients. Obtaining quantum-mechanical results for these quantities would require a complex calculation which would be inconsistent with the extrapolations used to obtain the InKr and TlKr curves. Consequently, we have used Gallagher's analysis [17], which is based on the classical Frank-Condon principle.

In order to obtain  $g_{\nu}$  and  $k_{\nu}$ , the CI curves are first fit by Morse potentials. The parameters for these Morse potentials are given in Table XI. These parameters can then be used in Gallagher's equations, along with the atomic transition rate, to obtain absorption and stimulated emission coefficients for pressure and excitation conditions of interest to experimentalists. We have calculated these coefficients for two different types of conditions. The high temperature results correspond to the case where the concentration of the metal is obtained from the vapor pressure of the metal itself, while the low temperature results correspond to obtaining the required concentration of the metal from vaporization of  $MI_3$  ( $M = Ga, In, or Tl$ ). This latter condition has been suggested by Gallagher as a possible means of obtaining high concentrations of the metal at low temperatures. In both cases the densities used are  $10^{20}/cm^3$  for Kr,  $10^{16}/cm^3 = 3[M^2P_{1/2}] = 1.5[M^2P_{3/2}]$  and  $2 \times 10^{14}/cm^3 = [M^2S_{1/2}]$ . The resulting absorption and stimulated

emission coefficients for GaKr , InKr and TlKr are given in Figures 10 to 15.

A paper has been published about the work presented in §2.  
See Appendix A.

References for §2

1. B. Cheron, R. Scheps and A. Gallagher, J. Chem. Phys. 65, 326 (1976).
2. Gallagher, private communication.
3. T. H. Dunning, Jr., J. Chem. Phys. 66, 1382 (1977).
4. R. C. Raffenetti, J. Chem. Phys. 58, 4452 (1973).
5. W. J. Hunt and W. A. Goddard III, Chem. Phys. Lett. 3, 414 (1969).
6. P. J. Hay and T. H. Dunning, Jr., J. Chem. Phys. 64, 5077 (1976).
7. P. J. Hay and T. H. Dunning, Jr., J. Chem. Phys. 66, 1306 (1977).
8. P. J. Hay, T. H. Dunning, Jr. and Richard C. Raffenetti, J. Chem. Phys. 65, 2679 (1976).
9. D. C. Eckstrom, R. A. Gutcheck, R. M. Hill, D. Huestis, and D. C. Lorents, "Studies of E-Beam Pumped Molecular Lasers", Semiannual Report No. 2, Stanford Research Institute, Menlo Park, CA. (1973).
10. J. S. Cohen and B. I. Schneider, J. Chem. Phys. 61, 3230 (1974).
11. B. Cheron, R. Scheps and A. Gallagher, J. Chem. Phys. 65, 326 (1976).
12. P. Bagus, Y. S. Lee, K. S. Pitzer, Chem. Phys. Lett. 33 408 (1975) (discussion of Lanthanide contraction).

Table I. Gaussian exponents and contraction coefficients

Exponents	Contraction coefficients				
	Gallium atom				
	1s	2s	3s	4s	4s'
457600.	.000222	-.000069	.000026	-.000006	0.0
68470.	.001732	-.000535	.000205	-.000048	0.0
15590.	.008952	-.002814	.001070	-.000247	0.0
4450.	.035874	-.011275	.004337	-.001007	0.0
1472.	.114000	-.038495	.014707	-.003399	0.0
541.3	.274138	-.100714	.039748	-.009279	0.0
214.8	.414793	-.211832	.084475	-.019587	0.0
88.81	.275395	-.175448	.079654	-.019104	0.0
27.18	.029561	.479840	-.291821	.072753	0.0
11.54	-.006815	.634145	-.527118	.134137	0.0
3.303	.002253	.069592	.583707	-.181778	0.0
1.334	-.001017	-.012299	.674103	-.358241	0.0
.1947	.000251	.002774	.028077	.615164	0.0
.07158	0.0	0.0	0.0	0.0	1.0
	5s	5s'			
.026	1.0	0.0			
.011	0.0	1.0			
	2p	3p	4p	4p'	5p
3274.	.001513	-.000576	.000094	0.0	0.0
765.4	.013070	-.004981	.000800	0.0	0.0
241.6	.067263	-.026421	.004337	0.0	0.0
89.39	.219542	-.089529	.014443	0.0	0.0
36.36	.421107	-.186734	.031377	0.0	0.0
15.60	.376515	-.144494	.021501	0.0	0.0
6.472	-.089425	.258956	-.046233	0.0	0.0
2.748	-.000502	.570187	-.125293	0.0	0.0
1.090	.001761	.325305	-.045636	0.0	0.0
.2202	-.000247	.016563	.452811	0.0	0.0
.06130	0.0	0.0	0.0	1.0	0.0
.01	0.0	0.0	0.0	0.0	1.0
	3d	4d			
59.66	.031949	0.0			
17.10	.163546	0.0			
6.030	.367457	0.0			
2.171	.456851	0.0			
.6844	.305161	0.0			
.160	0.0	1.0			



Table I. Gaussian exponents and contraction coefficients

Exponents	Contraction coefficients				
	Krypton atom				
	1s	2s	3s	4s	4s'
605700.	.000231	-.000073	.000029	-.000009	0.0
90300.	.001755	-.000551	.000221	-.000070	0.0
20920.	.009076	-.002894	.001159	-.000369	0.0
5889.	.036990	-.011834	.004781	-.001522	0.0
1950.	.116154	-.039826	.016056	-.005118	0.0
718.2	.278401	-.104801	.043454	-.013886	0.0
285.4	.415746	-.217093	.091899	-.029537	0.0
118.6	.267204	-.175562	.083789	-.027309	0.0
38.16	.027870	.471395	-.303023	.103498	0.0
16.45	-.005998	.636794	-.570620	.208810	0.0
5.211	.002217	.082255	.501751	-.235737	0.0
2.291	-.001092	-.014138	.760483	-.553570	0.0
.4837	.000306	.003289	.044857	.701123	0.0
.1855	0.0	0.0	0.0	0.0	1.0
	2p	3p	4p	4p'	
4678.	.001392	-.000569	.000156	0.0	
1120.	.011666	-.004777	.001286	0.0	
357.1	.060858	-.025631	.007059	0.0	
131.4	.210040	-.092159	.024990	0.0	
52.86	.421000	-.200936	.056870	0.0	
22.70	.383515	-.160784	.040225	0.0	
9.547	.097383	.267789	-.084756	0.0	
4.167	-.001087	.585908	-.240291	0.0	
1.811	.002209	.291397	-.038636	0.0	
.5337	-.000509	.015484	.599154	0.0	
.1654	0.0	0.0	0.0	1.0	
	3d	4d			
125.6	.019168	0.0			
33.31	.125638	0.0			
12.15	.366069	0.0			
4.350	.502482	0.0			
1.494	.264377	0.0			
.35	0.0	1.0			

Table II. Reference Configurations

$2_{\Sigma}^{+}$  states

1	$1\sigma^2 2\sigma^2 3\sigma^2 4\sigma 1\pi^4$
2	$1\sigma^2 2\sigma^2 3\sigma^2 5\sigma 1\pi^4$
3	$1\sigma^2 2\sigma^2 3\sigma^2 6\sigma 1\pi^4$

$2_{\Pi}$  states

1	$1\sigma^2 2\sigma^2 3\sigma^2 1\pi^4 2\pi$
2	$1\sigma^2 2\sigma^2 3\sigma^2 1\pi^4 3\pi$

$1_{\Sigma}^{+}$  state (GaKr<sup>+</sup>)

1	$1\sigma^2 2\sigma^2 3\sigma^2 1\pi^4$
---	--

Table III. POL-CI calculations on the low-lying states of GaKr and the ground state of GaKr<sup>+</sup>. All energies are relative to -4674. hartrees.

R	$1^2\Sigma^+$	$2^2\Sigma^+$	$1^2\Pi$	$1^1\Sigma^+$
$\infty$	-1.200042	-1.095050	-1.198917	-0.992860
15.00	-1.200121	-1.095025	-1.198978	-0.993044
10.00	-1.200290	-1.094061	-1.199328	-0.994018
8.00	-1.198650	-1.094202	-1.200204	-0.996703
7.00	-1.193963	-1.095454	-1.200450	-0.999505
6.00	-1.179381	-1.096768	-1.197718	-1.002018
5.00	-1.135164	-1.088552	-1.179245	-0.992868
4.50	-1.086883	-1.064404	-1.148099	-0.967583
4.00	-1.018697	-0.992381	-1.079327	-0.906827
3.75	-0.968656	-0.933786	-1.025394	-0.856247

Table IV. Potential well depths

Mole - cule	State	CI		Morse Fit		Gallagher	
		R	$\Delta E(\text{eV})$	R	$\Delta E(\text{eV})$	R	$\Delta E(\text{eV})$
GaKr	$I_{1/2}(X_{1/2})$		$\sim .018$	7.55	.021		
	$I_{3/2}(X_{3/2})$		$\sim .040$	7.18	.040		
	$II_{1/2}(A_{1/2})$	$\sim 10$	.006	10.15	.00642		
	$III_{1/2}(B^2\Sigma_{1/2})$	6.36	.064	6.26	.080		
GaKr <sup>+</sup>	$I_0$	6.28	.26	5.95	.252		
InKr	$I_{1/2}$	$\sim 8$	$\sim .013$	7.86	.00778		
	$I_{3/2}^a$						
	$II_{1/2}$	$\sim 10$	$\sim .006$	9.98	.0064		
	$III_{1/2}^a$						
	$I_0^a$						
TlKr	$I_{1/2}$	$\sim 8$	$\sim .010$	8.5	.012	7.01	.024
	$I_{3/2}^a$					6.58	.062
	$II_{1/2}$	$\sim 10$	$\sim .006$	9.88	.064		
	$III_{1/2}^a$					6.09	.107
	$I_0^a$						

<sup>a</sup> same as GaKr

Table V. Dipole and transition moments for the low-lying states of GaKr

R	$\chi^2_{\Pi}$	$1^2\Sigma^+$	$2^2\Sigma^+$	$1^2\Sigma^+-\chi^2_{\Pi}$	$2^2\Sigma^+-\chi^2_{\Pi}$	$2^2\Sigma^+-1^2\Sigma^+$
15.00	0.00598	0.00156	0.07558	0.00183	-1.29167	-1.31011
10.00	0.02605	0.02048	0.56872	0.01631	-1.28976	-1.29762
8.00	0.09152	0.14168	0.89914	0.04761	-1.27767	-1.23098
7.00	0.18861	0.30443	0.95672	0.07894	-1.26770	-1.19024
6.00	0.41543	0.62092	0.81671	0.11663	-1.25536	-1.18926
5.00	0.90382	1.20144	0.45889	0.09916	-1.23487	-1.44020
4.50	1.24437	0.96841	1.19373	-0.13653	-1.20897	-2.06755
4.00	1.64453	-1.27575	5.47300	-0.84619	-0.86801	- .30554
3.75	1.88349	-1.13125	6.45764	-0.90367	-0.78769	.40946

Table VI. Quantities for spin-orbit matrices

$\Omega = 1/2$	$2_{\Sigma^+}$	$2_{\Pi}$	$\Omega = 3/2$	$2_{\Pi}$
$2_{\Sigma^+}$	0	$\sqrt{2} \lambda$	$2_{\Pi}$	$+\lambda$
$2_{\Pi}$	$\sqrt{2} \lambda$	$-\lambda$		

Ga  $\lambda = .001255$  au

In  $\lambda = .00336$

Tl  $\lambda = .011835$

Table VII. Spin-orbit coefficients for the  $\Omega = 1/2$  states

	$R(a_0)$	$C_{\Sigma}$	$C_{\Pi}$
GaKr	3.75000	.99955	.02998
	4.00000	.99960	.02813
	4.50000	.99961	.02787
	5.00000	.99927	.03811
	6.00000	.99641	.08468
	7.00000	.98199	.18892
	8.00000	.93379	.35782
	10.00000	.82915	.55902
	15.00000	.81649	.57736
InKr	3.75000	.99704	.07690
	4.00000	.99738	.07238
	4.50000	.99742	.07175
	5.00000	.99534	.09644
	6.00000	.98063	.19588
	7.00000	.93712	.34900
	8.00000	.87677	.48091
	10.00000	.82132	.57047
	15.00000	.81649	.57736
TlKr	3.75000	.97505	.22197
	4.00000	.97731	.21180
	4.50000	.97763	.21034
	5.00000	.96502	.26219
	6.00000	.91737	.39803
	7.00000	.86679	.49867
	8.00000	.83612	.54854
	10.00000	.81788	.57540
	15.00000	.81649	.57736

Table VIII. Rydberg-valence transition moments in GaKr  
(with spin-orbit corrections)

R	III 1/2 - I 1/2		III 1/2 - II 1/2		III 1/2 - I 3/2
	Z	(X,Y)	Z	(X,Y)	(X,Y)
15.00	-0.75641	0.74574	-1.06969	-0.52733	-0.91335
10.00	-0.72540	0.75618	-1.07592	-0.50983	-0.91200
8.00	-0.44047	0.84363	-1.14948	-0.32327	-0.90345
7.00	-0.22486	0.88026	-1.16880	-0.16935	-0.89640
6.00	-0.10071	0.88449	-1.18499	-0.07517	-0.88767
5.00	-0.05489	0.87255	-1.43915	-0.03328	-0.87318
4.50	-0.05762	0.85454	-2.06674	-0.02383	-0.85487
4.00	-0.00859	0.61353	-0.30542	-0.01727	-0.61378



Table IX. Atomic states of Ga , In , and Tl

State	Excitation Energy					
	Ga		In		Tl	
	cm <sup>-1</sup>	eV	cm <sup>-1</sup>	eV	cm <sup>-1</sup>	eV
<sup>2</sup> P <sub>1/2</sub>	0.0	0.0	0.0	0.0	0.0	0.0
<sup>2</sup> P <sub>3/2</sub>	826.24	.10241	2212.56	.274228	7792.7	.965840
<sup>1</sup> S <sub>1/2</sub>	24788.58	3.07234	24372.87	3.020814	26477.5	3.281665
I.P.	48380.	5.9963	46669.93	5.784348	49264.2	6.105886

Table X. Rydberg-to-valence transition moments in model TIKr  
(with spin-orbit corrections)

R	III 1/2 - I 1/2		III 1/2 - II 1/2		III 1/2 - I 3/2
	Z	(X,Y)	Z	(X,Y)	(X,Y)
15.00	-0.75641	0.74574	-1.06969	-0.52733	-0.91335
10.00	-0.74665	0.74590	-1.06130	-0.52476	-0.91200
8.00	-0.67524	0.75539	-1.02925	-0.49558	-0.90345
7.00	-0.59354	0.77699	-1.03169	-0.44701	-0.89640
6.00	-0.47336	0.81433	-1.09099	-0.35332	-0.88767
5.00	-0.37761	0.84264	-1.38982	-0.22894	-0.87318
4.50	-0.43489	0.83575	-2.02130	-0.17981	-0.85487
4.00	-0.06471	0.59985	-0.29861	-0.13000	-0.61378

Table XI. Morse fitting parameters:

$$V(R) - V(\infty) = D_e[u^2 - 2u] \text{ where } u = \exp [B(R_e - R)]$$

Molecule	State	$D_e$	$R_e(a_0)$	$B(a_0^{-1})$
GaKr	$I_{1/2}$	.000772	7.56	.724
	$I_{3/2}$	.00147	7.19	.722
	$II_{1/2}$	.000625	10.14	.471
	$III_{1/2}$	.00295	6.26	.853
InKr	$I_{1/2}$	.000286	7.86	.817
	$I_{3/2}^a$			
	$II_{1/2}$	.000474	10.24	.483
	$III_{1/2}^a$			
TlKr	$I_{1/2}$	.00439	8.52	.633
	$I_{3/2}^a$			
	$II_{1/2}$	.000408	10.12	.502
	$III_{1/2}^a$			

<sup>a</sup>Same as for GaKr

Fig. 1. Orbital diagrams for the electronic states of Ga + Kr and Ga<sup>+</sup> + Kr. The lobes and circles represent the in-plane and out-of-plane p orbitals; the dashed circle denotes the Rydberg orbital.

### THE LOW-LYING ELECTRONIC STATES OF GaKr AND GaKr<sup>+</sup>

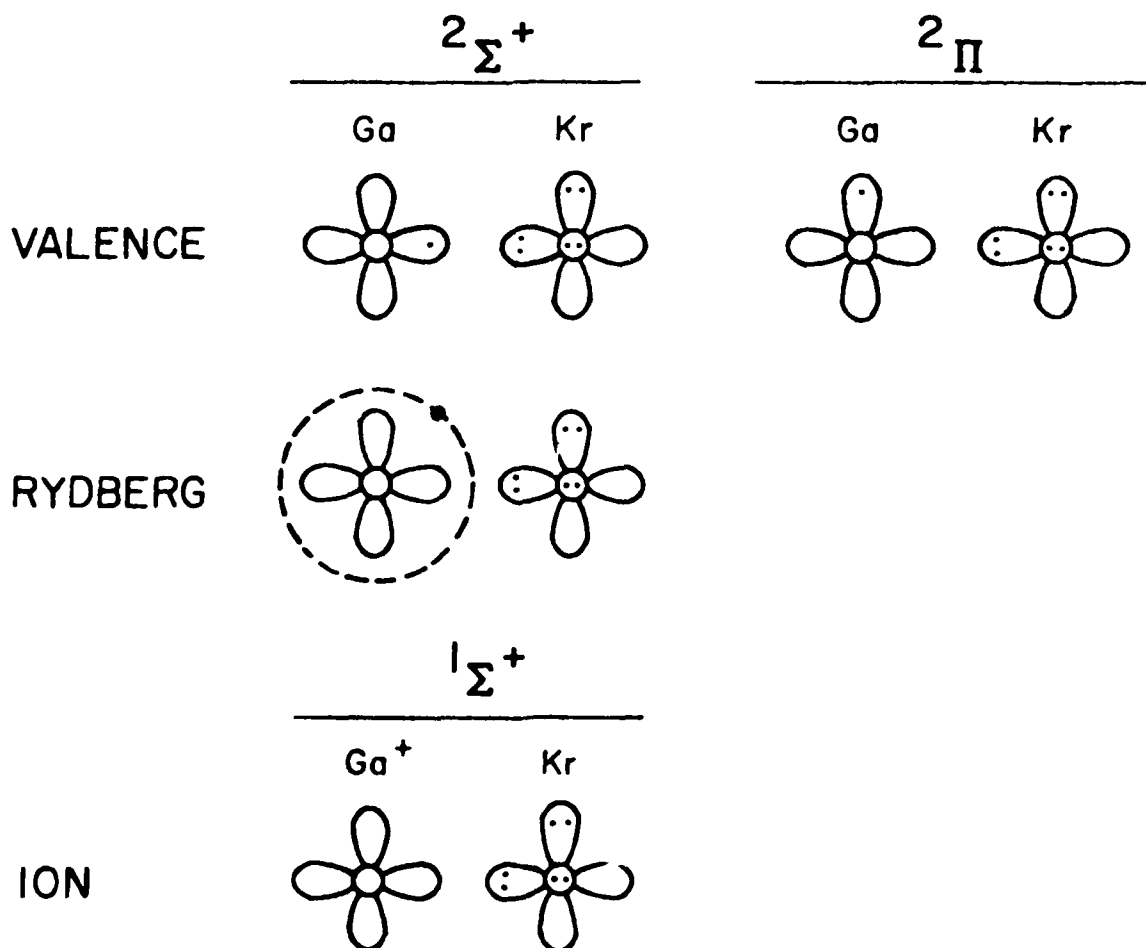


Figure 2.

### THE LOW-LYING STATES OF GaKr AND GaKr<sup>+</sup>

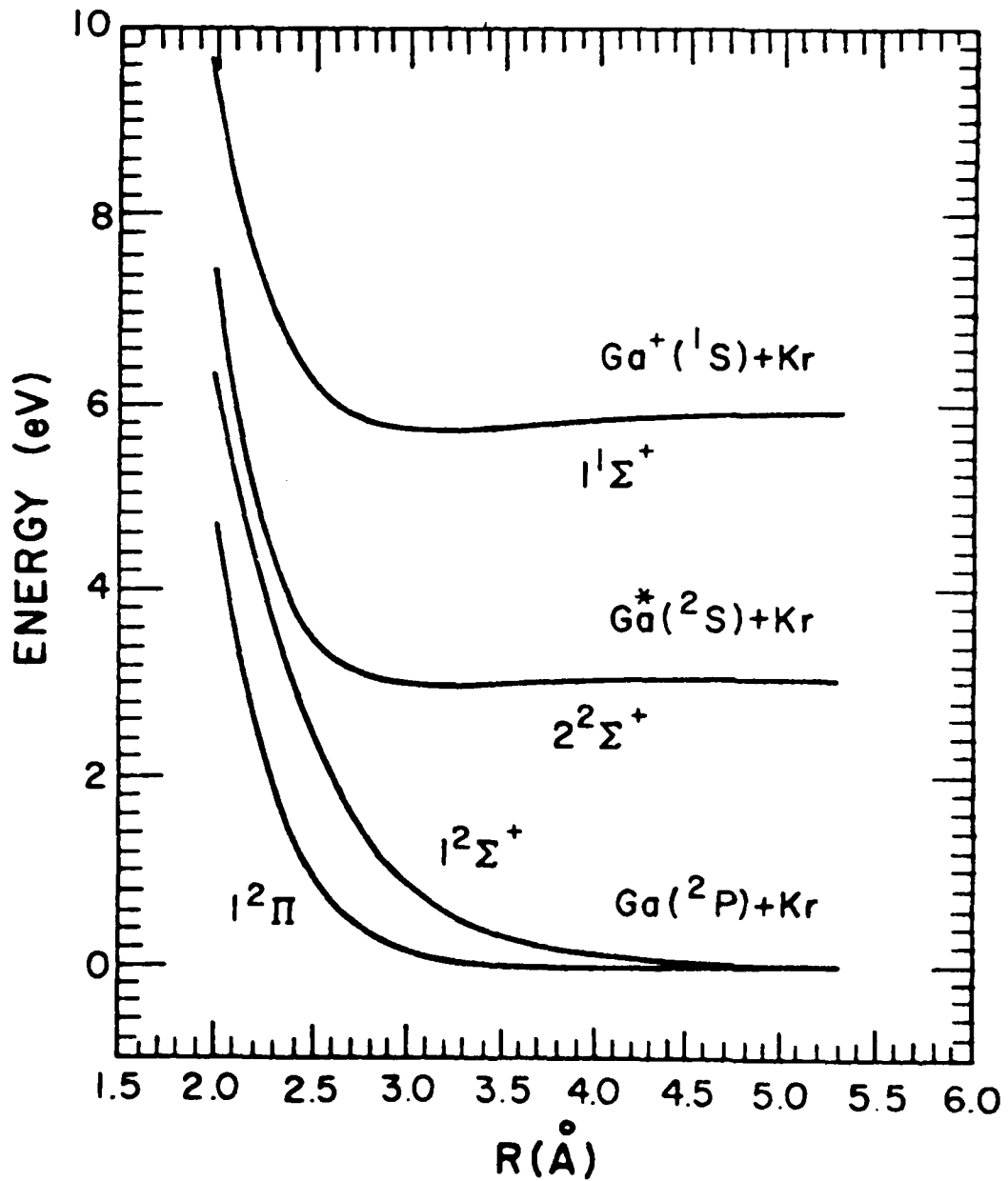


Figure 3.

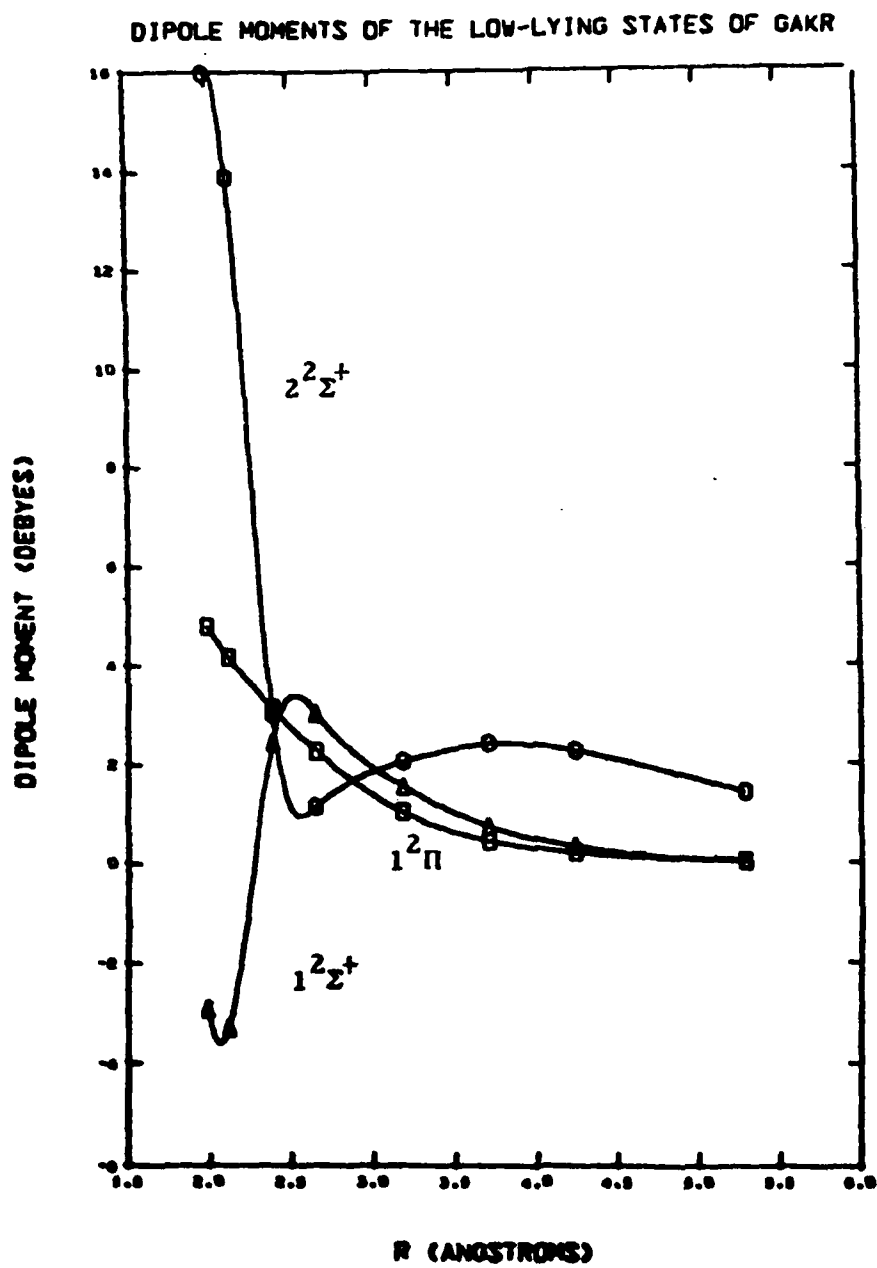


Figure 4.

### DIPOLE TRANSITION MOMENTS AMONG THE LOW-LYING STATES OF GaKr

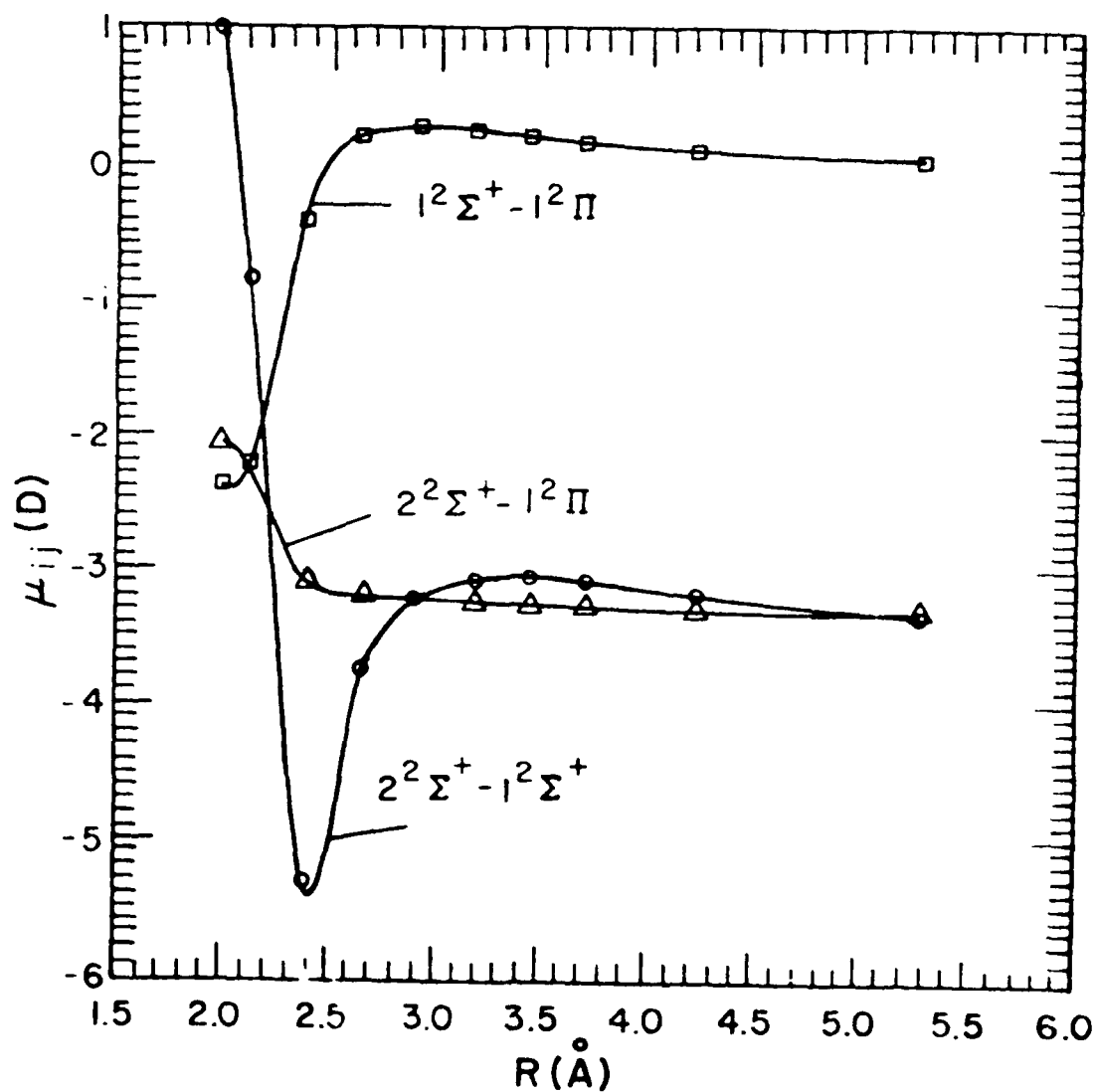


Figure 5.

### THE LOW-LYING STATES OF GaKr AND GaKr<sup>+</sup> WITH SPIN-ORBIT CORRECTIONS

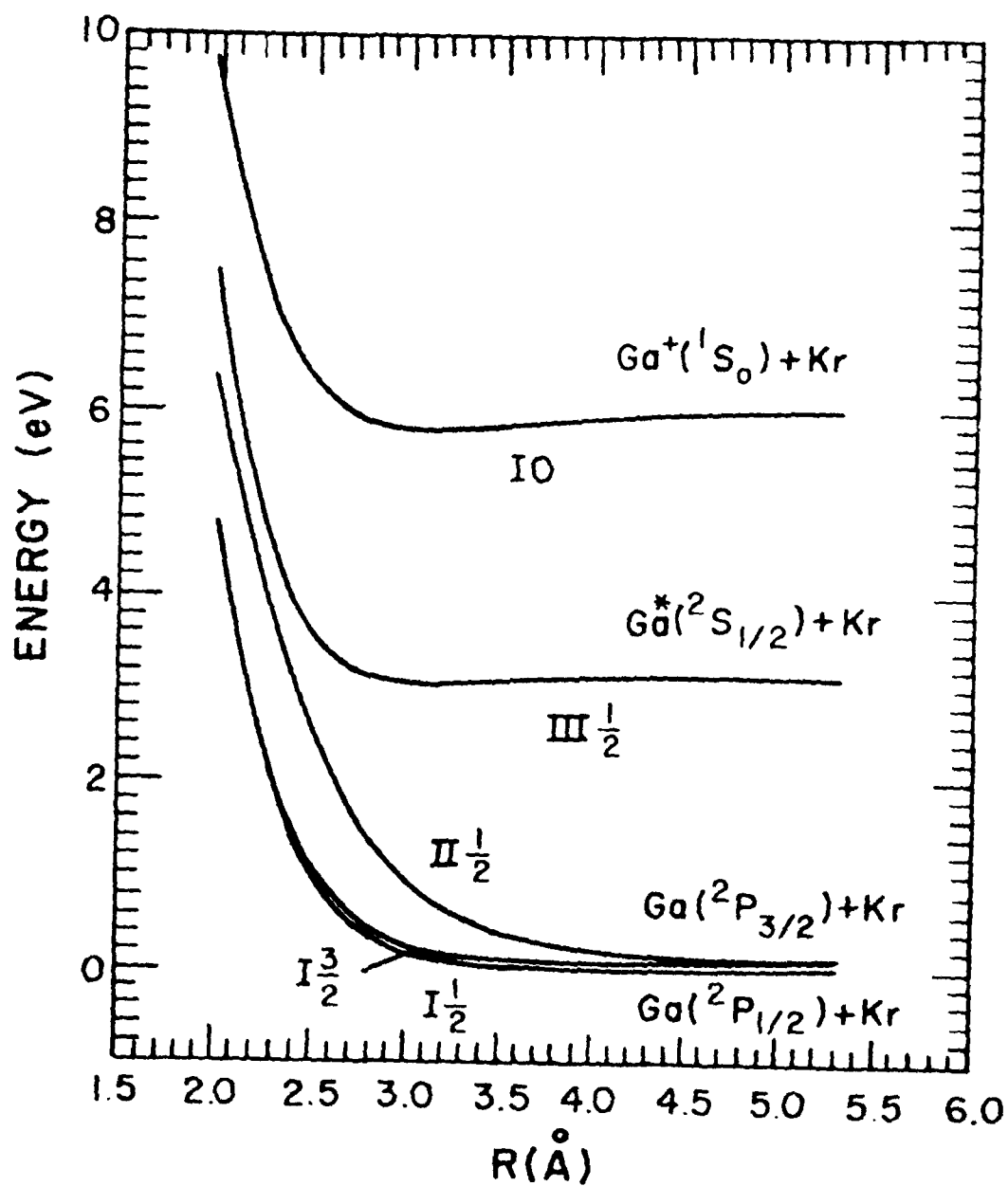




Figure 6.

DIPOLE TRANSITION MOMENTS AMONG  
THE LOW-LYING STATES OF GaKr WITH  
SPIN-ORBIT CORRECTIONS

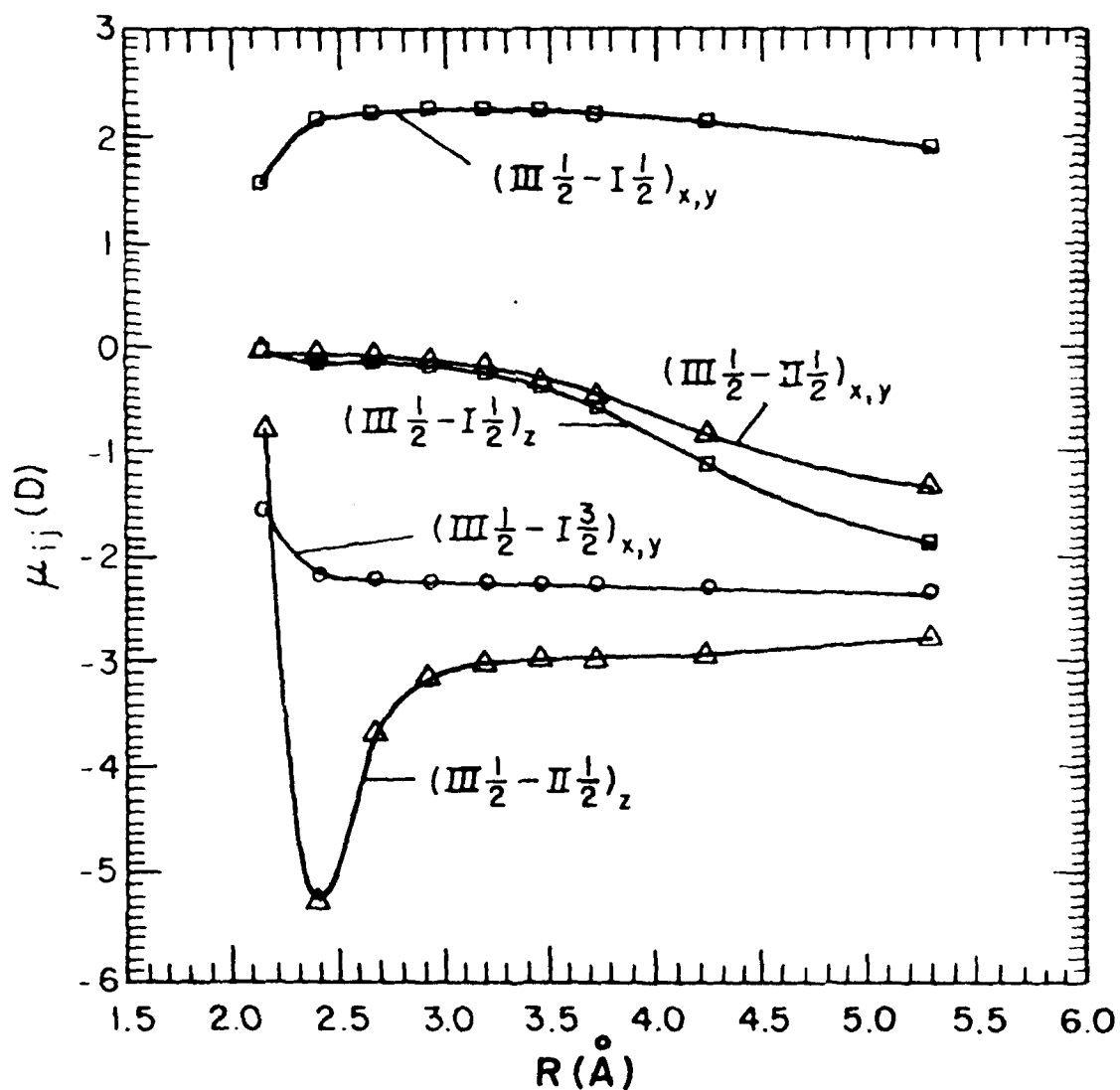


Figure 7.

### THE LOW-LYING STATES OF $\text{InKr}$ AND $\text{InKr}^+$ WITH SPIN-ORBIT CORRECTIONS

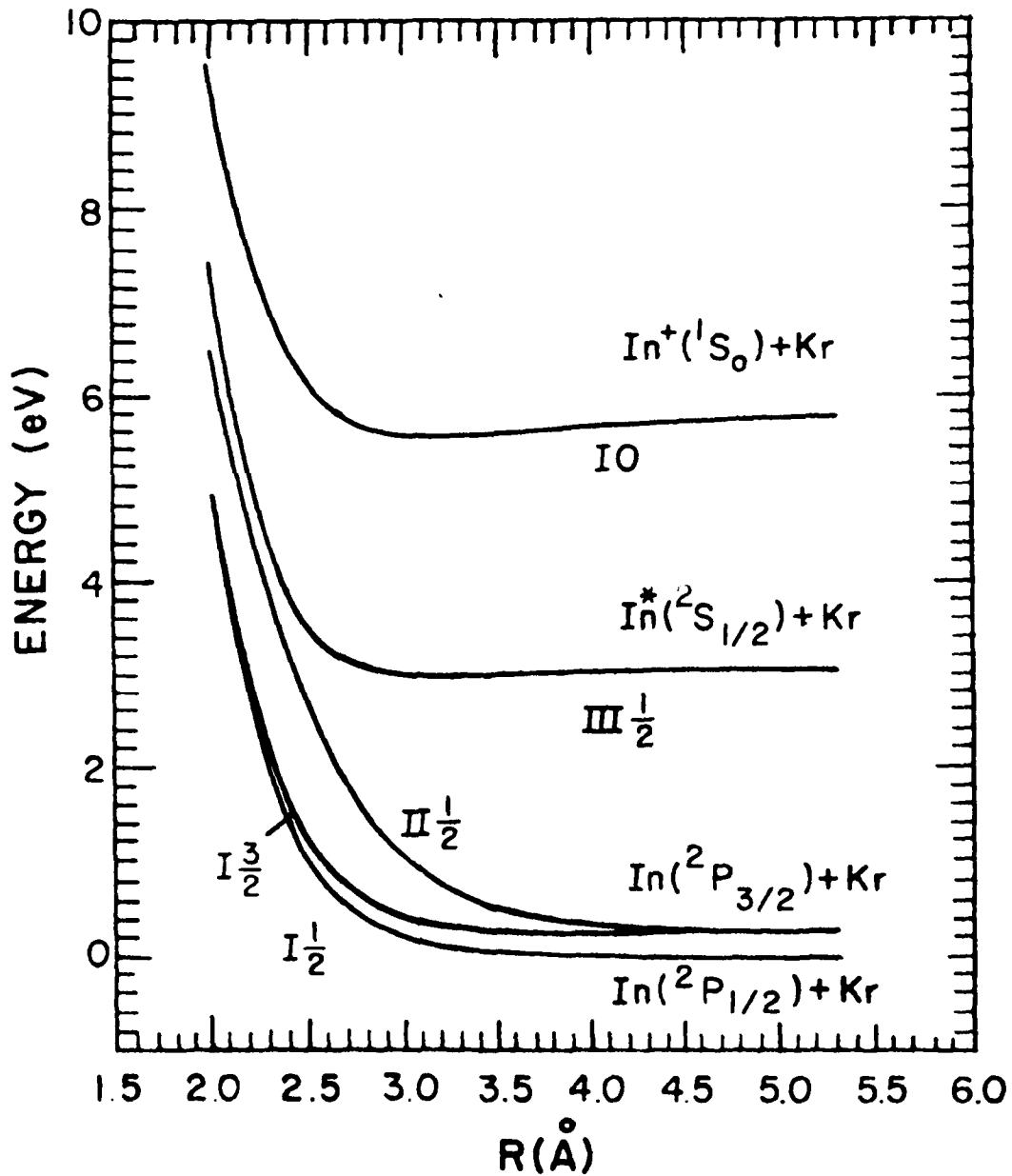


Figure 8.

### THE LOW-LYING STATES OF $\text{TiKr}$ AND $\text{TiKr}^+$ WITH SPIN-ORBIT CORRECTIONS

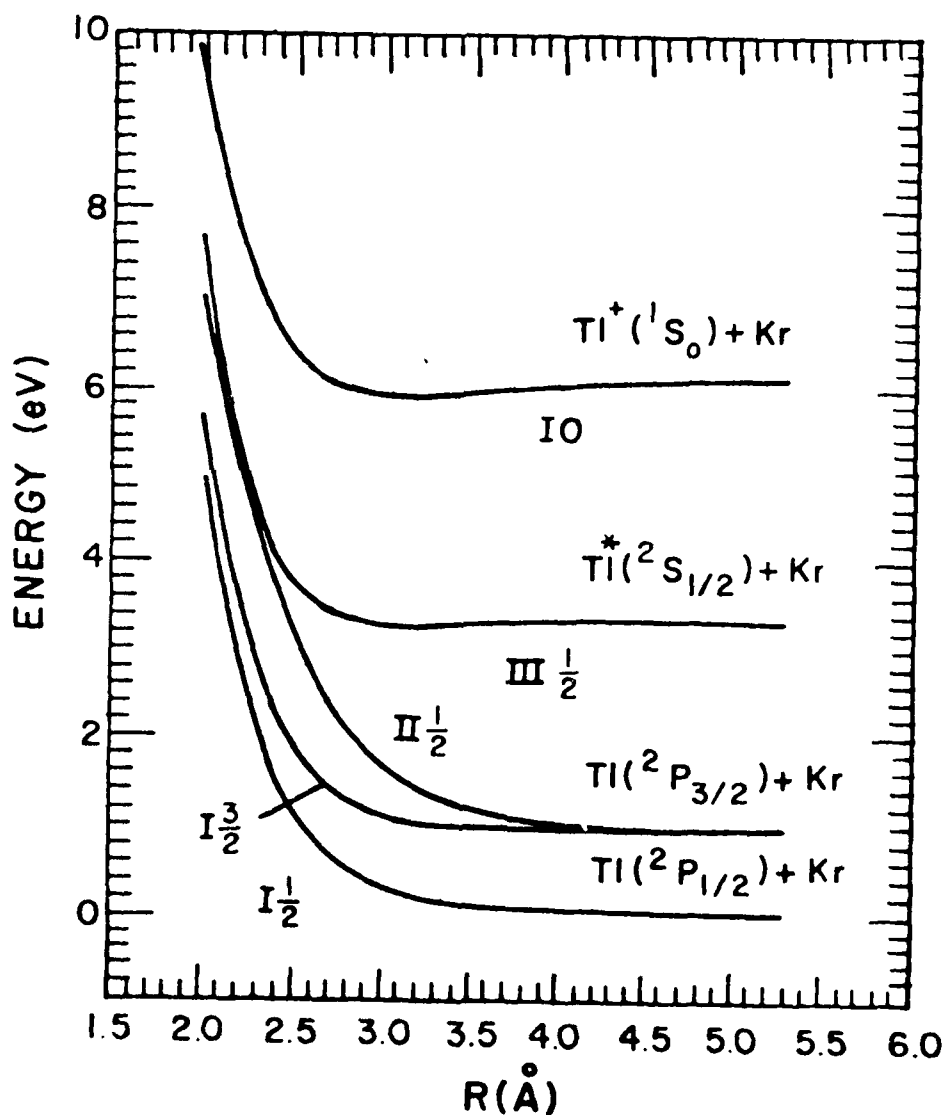


Figure 9.

DIPOLE TRANSITION MOMENTS CONNECTING  
THE LOW-LYING STATES OF  $\text{TiKr}$  WITH  
SPIN-ORBIT CORRECTIONS

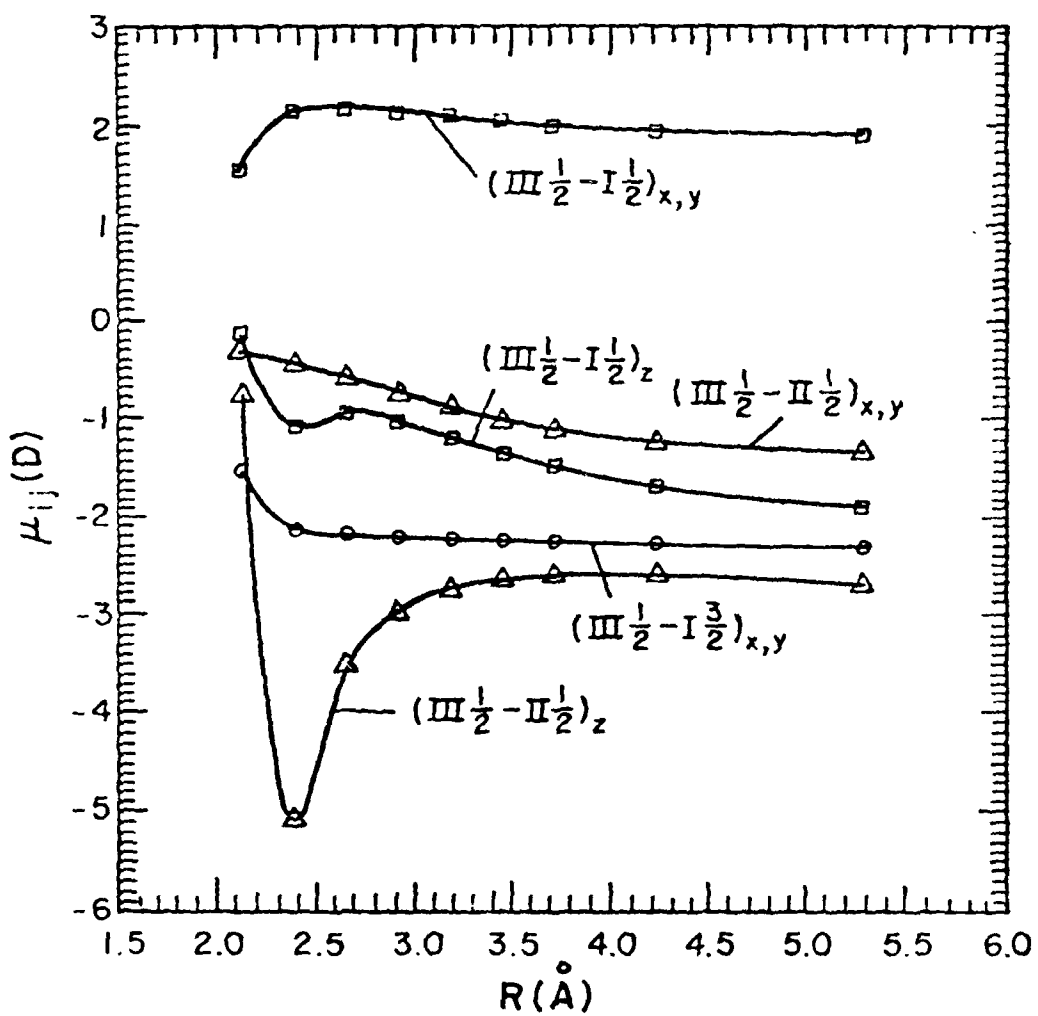


Figure 10.

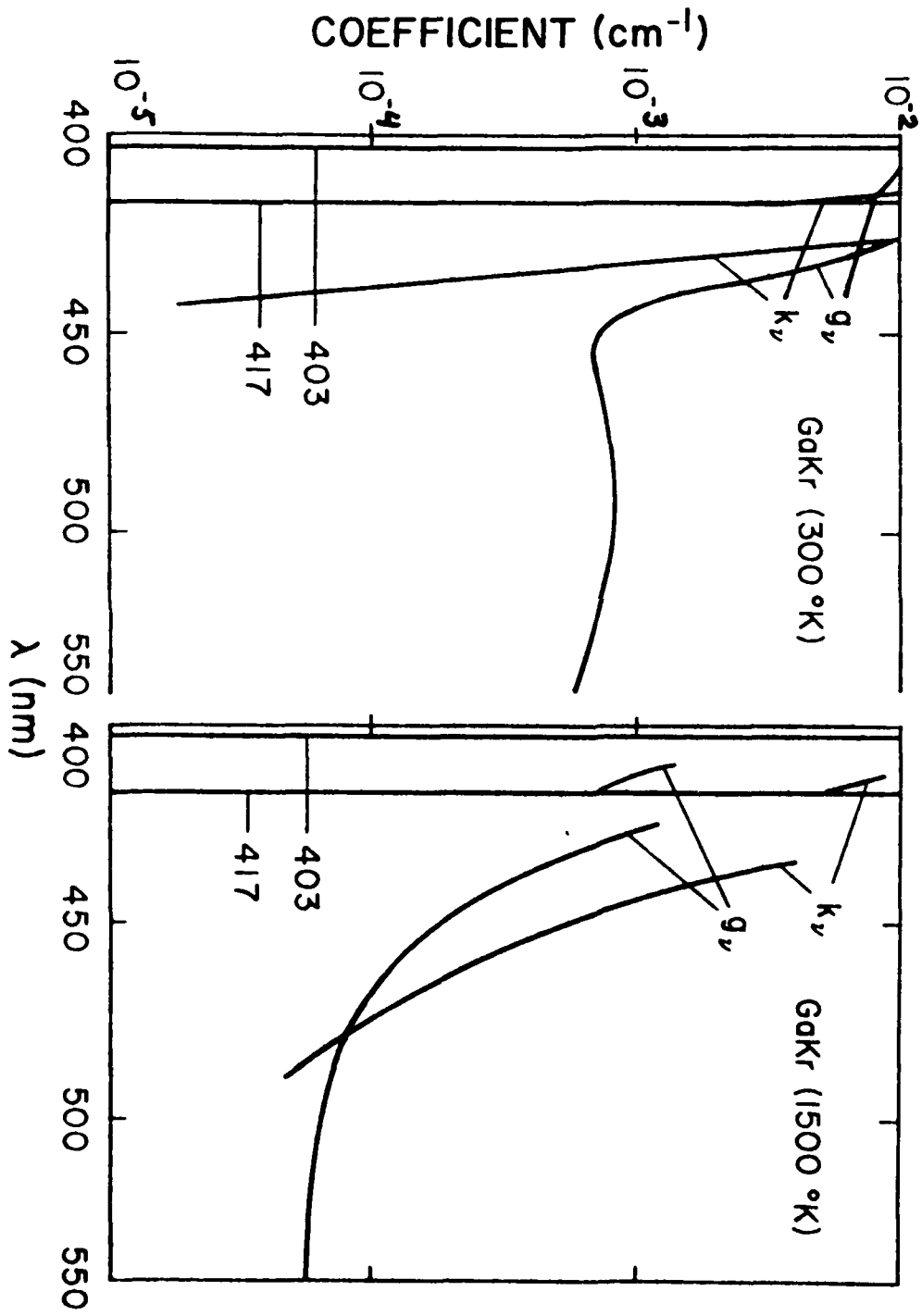


Figure 11.

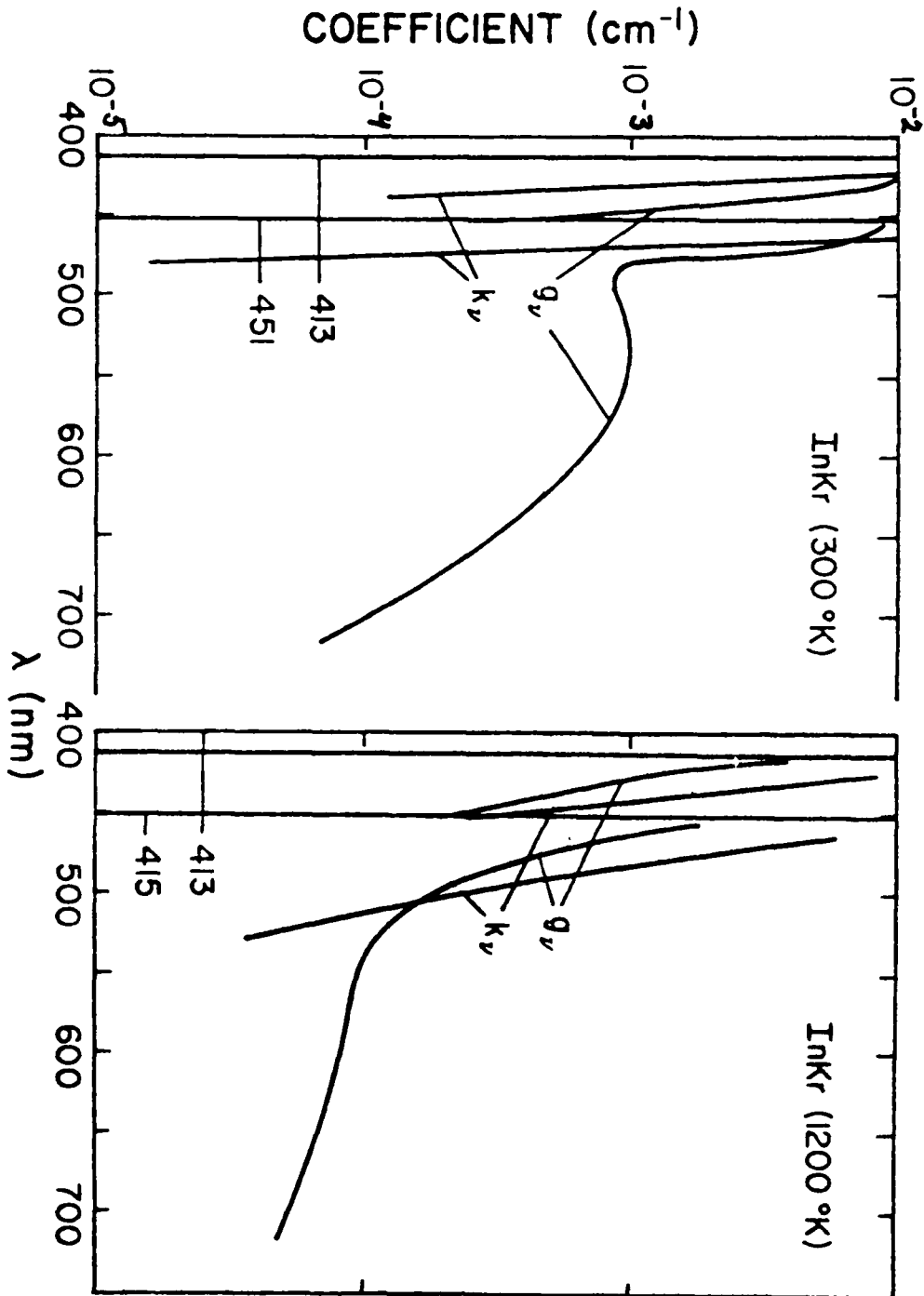
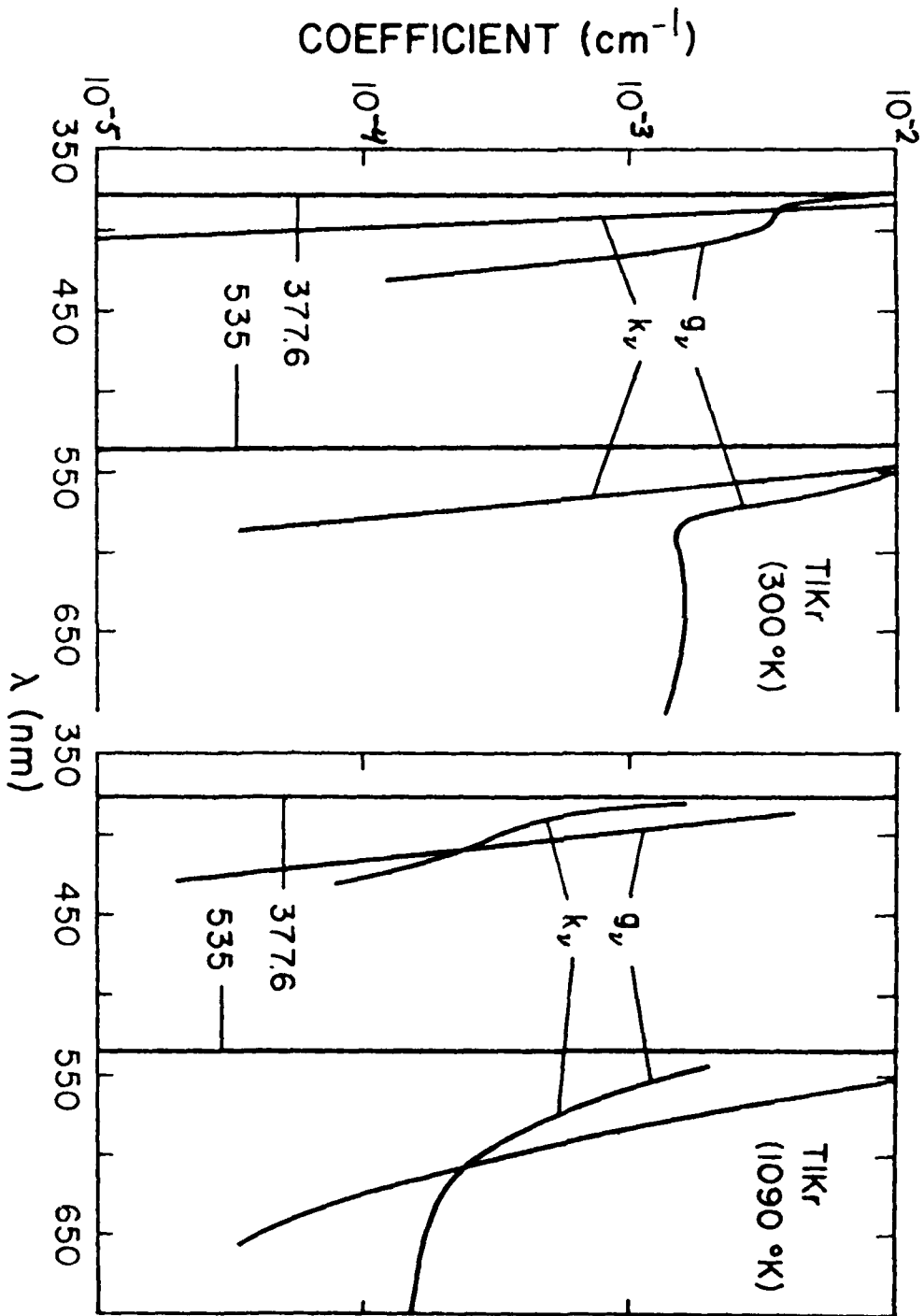


Figure 12.



Application of the Gordon-Kim theory to the group IIIB-rare gas systems.

In recent years, the electron gas methods developed by Gaydaenko and Nikulin [1], and Gordon and Kim [2] and modified by Rae [3] and Cohen and Pack [4] have proved successful in calculating the interaction energies of pairs of closed shell atoms or ions [1-5], of atom-molecule systems [6-7], of molecule-molecule systems [8], and, recently, of systems with one open shell atom [9]. These interaction energies are much more accurate than the simplicity of the Gordon-Kim (GK) method would lead one to expect.

The recent success of the GK method in calculating closed shell - open shell interaction energies has prompted us to use this method to calculate the interaction of group IIIB-noble gas pairs. The GK theory has been most successful in cases where the interaction is non-covalent and where the atoms are relatively undistorted. For these reasons, systems such as GaKr would seem to be ideal candidates for a GK calculation.

The electron-gas theory is briefly reviewed in part A, and our preliminary results on GaKr are given in part B.

#### A. The electron gas method

The method we have used is that of Gordon and Kim [2] as modified by Cohen and Pack [4]. A more detailed description of the theory is available in these two papers. Briefly the GK theory approximates the intermolecular



potential  $V(R)$  at the distance  $R$  by

$$V(R) \approx V^{GK}(R) = V_{HF}^{GK}(R) + V_{corr}^{GK}(R)$$

where

$$V_{HF}^{GK} = V_k + V_c + V_e$$

and these three terms represent the kinetic, Coulomb and exchange interaction energies, respectively. To calculate these interaction energies, the electronic charge density  $\rho$  is approximated by the sum of the atomic charge densities,

$$\rho = \rho_a + \rho_b .$$

With this approximation, the Coulomb interaction can be calculated directly, but the other terms are all estimated by the formulas for the energy density of a uniform electron gas [4]. An additional modification [3,4] is made to the exchange energy to avoid self-exchange contributions.

## B. Calculations

We have modified the molecule-molecule GK interaction program of Parker, Snow and Pack [8], which allows for non-spherical potentials, to calculate interaction energies for closed shell - open shell atomic pairs. The density of the open shell atom, in this case Ga, is divided into

the spherically symmetric core density plus the valence density. For Ga in the ground state ( $4s^2 4p^1$ ), the valence density is constrained to be in a p orbital directed along the internuclear axis, to form a  $\Sigma$  molecular state, or perpendicular to it to form a  $\Pi$  state.

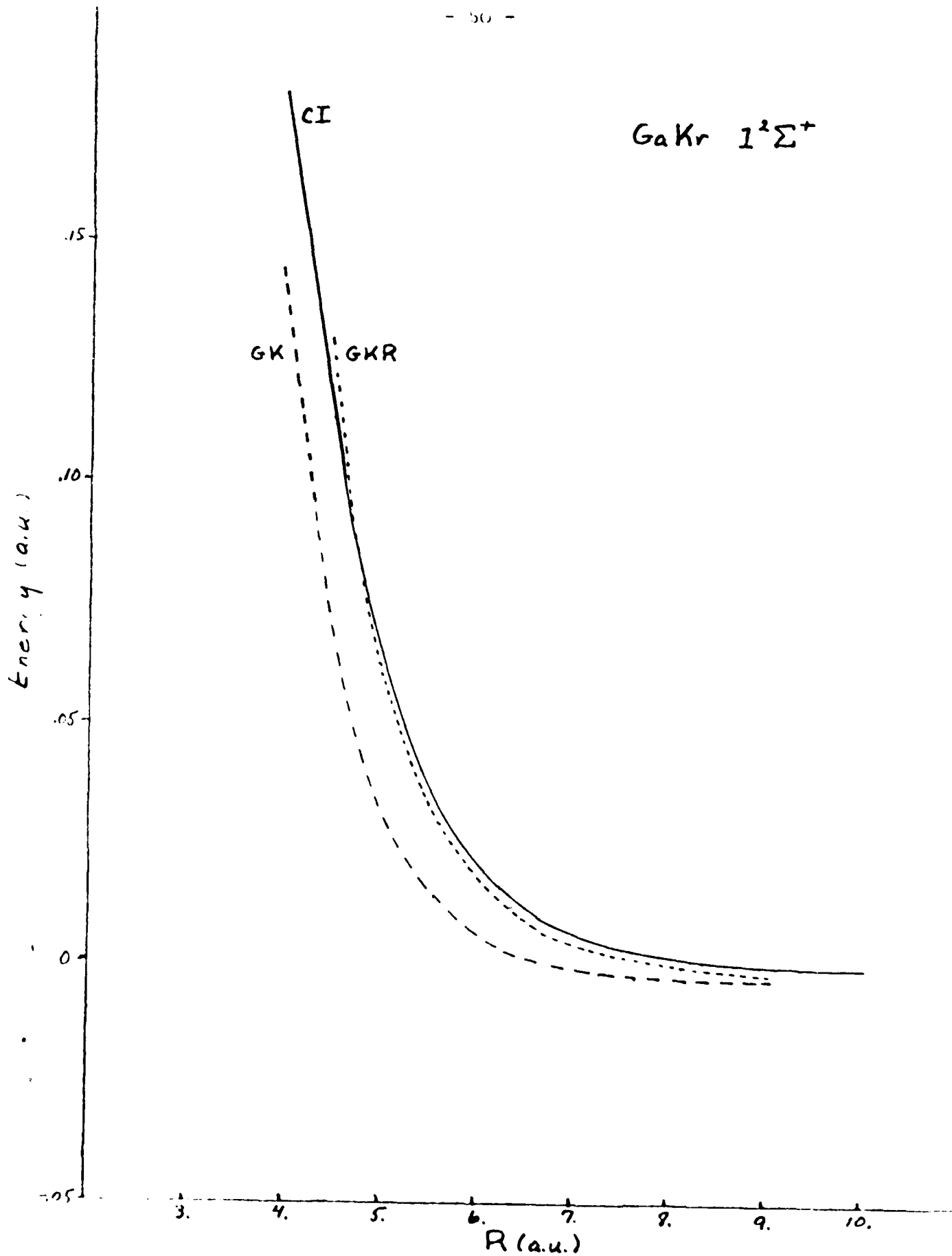
In order to expedite the evaluation of integrals, the atomic density is expanded in a set of Slater basis functions with the coefficients determined by a least-squares fit [4]. The basis set expansions for the density are then read into the GK program which calculates the interaction energy by three-dimensional numerical quadrature.

We have obtained numerically tabulated, relativistic Hartree-Fock densities for the group IIIB and rare gas atoms from Joseph Mann [10]. The densities of the  $4s^2 4p^1$  and  $4s^2 5s^1$  states of Ga and the ground state of Kr were fit with small sets of Slater functions. At this time the fit of the basis set expansion is not very good ( $\sim 10\%$ ).

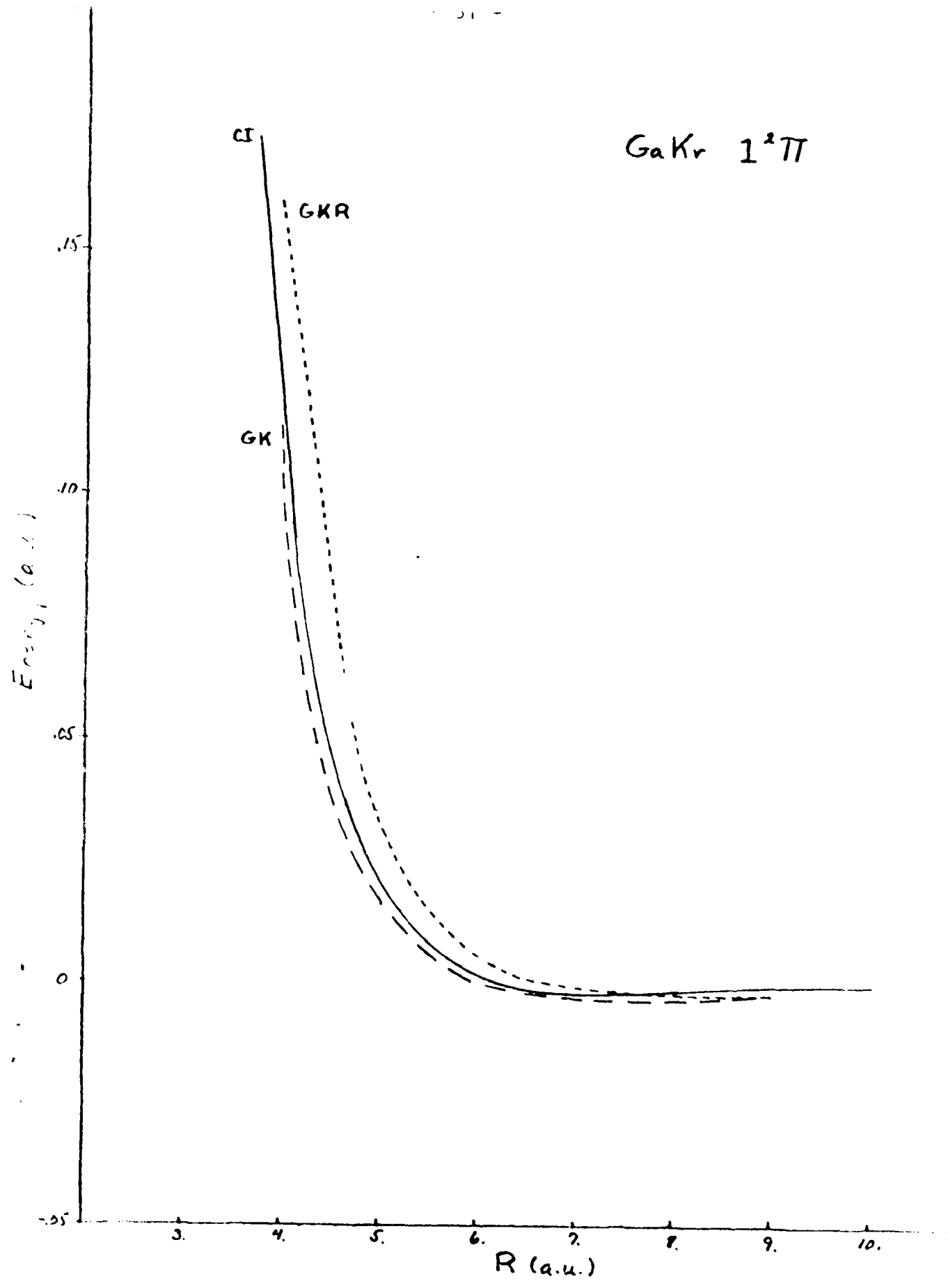
The basis set expansions obtained from this fitting procedure were then used to calculate the GK interaction energies. Because the fitting procedure does not normalize the density, the inaccuracy of the present expansions results in a spurious Coulomb repulsion between the two atoms. We hope that improving the basis set fit will correct this error.

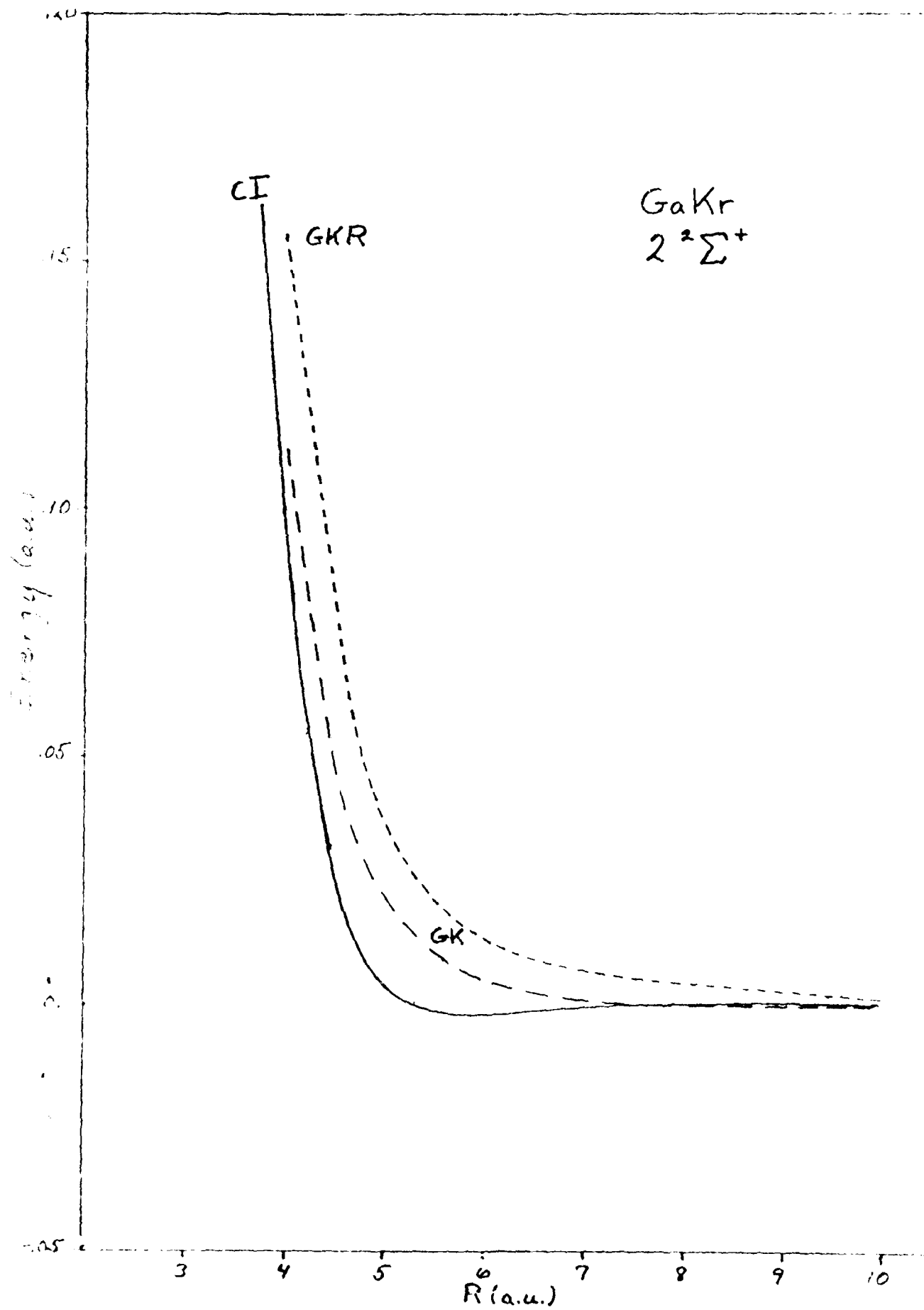
The GK potential curves are compared with the CI results (see Section II) in Figures 1-3. The energies are plotted with respect to the asymptotic energy of each state. The curve labeled GKR includes Rae's correction while the GK curve is the unmodified GK theory. The GKR curve for the  $1^2\Sigma^+$  state agrees remarkably well with the CI result. Unfortunately, the agreement for both the  $1^2\Pi$  and  $2^2\Sigma^+$  states are not as good. Specifically the depths and positions of the potential wells are not predicted accurately. We are currently working on improving the basis set fit and thereby the interaction energies.

GaKr  $1^2\Sigma^+$



GaKr  $1^2\Pi$





1. V. I. Gaydaenko and V. K. Nikulin, Chem. Phys. Letters 7, 360 (1970); V. K. Nikulin, Zh. Tekh. Fiz. 41, 41 (1970) [English transl. Soviet Phys. Tech. Phys. 16, 28 (1971)].
2. R. G. Gordon and Y. S. Kim, J. Chem. Phys. 56, 3122 (1972); Y. S. Kim and R. G. Gordon, J. Chem. Phys. 60 1842, 4323, 4332, (1974); 61 1, (1974).
3. A. I. M. Rae, Chem. Phys. Letters 18, 574 (1973).
4. J. M. Cohen and R. T. Pack, J. Chem. Phys. 61, 2372 (1974).
5. B. Schneider, J. Chem. Phys. 58 4447 (1973).
6. Y. S. Kim, Thesis, Harvard University (1973).
7. G. Green and P. Thaddeus, Astrophys. J. 191, 653 (1974).
8. G. A. Parker, R. L. Snow and R. T. Pack, Chem. Phys. Lett. 33 399 (1975).
9. M. J. Clugston and R. G. Gordon, J. Chem. Phys. 66, 239 (1977).
10. Joseph Mann, private communication.

§4

4.1 Theoretical basis

A. Introduction

This section describes the theoretical basis of our calculations using the effective potential method. For an excimer system AB, where A is a closed-shell system, most of the states of interest correspond to the asymptotic situation where B is excited but A is in its ground state. Fundamentally, what the electron scattering theory says is that any charged particle in B sees a potential ( $\Sigma_A$ ), due to the closed-shell system A, which is the same as if the charged particle were scattered off of A. This scattering potential is corrected for the fact that A is "depolarised" relative to the scattering problem, due to the presence of the nucleus and other electrons of B. The unique aspect of this work, which distinguishes it from many other high-quality attempts to produce such curves, is that it is based on the model interaction potentials and response functions that arise out of many body theory (using Schwinger Functional Derivatives). The use of this type of many body theory has characterized the work of this group over the last few years.<sup>16</sup>

The effective potential method will clearly give incorrect results when any of three situations are met: First, if charge transfer states mix with the excited states of interest; second, when states go asymptotically to two excited atoms; third, when covalent bonding is important. Only for charge transfer do we have a possible Class I solution. For the moment it is hoped that all three problem situations will be avoided for the lowest excimer excited states in the systems of interest to this proposal. If  $Zn_2$  and  $Mg_2$  are any guide the first two problems occur only for the higher excited states.<sup>17</sup>

In part B the basic equations are presented and possible methods for calculating the interaction energy are discussed in part C. The use of semiempirical forms for the effective potentials are discussed in part D.



## B. The Basic Equations

Using many-body field theoretic methods it has been shown that the change in energy,  $\epsilon$ , resulting from the addition of an electron to a closed-shell reference system (referred to here as A) is given by the one-particle Dyson equation

$$T(r)\phi(r) + \int dr' \Sigma^A(r;r';\epsilon)\phi(r) = \epsilon\phi(r) \quad (1)$$

where  $T$  is the kinetic energy operator and  $\phi$  is the Dyson amplitude with  $r$  and  $r'$  being space-spin coordinates. Thus, the problem reduces to an effective one-particle problem in which this particle experiences an effective potential,  $\Sigma^A$ , which represents all the other particles collectively, taking into account all effects such as polarization, correlation and exchange, etc. As might be expected, the cost of this simple formulation is that  $\Sigma^A$  is an extremely complicated entity which is both nonlocal and energy dependent and which cannot rigorously be brought into closed form. However, it has been possible to develop

excellent closed form approximations to this potential which are based on well founded physical concepts. Most notable among these is the Random Phase Approximation (RPA) potential,  $\Sigma_{\text{RPA}}$ , which has been very successfully used in calculating the ionization potentials, excitation energies, oscillator strengths, and elastic -scattering phase shifts for He [18].  $\Sigma_{\text{RPA}}$  has also been used to accurately calculate the ionization and excitation energies of Li [19] Moreover, it has been shown that this ab initio potential encompasses other phenomenologically derived semiempirical potentials which have been used by other workers with great success [20].

It has also been recently demonstrated that by applying the same many-body techniques to the problem of two electrons added to a closed-shell reference system (A) one obtains an effective two-particle equation for the resulting change in energy [21].

$$\left[ \sum_{i=1}^2 \left( T(r_i) + \int dr' \Sigma^A(r_i; r_i'; \epsilon) \right) + \frac{1}{|r_1 - r_2|} + \int dr_1' dr_2' W^A(r_1, r_2; r_1', r_2') \right] \phi(r_1, r_2) = \epsilon \phi(r_1, r_2), \quad (2)$$

where in addition to the individual one-particle potentials there now appear a two-particle effective potential,  $W^A$ , which represents how the presence of one particle affects the potential seen by the other particle and which reflects the fact that system A can act as a dielectric medium to shield the Coulombic interaction between two charged particles. As with  $\Sigma^A$ , this potential cannot be rigorously brought into closed form.

However, an excellent ab initio closed form approximation to this potential can be obtained with the Random Phase Approximation,  $W_{RPA}$ , which is completely compatible with the similarly obtained one-particle potential,  $\Sigma_{RPA}$ .

If we now proceed to the case of adding  $m$  electrons to our closed-shell reference system it follows by induction and can be proven formally that the change in energy is given by

$$\begin{aligned} & \left[ \sum_{i=1}^m \left( T(r_i) + \int dr'_i \Sigma^A(r_i; r'_i; \epsilon) \right) + \sum_{i>j}^m \left( \frac{1}{|r_i - r_j|} + \int dr'_i dr'_j W^A(r_i, r_j; r'_i, r'_j; \epsilon) \right) \right. \\ & \left. \int_{j>k}^m dr'_i dr'_j dr'_k U^A(r_i, r_j, r_k; r'_i, r'_j, r'_k; \epsilon) + \dots + \int dr'_1 \dots dr'_m V^A(r_1 \dots r_m; r'_1 \dots r'_m; \epsilon) \right] \Psi(r_1 \dots r_m) \\ & = \epsilon \Psi(r_1 \dots r_m), \end{aligned} \quad (3)$$

where our notation for three-particle and higher potentials is obvious.

In the above we only considered the addition of electrons to our closed-shell reference system A. However, we can also add nuclei as well; the only difference being that when acting on a nuclear coordinate all potential terms involving electron exchange must of course vanish. Since this can be trivially accomplished by choosing an appropriate (artificial) nuclear spin coordinate, we can immediately generalize (3) to include both nuclei and electrons by allowing the particles to carry different charges,  $z$ , (where  $z = -1$  for an electron) to give

$$\begin{aligned}
 & \left[ \sum_{i=1}^m (T(r_i) - \int dr'_i \Sigma^A(r_i; r'_i; \epsilon, z_i)) + \sum_{i>j}^m \left( \frac{z_i z_j}{|r_i - r_j|} + \int dr'_i dr'_j W^A(r_i, r_j; r'_i, r'_j; \epsilon, z_i, z_j) \right) \right. \\
 & \left. + \dots \right] \Psi(r_1 \dots r_m) = \epsilon \Psi(r_1 \dots r_m). \quad (4)
 \end{aligned}$$

We of course cannot solve (4) since the potentials involved cannot be written in closed form. However, we can replace these potentials by their RPA approximates which are in closed form. Furthermore, realizing that we are deriving a theory for intermolecular forces which is essentially perturbative in nature, we will now assume that all three-particle and higher potentials can be neglected so that our equation becomes simply

$$\begin{aligned}
 & \left[ \sum_{i=1}^m (T(r_i) - \int dr'_i \Sigma^A(r_i; r'_i; \epsilon, z_i)) + \sum_{i>j}^m \left( \frac{z_i z_j}{|r_i - r_j|} + \int dr'_i dr'_j W^A(r_i, r_j; r'_i, r'_j; \epsilon, z_i, z_j) \right) \right] \Psi(r_1 \dots r_m) \\
 & = \epsilon \Psi(r_1 \dots r_m). \quad (5)
 \end{aligned}$$

Since our interest lies in the calculation of potential energy surfaces, what we really want is an equation for the change in energy when  $m_e$  electrons and  $m_n$  nuclei are added to A with these nuclei held fixed at specific points in space (which we will refer to collectively as R with the actual spatial coordinate of nuclei i being  $R_i$ ). That is, we want to be able to separate electronic motion from nuclear motion so that this quantity,  $\mathcal{E}(R)$ , will be the total potential experienced by these nuclei and will satisfy the equation

$$\left[ \sum_{i=1}^{m_n} T(R_i) + \mathcal{E}(R) \right] X(R) = \epsilon X(R) \quad (6)$$

where  $X(R)$  is a function of the nuclear coordinates only. As it stands, (5) precludes such a separation because of the energy dependence of the potentials involved. To overcome this problem we will now assume that for those solutions to (5) we seek this energy dependence is not strong. Furthermore, we will also assume that the response of  $A$  to the added particles is instantaneous. In this way we can replace the non-adiabatic energy dependent potentials in (5) with their hermitian energy independent adiabatic approximates such as those given in ref.21. With these substitutions (5) does become separable, and by taking

$$\psi(r_1 \dots r_{m_e}) = \sum_j X_j(R) \psi_j(r_1 \dots r_{m_e}) ; \langle \psi_i | \psi_j \rangle = \delta_{ij} \quad (7)$$

where  $\psi(r_1 \dots r_{m_e})$  is a function of only the electronic coordinates we find that  $\mathcal{E}(R)$  is given by

$$\mathcal{E}(R) = E^A(R) - \sum_{i=1}^{m_n} \Sigma^A(R_i; z_i) + \sum_{i>j}^{m_n} \left( \frac{z_i z_j}{|R_i - R_j|} + W^A(R_i, R_j; z_i, z_j) \right), \quad (8)$$

where  $E^A$  is given by the equation

$$\begin{aligned} & [H(r_1 \dots r_{m_e}; R) + \sum_{i=1}^{m_e} \left( \int dr'_i \Sigma^A(r; r') \right) - \sum_{j=1}^{m_n} \int dr'_j W^A(r_i, R_j; r'_j; z_j) \\ & + \sum_{i>j}^{m_e} \int dr'_i dr'_j W^A(r_i, r_j; r'_i r'_j) ] \psi(r_1 \dots r_{m_e}) = E^A(R) \psi(r_1 \dots r_{m_e}) \quad (9a) \end{aligned}$$

where  $H$  is the usual hamiltonian for  $m_e$  electrons in the field of  $m_n$  fixed nuclei

$$\begin{aligned}
 H(r_1 \dots r_{m_e}; R) &= \sum_{i=1}^{m_e} (T(r_i) - \sum_{j=1}^{m_n} \frac{z_j}{|r_i - R_j|}) + \sum_{i>j}^{m_e} \frac{1}{|r_i - r_j|} \\
 &= \sum_{i=1}^{m_e} h(r_i) + \sum_{i>j}^{m_e} \frac{1}{r_{ij}} \tag{9b}
 \end{aligned}$$

and where all one- and two-particle effective potentials are taken to be hermitian adiabatic approximates to the true potentials. Note also that all potential terms involving the  $m_n$  nuclei are now written as local quantities thereby taking into account the previously mentioned fact that there are no exchange (i.e. nonlocal) terms in the potentials when nuclei are being considered.

If we now collectively refer to these  $m_e$  electrons and  $m_n$  nuclei which have a fixed internuclear geometry as being system B, then  $\mathcal{E}(R)$  is the change in energy resulting from the creation of system B in the vicinity (as measured by  $R$ ) of A. If  $R \rightarrow \infty$  then  $\mathcal{E} \rightarrow \mathcal{E}_B^0$  which is just the energy B itself. Therefore, the intermolecular potential of the system A-B as a function of the separation between A and B is

$$V_B^A(R) = E_B^A(R) - E_B^0 + V_{B,nuc}^A(R) \tag{10a}$$

where

$$V_{B,nuc}^A(R) = - \sum_{i=1}^{m_n} \Sigma^A(R_i; z_i^B) + \sum_{i>j}^{m_n} W^A(R_i, R_j; z_i^B, z_j^B) \tag{10b}$$

and where

$$E_B^0 = \mathcal{E}_B^0 + \sum_{i>j}^{m_n} z_i^B z_j^B \frac{1}{|R_i - R_j|} \quad (10c)$$

is just the electronic energy of isolated system B and where  $E_B^A(R)$  is given by

$$\begin{aligned} & [H(r_1 \dots r_{m_e}; R) + \sum_{i=1}^{m_e} \int dr'_i (\Sigma^A(r_i; r'_i) - \sum_{j=1}^{m_n} W^A(r_i, R_j; r'_i; Z_j^B)) \\ & + \sum_{i>j}^{m_e} \int dr'_i dr'_j W^A(r_i, r_j; r'_i r'_j)] \Psi_B^A(r_1 \dots r_{m_e}) = E_B^A(R) \Psi_B^A(r_1 \dots r_{m_e}) \quad (10d) \end{aligned}$$

Therefore, given that we know  $E_B^0$  and that we have available good closed form adiabatic approximates for  $\Sigma^A$  and  $W^A$  our problem reduces to finding the solutions (or rather a particular solution) to (10d). In the following section we will look at some ways of doing this.

C. Determination of  $E_B^A$

Our equation for  $E_B^A$  is of the form

$$(H + U^A) \psi_B^A = E_B^A \psi_B^A \quad (11a)$$

where

$$\begin{aligned} U^A(r_1 \dots r_{m_e}; R) &= \sum_{i=1}^{m_e} \int dr_i' [\Sigma^A(r_i; r_i') - \sum_{j=1}^{m_n} W^A(r_i, R_j; r_i'; Z_j^B)] \\ &+ \sum_{i>j}^{m_e} \int dr_i' dr_j' W^A(r_i, r_j; r_i', r_j') \\ &= \sum_{i=1}^{m_e} p^A(r) + \sum_{i>j}^{m_e} q_{12}^A(r_i, r_j) \end{aligned} \quad (11b)$$

where we note that  $\psi_B^A$  is an eigenfunction of the hermitian 'hamiltonian'  $(H + U^A)$  and that  $H$  is the electronic hamiltonian for isolated system  $B$ . If we now explicitly assume that  $U^A$  is small compared to  $H$  (this of course was implicit in our derivation of  $U^A$  in the first place) then  $U^A$  can be regarded as being a small perturbation on  $H$ . As a consequence, the solution,  $\psi_B^A$ , to (11) which we seek should resemble the electronic wavefunction for isolated system  $B$ ,  $\psi_B^0$ , and this wavefunction should therefore provide us with a proper starting point determining  $\psi_B^A$  and  $E_B^A$ .

1. First-Order Perturbation Treatment

Projecting (11a) against  $\psi_B^A$  and normalizing  $\psi_B^A$  to unity gives



$$E_B^A = \langle \psi_B^A | H + U^A | \psi_B^A \rangle ; \langle \psi_B^A | \psi_B^A \rangle = 1 , \quad (12a)$$

whereas if  $\psi_B^0$  is a self-consistent solution for isolated system B its energy is.

$$E_B^0 = \langle \psi_B^0 | H | \psi_B^0 \rangle ; \langle \psi_B^0 | \psi_B^0 \rangle = 1 . \quad (12b)$$

If we assume that  $U^A$  is a quite small perturbation to H then we can solve for  $E_B^A$  using standard first-order perturbation theory to obtain

$$E_B^A = E_B^0 + \langle \psi_B^0 | U^A | \psi_B^0 \rangle \quad (13)$$

so that our first-order perturbative expression for  $V_B^A$  is simply

$$V_B^A = V_{B,nuc}^A + \langle \psi_B^0 | U^A | \psi_B^0 \rangle . \quad (14)$$

This of course is equivalent to assuming that the wavefunction for system B remains virtually unchanged when in the presence of A .

In terms of the one- and two-particle density matrices,  $\rho_1^0$  and  $\rho_2^0$ , associated with  $\psi_B^0$ , (14) becomes

$$V_B^A = V_{B,nuc}^A + \int_{r'=r} dr \rho^A(r') \rho_1^0(r;r') + \int_{r'=r} dr_1 dr_2 q_{12}^A(r_1, r_2) \rho_2^0(r_1, r_2; r_1 r_2) . \quad (15)$$

If  $\psi_B^0$  is a single Slater determinant so that

$$\rho_2^0(r_1, r_2; r_1', r_2') = 1/2[\rho_1^0(r_1; r_1')\rho_1^0(r_2; r_2') - \rho_1^0(r_1; r_2')\rho_1^0(r_2; r_1')] \quad (16a)$$

with

$$\rho_1^0(r; r') = \sum_{i=1}^n \phi_i^*(r) \phi_i(r') \quad (16b)$$

where  $\{\phi_i\}$  are the  $n$  one-electron spin-orbitals comprising  $\psi_B^0$ ,  
then  $V_B^A$  takes on the form

$$V_B^A = V_{B,nuc}^A + \sum_{i=1}^n \langle \phi_i | p^A | \phi_i \rangle + 1/2 \sum_{i \neq j}^n [\langle \phi_i \phi_j | q_{12}^A | \phi_i \phi_j \rangle - \langle \phi_i \phi_j | q_{12}^A | \phi_j \phi_i \rangle] \quad (17)$$

where the two-electron integrals over  $q_{12}^A$  are written in the standard  $\langle 12 || 12 \rangle$  notation.

If  $\psi_B^0$  cannot be written as a single Slater determinant but can be written as a linear combination of determinants involving  $n$  one-electron spatial orbitals  $\{\phi_i^0\}$  then (12b) can always be written as

$$E_B^0 = \sum_{i,j}^n D_i^j \langle \phi_i^0 | h | \phi_j^0 \rangle + \sum_{i,j,k,l}^n D_{i,j}^{k,l} \langle \phi_i^0 \phi_j^0 | \frac{1}{r_{12}} | \phi_k^0 \phi_l^0 \rangle \quad (18)$$

where  $\{D_i^j, D_{i,j}^{k,l}\}$  are fixed coefficients which depend on the precise form of  $\psi_B^0$  and on orbital overlaps. Since  $U^A$  is of the same form as  $H$  and, like  $H$ , is spin independent (recall that isolated system  $A$  must be closed-shell) we can immediately write our first-order approximation for  $V_B^A$  as

$$V_B^A = V_{B,nuc}^A + \sum_{i,j}^n D_i^j \langle \phi_i^0 | p^A | \phi_j^0 \rangle + \sum_{i,j,k,l}^n D_{ij}^{kl} \langle \phi_i^0 \phi_j^0 | q_{12}^A | \phi_k^0 \phi_l^0 \rangle \quad (19)$$

where all operators and integrals are now explicitly taken to involve only spatial coordinates. Therefore, we can determine  $\langle \psi_B^0 | U^A | \psi_B^0 \rangle$  by using the general energy expression (18) but employing one- and two-electron integrals over the operators  $p^A$  and  $q_{12}^A$  instead of the usual integrals over  $h$  and  $\frac{1}{r_{12}}$ .

We could continue this perturbation treatment by going on to determine second-order and higher corrections. However we will stop here and next consider a self-consistent approach instead.

## 2. Self-Consistent Treatment

Let us now assume that while  $U^A$  is a small perturbation to  $H$  it is not small enough to justify a simple first-order perturbation treatment. That is, we will now assume that  $\psi_B^A$  can still be taken to be functionally the same as  $\psi_B^0$  but because of the presence of  $A$  the spatial orbitals themselves distort away from  $\{\phi_i^0\}$  to a meaningful extent. The problem is then to determine these new orbitals  $\{\phi_i\}$ . Since  $\psi_B^A$  is an eigenfunction of electronic motion satisfying (11) this can be done variationally. That is, we can determine these new distorted orbitals by requiring that  $E_B^A$  be stationary with respect to changes in these orbitals. If for simplicity (but not necessity) we assume that  $\psi_B^0$  can be written as a Hartree-Fock type wavefunction involving orthonormal

spatial orbitals (or orthonormal spin-orbitals for the case of an Unrestricted Hartree-Fock wavefunction) then (18) takes on the simple Roothaan form

$$E_B^0 = 2 \sum_{i=1}^n f_i \langle \phi_i^0 | h | \phi_i^0 \rangle + \sum_{i,j}^n [a_{ij} J_{\phi_i^0 \phi_j^0} + b_{ij} K_{\phi_i^0 \phi_j^0}] \quad (20a)$$

where

$$J_{\phi_i^0 \phi_j^0} = \langle \phi_i^0 | J_{\phi_j^0} | \phi_i^0 \rangle = \langle \phi_j^0 | J_{\phi_i^0} | \phi_j^0 \rangle = \langle \phi_i^0 \phi_j^0 | \frac{1}{r_{12}} | \phi_i^0 \phi_j^0 \rangle \quad (20b)$$

$$K_{\phi_i^0 \phi_j^0} = \langle \phi_i^0 | K_{\phi_j^0} | \phi_i^0 \rangle = \langle \phi_j^0 | K_{\phi_i^0} | \phi_j^0 \rangle = \langle \phi_i^0 \phi_j^0 | \frac{1}{r_{12}} | \phi_j^0 \phi_i^0 \rangle \quad (20c)$$

and where  $\{f_i; a_{ij}; b_{ij}\}$  are fixed coefficients (for the case of a multi-configurational wavefunction these coefficients are simply related to the variationally determined configurational coefficients) which depend on the precise form of  $\psi_B^0$ . Since  $\psi_B^A$  is being taken to have the same form as  $\psi_B^0$  and because of the similarities between  $H$  and  $U^A$  mentioned above, we can immediately write our equation for  $E_B^A$  as

$$E_B^A = 2 \sum_{i=1}^n f_i \langle \phi_i | h^A | \phi_i \rangle + \sum_{i,j} [a_{ij} \langle \phi_i \phi_j | g_{12}^A | \phi_i \phi_j \rangle + b_{ij} \langle \phi_i \phi_j | g_{12}^A | \phi_j \phi_i \rangle] \quad (21a)$$

where the operator  $h^A$  and  $g_{12}^A$  are given by

$$h^A = h + p^A ; g_{12}^A = \frac{1}{r_{12}} + q_{12}^A \quad (21b)$$

Therefore,  $\{\phi_i\}$  and therefore  $E_B^A$  can be determined using standard basis set expansion (LCAO) SCF techniques. The only difference is that instead of using the usual one- and two-electron integrals we must use integrals over the operators  $h^A$  and  $g_{12}^A$  instead. However, since these integrals serve only as input this difference is transparent to whatever available SCF procedure we employ.

### 3. Configuration Interaction Treatment

For the sake of completeness it should be mentioned that since  $\psi_B^A$  can be variationally determined there is no need to stop at the SCF level and we could solve for this function as a Configuration Interaction (CI) problem. The only difference from a standard CI calculation is that instead of using the usual one- and two-electron integrals we must use integrals over the  $h^A$  and  $g_{12}^A$  operators defined in (21b). It should be pointed out however that any solution for  $\psi_B^A$  which differs significantly from  $\psi_B^0$  implies that for that solution  $U^A$  can no longer be regarded as a small perturbation to  $H$  and in such a case the validity of the approximations made in our choice of  $U^A$  would become subject to question. This of course also applies in our SCF treatment as well.

#### D. The Potentials

The one- and two-particle effective potentials  $\Sigma^A$  and  $W^A$  appearing in our final equations in section II are hermitian adiabatic approximates to the true field theoretic potentials. As we have mentioned,

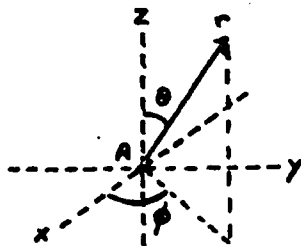
such potentials can be obtained in closed ab initio form using many-body theory within the framework of the RPA approximation and taking the adiabatic limits. However, while these potentials are tractable they are nonetheless quite complicated and their use would entail considerable computational effort. In view of the perturbative nature of our theory it is reasonable to expect that we could use potentials having simpler forms. Such simpler potentials can be obtained by making moment expansions of the RPA potentials and truncating these expansions in a physically meaningful manner [21]. When this is done, the resulting potentials can be cast in forms which are very similar to phenomenologically derived semiempirical potentials which have been used by other workers with considerable success [22]. Therefore, it would seem that the use of complicated ab initio potentials is not warranted (although we do reserve the option to do so) and that we can take our potentials to have semiempirical forms similar to those used by Dalgarno and by Victor [22], namely

$$\int dr' \Sigma^A(r;r') = -\frac{Z^A}{|r|} + \int dr' \Sigma_{HF}^A(r;r') - \frac{\alpha_d^A}{2|r|^4} W_6(k|r|) - \frac{\alpha_q^A}{2|r|^6} W_8(k|r|) + (a_0 + a_1|r| + a_2|r|^2)e^{-k|r|} \quad (22a)$$

and

$$\int dr'_1 dr'_2 W^A(r_1, r_2; r'_1, r'_2) = -\frac{\alpha_d^A}{|r_1|^2 |r_2|^2} W_3(k|r_1|) W_3(k|r_2|) P_1(\cos \gamma_{12}) - \frac{\alpha_q^A}{|r_1|^3 |r_2|^3} W_4(k|r_1|) W_4(k|r_2|) P_2(\cos \gamma_{12}) \quad (22b)$$

where we have chosen our coordinate system to be centered on A which for simplicity we now take to be an atom having a nuclear charge of  $z^A$



and where

- $W_n(x) = (1 - e^{-x^n})$  is a cutoff function
- $\gamma_{12}$  = angle between vectors  $r_1$  and  $r_2$
- $P_\ell(x)$  = legendre polynomial of the  $\ell^{\text{th}}$  degree
- $\alpha_d^A$  = dipole polarizability of A
- $\alpha_q^A$  = approximate quadrupole polarizability of A (adjustable)
- $k$  = approximately  $1/2 r_0$  where  $r_0$  is the effective radius of A (adjustable)
- $\{a_i\}$  = adjustable monopole parameters

and

$$\Sigma_{\text{HF}}^A(r; r') = \sum_{i=1}^{n_A} \frac{\phi_i^{A*}(r') [2 - P_{r,r'}] \phi_i^A(r')}{|r - r'|}$$

is the static Hartree-Fock potential of A with  $\{\phi_i^A\}$  being the  $n_A$  spatial Hartree-Fock orbitals for the electrons in A.  $P_{r,r'}$  is the permutation operator if  $r$  is an electronic coordinate whereas  $P_{r,r'} = 0$

if  $r$  is a nuclear coordinate. Note that all quantities are now purely spatial and that  $\Sigma^A$  and  $W^A$  are therefore explicitly spin independent.

In (22a) the first term is simply the potential due to the nucleus of  $A$  and the second term is the static Hartree-Fock potential for the electrons in  $A$  occupying the spatial orbitals  $\{\phi_i^A\}$ . The next two terms in (22a) are asymptotically correct induced dipole and quadrupole polarization potentials which die off rapidly at short distances from  $A$ . The final term is an induced monopole term which serves as a short range correction potential. The terms in (22b) describe an asymptotically correct dielectric potential which properly cancels out one-particle induced dipole and quadrupole polarizations of  $A$  due to two particles of the same charge when these particles are on opposite sides of  $A$ . That these potentials represent a significant simplification over the ab initio potentials is clear in that our two-particle potential is strictly local and the only nonlocal term in the one-particle potential is simply the usual Hartree-Fock exchange potential. However, despite their simplicity, potentials such as these have been used very successfully for a variety of problems in the past and should therefore be quite adequate for our purposes.

As it stands, (22b) is concise and to the point. However, one important property is obscured. This is that our two-particle potential can be written in terms of one-particle operators only. To see this we need only express the angle  $\gamma_{12}$  in terms of the spherical angles



for each vector. Thus, by making use of the expansion

$$P_\ell(\cos \gamma_{12}) = P_\ell(\cos \theta_1)P_\ell(\cos \theta_2) + 2 \sum_{m=1}^{\ell} \frac{(\ell-m)!}{(\ell+m)!} P_\ell^m(\cos \theta_1)P_\ell^m(\cos \theta_2) [\cos m\phi_1 \cos m\phi_2 + \sin m\phi_1 \sin m\phi_2] \quad (24)$$

where  $P_\ell^m(x)$  is an associated Legendre polynomial, we find that (22b) can be rewritten as

$$\int dr_1^i dr_2^i W^A(r_1, r_2; r_1^i, r_2^i) = - \sum_{i=1}^8 Q_i(r_1)Q_i(r_2) \quad (25a)$$

where

$$\begin{aligned} Q_1(r) &= \sqrt{\alpha_d^A} |r|^{-2} W_3(k|r|) P_1(\cos \theta) \\ Q_2(r) &= \sqrt{\alpha_d^A} |r|^{-2} W_3(k|r|) P_1^1(\cos \theta) \cos \phi \\ Q_3(r) &= \sqrt{\alpha_d^A} |r|^{-2} W_3(k|r|) P_1^1(\cos \theta) \sin \phi \\ Q_4(r) &= \sqrt{\alpha_q^A} |r|^{-3} W_4(k|r|) P_2(\cos \theta) \\ Q_5(r) &= 1/3 \sqrt{\alpha_q^A} |r|^{-3} W_4(k|r|) P_2^1(\cos \theta) \cos \phi \\ Q_6(r) &= 1/3 \sqrt{\alpha_q^A} |r|^{-3} W_4(k|r|) P_2^1(\cos \theta) \sin \phi \\ Q_7(r) &= 1/12 \sqrt{\alpha_q^A} |r|^{-3} W_4(k|r|) P_2^2(\cos \theta) \cos 2\phi \\ Q_8(r) &= 1/12 \sqrt{\alpha_q^A} |r|^{-3} W_4(k|r|) P_2^2(\cos \theta) \sin 2\phi \end{aligned} \quad (25b)$$

Consequently, the implementation of this method involves the addition of only one-electron integrals to existing SCF or CI programs. In addition, if  $\Sigma_{HF}^A$  is replaced by a pseudopotential, only the atomic orbitals of B will be used to calculate the potential for AB.



To perform an effective potential calculation, the program EFFPOT is inserted between steps 2a and 2b.

EFFPOT calculates the additional integrals required,  $\langle \phi_i | \Sigma^A | \phi_j \rangle$  and  $\langle \phi_i | Q_n | \phi_j \rangle$ , and modifies the integral tape so that the insertion of an effective potential is transparent to GVB II. These integrals have not been previously evaluated for gaussian basis sets, and because of the cut-off functions in  $\Sigma^A$  and  $Q_n$  and the angular dependence of  $Q_n$ , the evaluation of these integrals is rather complicated, especially for two-center integrals containing basis functions for  $l > 0$ .

Although it is relatively easy to construct an algorithm for evaluating these integrals, the algebraic detail rapidly becomes overwhelming. To alleviate this problem, we used the algebraic programming system REDUCE<sup>3</sup> to produce the FORTRAN code required to evaluate these integrals. An explanation of the algorithm used to derive the integral expressions and an example of the input to REDUCE are given below for one of the more complicated integrals.

The integral we shall consider is

$$\langle P_x^E | Q_4^B | P_x^F \rangle \quad (13)$$

where the superscripts indicate the atomic center on which the (basis or potential) function is centered,  $Q_4$  is defined by equation 10b and  $P_x$  indicates a "p<sub>x</sub>" gaussian basis function. This integral can be written explicitly as

$$\begin{aligned} \langle P_x^E | Q_4^B | P_x^F \rangle &= \\ & \sqrt{d_q^A/3} \int d\tau x_E e^{-\alpha r_E^2} r_0^{-3} W_4(kr_0) P_2(\cos \theta_0) x_F e^{-\beta r_F^2} \\ & = \sqrt{d_q^A/3} I. \end{aligned} \quad (14)$$

Using the relation

$$P_2(\cos \theta_0) = \frac{3z_0^2 - r_0^2}{2r_0^2}, \quad (15)$$

we can write

$$\begin{aligned} \mathbf{I} &= \frac{3}{2} \int d\tau x_E e^{-\alpha r_E^2} W_4(kr_0) z_0^2 r_0^{-5} x_F e^{-\beta r_F^2} \\ &\quad - \frac{1}{2} \int d\tau x_E e^{-\alpha r_E^2} W_4(kr_0) r_0^{-3} x_F e^{-\beta r_F^2} \\ &\equiv \mathbf{I}_1 + \mathbf{I}_2. \end{aligned} \quad (16)$$

In order to obtain the term  $z_B^2 e^{-cr_B^2}$ , we will set up a fake gaussian on center B,  $e^{-cr_B^2}$ , and move the  $W_4(kr_B)/r_B^5$  term to a fake center, D; after evaluating the resulting integral, we will take the limits  $D \rightarrow B$  and  $c \rightarrow 0$ . Using the relation

$$z_B^2 e^{-cr_B^2} = \frac{1}{2^2 c^2} \frac{\partial^2}{\partial B_z^2} e^{-cr_0^2} + \frac{1}{2c} e^{-cr_0^2}, \quad (17)$$

we obtain

$$\mathbf{I}_1 = \lim_{c \rightarrow 0} \lim_{D \rightarrow B} \frac{3}{2} \frac{1}{2^2 \alpha \beta} \frac{\partial^2}{\partial E_x \partial F_x} \left\{ \frac{1}{2^2 c^2} \frac{\partial^2}{\partial B_z^2} \mathbf{I}_3 + \frac{1}{2c} \mathbf{I}_3 \right\} \quad (18)$$

where

$$\mathbf{I}_3 = \int d\tau e^{-\alpha r_E^2} e^{-cr_0^2} r_0^{-5} W_4(kr_0) e^{-\beta r_F^2}. \quad (19)$$

We can also write

$$\mathbf{I}_2 = \frac{-1}{2^3 \alpha \beta} \frac{\partial^2}{\partial E_x \partial F_x} \mathbf{I}_4 \quad (20)$$

where

$$I_4 = \int d\tau e^{-\alpha r_E^2} e^{-\beta r_F^2} r_0^{-3} W_4(kr_0). \quad (21)$$

We can then apply the rule for combining gaussians on two centers,

$$e^{-\alpha r_E^2} e^{-\beta r_F^2} = e^{-\frac{\alpha\beta}{\gamma} R_{EF}^2} e^{-\gamma r_A^2} \quad (22)$$

where  $\gamma = \alpha + \beta,$  (22a)

$R_{EF}$  is the distance between centers E and F, and center A is defined by

$$A_x = (\alpha E_x + \beta F_x) / \gamma. \quad (22b)$$

We then use the Fourier Convolution Theorem to obtain the following expressions

for  $I_3$  and  $I_4$ :

$$I_3 = e^{-\frac{\alpha\beta}{\gamma} R_{EF}^2} e^{-\frac{\gamma c}{\delta} R_{AD}^2} I_5 \quad (23)$$

where

$$I_5 = \int d\tau e^{-\delta r_G^2} r_0^{-5} W_4(kr_0) \quad (24)$$

$$= \frac{\pi}{\delta R_{0G}} \int_0^\infty dr r^{-4} W_4(kr) \left\{ e^{-\delta(r-R_{0G})^2} - e^{-\delta(r+R_{0G})^2} \right\},$$

and

$$I_4 = e^{-\frac{\alpha\beta}{\gamma} R_{EF}^2} I_6 \quad (25)$$

where

$$I_6 = \int d\tau e^{-\gamma r_A^2} r_0^{-3} W_4(kr_0) \quad (26)$$

$$= \frac{\pi}{\delta R_{A0}} \int_0^\infty dr r^{-2} W_4(kr) \left\{ e^{-\gamma(r-R_{A0})^2} - e^{-\gamma(r+R_{A0})^2} \right\}.$$

If these equations  $\delta = \gamma + c$  and  $G$  is the center obtained by combining Gaussians on  $A$  and  $D$ . The derivatives and limits in equation 18 are obtained analytically by REDUCE and the result is that equation 18 is written as a sum of integrals with forms similar to those given by equations 24 and 26. These basic integrals are evaluated numerically and summed to give the result for  $\langle P_x^E | Q_4^B | P_x^F \rangle$ . To obtain expressions for this integral in the case where any of centers  $E, F, B$  coincide, REDUCE is used to obtain the appropriate limit ( $E \rightarrow F$ , for example). The REDUCE commands used to evaluate all  $Q_4$  integrals are given in Appendix B. The output from this REDUCE code is rearranged, using additional REDUCE commands, to produce FORTRAN code which can be inserted directly in the integral evaluation subroutines.

The present versions of the EFFPOT integral routines are restricted to two centers and  $s$  or  $p$  basis functions. Our tests of this program on LiHe are described in the next section.

The integration itself is done by a 32 point Gauß integration with the IBM library program DQG 32. The other FORTRAN-programs of the EFFPOT routine, developed by ourselves, are contained in Appendix C.

#### 4.III Test Calculations of EFFPOT on LiHe

In this section we present the results of the first stage of our tests of the effective potential method. We have chosen LiHe as the test system, and in this stage of the tests we assume that the parameters of our semi-empirical potential are known.

Values of  $\alpha_d$  and  $\alpha_q$  can easily be obtained; however, it should be pointed out that in a semi-empirical potential, each parameter plays a dual role. Besides describing the physical effect to which it most obviously corresponds, each parameter also serves to correct for the deficiencies of the semi-empirical model. Consequently in the best fit for the potential parameters, the values of  $\alpha_d$ ,  $\alpha_q$ , etc., should not be expected to equal the physical quantities. The values for the cut-off functions and for the short-range part of the potential are harder to obtain. Our initial desire was to use the parameters obtained by Peach.<sup>12</sup> She calculated the parameters for a model potential describing one electron outside of He by fitting the parameters to electron-He atom scattering data. Her model also included a pseudopotential to represent the Hartree-Fock potential of He; this fact makes it impossible to separate the pseudopotential from the short-range terms needed for the effective potential (see equation 7). Consequently, for our test calculations, we use Peach's values for  $\alpha_d$ ,  $\alpha_q$ ,  $\beta$  and her cut-off functions. In addition, we have guessed a value for  $a_0$  (equation 7), so that the short-range potential has only one term.

The exact forms of the potentials used in our test calculations are



$$\int dr' \Sigma^A(r; r'; z) = \frac{Z^A z}{r} + z \int dr' \Sigma_{HF}^A(r; r') + z^2 a_0 e^{-\gamma r} - \frac{\alpha_d z^2}{2 r^4} W_2(\beta r) - \frac{\alpha'_d z^2}{2 r^6} W_3(\beta' r) \quad (27)$$

$$\int dr'_1 dr'_2 W^A(r_1, r_2; r'_1, r'_2; z_1, z_2) = \frac{-\alpha_d z_1 z_2}{2 r_1^2 r_2^2} X_2(\beta r_1) X_2(\beta r_2) P_1(\cos \gamma_{12}) - \frac{-\alpha'_d z_1 z_2}{2 r_1^3 r_2^3} X_3(\beta r_1) X_3(\beta r_2) P_2(\cos \gamma_{12}) \quad (28)$$

Where  $W_n$  is defined by

$$W_n(x) = [X_n(x)]^2 \quad (29a)$$

and

$$X_n(x) = 1 - \exp(-x) \sum_{m=0}^n \frac{x^m}{m!} \underset{x \rightarrow 0}{\approx} \frac{x^{n+1}}{(n+1)!} \quad (29b)$$

$$\alpha' = (\alpha'_d - 6\beta_1/M).$$

The values of the parameters used are given in table 1.

In tables 2 and 3 and figures 1 and 2, we compare the effective potential-SCF (EP-SCF) calculations with SCF<sup>13</sup> and restricted CI calculations for the same basis set. The basis set is that of Krauss, Maldonado and Wahl<sup>13</sup>.

The restricted CI calculations presented here have the same asymptotic limit as the EP-CI calculations, but do not fully allow for distortion of He at intermediate distances. In comparing these results, it should be noted that the EP-SCF results have the same  $R \rightarrow \infty$  limit as the SCF calculation, but that at intermediate distances, the EP-SCF results go as  $1/R^6$  while the SCF calculations cannot give this dependence. Also, the full CI calculations, which allow for more He polarization, should give more attractive interaction

Table 1. Parameters for the potential defined by equations 27 to 29, for He<sup>a</sup>

Z <sub>a</sub>	2.
a <sub>0</sub>	.05
γ	1.59
α <sub>d</sub>	1.3834
β	2.09928
α'	-2.1222
β'	0.551429
α' <sub>q</sub>	2.11380

<sup>a</sup>All the parameters except a<sub>0</sub> and γ are taken from Peach.<sup>12</sup>

Table 2. LiHe total energies (in Hartrees)

N(a.u.)	EP-SCF		SCF <sup>a</sup>		CI (restricted)	
	2 $\Sigma$	2 $\Pi$	2 $\Sigma$	2 $\Pi$	2 $\Sigma$	2 $\Pi$
2.	-10.19137	-10.14751	-10.18797	-10.14029	-10.20229	-10.15458
3.	-10.27436	-10.22475	-10.27465	-10.22372	-10.29037	-10.23938
4.	-10.28454	-10.22723	-10.28397	-10.22646	-10.29993	-10.24232
5.	-10.28933	-10.22603	-10.28840	-10.22546	-10.30449	-10.24138
6.	-10.29166	-10.22533	-10.29113	-10.22500	-10.30722	-10.24090
8.	-10.29321	-10.22486	-10.29304	-10.22477	-10.30911	-10.24067
10.	-10.29339	-10.22476	-10.29335	-10.22473	-10.30944	-10.24065

<sup>a</sup>Krauss, Maldonado, and Wahl<sup>13</sup>

Table 3. LiHe interaction energies (in Hartrees)

i(a.u.)	EP-SCF		SCF <sup>a</sup>		CI(restricted)		Full CI
	2 $\Sigma$	2 $\Pi$	2 $\Sigma$	2 $\Pi$	2 $\Sigma$	2 $\Pi$	
2.	.10201	.07735	.10541	.08457	.10723	.09608	
3.	.01902	-.00004	.01873	.00099	.01915	.00128	.02000
4.	.00884	-.00252	.00941	-.00175	.00959	-.00166	
5.	.00405	-.00132	.00498	-.00075	.00503	-.00072	
6.	.00172	-.00062	.00225	-.00029	.00230	-.00024	
8.	.00017	-.00015	.00034	-.00006	.00041	-.00001	
10.	-.00001	-.00005	.00004	-.00002	.00008	.00001	

<sup>a</sup>Krauss, Maldonado, and Wahl<sup>13</sup>

Figure Captions

1. Interaction energy for LiHe  $^2\Sigma$  state.

⊙ connected by solid line; EP-SCF results.

▣ SCF results of Krauss, Maldonado, and Wahl<sup>13</sup>.

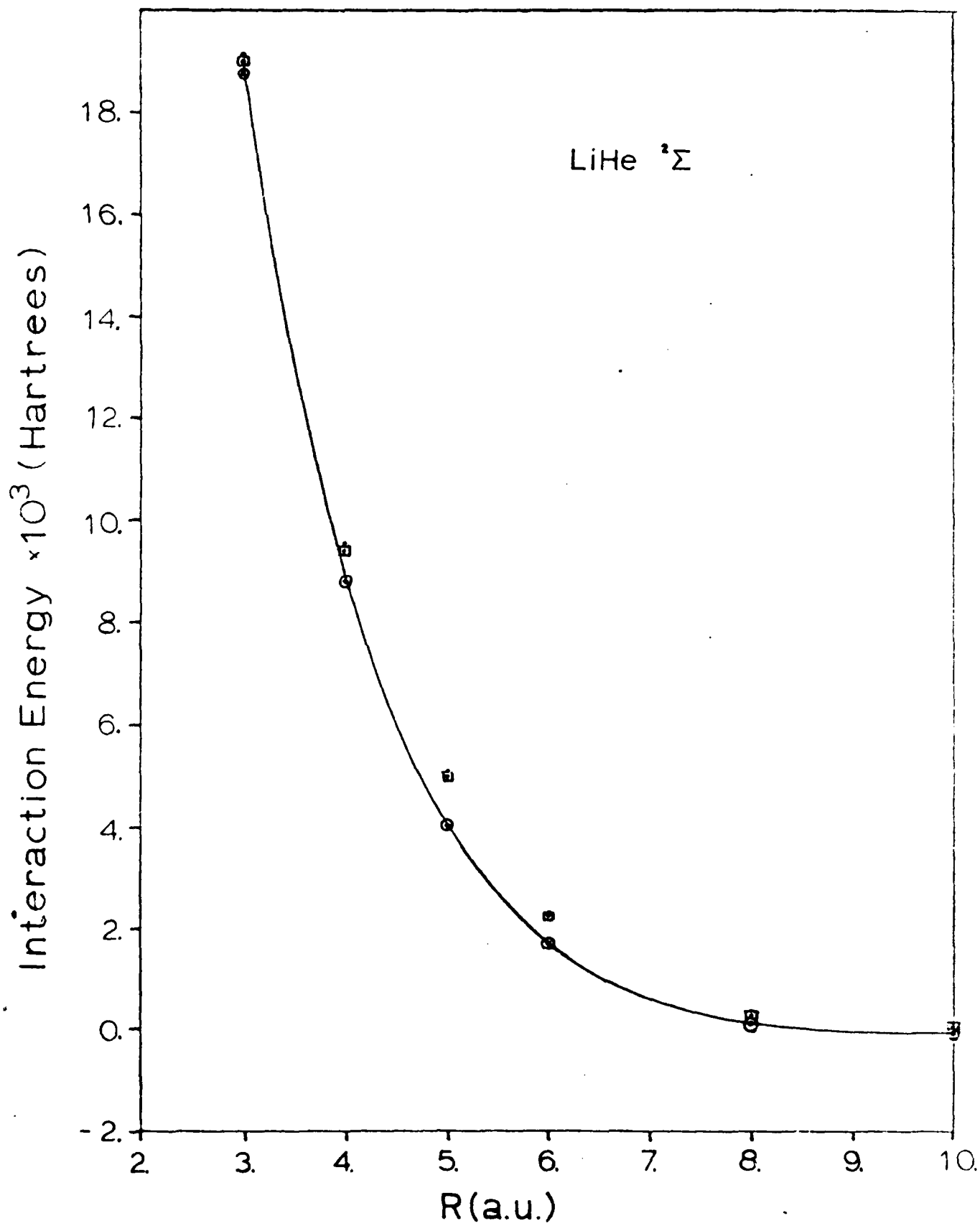
• restricted CI calculation.

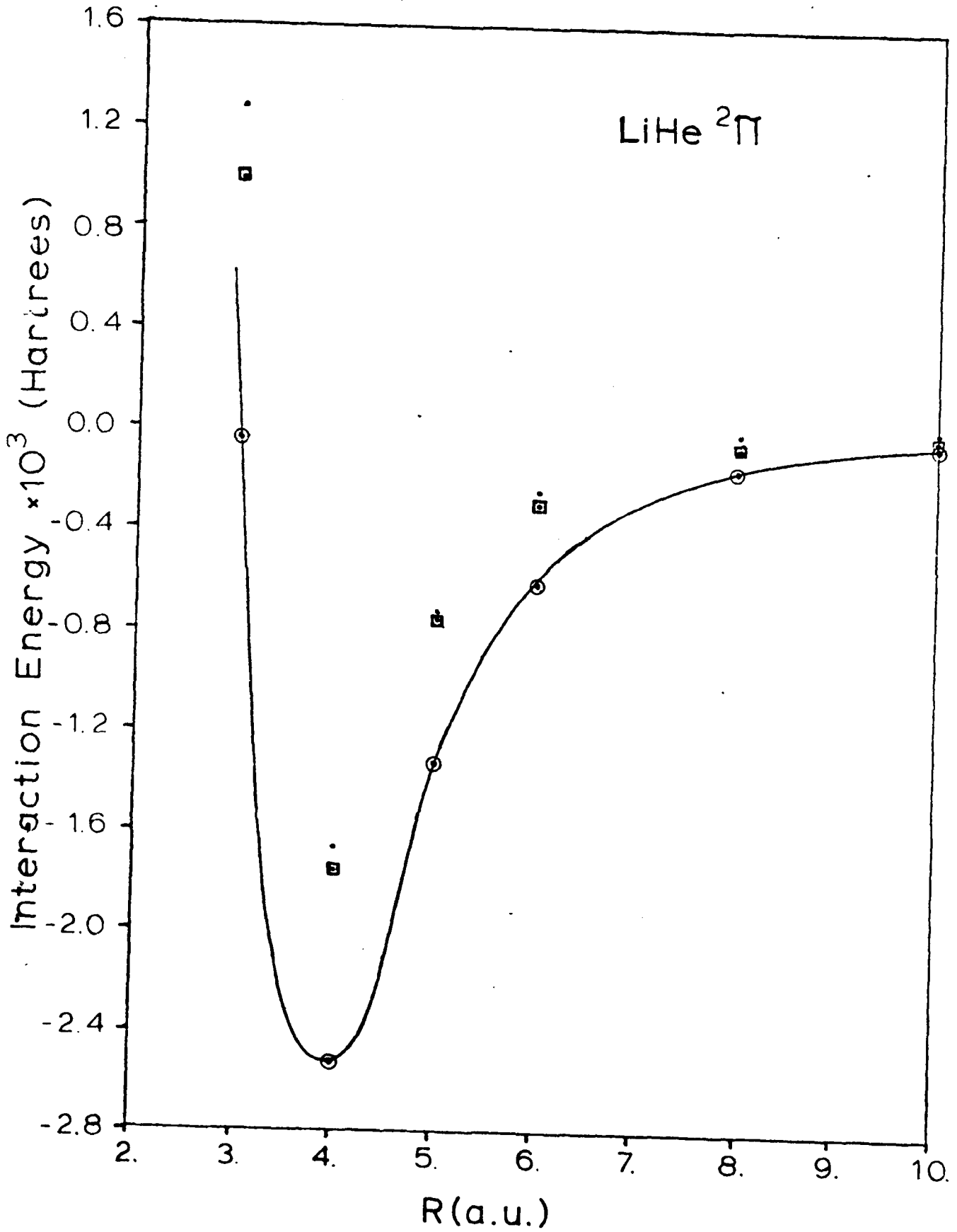
2. Interaction energy for LiHe  $^2\Pi$  state.

⊙ connected by solid line; EP-SCF results.

▣ SCF results of Krauss, Maldonado, and Wahl<sup>13</sup>.

• restricted CI calculation.





#### 4.IVa Test calculations of the fit program

In fig. 2 in the last paragraph it has become obvious that the initial values for the parameters in the effective potential (the ones given in table 1 in section III, let us call this set of parameters  $p_0$  in the following) do not give a sufficiently good agreement between the calculated molecular potential curve and the curve of our CI calculation or the results of Krauss et al. One method to find a better fit would be to repeat the calculations for a large number of parameter values and so to calculate a potential curve for each point on a dense grid in the 10-dimensional parameter space. This would be the safest method to come close to the best possible fit but it would consume an enormous amount of computer time and therefore it would be contrary to our initial goal. A faster alternative is, to apply a fit program which uses as input the results of section III and tries to improve the molecular potential curve by some kind of first order perturbation calculation.

In order to explain what kind of fitting method has been used here let us for this section introduce the following notation.  $p$  is a set of 10 parameters which go into the effective potential,  $W(p,R)$  is the complete effective potential for the set  $p$  of parameters and for the nuclear distance  $R$ ,  $\Psi(p,R)$  is the exact electronic SCF wavefunction for the nuclear distance  $R$  and for the effective potential  $W(p,R)$  calculated according to the method given in section III.  $V(p,R)$  is the molecular potential calculated according to the method given in section III with the effective potential  $W(p,R)$  and at a nuclear distance  $R$ .

The idea of our first order perturbation approach is to calculate first the difference between the effective potentials for two sets



of parameters  $p_0$  and  $p$ , then calculate the expectation value of this difference potential with the exact wavefunction belonging to parameter set  $p$ , and interpret this expectation value as difference in the molecular potential. In formula

$$V(p, R) = V(p_0, R) + \langle \psi(p_0, R) | W(p, R) - W(p_0, R) | \psi(p_0, R) \rangle \quad (30)$$

as justification for the application of a first order perturbation method we have first to show that the results of the exact calculation are highly linear at variation of a parameter in the effective potential. In fig. 3 the electronic energy has been calculated with the method given in section III for various values of the dipole parameter  $\alpha_d$  and always the same values for the other parameters at the same nuclear distance of  $R = 3.5$ . It can be seen that the dependence of the energy on the parameter  $\alpha_d$  is highly linear. Similar results hold for the other parameters. These calculations have also shown that the wavefunction does not change significantly under a change of a parameter. Therefore it seems that a first order perturbation approach to the fitting problem is justified. One of the inputs in any fitting program must be a value to which we want to come close. In the case here, the assumed true molecular potential curve for the He-Li  $2\pi$  state is the one given by Krauss et al. We denote it in the following by  $V_K(R)$ . In addition, it is necessary to define the quantity, a measure of the error, which should be minimized.

We have chosen as measure of the error of the molecular potential curve  $V(p, R)$  the following quantity

$$D(p) = \sum_i [V_K(R_i) - V(p, R_i)]^2 / V_K^2(R_i). \quad (31)$$

The sum  $i$  goes over all those nuclear distances at which we try to improve the function  $V(p,R)$  at the moment.

This fitting for the relative error is a disadvantage in so far, that those nuclear distances  $R_i$  at which  $V_K(R_i)$  is small have a higher weight than those distances at which  $V_K(R_i)$  is big. Therefore the computer tries to fit  $V(p,R_i)$  with the higher priority near zeros of  $V_K(R_i)$ .

The fitting program and all subroutines which belong to it and all those programs which are necessary in addition to the previous programs are shown in Appendix D.

Our experience running this fitting program can be summarized as follows: The fitting program is started with a particular set  $p_i$  of 10 parameters and in its 0th step it calculates the quantity  $V(p_i,R)$  according to (30). For this initial step it takes about 6 minutes times the number of points, on which the curve is fitted, to calculate the integrals. Such a long time is necessary because up to now there are no optimised standard programs of quantum chemistry available for these types of integrals. It takes a long time to transform the expressions of the functions to be integrated into such a form that a library integration program can be applied. (The 32 point Gaussian integration program DQG32 by IBM ultimately has been used. If in a next step one of the parameters  $a_d, a_q, \beta, a_0, a_1, a_2, a_3$  is changed then it is not necessary to evaluate the integrals again because these 7 parameters do not change the shape of  $W(p,R)$ . They go linearly into  $W(p,R)$  and also the corresponding integrals are linear in these parameters. Therefore it takes only a few seconds to calculate a new  $V(p_j,R)$  when  $p_j$  differs from  $p_i$  only in a parameter which goes into  $W(p,R)$  linearly. The situation

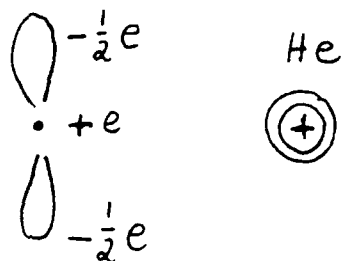
is completely different if one of the cut-off parameters is changed. Then the shape of the function  $W(p,R)$  is different and it is necessary to calculate from the start the corresponding integrals again. This takes at least several minutes time. Hence it is quite time consuming to fit cut-off parameters by this fitting program. Therefore we have done the fit of cut-off parameters partly by hand.

In Fig. 4 the results of the fit can be seen for two sets of parameters which gave the best fits we could obtain for the molecular potential curve of the  $^2\pi$  state of HeLi. For comparison we show in addition the curve calculated by Krauss et al. as solid line. This curve agrees quite well with our CI calculations (see Fig. 2 in section III). The result of the SCF calculations from section III is shown as dotted line also for comparison. This line is the molecular potential curve which belongs to the parameter set  $p_0$  and it is the 0th order result of the fitting procedure in this section. The broken line and the chain line show the 1st order results for two different sets of parameters. It is obvious that the deviation between these first order curves and the Krauss et al. curve is a lot less than the deviation between the 0th order curve and the Krauss et al. curve. The worst error of our 1st order curves is in the region near  $R=5$  to  $R=6$ . In this region it has not been possible to get a curve which is steep enough. All considered 1st order curves with a reasonable over all shape have been too horizontal in this interval. Up to now we did not yet have time to make calculations for molecular potential curves of other states of LiHe than the  $^2\pi$  state. Before we do this, it would be useful to try out a new fitting strategy described in the next section.

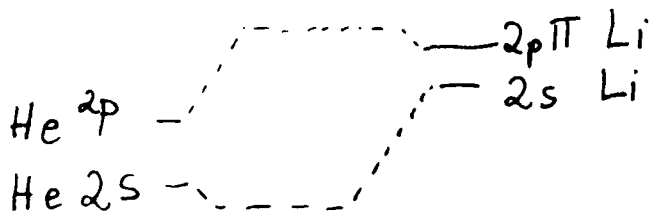
IVb. A strategy to achieve a better fit to the  $\pi$  state of LiHe

As was seen in IVa we did not get an ideal fit in the  $R=5$  region as we did not seem to get the fitted curve to be steep enough. It is to be noted that so far we have fitted to Krauss et al. LiHe,  $\pi$  state. It is also to be noted that we have not exhausted, because of lack of computer time, the fit routine and tried to guess the best parameter regions. In this subsection we suggest a new strategy which we plan to carry out in the fall of 1980 when U.S.C. will replenish our computer budget. The strategy is based on the comparison of the shape of the ground  $\text{LiHe}^+$  potential curve (which goes asymptotically to  $\text{Li}^+ + \text{He}$ ) to that of the  $\text{SCF}\pi\text{LiHe}$  curve (which dissociates properly) as given in the figures in Krauss et al. In this we see the striking fact that the two curves are parallel in the  $R=5$  to 6 region and almost parallel at short range; the LiHe has a slightly smaller  $R_e$ . This suggests the much of the curve in  $\pi$  LiHe is like the  $X^1\Sigma\text{LiHe}^+$  and this is clearly charge-induced dipole at large distance ( $R > 4.5$ ) as it goes at  $R^{-4}$  and  $\text{Li}^+ - \text{Helium}$  repulsion at short distance. Now the former effect is in our model due to the  $\alpha/r^4$  term and the latter in the static and monopole term. (in which  $e^{-ar}$  (a chosen so that the term effects the very short range part of the curve only)) is always automatically fit with a negative coefficient). This suggests that as a first run at fitting the  $\pi$ , that we work with the ionic state (a simpler problem) and set our quadrupole term to zero and perhaps again start with the physical value of the polarizability for Helium. This simpler system should be able to be fit. The ionic system then determines the  $\alpha$ , its short range cut-off parameters and will give a first guess of the monopole term.

Now we will return to the  $\pi$  Li-He fit, and retain the  $\text{LiHe}^+$  parameters as a start. We will then work at large R,  $R > 7$  only, fit the quadrupole term and its cut-off parameters. This is suggested again by the  $2\pi$  state to  $X^1\Sigma$  ionic state comparison figure in Krauss where we see that at large R the LiHe system deviates from the ionic system and is less attractive, i.e. the effect of a  $R^6$  comes in. This effect can only be found in the  $\pi$  state as at large R, the Li P state can be reviewed roughly as



i.e. Helium sees a  $\{\bar{\pi}\}$  charge distribution and the L  $\pi$  orbit feels the Helium quadrupole moment. The next step will be to now fit again at small R, the monopole term, starting with our ionic result. The small shift must be due to a chemical effect which can be described as:



We should be able to account for this with our monopole parameter.

Hopefully this new strategy will yield a better fit with little computing. The effective potential will then be used to construct the  $X^2\Sigma$  state.

Failure in fitting by the procedure of this subsection or in the construction of the  $\Sigma$  state will forebode badly for the ultimate success of this theory.

Figure Captions

Figure 3:

Plot of the electronic energy for the He-Li  $2\pi$  state calculated according to the method given in section III for various values of the parameter  $\alpha_d$  and otherwise always the parameters given in table 1 in section III. The nuclear distance is always  $R=3.5$ .

Figure 4:

Plot of potential curves for the He-Li  $2\pi$  state calculated with various parameters for the effective potential and the curve given by Krauss et al. for comparison.

Solid line: result of Krauss et al.

Dotted line: SCF calculation from section III with parameter set  $p_0$

Broken line: calculation with the method given in section IV and

parameter values  $\alpha_d = 0.8$   
 $\alpha_q = 1.65$   
 $\beta = 1.9$   
 $c_1 = 4$   
 $c_2 = 1.3$   
 $c_3 = 0.6$   
 $a_0 = -0.8$   
 $a_1 = 0$   
 $a_2 = 0$   
 $a_3 = 0$

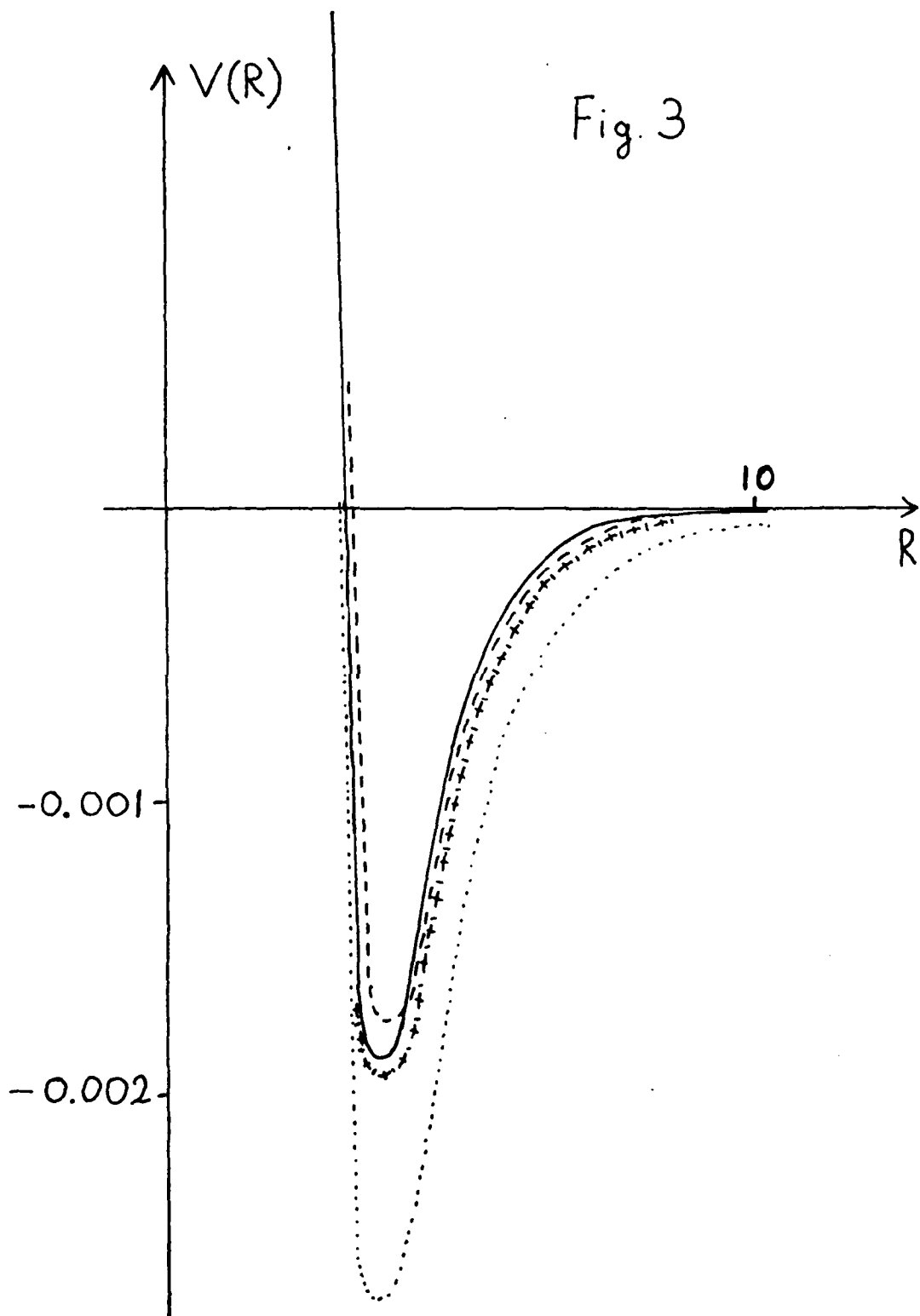
Chain line: calculation with the method given in section IV

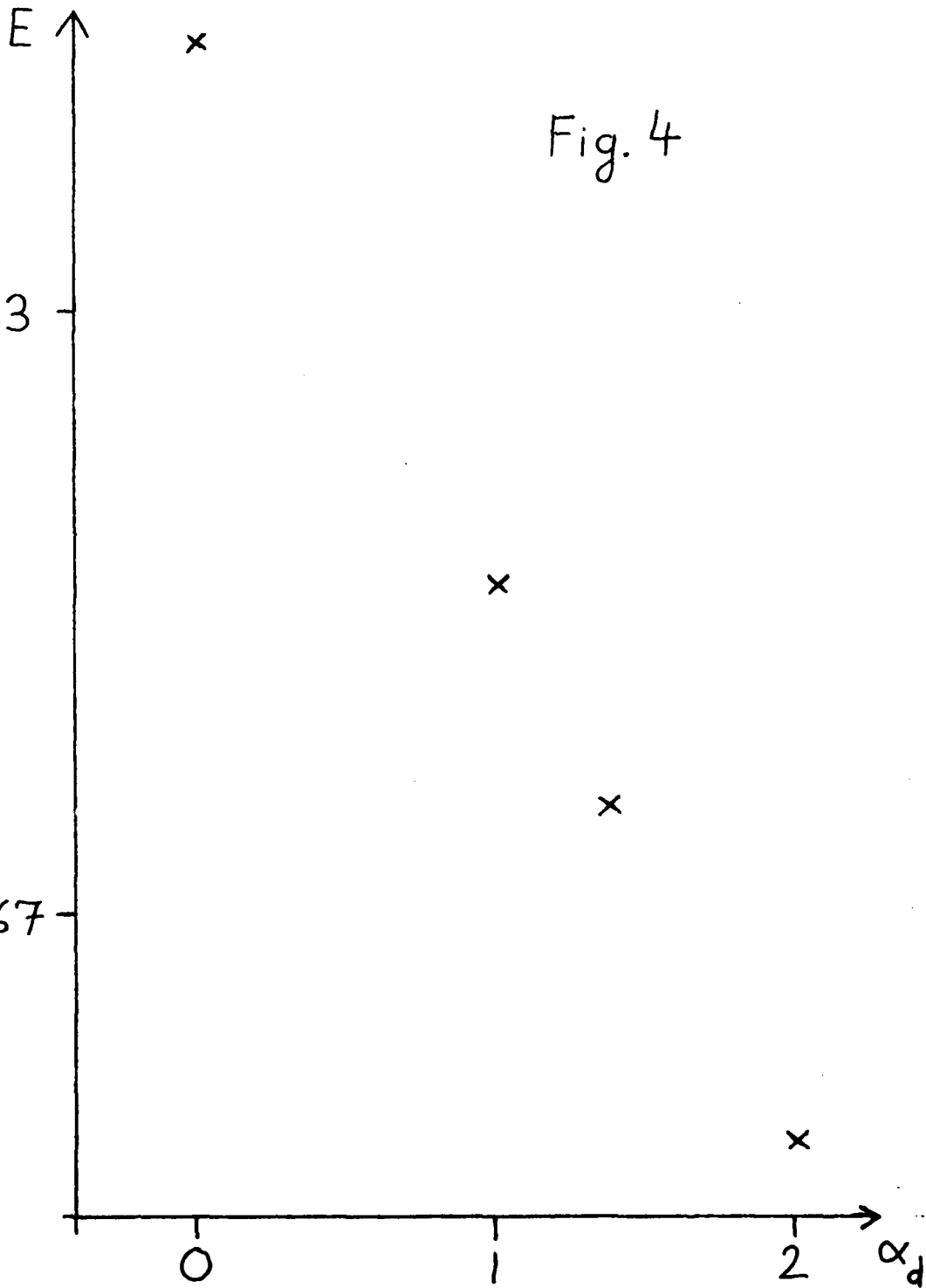
and parameter values

$a_d$	=	0.9
$\alpha_q$	=	1.75
$a_o$	=	-0.46
$a_1$	=	0
$\beta$	=	1.56
$C_1$	=	4
$a_2$	=	0
$C_2$	=	1.3
$C_3$	=	0.6
$a_3$	=	0



Fig. 3





References to §4

1. H.S. Taylor, M. Valley, C. Watts, and F. Bobrowicz, "Excimer potential curves," Annual Report No. 1, ARPA contract no. N00014-77-C-0102, Feb. 1, 1978.
2. T.H. Dunning, Jr., M. Valley and H.S. Taylor, J.Chem Phys. 69, 2672 (1978).
3. A.C. Hearn, REDUCE 2 Users's Manual, Second Edition, 1974.
4. B. Schneider, H.S. Taylor and R. Yaris, Phys. Rev. A1, 855 (1970), G. Csanak and H.S. Taylor, Phys. Rev. A6, 1843 (1972).
5. B.S. Yarlagadda, G. Csanak, H.S. Taylor, B. Schneider and R. Yaris, Phys. Rev. A7, 146 (1973); L.D. Thomas, G. Csanak, H.S. Taylor and B.S. Yarlagadda, J. Phys. B7, 1719 (1974).
6. B. Schneider, H.S. Taylor, R. Yaris, and B.S. Yarlagadda, Chem. Phys. Letters 22, 381 (1973).
7. G. Csanak and H.S. Taylor, Phys. Rev. A6, 1843 (1972); G. Csanak and H.S. Taylor, J. Phys. B6, 2055 (1973).
8. S.W. Wang, H.S. Taylor and R. Yaris, Chem. Phys. 14, 53 (1976).
9. A. Dalgarno, C. Bottcher and G.A. Victor, Chem. Phys. Lett. 7, 265 (1970), C. Bottcher and A. Dalgarno, Proc. R. Soc. Lond. A 340 187 (1974); D.K. Watson, C.J. Cerjan, S. Guberman and A. Dalgarno, submitted to Chem. Phys. Lett. 1977.  
C. Laughlin and G.A. Victor, Atomic Physics 3, 247 (1973).
10. N.W. Winter, F.W. Bobrowicz and W.A. Goddard III, J. Chem. Phys. 62 4325 (1975).
11. Y.S. Lee, W.C. Ermler and K.S. Pitzer, J. Chem. Phys. 67, 5861 (1977) W.R. Wadt, P.J. Hay and L.R. Kahn, J. Chem. Phys. 68 1752 (1978).
12. G. Peach, J. Phys. B 11, 2107 (1978).
13. M. Krauss, P. Maldonado and A.C. Wahl, J. Chem. Phys. 54, 4944 (1971).

16. B. Schneider, H. S. Taylor and R. Yaris, Phys. Rev. A1, 855 (1970), G. Csanak and H. S. Taylor, Phys. Rev. A6, 1843 (1972).
17. P. J. Hay, T. H. Dunning, Jr. and R. C. Raffanetti, J. Chem. Phys. 65, 2679 (1976); W. J. Stevens and M. Krauss, J. Chem. Phys. 67, 1977 (1977).
18. B. S. Yarlagadda, G. Csanak, H. S. Taylor, B. Schneider and R. Yaris, Phys. Rev. A7, 146 (1973); L. D. Thomas, G. Csanak, H. S. Taylor and B. S. Yarlagadda, J. Phys. B7, 1719 (1974).
19. B. Schneider, H. S. Taylor, R. Yaris and B. S. Yarlagadda, Chem. Phys. Lett. 22, 381 (1973).
20. G. Csanak and H. S. Taylor, Phys. Rev. A6, 1843 (1972); G. Csanak and H. S. Taylor, J. Phys. B6, 2055 (1973).
21. S. W. Wang, H. S. Taylor and R. Yaris, Chem. Phys. 14, 53 (1976).
22. A. Dalgarno, C. Bottcher and G. A. Victor, Chem. Phys. Lett. 7, 265 (1970), C. Bottcher and A. Dalgarno, Proc. R. Soc. Lond. A 340 187 (1974); D. K. Watson, C. J. Cerjan, S. Guberman and A. Dalgarno, submitted to Chem. Phys. Lett. 1977; C. Laughlin and G. A. Victor, Atomic Physics 3, 247 (1973).

**Appendix A**

# Theoretical studies of the low-lying electronic states of GaKr, including extrapolation to InKr and TlKr<sup>a)</sup>

Thom. H. Dunning, Jr.<sup>b)</sup>

Chemistry-Nuclear Chemistry Division, Los Alamos Scientific Laboratory, Los Alamos, New Mexico 87545

Marcy Valley and Howard S. Taylor

Department of Chemistry, University of Southern California, Los Angeles, California 90007  
(Received 25 April 1978)

We report *ab initio* configuration interaction calculations on the states of the gallium krypton (GaKr) molecule arising from the  $\text{Ga}(^2P_{1/2,3/2}, ^2S_{1/2}) + \text{Kr}(^1S_0)$  and  $\text{Ga}^+(^1S_0) + \text{Kr}(^1S_0)$  separated atom limits. The potential energy curves for the states arising from the  $\text{Ga}(^2P_{1/2,3/2})$  limits, the  $1\ 1/2$ ,  $1\ 1/2$ , and  $1\ 3/2$  states, are found to be repulsive. The potential energy curves for the states arising from the  $\text{Ga}(^2S_{1/2})$  and  $\text{Ga}^+(^1S_0)$  limits, the  $1\ 1/2$  and  $1\ 0$  states, are both found to be weakly bound;  $D_e(1\ 1/2) = 0.047$  eV and  $D(1\ 0) = 0.24$  eV. The potential energy curves and transition moments obtained in the GaKr calculations have been used to simulate the curves and moments for InKr and TlKr. Using this data the absorption and emission coefficients of all three molecules have been calculated.

## I. INTRODUCTION

The Group IIIA-rare gas excimer molecules are considered to be attractive candidates for developing an efficient, high power, tunable laser in the visible region of the spectrum.<sup>1</sup> The transition under consideration is a perturbed  $(n+1)^2S_{1/2} - n^2P_{1/2,3/2}$  transition of the Group IIIA atom. While current experimental studies have concentrated on the thallium-rare gas systems, especially TlXe, as the most promising candidates, Gallagher<sup>2</sup> has recently raised the possibility of using the gallium-rare gas systems by obtaining gallium atoms from the dissociation of Ga<sub>2</sub>.

To provide further information on the nature of the excimer states involved in these studies, we report here *ab initio* configuration interaction calculations on a prototype Group IIIA-rare gas diatomic molecule, GaKr. We present the potential energy curves for all of the states arising from the neutral  $\text{Ga}(^2P_{1/2,3/2}, ^2S_{1/2}) + \text{Kr}(^1S_0)$  and ionic  $\text{Ga}^+(^1S_0) + \text{Kr}(^1S_0)$  separated atom limits and the dipole transition moments radiatively coupling the states. We then use the computed potential curves and transition moments for GaKr, along with the experimental atomic spin-orbit coupling constants, to model the curves and moments for InKr and TlKr. With this data we calculate the emission and absorption coefficients for all three systems using the classical technique developed by Gallagher and co-workers.<sup>1b</sup>

## II. ELEMENTARY THEORETICAL CONSIDERATIONS

Let us first consider the description of the states of the Group IIIA-rare gas molecules without spin-orbit corrections. The valence  $\text{Ga}(^2P) + \text{Kr}(^1S)$  separated atom limit gives rise to a  $^2\Pi$  state and a  $^2\Sigma^+$  state, the Rydberg  $\text{Ga}(^2S) + \text{Kr}(^1S)$  limit gives rise to another  $^2\Sigma^+$  state

<sup>a)</sup>Research supported in part by the U. S. Department of Energy and by the Advanced Research Projects Agency under contract N00014-77-C-0102.

<sup>b)</sup>Present address: Theoretical Chemistry Group, Chemistry Division, Argonne National Laboratory, Argonne, Illinois 60439.

and the ionic  $\text{Ga}^+(^1S) + \text{Kr}(^1S)$  limit gives rise to a  $^1\Sigma^+$  state. We will label the states which arise from the valence limit the  $1^2\Pi$  and  $1^2\Sigma^+$  states, that from the Rydberg limit the  $2^2\Sigma^+$  state and that from the ionic limit the  $1^1\Sigma^+$  state.

The orbital diagrams for the  $1^2\Pi$ ,  $1^2\Sigma^+$ , and  $1^1\Sigma^+$  states of a Group IIIA-rare gas molecule are given in Fig. 1. From these diagrams it is evident that none of the resulting potential energy curves are expected to be chemically bound. In the ionic state, however, weak binding can result from the charge-induced dipole interaction of the Group IIIA ions and the rare gas atoms. In fact, this interaction might also be expected to give rise to a weak binding in the  $2^2\Sigma^+$  state. Since the Rydberg orbital of the Group IIIA atom is diffuse, the approaching rare gas atom can easily polarize the Rydberg orbital out of the

THE LOW-LYING ELECTRONIC STATES OF GaKr AND GaKr<sup>+</sup>

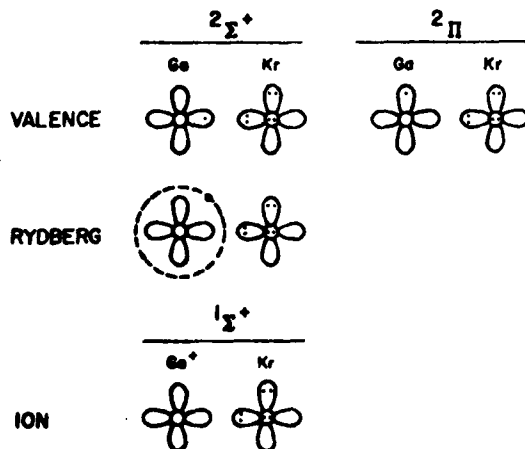


FIG. 1. Orbital diagrams for the low-lying electronic states of GaKr and GaKr<sup>+</sup>. The two lobed figures represent 4p orbitals in the plane of the paper; the circle represents a 4p orbital perpendicular to the plane of the paper; the 5s Rydberg orbital is represented by a large dashed circle.

interatomic region, thus partially unshielding the Group IIIA ionic core. The binding in the  $2^3\Sigma^*$  state should, of course, be substantially less than that in the  $1^1\Sigma^*$  state.

For the valence states the repulsiveness of the curves should be roughly proportional to the number of  $p\sigma$  electrons since the overlap of the two atomic charge distributions is dominated by the overlap of the  $p\sigma$  orbitals. Thus, the potential curve for the  $1^3\Pi$  state with two  $p\sigma$  electrons should be less repulsive than that for the  $1^2\Sigma^*$  state with three  $p\sigma$  electrons.

As we shall later see, at short internuclear separations the energies of the  $1^2\Sigma^*$  and  $2^2\Sigma^*$  states are nearly equal and there is a strong interaction between the two states. This mixing is strong in spite of the fact that one state is a valence state and the other a Rydberg state because the two zero-order configurations (see the next section) differ by only a single excitation.

A complete treatment of the electronic states of the Group IIIA-rare gas molecules must include the effects of spin-orbit coupling. Using the simple model developed in earlier papers for including the effects of spin-orbit coupling in diatomic molecules,<sup>3</sup> only the  $1^3\Pi$  and  $1^2\Sigma^*$  states are affected by the spin-orbit interaction, and the coupling arises solely from the spin-orbit interaction in the Group IIIA atom. For gallium the  $^2P_{1/2}$ - $^2P_{3/2}$  splitting is only 0.10 eV<sup>4</sup>; however, by thallium this splitting has increased to 0.97 eV.<sup>4</sup>

In a molecule only the  $z$  component of the total angular momentum,

$$\Omega = \Lambda + S_z,$$

is a good quantum number. Thus, from the  $\text{Ga}(^2P_{1/2,3/2}) + \text{Kr}(^1S_0)$  separated atom limits we obtain two  $\Omega = 1/2$  states and one  $\Omega = 3/2$  state (the  $I\ 1/2$ ,  $II\ 1/2$ , and  $I\ 3/2$  states), from the  $\text{Ga}(^2S_{1/2}) + \text{Kr}(^1S_0)$  limit another  $\Omega = 1/2$  state (the  $III\ 1/2$  state), and from the  $\text{Ga}(^1S_0) + \text{Kr}(^1S_0)$  limit an  $\Omega = 0$  state (the  $I\ 0$  state). At large internuclear distances the  $I\ 3/2$  and  $II\ 1/2$  potential curves are degenerate and are separated from the  $I\ 1/2$  (ground state) curves by the group IIIA  $^3P_{3/2}$ - $^3P_{1/2}$  splitting. As the distance decreases the  $1^3\Pi$  and  $1^2\Sigma^*$  curves rapidly separate, the separation increasing approximately exponentially. As a result at short distance the atomic spin-orbit coupling is nearly quenched and the  $I\ 1/2$  and  $II\ 3/2$  curves approximate the  $1^3\Pi$  curve and the  $II\ 1/2$  curve approximates the  $1^2\Sigma^*$  curve. The potential curves of the  $2^3\Sigma^*$  ( $III\ 1/2$ ) and  $1^1\Sigma^*$  ( $I\ 0$ ) states are unaffected by the inclusion of spin-orbit coupling.

### III. DETAILS OF THE CALCULATIONS

#### A. Basis sets

The calculations employed an atomic (14s11p5d) primitive Gaussian basis set for both the gallium and krypton atoms.<sup>5</sup> The core orbitals (1s, 2s, 3s, 2p, 3p, and 3d) were contracted to a single function while the valence orbitals (4s and 4p) were contracted to two functions using the general contraction method of Raffanetti<sup>6</sup> (see also Ref. 7). These atomic basis sets were augmented

with a single set of 3d functions,  $\zeta_{0d} = 0.16$  and  $\zeta_{4d} = 0.35$ , to describe molecular polarization effects. The values of these exponents were based on calculations on other excimer laser systems.<sup>3,8</sup>

Since the transition of interest involves the first Rydberg state of the gallium atom, the gallium basis set was augmented with two diffuse s functions,  $\zeta_s = 0.026$  and 0.011, and a diffuse p function,  $\zeta_p = 0.010$ , to describe this state. The exponents of these functions were obtained from Hartree-Fock (HF) calculations on the  $^2S$  and  $^2P$  Rydberg states of the gallium atom.

The final basis sets thus consisted of a (16s12p6d) primitive set contracted to [7s5p2d] for gallium and a (14s11p6d) primitive set contracted to [5s4p2d] for krypton.

#### B. Calculations on the gallium atom

The reference orbitals for the configuration interaction (CI) calculations on the gallium atom were obtained from a Hartree-Fock (HF) calculation of the  $^2P$  state of the atom with the configuration

$$^2P: \dots 4s^2 4p \quad (1)$$

(The 4p set includes all three cartesian components and all are equivalent.) The Rydberg 5s orbital was obtained from an IVO calculation<sup>9</sup> using the  $4s^2$  core. In terms of these orbitals the reference configurations for the other states of interest are

$$^2S: \dots 4s^2 5s \quad (2)$$

$$^1S: \dots 4s^2 \quad (3)$$

Both polarization CI (POL-CI)<sup>10</sup> and full CI calculations have been carried out on the above states of the gallium atom. The POL-CI calculations include all single and double excitations relative to configurations (1)-(3) with the restrictions that

(1) all core orbitals (1s-3s, 2p-3p, and 3d) remain doubly occupied and

(2a) no more than one electron occupy the Rydberg 5s and virtual orbitals ( $^2P$  and  $^1S$  states) or

(2b) no more than one electron occupy the Rydberg 5s orbital and no more than one electron occupy the virtual orbitals ( $^2S$  state).

The POL-CI calculations involve 22 space and 33 space/spin configurations for the  $^2P$  state, 27 space and 43 space/spin configurations for the  $^2S$  state, and 15 space and 15 space/spin configurations for the  $^1S$  state.<sup>11</sup> Note that the POL-CI wavefunction accounts for the  $4s^2 - 4p^2$  near-degeneracy effect.

The less restrictive condition, (2b), for the  $^2S$  state is necessary to obtain a comparable description of this state. Only by relaxing condition (2a) can configurations such as

$$\dots [4p\pi]5s$$

be included in the POL-CI wavefunction of the  $^2S$  state. These configurations account for the first-order difference between the 4p orbital obtained from the calcula-

tions on the  $^2P$  state and the  $p$  orbital needed to describe the angular correlation of the  $4s^2$  pair ( $4s-4p$  near degeneracy) and are quite important. Comparable configurations are automatically included in the POL-CI wavefunctions of the  $^2P$  and  $^1S$  states.

The full CI calculations include all excitations (single-triple) relative to the configurations (1)-(3) with only restriction (1) above. The full CI calculations include 157 space and 263 space/spin configurations for the  $^2P$  state, 204 space and 306 space/spin configurations for the  $^2S$  state, and 42 space and 42 space/spin configurations for the  $^1S$  state.<sup>11</sup> Within the frozen core approximation the accuracy of the results obtained from the full CI calculations is only limited by the completeness of the basis set.

### C. Hartree-Fock calculations on GaKr

The *reference orbitals* for the POL-CI calculations<sup>10</sup> on the GaKr molecule were obtained from an HF calculation on the  $1^2\Sigma^+$  state with configuration<sup>12</sup>

$$\dots 13\sigma^2 14\sigma^2 15\sigma^2 16\sigma^2 7\pi^4 \quad (1a)$$

In the POL-CI calculations the core orbitals (12  $\sigma$  orbitals, 12  $\pi$  orbitals, and 4  $\delta$  orbitals) are always required to be doubly occupied and so it is convenient to renumber the *valence orbitals* so that (1a) becomes

$$1^2\Sigma^+: 1\sigma^2 2\sigma^2 3\sigma^2 4\sigma 1\pi^4 \quad (1b)$$

As  $R \rightarrow \infty$  the above orbitals become

$$1\sigma - 4s_{Kr} \quad 1\pi - 4p_{Kr}$$

$$2\sigma - 4p\sigma_{Kr}$$

$$3\sigma - 4s_{Ga}$$

$$4\sigma - 4p\sigma_{Ga}$$

The IVO method,<sup>9</sup> with a  $1\sigma^2 2\sigma^2 3\sigma^2 1\pi^4$  core, was used to generate the *valence*  $2\pi$  and *Rydberg*  $5\sigma$  orbitals. As  $R \rightarrow \infty$  these orbitals become the  $4p\pi$  and  $5s$  orbitals of the gallium atom. The virtual orbitals were also obtained from the IVO calculations.

In terms of the orbitals defined in this way the *reference configurations* for the other states of interest are<sup>12</sup>

$$1^2\Pi: 1\sigma^2 2\sigma^2 3\sigma^2 1\pi^4 2\pi \quad (2)$$

$$2^2\Sigma^+: 1\sigma^2 2\sigma^2 3\sigma^2 5\sigma 1\pi^4 \quad (3)$$

$$1^1\Sigma^+: 1\sigma^2 2\sigma^2 3\sigma^2 1\pi^4 \quad (4)$$

### D. Polarization configuration interaction calculations on GaKr

The POL-CI calculations<sup>10</sup> on GaKr included all single and double excitations relative to the reference configurations given above with the restrictions that

(1) all core orbitals remain doubly occupied and

(2a) no more than one electron occupy the Rydberg  $5\sigma$  and virtual orbitals ( $^2\Pi$  and  $^1\Sigma^+$  states) or

(2b) no more than one electron occupy the Rydberg  $5\sigma$  orbital and no more than one electron occupy the virtual orbitals ( $^2\Sigma^+$  states).

For the  $^2\Sigma^+$  states the calculations considered both states simultaneously. This procedure results in 556 space and 1565 space/spin configurations for the  $^2\Pi$  states, 764 space and 2314 space/spin configurations for the  $^2\Sigma^+$  states, and 368 space and 558 space/spin configurations for the  $^1\Sigma^+$  state.

The less restrictive condition, (2b), is necessary for the  $^2\Sigma^+$  states to allow for configurations such as

$$1\sigma^2 2\sigma^2 \{2\pi\pi\} 5\sigma 1\pi^4,$$

which are important in the description of the Rydberg  $^2\Sigma^+$  state. As was the analogous case in the gallium atom, these configurations are necessary to allow for the inclusion of the  $4s^2-4p^2$  near-degeneracy effect in the molecular wavefunction.

### E. Inclusion of spin-orbit coupling in GaKr

As in our earlier calculations on excimer systems,<sup>3,13</sup> we have adopted a simple model<sup>3</sup> for including the effects of spin-orbit coupling on the calculated potential energy curves and wavefunctions. The experimental spin-orbit parameters for the open-shell atom, gallium in the present case, are used to determine the matrix elements of the spin-orbit Hamiltonian,  $H_{so}$ , coupling the molecular states at  $R = \infty$ . These matrix elements are then assumed to be independent of  $R$  and are added to the diagonal matrix of the electronic energies

$$H^0(R) = \delta_{ij} E_i(R) + H_{so} \quad (5)$$

The energies and wavefunctions with spin-orbit corrections are obtained by diagonalizing  $H^0(R)$ . This procedure is reasonable only so long as (1) the molecular states retain the identity of the atomic states from which they arise and (2) the atomic contributions to the molecular spin-orbit interactions are dominant.

For GaKr the spin-orbit interaction affects only those states which arise from the  $Ga(^2P) + Kr(^1S)$  limit. The Hamiltonian matrix for the  $\Omega = 1/2$  states arising from this limit is

$$H^{\Omega=1/2} = \begin{bmatrix} E(1^2\Sigma^+) & \sqrt{2}\lambda_{\sigma_a} \\ \sqrt{2}\lambda_{\sigma_a} & E(1^2\Pi) - \lambda_{\sigma_a} \end{bmatrix} \quad (6a)$$

and for the  $\Omega = 3/2$  state is

$$H^{\Omega=3/2} = E(1^2\Pi) + \lambda_{\sigma_a} \quad (6b)$$

In (6)  $\lambda_{\sigma_a}$  is one third of the  $^2P_{3/2} - ^2P_{1/2}$  splitting in the gallium atom. The energies of the  $2^2\Sigma^+$  and  $1^1\Sigma^+$  states of GaKr are unaffected by the inclusion of spin-orbit coupling. The wavefunctions for the states obtained by diagonalizing (6) may be written in the form

$$|I1/2\rangle = \cos\theta |1^2\Pi, \beta\rangle + \sin\theta |1^2\Sigma^+, \alpha\rangle \quad (7a)$$

$$|II1/2\rangle = -\sin\theta |1^2\Pi, \beta\rangle + \cos\theta |1^2\Sigma^+, \alpha\rangle \quad (7b)$$

$$|I3/2\rangle = |1^2\Pi, \alpha\rangle, \quad (7c)$$

where  $\theta$  is the spin rotation angle. The wavefunctions for the  $|III1/2\rangle$  and  $|I0\rangle$  states are

$$|III1/2\rangle = |2^2\Sigma^+, \alpha\rangle \quad (7d)$$

$$|I0\rangle = |1^1\Sigma^+\rangle, \quad (7e)$$



TABLE I. Calculations on the  $^2P$ ,  $^2S$ , and  $^1S$  (ion) states of Ga and the  $^1S$  state of krypton. For Ga the experimental results have been corrected for spin-orbit effects (see the text). Units are as indicated.

Atom state	$^2P$	Ga(Ga $^+$ ) $^2S$	$^1S$	Kr $^1S$
Total energies (hartree) <sup>a</sup>				
POL-CI	0.22523	0.12130	0.01912	0.97377 <sup>b</sup>
Full CI	0.23484	0.12750	0.02305	...
Excitation energies (eV)				
POL-CI	0.00	2.83	5.61	...
Full CI	0.00	2.92	5.76	...
Expt'l <sup>c</sup>	0.000	3.005	5.930	...
Transition moment ( $e a_0$ )				
POL-CI	...	-1.298 <sup>d</sup>	...	...
Lifetimes (nsec)				
POL-CI	...	8.2 <sup>e</sup>	...	...
Expt'l	...	6.8 <sup>f</sup>	...	...

<sup>a</sup>For Ga the energies are relative to -1923 hartree; for Kr the energies are relative to -2751 hartree.

<sup>b</sup>For Kr the POL-CI wavefunction is equivalent to the HF wavefunction.

<sup>c</sup>Reference 4.

<sup>d</sup>This is the matrix element  $1/3[\langle ^2S | x | ^2P_x \rangle + \langle ^2S | y | ^2P_y \rangle + \langle ^2S | z | ^2P_z \rangle]$ .

<sup>e</sup>Using the experimental excitation energy we obtain 6.9 nsec.

<sup>f</sup>Reference 14.

With the definitions (7) the dipole transition moments coupling the  $III\ 1/2$  state with all of the lower states are

$$\mu_z(III\ 1/2 - I\ 1/2) = \sin\theta \langle 2^2\Sigma^+ | z | 1^2\Sigma^+ \rangle \quad (8a)$$

$$\mu_x(III\ 1/2 - I\ 1/2) = \cos\theta \langle 2^2\Sigma^+ | x | 1^2\Pi_x \rangle / \sqrt{2} \quad (8b)$$

$$\mu_z(III\ 1/2 - II\ 1/2) = -\cos\theta \langle 2^2\Sigma^+ | z | 1^2\Sigma^+ \rangle \quad (9a)$$

$$\mu_x(III\ 1/2 - II\ 1/2) = \sin\theta \langle 2^2\Sigma^+ | x | 1^2\Pi_x \rangle / \sqrt{2} \quad (9b)$$

$$\mu_z(III\ 1/2 - I\ 3/2) = -\langle 2^2\Sigma^+ | z | 1^2\Pi_z \rangle / \sqrt{2} \quad (10)$$

Since the  $\langle 2^2\Sigma^+ | x | 1^2\Pi_x \rangle$  transition moment is expected to be comparable in magnitude to the  $\langle 2^2\Sigma^+ | z | 1^2\Sigma^+ \rangle$  moment (at  $R = \infty$  they are identical), it is clear from (8) and (9) that the transitions from the  $III\ 1/2$  state of the  $I\ 1/2$  and  $II\ 1/2$  states can have both large parallel and perpendicular components.

#### IV. RESULTS FOR Ga, GaKr, AND GaKr $^+$

##### A. Electronic states of Ga, without spin-orbit corrections

The results of the calculations on the Ga atom are summarized in Table I. The computed  $^2S$ - $^2P$  excitation energy is 2.83 eV (POL-CI) and 2.92 eV (full CI). Averaging the multiplet energies for the  $^2P_{1/2}$  and  $^2P_{3/2}$  states of gallium from Moore,<sup>6</sup> the experimental  $^2S$ - $^2P$  splitting is calculated to be 3.005 eV, just 0.08-0.17 eV larger than the computed spacing. The errors in the calculated ionization potentials, 5.61 eV (POL-CI) and 5.76 eV (full CI), are somewhat larger, being 0.32 and 0.17 eV, respectively.

The lifetime of the  $^2S$  state of gallium has been determined by Norton and Gallagher<sup>14</sup> to be  $6.8 \pm 0.3$  nsec. For the model used here the lifetime of the  $^2S$  state is independent of the spin-orbit corrections. From the POL-CI wavefunctions we calculate a lifetime of 8.2 nsec for the  $^2S$  state (6.9 nsec, if the experimental excitation energy is used instead of the calculated excitation energy).

##### B. Electronic states of GaKr and GaKr $^+$ , without spin-orbit corrections

The energies of the  $1^2\Pi$ ,  $1,2^2\Sigma^+$ , and  $1^1\Sigma^+$  states of GaKr and GaKr $^+$  obtained from the POL-CI calculations are listed in Table II and the resulting potential energy curves are plotted in Fig. 2. As is usual in such calculations,<sup>3,6,13</sup> the energies of the  $1^2\Pi$  and  $1^2\Sigma^+$  states, both of which arise from the  $^2P$  limit, are not exactly equal at  $R = 15.0 a_0$  (the largest value of  $R$  considered). The difference, 0.00114 hartree (0.031 eV), is attributable to the inequivalence of the  $4p\sigma$  and  $4p\pi$  orbitals and to core polarization effects (the core orbitals were obtained from HF calculations on the  $1^2\Sigma^+$  state which does not have the full rotational symmetry of the atom). In the plots the asymptotic energies of the states have been adjusted to give the experimental atomic energy splittings.

In line with the discussion in Sec. II, the potential energy curve for the  $1^2\Pi$  state is found to be less repulsive than that of the  $1^2\Sigma^+$  state, thus making the  $1^2\Pi$  state the ground state of the system. In fact, we find that the  $1^2\Pi$  curve is slightly bound,  $D_e \sim 0.04$  eV (see Table III). Although spurious minima have been found in previous calculations on excimer systems<sup>6,13</sup> and attributed to basis set limitations, the well in the  $1^2\Pi$  curve is substantially larger than has been observed heretofore. We thus suspect that the minimum in the  $1^2\Pi$  curve is not just a result of calculational limitations. The depth of the well in the real  $1^2\Pi$  curve is, of course, expected to be significantly larger than that calculated here since the POL-CI method is not designed to account for the attractive van der Waals' interaction.

As predicted in Sec. II both the  $2^2\Sigma^+$  and  $1^1\Sigma^+$  curves

TABLE II. Energies obtained from the POL-CI calculations on the low-lying electronic states of GaKr and GaKr $^+$ . Distances are in bohr; energies are in hartree. Energies are relative to -4674 hartree.

R	$1^2\Pi$	GaKr $1^2\Sigma^+$	$2^2\Sigma^+$	GaKr $^+$ $1^1\Sigma^+$
3.75	-1.02539	-0.96866	-0.93379	-0.85625
4.00	-1.07933	-1.01870	-0.99238	-0.90683
4.50	-1.14810	-1.08688	-1.06440	-0.96758
5.00	-1.17924	-1.13516	-1.08855	-0.99287
5.50	-1.19225	-1.16324	-1.09545	-1.00070
6.00	-1.19772	-1.17938	-1.09677	-1.00202
6.50	-1.19984	-1.18865	-1.09631	-1.00107
7.00	-1.20045	-1.19396	-1.09545	-0.99950
8.00	-1.20020	-1.19865	-1.09420	-0.99670
10.00	-1.19833	-1.20029	-1.09406	-0.99402
15.00	-1.18878	-1.20012	-1.09502	-0.99304

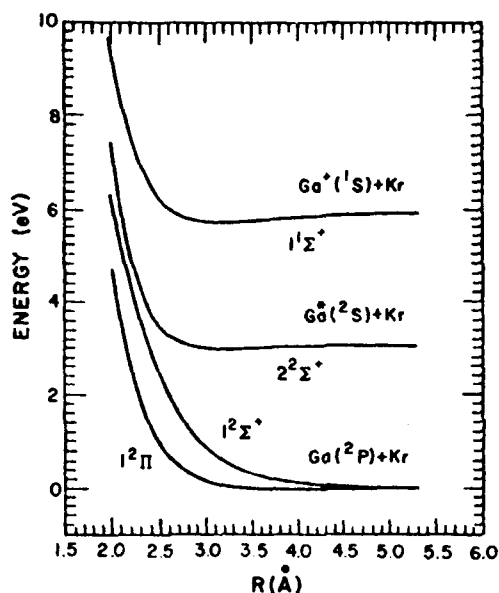
THE LOW-LYING STATES OF GaKr AND GaKr<sup>+</sup>

FIG. 2. Calculated potential energy curves for the states of GaKr and GaKr<sup>+</sup> arising from the Ga(2P, 2S) + Kr(1S) and Ga<sup>+</sup>(1S) + Kr(1S) separated atom limits. The curves have been uniformly shifted to correct for the errors in the gallium atom excitation energies.

are found to be bound with calculated dissociation energies of 0.047 and 0.24 eV, respectively. Again, inclusion of the attractive van der Waals' interaction would be expected to significantly increase the calculated well depths. There is a slight hump in the calculated potential curve of the 2<sup>2</sup>Σ<sup>+</sup> state, -0.026 eV, since the long-range interaction of the excited Ga and Kr atoms is repulsive. This hump could, however, disappear when the van der Waals' attraction is added to the calculated curve.

The dipole transition moments radiatively coupling the states of GaKr are given in Table IV and plotted in Fig. 3. At  $R = \infty$  the transition moment coupling the 1<sup>2</sup>Π and 1<sup>2</sup>Σ<sup>+</sup> states is identically zero and those coupling the (1<sup>2</sup>Π, 1<sup>2</sup>Σ<sup>+</sup>) states with the 2<sup>2</sup>Σ<sup>+</sup> state are approximately equal to the 2S-2P atomic transition moment (after properly accounting for differences in degeneracy

TABLE III. Spectroscopic constants for the bound states of <sup>69</sup>Ga<sup>84</sup>Kr and <sup>68</sup>Ga<sup>84</sup>Kr<sup>+</sup>. Units are as indicated.

	GaKr		GaKr <sup>+</sup>
	1 <sup>2</sup> Π	2 <sup>2</sup> Σ <sup>+</sup>	1 <sup>2</sup> Σ <sup>+</sup>
T <sub>0</sub> , eV	0.00	2.82	5.40
R <sub>0</sub> , Å	3.78	3.17	3.14
D <sub>0</sub> , eV	0.041	0.047	0.24
ω <sub>e</sub> , cm <sup>-1</sup>	36	86	83
B <sub>e</sub>	0.0312	0.0442	0.0452

TABLE IV. Dipole transition moments coupling the low-lying states of GaKr obtained from the POL-CI calculations.

R	1 <sup>2</sup> Σ <sup>+</sup> -1 <sup>2</sup> Π <sup>a</sup>	2 <sup>2</sup> Σ <sup>+</sup> -1 <sup>2</sup> Π <sup>a</sup>	2 <sup>2</sup> Σ <sup>+</sup> -1 <sup>2</sup> Σ <sup>+</sup>
3.75	-0.9037	-0.7877	0.4095
4.00	-0.8462	-0.8680	-0.3055
4.50	-0.1365	-1.2090	-2.0676
5.00	0.0992	-1.2349	-1.4402
5.50	0.1257	-1.2469	-1.2456
6.00	0.1166	-1.2554	-1.1893
6.50	0.0984	-1.2619	-1.1800
7.00	0.0789	-1.2677	-1.1902
8.00	0.0476	-1.2777	-1.2310
10.00	0.0163	-1.2898	-1.2976
15.00	0.0018	-1.2917	-1.3101

<sup>a</sup>The matrix element given is  $\langle \pi^2 \Sigma^+ | x | 1^2 \Pi_x \rangle$ .

factors). As  $R$  decreases rather minor changes occur until  $R \sim 2.5$  Å. For  $R < 2.5$  Å substantial changes are noted in all of the transition moments, although the change in the 2<sup>2</sup>Σ<sup>+</sup>-1<sup>2</sup>Π moment is less dramatic than for the 2<sup>2</sup>Σ<sup>+</sup>-1<sup>2</sup>Σ<sup>+</sup> and 1<sup>2</sup>Σ<sup>+</sup>-1<sup>2</sup>Π moments. The erratic behavior of the transition moments for  $R < 2.5$  Å is one manifestation of the strong interaction of the 1<sup>2</sup>Σ<sup>+</sup> and 2<sup>2</sup>Σ<sup>+</sup> states at short  $R$ .

Although, as noted above, substantial changes are found in the transition moments for  $R < 2.5$  Å, such behavior can be expected to have little effect on the observable properties of the system. At  $R = 2.5$  Å the energy of the 2<sup>2</sup>Σ<sup>+</sup> state is >0.5 eV above its asymptote so that the region  $R < 2.5$  Å would be thermally inaccessible.

## DIPOLE TRANSITION MOMENTS AMONG THE LOW-LYING STATES OF GaKr

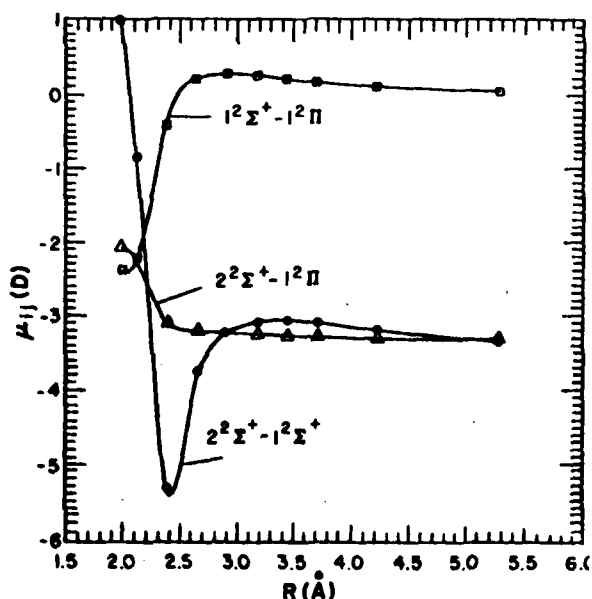


FIG. 3. Calculated dipole transition moments for the 1<sup>2</sup>Σ<sup>+</sup>-1<sup>2</sup>Π, 2<sup>2</sup>Σ<sup>+</sup>-1<sup>2</sup>Π, and 2<sup>2</sup>Σ<sup>+</sup>-1<sup>2</sup>Σ<sup>+</sup> transitions in GaKr.

THE LOW-LYING STATES OF GaKr AND  
GaKr<sup>+</sup> WITH SPIN-ORBIT CORRECTIONS

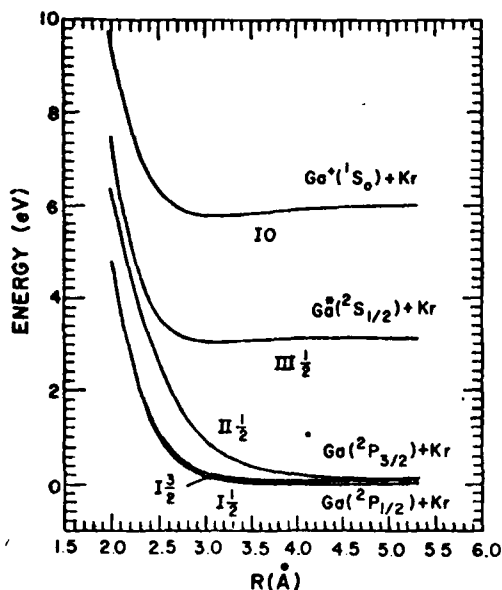


FIG. 4. Calculated potential energy curves for the states of GaKr and GaKr<sup>+</sup> arising from the Ga(<sup>2</sup>P<sub>1/2, 3/2</sub>, <sup>2</sup>S<sub>1/2</sub>) + Kr(<sup>1</sup>S<sub>0</sub>) and Ga(<sup>1</sup>S<sub>0</sub>) + Kr(<sup>1</sup>S<sub>0</sub>) separated atom limits. The curves have been uniformly shifted to correct for the errors in the gallium excitation energies.

C. Electronic states of GaKr and GaKr<sup>+</sup>, with spin-orbit corrections

The energies of the states of GaKr and GaKr<sup>+</sup> with spin-orbit corrections are given in Table V and the resulting potential energy curves are plotted in Fig. 4. In calculating the spin-orbit corrected energies we shifted the 1<sup>2</sup>Π energies to agree with the 1<sup>2</sup>Σ<sup>+</sup> energy at the largest value of R considered (R = 15.0a<sub>0</sub>). Again, in plotting the potential energy curves, the asymptotic energies of the states have been adjusted to give the correct atomic energy splittings.

As predicted in Sec. II, at short R the curves for the

TABLE V. Calculated energies of the I 1/2, II 1/2, and I 3/2 states of GaKr with spin-orbit corrections. Distances are in bohr; energies are in hartree. Energies are relative to the energy of the 1<sup>2</sup>Σ<sup>+</sup> state at R = 15 a<sub>0</sub>.

R	I 1/2	I 3/2	II 1/2
3.75	0.17228	0.17484	0.23152
4.00	0.11835	0.12091	0.18147
4.50	0.04957	0.05213	0.11329
5.00	0.01841	0.02099	0.06502
5.50	0.00538	0.00799	0.03698
6.00	-0.00015	0.00252	0.02089
6.50	-0.00234	0.00040	0.01170
7.00	-0.00307	-0.00022	0.00650
8.00	-0.00316	0.00003	0.00215
10.00	-0.00280	0.00090	0.00103
15.00	-0.00251	0.00126	0.00126

TABLE VI. Calculated dipole transition moments coupling the III 1/2 and I 1/2, II 1/2 and I 3/2 states of GaKr with spin-orbit corrections. Distances are in bohr; moments are in atomic units.

R	III 1/2-I 1/2		III 1/2-II 1/2		III 1/2-I 3/2
	x	(x, y)	z	(x, y)	(x, y)
4.00	-0.0086	0.6135	-0.3054	-0.0173	-0.6138
4.50	-0.0576	0.8545	-2.0667	-0.0238	-0.8549
5.00	-0.0549	0.8726	-1.4392	-0.0333	-0.8732
5.50	-0.0701	0.8803	-1.2437	-0.0496	-0.8817
6.00	-0.1007	0.8845	-1.1850	-0.0752	-0.8877
6.50	-0.1504	0.8850	-1.1704	-0.1138	-0.8923
7.00	-0.2249	0.8803	-1.1688	-0.1694	-0.8964
8.00	-0.4405	0.8436	-1.1495	-0.3233	-0.9035
10.00	-0.7254	0.7562	-1.0759	-0.5098	-0.9120
15.00	-0.7564	0.7457	-1.0697	-0.5273	-0.9134

I 1/2 and I 3/2 states become nearly degenerate and just represent the curves for the two spin-orbit components of the 1<sup>2</sup>Π state. Also, at short R the II 1/2 curve closely approximates the curve for the 1<sup>2</sup>Σ<sup>+</sup> state. The potential energy curves for the 2<sup>2</sup>Σ<sup>+</sup> (III 1/2) and 1<sup>1</sup>Σ<sup>+</sup> (I 0) states are unchanged by the inclusion of spin-orbit corrections.

The dipole transition moments radiatively coupling the states of GaKr with spin-orbit corrections are given in Table VI and are plotted in Fig. 5. It should be noted that both the z component of the III 1/2-I 1/2 transition and the x component of the III 1/2-II 1/2 transition are now found to vary significantly even for R > 2.5 Å. This is due to the changing nature of the I 1/2 and II 1/2 states

DIPOLE TRANSITION MOMENTS AMONG  
THE LOW-LYING STATES OF GaKr WITH  
SPIN-ORBIT CORRECTIONS

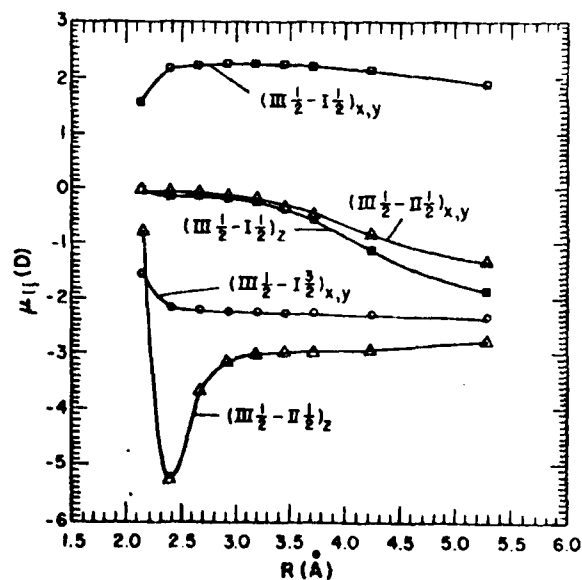


FIG. 5. Calculated dipole transition moments for the III 1/2-I 1/2, III 1/2-I 3/2, and III 1/2-II 1/2 transitions in GaKr.

TABLE VII. Excitation energies and ionization potentials for the Ga, In, and Tl atoms, in eV. Taken from Ref. 4.

State	Group IIIA atoms		
	Ga	In	Tl
$^2P_{1/2}$	0.000	0.000	0.000
$^2P_{3/2}$	0.102	0.274	0.966
$^2S_{1/2}$	3.073	3.022	3.282
$^1S_0$	5.998	5.786	6.108

as the atomic spin-orbit coupling is quenched by molecular formation.

### V. EXTRAPOLATION TO InKr AND TIKr

To provide information on the InKr and TIKr molecules, the latter being the most experimentally accessible of the Group IIIA-krypton molecules, the potential curves for InKr and TIKr have been estimated from the GaKr curves. The excitation energies and ionization potentials for the series Ga, In, and Tl are given in Table VII. As can be seen, this series does not form a steady progression: In has a lower ionization potential and excitation energies than Ga, as expected, but Tl has a higher ionization potential and excitation energies. This anomalous behavior in Tl is due in part to the filling of the 4f shell ("lanthanide contraction") and to the larger spin-orbit interactions.<sup>15</sup> These effects are only partially accounted for in the present models.

To simulate InKr and TIKr, the experimental spin-

### THE LOW-LYING STATES OF InKr AND InKr<sup>+</sup> WITH SPIN-ORBIT CORRECTIONS

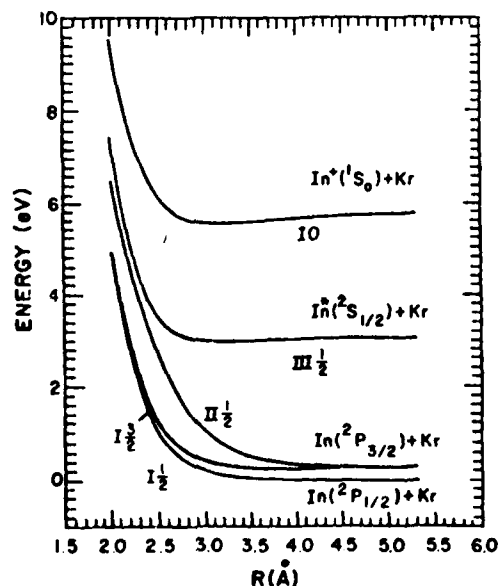


FIG. 6. Model potential energy curves for the states of InKr and InKr<sup>+</sup> arising from the  $\text{In}(^2P_{1/2,3/2}, ^2S_{1/2}) + \text{Kr}(^1S_0)$  and  $\text{In}(^1S_0) + \text{Kr}(^1S_0)$  separated atom limits, see the text.

### THE LOW-LYING STATES OF TIKr AND TIKr<sup>+</sup> WITH SPIN-ORBIT CORRECTIONS

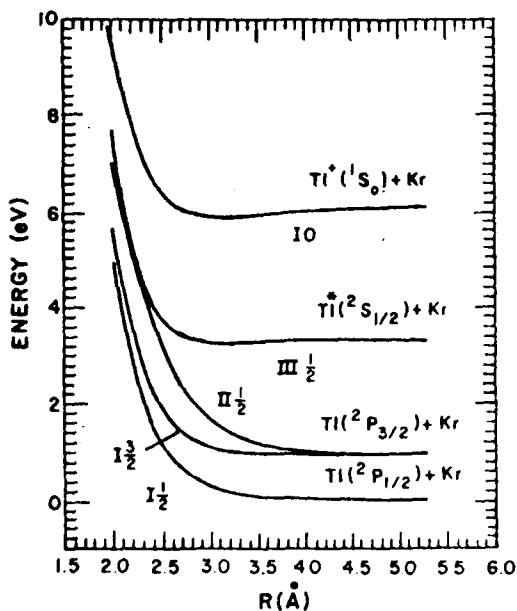


FIG. 7. Model potential energy curves for the states of TIKr and TIKr<sup>+</sup> arising from the  $\text{Tl}(^2P_{1/2,3/2}, ^2S_{1/2}) + \text{Kr}(^1S_0)$  and  $\text{In}(^1S_0) + \text{Kr}(^1S_0)$  separated atom limits, see the text.

orbit parameters for In and Tl, see Table VII, were used to couple the curves calculated for GaKr. The potential energy curves for InKr and TIKr obtained in this way are expected to be qualitatively correct; the curves are plotted in Figs. 6 and 7. As before, the plotted

### DIPOLE TRANSITION MOMENTS CONNECTING THE LOW-LYING STATES OF TIKr WITH SPIN-ORBIT CORRECTIONS

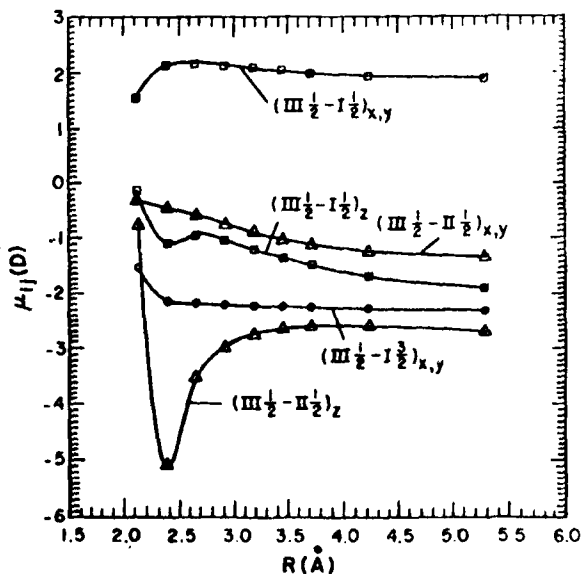


FIG. 8. Model dipole transition moments for the  $\text{III } 1/2 - \text{I } 1/2$ ,  $\text{III } 1/2 - \text{I } 3/2$ , and  $\text{III } 1/2 - \text{II } 1/2$  transitions in TIKr.

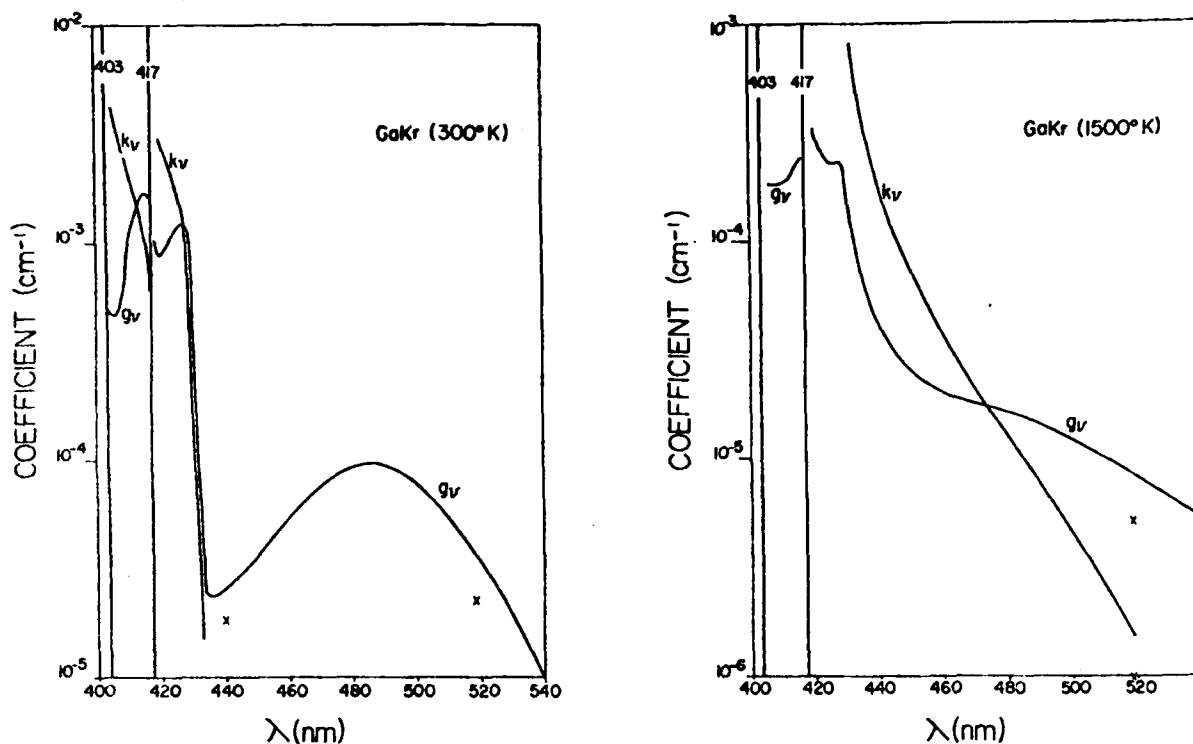


FIG. 9. Calculated absorption,  $K_v(T)$ , and stimulated emission,  $g_v(T)$ , coefficients for GaKr at  $T = 300$  and  $1500^\circ\text{K}$ .

curves have been shifted to give the correct atomic excitation energies. The effect of the increasing spin-orbit interaction in the sequence  $\text{Ga} < \text{In} < \text{Tl}$  is evident in Figs. 4, 6, and 7.

Using the transition moments obtained from the calculations on GaKr and the wavefunctions obtained from the TIKr simulation, the transition moments of TIKr have been estimated. The moments so obtained are plotted in Fig. 8.

## VI. ABSORPTION AND STIMULATED EMISSION COEFFICIENTS FOR GaKr, InKr, AND TIKr

The interest in the Group IIIA-rare gas systems arises from the possibility of their use as visible laser systems. In order to judge their usefulness as lasers it is convenient to calculate the pure absorption,  $K_v(T)$ , and stimulated emission,  $g_v(T)$ , coefficients for the perturbed atomic transitions. Obtaining quantum mechanical results for these quantities would require a complex calculation which is not justified by the extrapolations used to obtain the InKr and TIKr curves. Consequently, we have used instead the method of Gallagher and co-workers,<sup>10</sup> which is based on the classical Franck-Condon principle. In this approximation

$$g_v(T) = [M^* [X] (\lambda^2 / 8\pi) A_0(J(\lambda/\lambda_0)) I'_J(\nu T)]$$

$$K_v(T) = [M [X] (g^*/g) g_v(T) \exp\{h(\nu - \nu_0)/kT\}]$$

and

$$I'_J(\nu, T) = 4\pi R(\nu)^2 \left(\frac{\nu}{\nu_0}\right)^4 \frac{1}{d\nu/dR(\nu)} \frac{D[R(\nu)] g_m}{D(\infty) g_A} \times \exp\{-V^*[R(\nu)]/kT\}.$$

In these equations,  $J$  refers to the bands associated with the  $^2S_{1/2} - ^2P_J$  transition,  $\nu_0$  and  $\lambda_0$  are the frequency and wavelength of the atomic transition with a transition rate of  $A_0(J)$ ,  $g^* = 2$  for the  $^2S_{1/2}$  state and  $g = 2J + 1$  for the  $^2P_J$  states,  $D(R)$  is the transition dipole moment at  $R$ ,  $g_m$  and  $g_A$  are the statistical weights of the excited molecular and parent atomic state, and  $V^*(R)$  is the excited state potential curve relative to the energy of the excited atomic state.  $[M]$ ,  $[M^*]$ , and  $[X]$  are the concentrations of ground and excited metal atoms and of rare gas atoms at the temperature  $T$ .

In order to obtain  $g_v(T)$  and  $K_v(T)$ , the calculated curves were first fit with cubic splines. The spline fit was then used to calculate  $d\nu/dR$ , and these quantities, along with the atomic transition rates,<sup>14</sup> were used to calculate the absorption and stimulated emission coefficients for pressure and excitation conditions relevant to the experimental studies. We have calculated the coefficients for two different types of conditions. The high temperature results correspond to the case where the concentration of the metal is obtained from the vapor pressure of the metal itself, while the low temperature results correspond to obtaining the required concentration of the metal from vaporization of  $\text{M}_3$ . This latter condition has been suggested by Gallagher<sup>2</sup> as a possible means of obtaining high concentrations of the metal at low temperatures. In both cases the densities used are

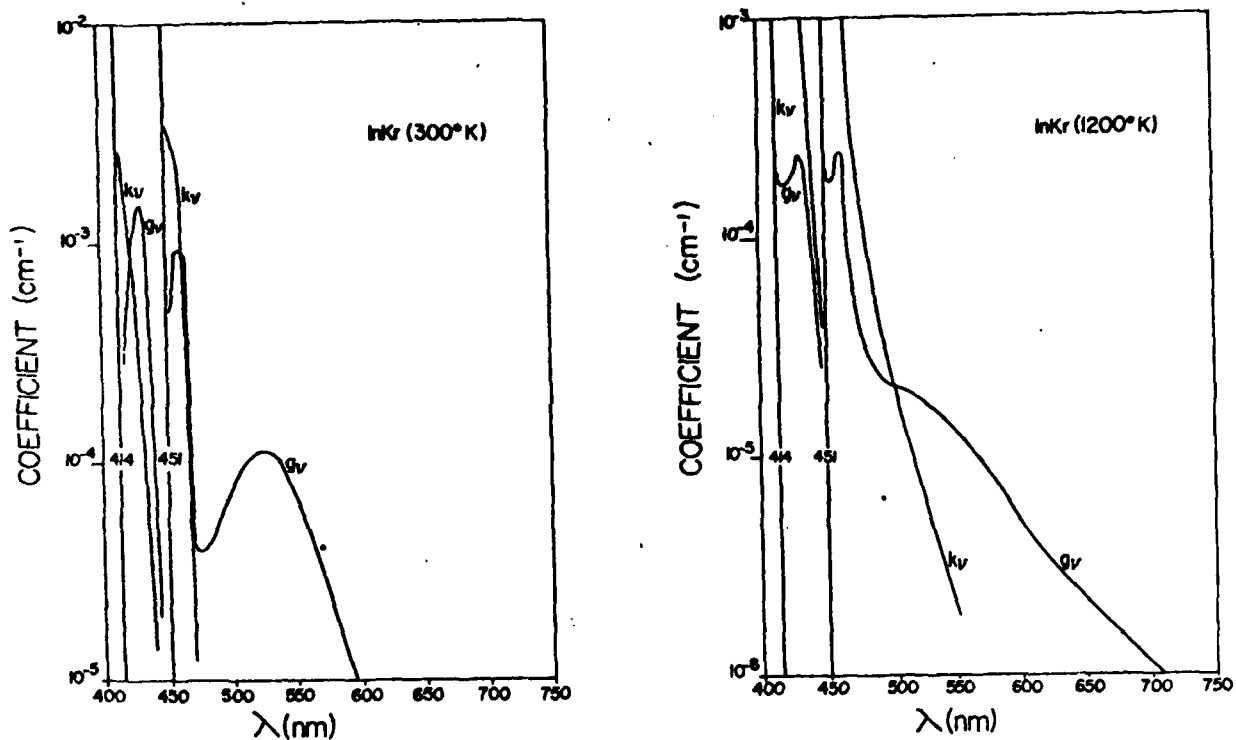


FIG. 10. Model absorption,  $K_v(T)$ , and stimulated emission,  $g_v(T)$ , coefficients for InKr at  $T = 300$  and  $1200^\circ\text{K}$ .

$10^{20}/\text{cm}^3$  for [Kr],  $10^{16}/\text{cm}^3 = 3[M(^2P_{1/2})] = 1.5[M(^2P_{3/2})]$ , and  $2 \times 10^{14}/\text{cm}^3$  for  $[M(^2S_{1/2})]$ . Since the blue wings of the  $^2S_{1/2} - ^2P_{1/2,3/2}$  bands are due to transitions occurring at large  $R$ , where our curves are not expected to be

especially accurate, we have not calculated  $g_v$  and  $K_v$  in these regions.

The resulting absorption and stimulated emission coefficients for GaKr, InKr, and TlKr are given in Figs.

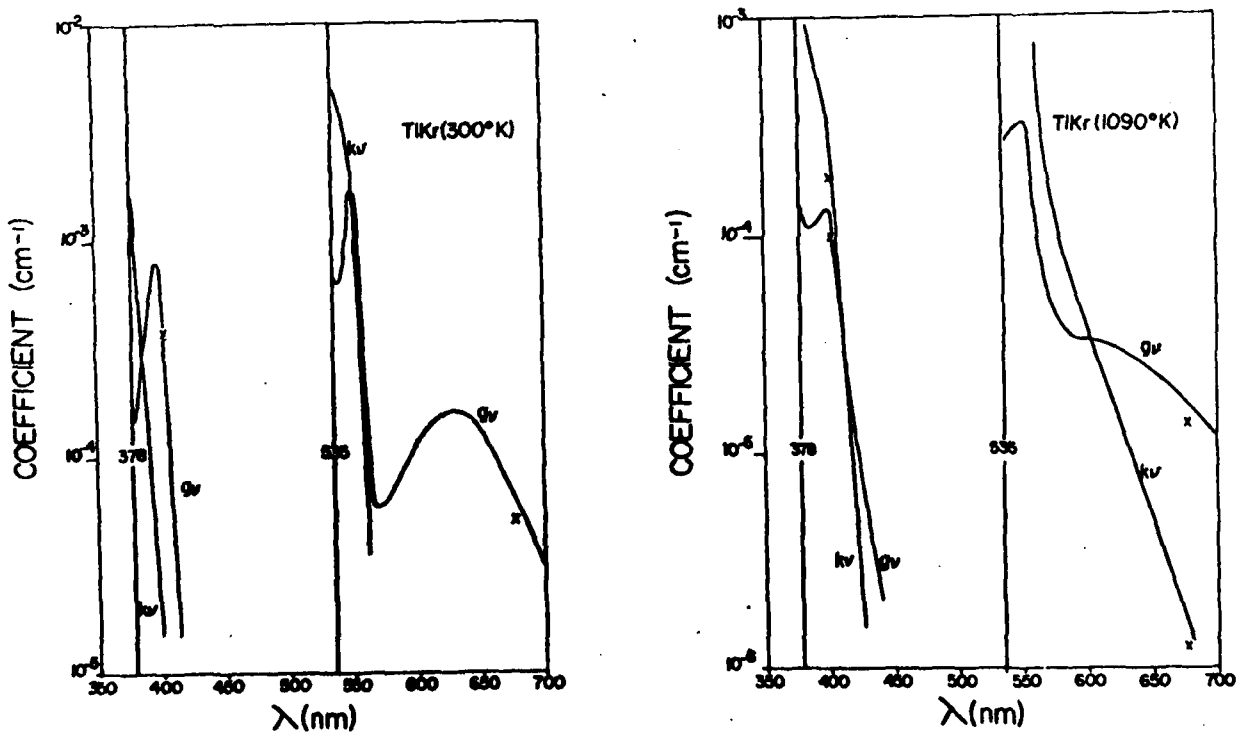


FIG. 11. Model absorption,  $K_v(T)$ , and stimulated emission,  $g_v(T)$ , coefficients for TlKr at  $T = 300$  and  $1090^\circ\text{K}$ .

9-11. In these figures the solid lines are the total coefficients calculated by assuming that the transition moment,  $D(R)$ , is a constant. The  $X$ 's are the coefficients obtained by using the spatially averaged values of  $D(R)$  calculated from Table VI and the appropriate spin-orbit parameters. For GaKr at 1500 °K (Fig. 10) and for  $403.4 < \lambda < 417.3$  nm,  $K_v > 10^{-3}$  cm<sup>-1</sup>. The dip in  $g_v$  close to the line center is due to the positive value of  $V^*(R \sim 8a_0) - V^*(R = \infty)$ .

The gain coefficient, which is approximately equal to  $g_v - K_v$ , can be estimated from these curves. For the frequencies at which gain occurs, the use of  $D(R)$  decreases  $g_v$ ,  $K_v$ , and the gain by 30-40% for GaKr and by 9-15% for TIKr. For TIKr the errors introduced by the extrapolation procedure are likely to be larger than those produced by using  $D(\infty)$  rather than  $D(R)$ . The maximum gain occurs approximately at the minimum in the III 1/2 curve. Because  $g_v$  depends exponentially on  $V^*$ , changes in the well depth of the excited state would have a significant effect on  $g_v$ . If the well depth were larger for TIKr, as Gallagher and co-workers predict,<sup>1</sup>  $g_v$  and the gain would be larger. Likewise, since the excited state in TlXe is predicted<sup>1</sup> to be more bound than in TIKr, the gain should be larger for TlXe than for TIKr.

<sup>1</sup>B. Cheron, R. Scheps, and A. Gallagher, *J. Chem. Phys.* **65**, 326 (1976).

<sup>2</sup>A. Gallagher, private communication.

<sup>3</sup>P. J. Hay, T. H. Dunning, Jr. and R. C. Raffanetti, *J.*

*Chem. Phys.* **65**, 2679 (1976).

<sup>4</sup>C. E. Moore, *Atomic Energy Levels*, National Bureau of Standards, Circular No. 467, Vols. I-III. (U.S. GPO, Washington, D. C., 1949).

<sup>5</sup>T. H. Dunning, Jr., *J. Chem. Phys.* **66**, 1382 (1977).

<sup>6</sup>R. C. Raffanetti, *J. Chem. Phys.* **58**, 4452 (1973).

<sup>7</sup>T. H. Dunning, Jr. and P. J. Hay in *Methods of Electronic Structure Theory*, edited by H. F. Schaefer, III (Plenum, New York, 1977), Chap. 1.

<sup>8</sup>T. H. Dunning, Jr. and P. J. Hay, *J. Chem. Phys.* **66**, 3767 (1977).

<sup>9</sup>W. J. Hunt and W. A. Goddard, III, *Chem. Phys. Lett.* **3**, 414 (1969).

<sup>10</sup>P. J. Hay and T. H. Dunning, Jr., *J. Chem. Phys.* **64**, 5077 (1976); T. H. Dunning, Jr., *J. Chem. Phys.* **65**, 3854 (1976). The POL-CI wavefunction is closely related to the first-order wavefunction of Schaefer, Harris, and co-workers, see, e.g., H. F. Schaefer, III, R. A. Klemm, and F. E. Harris, *J. Chem. Phys.* **51**, 4643 (1969).

<sup>11</sup>The CI program cannot make full use of the atomic or diatomic symmetry. The numbers of configurations quoted in the text are for  $C_{2v}$  symmetry.

<sup>12</sup>For the states of interest here the generalized valence bond wavefunctions would also include the  $s-p$  near-degeneracy configurations. As noted in the text these configurations are included in the POL-CI wavefunctions.

<sup>13</sup>P. J. Hay and T. H. Dunning, Jr., *J. Chem. Phys.* **66**, 1306 (1977).

<sup>14</sup>M. Norton and A. Gallagher, *Phys. Rev. A* **3**, 915 (1971).

<sup>15</sup>P. Bagus, Y. S. Lee, and K. S. Pitzer, *Chem. Phys. Lett.* **33**, 408 (1975).

<sup>16</sup>R. Scheps, Ch. Ottinger, G. York, and A. Gallagher, *J. Chem. Phys.* **63**, 2581 (1975).

Appendix B









! <WATTS>0020.31:IO WFT 15-NOV-74 9:55AM

```

q21 := q21;
write ("copy");
q24 := q24;
write ("sm7");
q27 := q27;
q28 := q28;
write ("comment (px,ox)");
q31 := q31;
q32 := q33;
q33 := q33;
write ("comment (oy,oy)");
q34 := q34;
q35 := q35;
q36 := q36;
write ("comment (oz,oz)");
q37 := q37;
q38 := q38;
q39 := q39;
write "end";
snut 7fn;
on nati;

```

APPENDIX C

```

0001 SURROUT INE JKPOF (F,DJ,CK,ISNX,IUNIT,HO,DKO,CLOSED)
0002 IMPLICIT REAL*8(A-H,C-Z)
0003 LCGICAL CLOSEC
0004 DIMENSION H(1275),DJ(1275),DK(1275),HC(1),DKO(1)
0005 INTEGER*2 ISNX(50),IA,IB,IC,ID,IMU,IF
0006 COMMON/INTS/NINTS,IA(500),IB(500),IC(500),ID(500),
/ IMU(500),IF(500),V(500)

```

```

C WILL ADD 2J-K TC H
C IF CLOSED = FALSE, WILL ALSO ACC -K FOR OPEN SHELL TO HO
C DJ AND DK ALWAYS CONTAIN TOTAL (CLOSED + OPEN) DENSITY
C MATRICES
C DKO CONTAINS "DK" DENSITY MATRIX FOR OPEN SHELL CREATALS
C ONLY
C TOTAL COULOMB + EXCHANGE INTERACTION IS
C TR(DB*H)+ TR(DO*HO)
C READ(IUNIT)NINTS,IA,IB,IC,ID,IMU,IF,V
11 IF(NINTS.EQ.0) GO TO 30
DC 29 M=1,NINTS
I=IA(M)
J=IB(M)
K=IC(M)
L=ID(M)
MU=IMU(M)
VAL=V(M)
GO TO (12,13,14,15,16,17,18,19,20,21,22,23,24,25),MU

```

```

0007 H(II)=H(II)+I
0008 IF(CLOSED) GO TO 29
0009 FC(II)=HO(II)+VAL*DKC(II)
0010 GO TO 29
0011 IJ=ISNX(I)+J
0012 II=ISNX(I)+I
0013 JJ=ISNX(J)+J
0014 H(IJ)=H(IJ)+VAL*(CJ(IJ)+DJ(IJ)+DK(IJ))
0015 H(II)=H(II)+VAL*DK(JJ)
0016 H(JJ)=H(JJ)+VAL*DK(II)
0017 IF(CLOSED) GC TC 29
0018 HO(IJ)=HO(IJ)+VAL*DKO(IJ)
0019 HO(II)=HO(II)+VAL*DKO(JJ)
0020 HG(JJ)=HG(JJ)+VAL*DKC(II)
0021 GO TO 29
0022 IJ=ISNX(I)+J
0023 II=ISNX(I)+I
0024 JJ=ISNX(J)+J
0025 H(IJ)=H(IJ)+VAL*(CJ(IJ)+DJ(IJ)+DK(IJ))
0026 H(II)=H(II)+VAL*DK(JJ)
0027 H(JJ)=H(JJ)+VAL*DK(II)
0028 IF(CLOSED) GC TC 29
0029 HO(IJ)=HO(IJ)+VAL*DKO(IJ)
0030 HO(II)=HO(II)+VAL*DKO(JJ)
0031 HG(JJ)=HG(JJ)+VAL*DKC(II)
0032 GO TO 29
0033 II=ISNX(I)+I
0034 KK=ISNX(K)+K
0035 IK=ISNX(I)+K
0036 H(II)=H(II)+VAL*DJ(KK)
0037 H(KK)=H(KK)+VAL*DJ(II)
0038 H(IK)=H(IK)+DK(IK)*VAL
0039 IF(CLOSED) GC TO 29
0040 HO(IK)=HO(IK)+VAL*DKO(IK)
0041 GC TO 29
0042 IL=ISNX(I)+L
0043 II=ISNX(I)+I
0044 H(IL)=H(IL)+VAL*(CJ(IJ)+DK(II))
0045 H(II)=H(II)+ (VAL+VAL)*(CJ(IL)+DK(IL))
0046 IF(CLOSED) GO TO 29
0047 HC(IL)=HC(IL)+VAL*DKC(II)
0048 HO(II)=HO(II)+VAL*DKO(IL)*2.D0
0049 GC TO 29

```

```

0050 16 KL=ISNX(K)+L
0051 II=ISNX(I)+I
0052 IL=ISNX(I)+L
0053 IK=ISNX(I)+K
0054 H(KL)=H(KL)+VAL*DJ(I I)
0055 P(I I)=H(I I)+(VAL+VAL)*DJ(KL)
0056 H(IL)=H(IL)+VAL*DK(IK)
0057 H(IK)=H(IK)+VAL*DK(IL)
0058 IF(CLOSED) GO TC 29
0059 HO(IL)=HO(IL)+VAL*DKC(IK)
0060 HO(IK)=HO(IK)+VAL*DKO(IL)
0061 GC TO 29
0062 JJ=ISNX(J)+J
0063 IJ=ISNX(I)+J
0064 H(JJ)=H(JJ)+(VAL+VAL)*(CJ(IJ)+CK(IJ))
0065 P(IJ)=H(IJ)+VAL*(DJ(JJ)+DK(JJ))
0066 IF(CLOSED) GO TO 29
0067 HO(JJ)=HO(JJ)+VAL*DKC(IJ)*2.00
0068 HO(IJ)=HO(IJ)+VAL*DKO(JJ)
0069 GC TO 29
0070 JK=ISNX(J)+K
0071 GO TO 27
0072 JK=ISNX(K)+J
0073 KK=ISNX(K)+K
0074 IJ=ISNX(I)+J
0075 IK=ISNX(I)+K
0076 H(KK)=H(KK)+(VAL+VAL)*DJ(IJ)
0077 H(IJ)=H(IJ)+VAL*DJ(KK)
0078 H(JK)=H(JK)+VAL*DK(IK)
0079 P(IK)=H(IK)+VAL*DK(JK)
0080 IF(CLOSED) GC TC 29
0081 HO(JK)=HO(JK)+VAL*DKO(IK)
0082 HC(IK)=HO(IK)+VAL*DKC(JK)
0083 GO TO 29
0084 IJ=ISNX(I)+J
0085 JL=ISNX(J)+L
0086 JJ=ISNX(J)+J
0087 IL=ISNX(I)+L
0088 H(JL)=H(JL)+VAL*(DJ(IJ)+DK(IJ)+CK(IJ))
0089 H(IJ)=H(IJ)+VAL*(DJ(JL)+DK(JL)+DK(JL))
0090 H(JJ)=H(JJ)+(VAL+VAL)*DK(IL)
0091 H(IL)=H(IL)+VAL*DK(JJ)
0092 IF(CLOSED) GO TO 29
0093 HC(JL)=HO(JL)+VAL*DKC(IJ)
0094 HO(IJ)=HO(IJ)+VAL*DKO(JL)
0095 HO(JJ)=HO(JJ)+VAL*DKC(IL)*2.00
0096 HO(IL)=HO(IL)+VAL*DKO(JJ)
0097 GO TO 29
0098 IL=ISNX(I)+L
0099 IJ=ISNX(I)+J
0100 II=ISNX(I)+I
0101 JL=ISNX(J)+L
0102 H(IL)=H(IL)+VAL*(DJ(IJ)+DK(IJ)+DK(IJ))
0103 H(IJ)=H(IJ)+VAL*(CJ(IL)+DK(IL)+DK(IL))
0104 H(II)=H(II)+(VAL+VAL)*DK(JL)
0105 H(JL)=H(JL)+VAL*DK(II)
0106 IF(CLOSED) GC TC 29
0107 HO(IL)=HO(IL)+VAL*DKO(IJ)
0108 HO(IJ)=HO(IJ)+VAL*DKO(IL)

```

```

0109 H(C(I I))=H(C(I I))+VAL*DKO(JL)*2.D0
0110 H(C(JL))=H(C(JL))+VAL*DKC(I I)
0111 GO TO 29
0112 IJ=ISNX(I)+J
0113 KJ=ISNX(K)+J
0114 JJ=ISNX(J)+J
0115 IK=ISNX(I)+K
0116 H(KJ)=H(KJ)+VAL*(CJ(I J)+CJ(I J)+DK(I J))
0117 H(IJ)=H(IJ)+VAL*(CJ(KJ)+DJ(KJ)+DK(KJ))
0118 H(JJ)=H(JJ)+(VAL+VAL)*DK(IK)
0119 H(IK)=H(IK)+VAL*DK(JJ)
0120 IF(CLCSED) GO TO 29
0121 H(KJ)=H(KJ)+VAL*DKC(I J)
0122 H(IJ)=H(IJ)+VAL*DKO(KJ)
0123 H(C(JJ))=H(C(JJ))+VAL*DKC(IK)*2.D0
0124 H(C(IK))=H(C(IK))+VAL*DKC(JJ)
0125 GC TO 29
0126 JL=ISNX(J)+L
0127 JK=ISNX(K)+K
0128 GC TO 25
0129 JL=ISNX(J)+L
0130 JK=ISNX(K)+J
0131 GC TO 26
0132 JL=ISNX(L)+J
0133 JK=ISNX(K)+J
0134 KL=ISNX(K)+L
0135 IJ=ISNX(I)+J
0136 IL=ISNX(I)+L
0137 IK=ISNX(I)+K
0138 H(JL)=H(JL)+VAL*DK(IK)
0139 H(IK)=H(IK)+VAL*DK(JL)
0140 H(IL)=H(IL)+VAL*DK(JK)
0141 H(JK)=H(JK)+VAL*DK(IL)
0142 IF(CLCSED) GC TO 290
0143 H(C(JL))=H(C(JL))+VAL*DKC(IK)
0144 H(C(IK))=H(C(IK))+VAL*DKC(JL)
0145 H(C(IL))=H(C(IL))+VAL*DKC(JK)
0146 H(C(JK))=H(C(JK))+VAL*DKC(IL)
0147 VAL=VAL+VAL
0148 H(KL)=H(KL)+VAL*DJ(I J)
0149 H(IJ)=H(IJ)+VAL*DJ(KL)
0150 CCNTINUE
0151 IF(LAST.EQ.0) GO TO 11
0152 RETURN
0153 EN*

```



```

0001 REAL FUNCTION QINT*(K)
0002 IMPLICIT REAL*(A-H,O-Z)
0003 EXTERNAL DS1,DS2,DS3,CS4,CS5,CS6,CS7,CS8,CS9
0004 LOGICAL INTG
0005 COMMON/INT/C,DK,RAB,DKG,IITYPE
0006 COMMON/SCLR/EXI,EXJ,IITYPE,JTYPE,ICNTR,JC NTR,H,CUT,CUT2,CUT3,
0007 U,ALPHAD,ALPHAQ,AP(4)
0008 CCMGCM/FCT/FCTCK(15),IPCT
0009 DATA SQ3/1.732050E0756887D0/
0010 DATA PI/3.14159265358979C0/
0011 DATA NAPP,STEPM/4.200C.C0/
0012 DATA EPR/1.D-16/
0013 DATA NGC/6/
C***** WARNING INTERVALS FOR G032 DECREASED*****
C***** INCREASED INTEGRATION PARAM
C PROGRAM USES INTEGRAL EXPRESSIONS OBTAINED FROM REDUCE
C IITYPE=1,S
C 2,FX
C 3,PY
C 4,PZ,Z ASSUMED ALONG DIRECTION OF BOND
C ICNTR=1, FOR A THE CLOSED SHELL ATOM ON WHICH EFFECTIVE POTENTIAL
C IS CENTERED
C 2 FOR ATOM B, NON-CLOSED SHELL
C WARNING 01 AND 04 CODE DOES NOT CONTAIN EFX,EFY ETC TERMS
C WHICH WOULD BE NEEDED FOR MOLECULES
0013 IF(IPCT.EQ.0) GO TO 100
0014 DK=CUT2
0015 DKQ=CUT3
0016 GO TO 99
0017 DK=CUT
0018 QINT=0.0D0
0019 IF(IITYPE.LE.4.AND.JTYPE.LE.4.OR.K.GT.8.OR.K.LE.0) GO TO 101
0020 WRITE(6,600) IITYPE,JTYPE,K
0021 FCORMAT(1H,25P*****ERFCFR***** /
0022 U 1H,24HONLY TYPE,LE,A ALLOWED /
0023 U 1H,24HK=15,5X,16HK MUST BE 1 TO 8 /
0024 I 1H,20H***** /
0025 RETURN
0026 I JTYPE=IITYPE+JTYPE
0027 I JCNTR=ICNTR+JCNTR
0028 GC TO (111,112,113,111,112,113,111,112,113,117,118),K
0029 IF(IITYPE.NE.1.OR.JTYPE.NE.4).AND.(JTYPE.NE.1.OR.IITYPE.NE.4)
0030 U .AND.(IITYPE.NE.JTYPE)) GO TO 115
0031 IF(K.F2).1.AND.((IITYPE.EQ.2.CR.IJTYPE.EQ.8).AND.IJCNTR.EQ.2)
0032 U .OR.((IITYPE.EQ.4.OR.IJTYPE.EQ.6).AND.IJCNTR.EQ.2)) GO TO 115
0033 IF(K.EQ.4.AND.(IITYPE.EQ.1.OR.JTYPE.EQ.1).AND.IJCNTR.EQ.2)) GO TO 115
0034 GO TO 120
0035 IF(IJTYPE.NE.2.OR.(IITYPE.NE.1.AND.IITYPE.NE.4))
0036 U .AND.(IITYPE.NE.2.OR.(JTYPE.NE.1.AND.JTYPE.NE.4))) GO TO 115
0037 IF(K.EQ.2.AND.(IITYPE.EQ.4.OR.JTYPE.EQ.4).AND.IJCNTR.EQ.2)
0038 U GO TO 115
0039 IF(K.EQ.5.AND.(IITYPE.EQ.1.OR.JTYPE.EQ.1).AND.IJCNTR.EQ.2)
0040 U GO TO 115
0041 GO TO 120
0042 IF(IJTYPE.NE.3.OR.(IITYPE.NE.1.AND.IITYPE.NE.4))
0043 U .AND.(IITYPE.NE.1.CR.(IITYPE.NE.1.AND.JTYPE.NE.4))) GO TO 115
0044 IF(K.FO.3.AND.(IITYPE.EQ.4.OR.JTYPE.EQ.4).AND.IJCNTR.EQ.2)
0045 U GO TO 115

```

```

0036      IF(K.EQ.6.AND.(ITYPE.EQ.1.OR.JTYPE.EQ.1).AND.IJCNTR.EQ.2)
0037      U GO TC 115
0038      GO TO 120
0039      IF((ITYPE.NE.JTYPE).OR.(ITYPE.NE.2.AND.IJTYPE.NE.3)) GO TO 115
0040      IF((ITYPE.NE.2.OR.JTYPE.NE.3)
0041      U .AND.(ITYPE.NE.3.OR.JTYPE.NE.2)) GO TO 115
0042      GO TO 120
0043      RETURN
0044      C=EXI+EXJ
0045      HM3=0.000
0046      HVA=0.000
0047      HM5=0.000
0048      FXP0=1.00
0049      IF(ICNTR.EQ.JCNTR) GC TC 130
0050      EXPREF=EXP(-EXI*EXJ**2/C)
0051      IF(EXPREF.EQ.0.000) RETURN
0052      IF(ICNTR.EQ.1) GC TC 125
0053      RAB=EXI#R/C
0054      GC TC 130
0055      RAB=EXJ#R/C
0056      GC TO 150
0057      EXPREF=1.00
0058      RAB=R
0059      IF(ICNTR.EQ.1) GO TO 135
0060      GO TO 150
0061      RAB=0.000
0062      EXP5M=1.00
0063      C2=C*C
0064      C3=C2*C
0065      RAB2=PAB#RAB
0066      PAR3=RAB2#RAB
0067      IF(IJTYPE.EQ.2) GC TC 190
0068      AEX=0.000
0069      ABY=0.000
0070      AHZ=RAB
0071      FFY=0.000
0072      EFY=0.000
0073      EFZ=0.000
0074      IF(ICNTR.NE.JCNTR) EFZ=R
0075      RAB4=RAB2#RAB2
0076      RAB5=RAB2#RAB3
0077      RAB6=RAB3#RAB3
0078      RAB7=RAB3#RAB4
0079      C4=C2*C2
0080      ABX2=C.000
0081      ABY2=0.000
0082      ABZ2=ABZ*ABZ
0083      ADZ3=ADZ*ADZ2
0084      IF(ITYPE.NE.1)A=EXJ
0085      IF(JTYPE.NE.1)A=EXI
0086      IF(ITYPE.EQ.1.OR.JTYPE.EQ.1) GC TC 190
0087      C DEFINITION AF A AND B IMPRTANT IF EXX,RFY.NE./
0088      IF(ICNTR.NE.2) GC TO 188
0089      A=EXI
0090      B=EXJ
0091      GO TO 199
0092      A=EXJ
0093

```

```

0092      P=EXI
0093      C5=C4*C
0094      RAR9=PAB1*RAB4
0095      RAR9=PAB3*RAB
0096      ABX3=0.000
0097      ABY3=0.000
0098      ABX4=C.000
0099      ABY4=C.000
0100      AB74=ABZ2*ABZ2
0101      EFY2=C.000
0102      EFY2=0.000
0103      FFZ2=FFZ*FFZ
0104      GO TO 191
0105      IF(ICNTR+ITYPE.EQ.2.OR.JCNTR+JTYPE.EQ.2) EFZ=-EFZ
0106      REXP=DSQRT(-DLGG(1.D-16)/C)
C**BETTER INT LIMITS*****
C**MIN=CMAX1(RAE-REXP,0.0C0)
RMAX=AB+REXP
HIN=HFXP*2.*(NAPF-1)
INTC=(C.LE.100.AND.RAB.LE.10.000).CR.
U (C.GE.1.D3.AND.RAB.LT.1C0)
IF(K.GE.4) GC TC 400
IF(INTC) GO TO 195
C*****WARNING: ALL INTEGRALS DONE BY GAUSSIAN QUAD*****
C** REMOVE C FOR ITROMB
C*****WARNING: GAUSSIAN QUAD CHANGED TO 4 INTERVALS
CALL NDDG32(RMIN,FMAX,DS1,HM1,NGG)
IF(RAB.GE.1.D-10) CALL NDDG32(RMIN,FMAX,DS2,HM2,NGG)
GC TO 199
195 CALL ITROM9(DS1,HIN,ERR ,NAPP,HM1,IERR,RMIN)
IF(RAE.GE.1.D-10)
.CALL ITROMB(DS2,HIN,ERR ,NAPP,HM2,IERR,RMIN)
CONTINUE
601 FCRMAT(IH ,4+HM1=.E27.16,5X,4HHM2=.E27.16)
608 FCRMAT(IH ,5HRMIN=.E15.6,5X,5HRMAX=.E15.6)
IF(IJTYPE.NE.2) GO TO 200
C G1
QINT=PI*(2.*HM2/(C*RAE)-HM1/(C2*RAB2))/EXP0
GINT=GINT*EXPREF
RETURN
200 CONTINUE
IF(ITYPE.EQ.1.OR.JTYPE.EQ.1).AND.K.NE.1) GO TO 205
IF(INTC) GO TC 204
IF(RAB.GE.1.D-10) CALL NDDG32(RMIN,RMAX,DS3,HM3,NGG)
GC TO 205
204 IF(RAB.GE.1.D-10)
.CALL ITROMB(DS3,HIN,ERR ,NAPP,HM3,IERR,RMIN)
CONTINUE
602 FCRMAT(IH ,4HHM3=.E27.16)
IF(ITYPE.NE.1.AND.JTYPE.NE.1) GO TO 300
GO TO (201,202,203),K
C G1= < S / Q1 / PZ >
201 IF(RAB.LT.1.C-10) GC TC 211
Q1= (-PI*(6*RAB*HM2*ABZ2*C-2*HM2*RAB3*(2*ABZ*EFZ*C*A-(2*C2*
.ABZ2-C))+2*ABZ*HM1*FAR2*EFZ*A-(HM1*(RAB2*(2*ABZ2*C-1)+3*ARZ2)
.ABZ*ABZ2*C2*HM3*ABZ2)))/(2*EXFO*EXP5*C3*RAB5)
GINT=G1*EXPREF
RETURN
0136
0137

```

```

0139 GINT=4.*PI*HM1/3.
0140 RETURN
0141 IF(RAF.LT.1.D-10) GO TO 212
C U2= < S / Q2 / PX >
0142 Q2= (((2*C*PAB2*ABX2-RAR2+3*ABX2)-2*ABX*EFX*A*RAB2)*HM1+2*((C
* C2*AR2*ABX2)*PI)/(2*E*PC*E*XP5*C3*RAB5)
0143 GINT=C2*EXPREF
0144 RETURN
0145 QINT=4.*PI*HM1/3.
0146 IF(RAB.LT.1.D-10) GO TO 213
C O3= < S / Q3 / PY >
0147 Q3= (-PI*(6*RRAB*HM2*AEY2*C+2*ABY*(HM1*RAB2-2*HM2*RAB3*C))*EFY*A
* HM3*C2*RAB2*ABY2))*EXP5M)/(2*C3*RAB5)*EXPREF
0148 QINT=C3
0149 RETURN
0150 GINT=4.*PI*HM1/3.
0151 RETURN
0152 CONTINUE
0153 IF(IJTYPE.NE.8) GC TC 302
C IF(INIC) GO TO 301
0154 IF(RAB.GE.1.D-10) CALL NDCG32(RMIN,RMAX,DS4,HM4,NGQ)
0155 GO TO 302
0156 IF(RAE.GE.1.D-10)
/ CALL ITRDMR(DS4,HIN,FFR ,NAPP,HM4, IERR, RMIN)
0157 CONTINUE
0158 FCRMAT(IH, 4,HM4=,F27.16)
0159 GO TO (310,320,330),K
0160 GO TO (115,212,313,314),I,TYPE
C < PX(E) / Q1(F) / PY(E) >
0161 Q1= (-ABZ*PI*(6*HM2*HAB3*C-(3*HM1*RAB2+4*C2*HM3*FAB4)))/(4*
* EXP0*EXP5*RAE7*C4)
0162 QINT=C1*EXPREF
0163 RETURN
C < PY(E) / Q1(F) / PY(E) >
0164 Q1= (-ABZ*PI*(6*HM2*RAB3*C-(3*HM1*RAD2+4*C2*HM3*RAB4)))/(4*
* EXP0*EXP5*RAE7*C4)
0165 QINT=C1*EXPREF
0166 RETURN
C < PZ / Q1 / PZ >
0167 Q1= (PI*(30*RAB*HM2*AEZ3+C-2*HM2*(ABZ*(9*RAB3*C+4*C2*RAB5+4*
RAB5*RAE22*C*A)-2*(3*RAB3*(2*C2*APZ3+ABZ2*EFZ*(B-A)*C)+2*C2*
RAB5*ABZ2*EFZ*(B-A)+2*C3*RAE5*AEZ3-HAB5*EFZ*(B-A)*C))+ABZ*(
HM1*(9*RAB2+4*RAB4*(B*EFZ2*A+C))+12*C2*HM3*RAB4)-(HM1*(6*RAB2
*(ABZ2*EFZ*(B-A)+12*AEZ3*(C)+4*C2*RAE4*ARZ3+4*HM3*EFZ2*RAB4*(B-
A)*C-2*EFZ*RAB4*(B-A)+15*ABZ3)+24*RAE2*C2*HM3*ABZ3-8*RAB3*C3*
HM4*ABZ1+8*C2*HM3*ABZ2*EFZ*RAB4*(B-A)+16*HM3*C3*RAB4*ABZ3)))/
(4*EXP0*EXP5*RAE7*C4)
0168 QINT=C1*EXPREF
0169 RETURN
C < PX / Q2 / PZ >
0170 IF(I,TYPE.EQ.2) GO TO 321
0171 A=EXI
0172 B=EXJ
0173 IC(ICNTR.EQ.1) EFZ=-R
0174 GC TO 322
0175 R=EXI
321

```

```

0176 A=EXJ
0177 IF(JCNTR.EQ.1) EFZ=-R
0178 Q2= (-PI*(2*8*(HMI*(2*C*AB4*AEX2+3*AB2*ABX2-R*AB4)-2*ABX*EFX
322 *A*AB4)-2*HM2*((3*AB3*ABX2-R*AB5)*C+2*C*AB5*ABX2)-2*ABX*
*EFX*C*AB5)+4*HM3*(2*AE4*ABX2)*EFZ+HM1*ABZ*((2*(6*AB2*
ABX2-R*AB4)*C+4*C2*AE4*ABX2-3*AB2+15*ABX2)-2*(2*C*AB4+3*
AB2)*ABX*EFX)+2*HM2*ABZ*((2*(6*AB3*ABX2-R*AB5)*C2-3*C*AB3
+4*C3*AB5*ABX2)-2*(3*(C*AB3+2*C2*AB5)*ABX*EFX)+15*ABX*
ABX2)+4*HM3*ABZ*((6*AB2*ABX2-R*AB4)*C2+4*C3*AB4*ABX2)-2*ABX
*EFX*A*C2*AB4)-8*HM4*ABZ*(C3*AB3*ABX2))/(4*EXP0*E*XP5*AB7*C4
)
0179 QINT=Q2*EXPREF
0180 RETURN
C < S / Q3 / PZ >
330 IF(IJTYPE.EQ.3) GO TO 331
A=FXJ
R=EXI
IF(JCNTR.EQ.1) EFZ=-R
GO TO 332
331 A=EXI
R=EXJ
IF(IJTYPE.EQ.1) EFZ=-R
332 Q3= (PI*EXP54*(30*AB4*AB7*HM2*ABY2*C+2*ABY*AB*EFY*(2*EFZ*(HMI*
AB4-2*HM2*AB5*C)+4*HM3*AB2+2*HM1*AB4)*C-4*HM2*C2*
RAB5-6*HM2*AB3*ABX2+4*HM3*AB2+2*HM1*AB4)*C+2*EFZ*(HMI*(2*ABY2*C-1)*
RAB4+3*AB2*ABY2)-2*HM2*(2*AB5*ABY2+3*AB3*ABY2*C-RAB5*C)
+4*HM3*AB2*ABY2)*A-AEZ*(4*HM1*C2*AB4*ABY2+12*HM1*ABE2*
ABY2*C-3*HM1*AB4*ABY2)-2*HM1*AB4*ABY2+15*HM1*ABY2-2*HM2*AB3*
ABY2+4*HM2*C2*AB5-8*HM2*AB3*AB5*ABY2+6*HM2*AB3*ABY2+2*HM3*ABY2*
RAB2*ABY2)-4*HM3*AB4+16*HM3*AB4*16*HM3*AB4*16*HM3*AB4*16*HM3*
ABY2)))/(4*C4*EXP0*RAE7)
QINT=Q3*EXPREF
RETURN
400 CCNTINUE
IF(IJTYPE.EQ.1) GO TO 401
CALL NDCG32(RMIN,RMAX,DS5,HM1,NGQ)
IF(RAB.LT.1.D-10) GC TC 449
CALL NDCG32(RMIN,RMAX,DS6,HM2,NGQ)
CALL NDCG32(RMIN,RMAX,DS7,HM3,NGQ)
GC TO 449
401 CALL ITRMB(DS5,HIN,ERR,NAPP,HM1,IERR,RMIN)
IF(RAB.LT.1.D-10) GC TO 449
CALL ITRMB(DS6,HIN,ERR,NAPP,HM2,IERR,RMIN)
CALL ITRMB(DS7,HIN,ERR,NAPP,HM3,IERR,RMIN)
CCNTINUE
449 FORMAT(IH,4HM2=E27.16,EX,4HM2=E27.16,5X,4HM3=E27.16)
605 IF(IJTYPE.EQ.2) GC TC 450
C < S / 34 / S >
QINT=PI*(2*HM3+3*HM1)/(2*C2*AB2)-3*HM2/(C*AB))/(C*AB*EXP0)
QINT=QINT*EXPREF
RETURN
450 CONTINUE
IF(IJTYPE.EQ.1) OR(JTYPE.EQ.1) AND(K.NE.4) OR(K.EQ.7) GO TO 452
IF(INTC) GO TO 451
IF(RAB.GE.1.D-10) CALL NDCG32(RMIN,RMAX,DS8,HM4,NGQ)
GO TO 452
451 IF(RAB.GE.1.D-10)
/CALL ITRMB(DS8,HIN,ERR,NAPP,HM4,IERR,RMIN)
452 CONTINUE

```

```

0214 FORMAT(1H,4HHM4=.E27.16)
0215 IF(ITYPE.NE.1.AND.JTYPE.NE.1) GO TO 500
0216 GO TO (115,115,115,454,455,456).K
C < S / Q4 / PZ >
0217 Q4= (PI*(90*RAR*HM2*AE73*(C-6*PM2*(6*ABZ2*ABZ3*EFZ*C*A-(2*C2*(3
*ABZ3-ABZ3-RAB5*ARZ)-9*PAB3*ABZ*C+2*PAB5*EFZ*C*A))+6*ABZ2*EFZ
*(3*PM1*ABZ2+ARAB4*C2*PM3)*A-(18*HM1*ABZ2*ABZ3*C-27*HM1*ABZ2
*AEZ2+6*HM1*ABZ4*EFZ*A-6*PM1*AE4*ABZ*C+45*HM1*AEZ3+72*ABZ2*C2
*HM3*ABZ3-40*ABZ4*C2*HM3*ABZ+24*ABZ4*HM3*C3*ABZ3+8*C2*HM3*
RAB6*EFZ*A-24*RAE3*C3*PM4*AEZ3+8*ABZ5*C3*HM4*ABZ-8*HM3*ABZ6*
C3*ABZ)))/(8*EXP5*C4*EXP0*ABZ7)
CINT=C4*EXPREF
RETURN
0218
0219
C < S / Q5 / PX >
0220 Q5= (ARZ*PI*(30*RAE*PM2*C*ABX2+(2*ABX*EFX*(3*HM1*ABZ2-6*HM2*C*
RAB3+4*HM3*C2*ABZ4)*A-3*(2*C*ABZ2*ABX2-RAB2+5*ABX2)*HM1-6*(C-
2*C2*ARX2)*PM2*ABZ3-4*(C*ABZ2*ABX2-RAB4)*C2+2*C3*ABZ4*ABX2)*
HM3+8*HM4*C3*ABZ3*ABX2)))/(4*EXP0*EXP5*ABZ7*C4)
CINT=Q5*EXPREF*SQ2
RETURN
0221
0222
C < S / Q6 / PY >
0223 Q6= (ARZ*PI*EXP5M*(30*ABZ*ABY2*HM2*C+2*ABY*EFY*(4*C2*ABZ4*HM3+
3*ABZ2*HM1-6*ABZ3*HM2*C)*A-(4*C2*(6*ABZ2*ABY2*HM3-3*ABZ3*ABY2
*HM2-RAB4*HM3)-8*C3*ABY2*(RAB3*HM4-RAB4*HM3)+3*ABZ2*HM1*(2*
ABY2*C-1))+5*ABZ3*HM2*C+15*ABY2*HM1)))/(4*C4*EXP0*ABZ7)
CINT=C6*EXPREF*SQ3
RETURN
0224
0225
0226 CCNTINJE
0227 IF(IJTYPE.NE.8) GC TO 502
C IF(INTC) GO TO 501
0228 IF(RAB.GE.1.D-10) CALL NCGG32(RMIN,RMAX,DS9,HM5,NGQ)
0229 GO TO 502
0230 IF(RAE.GE.1.D-10)
/CALL ITRM3(DS9,HIN,EFR,NAPP,HMS,IERR,RMIN)
0231 CCNTINJE
0232 FCRTM(1H,4HMS=.E27.16)
0233 GO TO (115,115,115,540,560,570,580).K
0234 GC TO (115,542,543,544).ITYPE
C < PX / Q4 / PY >
0235 IF(RAB.LT.1.D-10) GO TO 532
0236 Q4= (PI*(18*HM2*(5*ABZ2*ABZ3-RAB5)*C-3*ABZ2*(15*HM1*ABZ2+24*
PAB4*C2*HM3-8*ABZ5*C3*HM4)+(9*HM1*ABZ4+16*C2*HM3*ABZ6-8*C3*
HM4*ABZ7)))/(16*EXP5*EXP0*C5*ABZ9)
CINT=C4*EXPREF
RETURN
0237
0238
0239
0240 QINT=-4.*PI*HM1/15.
RETURN
C < PY / Q4 / PY >
0241 IF(RAB.LT.1.D-10) GO TO 532
0242 Q4= (PI*(18*HM2*(5*ABZ2*ABZ3-RAB5)*C-3*ABZ2*(15*HM1*ABZ2+24*
PAB4*C2*HM3-8*ABZ5*C3*HM4)+(9*HM1*ABZ4+16*C2*HM3*ABZ6-8*C3*
HM4*ABZ7)))/(16*EXP5*EXP0*C5*ABZ9)
CINT=C4*EXPREF
RETURN
0243
0244
0245 IF(RAB.LT.1.D-10) GO TO 545
0246 Q4= (-9)*(30*ABZ*HM2*C*AEZ4-6*HM2*(2*ABZ2*(18*C2*ABZ5+45*ABZ3
*C+5*ABZ5)*C4*EFZ2+2*C3*ABZ7)-(4*C2*(15*ABZ3*ABZ4+3*ABZ5*
ABZ3*EFZ*(B-A)-ABZ7*EFZ*AEZ*(B-A))+30*ABZ3*ABZ3*EFZ*(B-A)*C+3

```

```

. *PAB5*(4*C3*ABZ4-6*EFZ*ABZ*(B-A)*C+3*C)+4*AB7*8*C*A*EFZ2))+2
. *ABZ2*((135*HM1*AB2+18*HM1*AB4*B*A*EFZ2+54*HM1*RAP4*C+6*HM1)*
. C2*AB6+222*AB4*C2*PM3+24*C2*HM3*AB6*8*A*EFZ2-84*AB5*C3*
. HM4+20*HM3*AB6*C3+8*HM3*C4*FAB8+8*AB6*C4*HM5-16*HM4*C4*AB7
. )-(3*HM1*(30*AB2*(AB73*EFZ*(B-A)+2*C*ABZ4)+3*AB4*(4*C2*ABZ4
. +4*ABZ3*EFZ*(B-A)*C-6*EF7*ABZ*(B-A)+3)-4*AB6*(EFZ*ABZ*(B-A)*
. C-R*A*EFZ2)+105*AB74)+54*C*AB2*C2*HM3*ABZ4+48*AB4*(3*C2*HM3*
. ABZ3*EFZ*(B-A)+6*HM3*C3*ABZ4+C4*HM5*ABZ4)-8*C2*HM3*(5*AB6*(2
. *EFZ*ABZ*(B-A)-1)-2*FAB8*E*A*EFZ2)-240*AB3*C3*HM4*ABZ4-48*
. AB5*HM4*(C3*ABZ3*EFZ*(B-A)+2*C4*ABZ4)+16*HM3*(3*AB6*(C3*
. ABZ3*EFZ*(B-A)+C4*AEZ4)-(C3*EFZ*ABZ*AB8*(B-A))+8*C3*HM4*AB7*
. (2*EFZ*ABZ*(B-A)-1)))/(16*EXP5*EXP0*C5*AB9)
. QINT=64*EXPREF
. RETURN
. QINT=8.*PI*HM1/15.
. RETURN

```

0247  
0248  
0249  
0250

545

```

C < PX / Q5 / PZ >
550 IF(RAB.LT.1.D-10) GO TO 551
551 IF(ITYPE.EQ.2) GO TO 553

```

0251  
0252  
0253  
0254  
0255  
0256  
0257  
0258  
0259  
0260

```

553 R=EXI
554 A=EXJ
555 IF(JCNTR.EQ.1) EFZ=-R
556 GO TO 552

```

```

552 IF(JCNTR.EQ.1) EFZ=-R
553 Q5= (-PI*(ABZ2*(210*AB7*HM2*C*ABX2+(2*ABX*EFZ*(8*AB6*HM3*C3+6
. *HM1*C*AB4+15*HM1*AB2-30*HM2*C*AB3-12*HM2*C2*AB5+24*HM3*
. C2*AB4-8*HM4*C3*RAPE)*A+8*AB6*PM3*(C3-2*C4*ABX2)-3*HM1*(2*(
. 10*AB2*ABX2-RAB4)*C+4*C2*RAE4*ABX2-5*RAE2+35*ABX2)+6*HM2*(2*
. (10*FAB3*ABX2-RAB5)*C2-5*C*RAE3+4*C3*RAE5*ABX2)-12*HM3*(15*
. RAB2*ABX2-2*RAB4)*C2+8*C3*RAE4*ABX2)+8*HM4*((10*AB3*ABX2-
. RAB5)*C3+4*C4*RAE5*ABX2)-16*HM5*C4*RAE4*ABX2))+2*ABZ*B*EFZ*(2
. *ABX*EFZ*(4*AB6*HM3*C2+3*(HM1*AB4-2*HM2*C*AB5)))+A*(4*AB6*
. HM3*(C2-2*C3*ABX2)-(3*HM1*(2*C*RAE4*ABX2+5*RAE2*ABX2-RAB4)-6*
. HM2*(15*RAE3*ABX2-RAB5)*C2+2*C2*RAE5*ABX2)+24*HM3*C2*RAE4*ABX2
. -8*HM4*C3*RAE5*ABX2))-(2*AEX*EFZ*(4*AB6*HM3*C2+3*HM1*AB4-6
. *HM2*C*RAE5)*A+4*RAE4*HM3*(C2-2*C3*ABX2)-3*HM1*(2*C*RAE4*ABX2
. +5*RAE2*ABX2-RAB4)+6*HM2*(15*RAE3*ABX2-RAB5)*C2+2*C2*RAE5*ABX2
. )-24*HM3*C2*RAE4*ABX2+8*HM4*C3*RAE5*ABX2)))/(8*EXP0*EXP5*C5*
. RAB9)
. QINT=C5*EXPREF*C3
. RETURN

```

0261  
0262  
0263  
0264

```

551 QINT=4.*PI*HM1/15.*S03
. RETURN
. RETURN

```

```

C < PY / Q6 / PZ >
560 IF(RAB.LT.1.D-10) GO TO 561
561 IF(ITYPE.EQ.3) GO TO 561

```

0265  
0266  
0267  
0268  
0269  
0270  
0271  
0272  
0273  
0274

```

561 B=EXI
562 A=EXJ
563 IF(JCNTR.EQ.1) EFZ=-R
564 GO TO 562

```

```

562 IF(JCNTR.EQ.1) EFZ=-R
563 Q6= (-PI*EXP5*((210*AB7*HM2*ABY2*ABZ2*HM2*C+2*ABY*8*EFY*(2*ABZ*EFZ
. *A*(4*C2*AB6*HM3+3*AB4*HM1-6*AB5*HM2*C)-4*C2*(6*AB4*ABZ2
. *HM3-3*AB5*ABZ2*HM2-RAE6*HM3)-8*C3*ABZ2*(RAE5*PM4-HAB6*HM3)+
. 15*AB92*ABZ2*HM1-30*AB83*ABZ2*HM2*C+3*AB4*HM1*(2*ABZ2*C-1))+6

```

```

* RAB5*HM2*C)) + 2*ABZ*EFZ*(4*C2*(6*RAB4*ARY2*HM3-3*PAB5*ABY2*
HM2-RAB6*HM3)-8*C3*AEY2*(RAE5*HM4-RAB6*HM3)+15*RAB*ABY2*HM1-
30*RAB3*ABY2*HM2*C+3*RAB4*HM1*(2*ABY2*C-1)+6*RAE5*HM2*C)*A-(
16*(RAB4*HM5-2*RAB5*HM4+RAB6*HM3)*C4*ABY2*ABZ2+4*C2*(45*RAB2*
ABY2*ABZ2*HM3-30*RAB3*ABY2*ABZ2*HM2+3*RAE4*(ABY2*(ABZ2*HM1-2*
HM3)-2*ABZ2*HM3)+3*RAB5*(ABY2*ABZ2)*HM2+RAB6*HM3)-8*C3*(10*
RAB3*ABY2*ABZ2*HM4-12*RAE4*ABY2*ABZ2*HM3+RAB5*(ABY2*(3*ABZ2*
HM2-HM4)-ABZ2*HM4)+ABY2*FAC6*HM3+ABZ2*RAE6*HM3)+15*RAB2*(ABY2
*(4*ABZ2*C-1)-ABZ2)*HM1+30*RAB3*(ABY2*ABZ2)*HM2*C-3*RAB4*(2*
ABY2*C+2*ABZ2*C-1)*HM1-6*RAE5*HM2*C+105*ABY2*ABZ2*HM1))/(8*
C5*RAE9*EXP0)

```

0275  
0276  
0277  
0278  
0279  
0280

GINT=C5\*EXPREF\*S03  
RETURN

570  
572  
573

```

GO TO (115,572,573),I TYPE
IF(RAB.LT.1,D-10) GO TO 574
ANS5=-8*((15*ABX2-ABY2)*RAB5+10*RAB3*(ABX2*ABY2-ABX4))*C3+4*C4
*RAB5*(ABX2*ABY2-ABX4)*HM4+16*HM5*C4*RAE4*(ABX2*ABY2-ABX4)
ANS4=2*ABX*EFX*(8*(15*HM1*RAE2*ABY2+6*HM1*RAE4*AEY2*C+6*HM1*
RAB4-12*HM2*C2*RAB5*ABY2-30*HM2*RAB3*ABY2*C-12*HM2*RAE5*C+24*
HM3*C2*RAB4*ABY2+8*HM3*C2*RAB6+8*HM3*C3*ABY2*RAE6-8*HM4*C3*
RAB5*ARY2)-3*HM1*(5*FAE2*ABY2+2*RAB4*(ABY2*C+1))*A+6*HM2*(2*
C2*RAE5*ABY2+5*RAB3*ABY2*C+2*RAD5*C)*A-8*HM3*A*(C2*(3*RAB4*
ABY2+RAB6)+C3*ABY2*RAB6)+8*HM4*C3*RAE5*ABY2*A)-2*EFX*ABX3*(8*
(15*HM1*RAE2+6*HM1*RAE4)*C-12*HM2*C2*RAE5-30*HM2*RAE3*C+24*HM3
*C2*RAB4+8*HM3*C3*RAE6-8*HM4*C3*RAE5)*C-8*HM3*A*(3*C2*RAE4+C3*RAE6)+8
C)+6*HM2*A*(2*C2*RAE5+5*RAE3*C)-8*HM3*A*(3*C2*RAE4+C3*RAE6)+8
*HM4*C3*RAE5*A)+4*(3*HM1*RAE4-6*HM2*RAE5*C+4*HM3*C2*RAB6)*B*
EFX2*(ABX2-ABY2)*A+3*(5*((4*ABY2*C+5)*ABX2-4*ABX4)*C-ABY2)*
RAB2+2*(4*ABX2*C-1)*RAB4+4*C2*RAE4*(ABX2*ABY2-AEX4)+35*ABX2*
ABY2-35*ABX4)*HM1-6*(4*(F*RAE3*(ABX2*ABY2-ABX4)+2*RAE5*ABX2)*
C2+5*(5*ABX2-ABY2)*RAB3*(C+4*C3*RAE5*(ABX2-ABX4)-2*RAE5*C
)*HM2+4*((6*(5*ABX2-ABY2)*RAB4+45*RAE2*(ABX2*ABY2-AEX4))-2*
RAB6)*C2+8*(3*RAE4*(ABX2*ABY2-ABX4)+ABX2*RAE6)*C3+4*C4*RAE6*(
ABX2*ABY2-ABX4))*HM3+A*NS5
ANS3=-ANS4
ANS2=210*RAB*HM2*(ABX2*ABY2-AEX4)*C+ANS3
ANS1=PI*ANS2*EXP5M
G7=ANS1/(8*C5*RAE9)*EXPREF
GINT=Q7*S03/2.D0
RETURN

```

0281  
0282  
0283  
0284  
0285  
0286  
0287  
0288

573

```

IF(RAB.LT.1,D-10) GO TO 575
ANS4=-((2*ABY*EFY*(15*HM1*RAE2*ABX2+6*HM1*RAE4*ABX2*C+6*HM1*
RAB4-12*HM2*C2*RAE5*ABX2-30*HM2*RAE3*ABX2*C-12*HM2*RAE5*C+24*
HM3*C2*RAE4*ABX2+8*HM3*C2*RAE6+8*HM3*C3*ABX2*RAE6-8*HM4*C3*
RAB5*ABX2)*(B-A)-2*B*(EFY*ABY3*(15*HM1*RAE2+6*HM1*RAE4)*C-12*
HM2*C2*RAE5-30*HM2*RAE3*C+24*HM3*C2*RAE6+8*HM3*C3*RAE6-8*HM4*
C3*RAE5)+6*HM1*RAE4*EFY2*(ABX2-ABY2)*A)-12*HM2*RAE5*EFY2*(ABX2
-ABY2)*C+A+3*HM3*C2*EFY2*RAE6*(ABX2-ABY2)*A)+2*EFY*ABY3*A*(15
*HM1*RAE2+6*HM1*RAE4)*C-12*HM2*C2*RAE5-30*HM2*RAE3*C+24*HM3*C2
*RAE4+9*HM3*C3*RAE6-6*HM4*RAE2*RAE2)*C+5*HM1*(4*C2*RAE4*ABX2*ABY2
-4*C2*RAE4*ABY4+20*RAE2*RAE2*ABY2*C-5*RAE2*ABX2-20*RAE2*ABY4*
C+25*RAE2*ABY2+8*RAE4*ABY2*C-2*RAE4+35*ABX2*ABY2-35*ABY4)-6*
HM2*(4*C2*(15*RAE3*(ABX2*ABY2-ABY4)+2*RAE5*ABY2)+4*C3*RAE5*(
ABX2*ABY2-ABY4)-5*RAE3*C*(AEX2-5*ABY2)-2*RAE5*C*(C2*(
45*RAE2*(ABX2*ABY2-ABY4)-6*RAE4*(ABX2-5*ABY2)-2*RAE6)+8*C3*(3
*RAB4*(ABX2*ABY2-ABY4)+AEY2*RAE6)+4*C4*RAE6*(ABX2*ABY2-ABY4))
-RAB4*(C3*(10*RAE3*(ABX2*ABY2-ABY4)-RAB5*(ABX2-5*ABY2))+4*C4
*RAB5*(ABX2*ABY2-ABY4))+16*HM5*C4*RAE4*(ABX2*ABY2-ABY4))
ANS3=210*RAB*HM2*(ABX2*ABY2-ABY4)*C+ANS4

```

0289



```

0290 ANS2=PI*ANS3*EXP5 M
0291 ANS1=-ANS2
0292 Q7= ANS1/(8*C5*RAE9)*EXPREF
0293 QINT=Q7*S03/2.D0
0294 RETURN
0295 HVI=-HMI
0296 QINT=2.*PI*HMI/15.*S03
0297 RETURN
C < PX / QR / PY >
0298 IF(RAB.LT.1.D-10) GO TO 581
0299 IF(ITYPE.EQ.2) GO TO 583
0300 A=FXJ
0301 P=FXI
0302 IF(JCINT.H.EQ.1) EFZ=-R
0303 GO TO 582
0304 A=FXI
0305 R=EXJ
0306 IF(ICNTR.EQ.1) EFZ=-R
0307 IF(ICNTR.EQ.1)
  Q8= (-PI*(210*RRAB*ABY*FM2*C*ABX2+ABY*(2*ABX*EFX*2*(8*RRAB6*HM3*
  (FFY*A*C2-C3)+6*EFY*(HMI*RRAB4-2*HM2*C*RRAB5)*A-3*(2*C*RRAB4+5*
  RAB2)*HMI+6*(5*C*RAE2+2*(2*RRAB5)*HM2-2*HM3*C2*RRAB4+8*HM4*C3*
  RAB5)-8*RRAB6*HM3*(EFY*(C2-2*C3*ABX2)*A-(C3-2*CA*ABX2))+2*EFY*
  (3*HMI*(15*RRAB2*ABX2-RAB4)+2*C*RRAB4*ABX2)-6*HM2*((5*RRAB3*ABX2
  -RAB5)*C+2*C2*RAE5*AEX2)+2*HM3*C2*RRAB4*ABX2-8*FM4*C3*RRAB5*
  ABX2)*A-3*HMI*(2*(10*RRAB2*ABX2-RAB4)*C+4*C2*RRAB4*ABX2-5*RRAB2+
  35*AEX2)+6*FM2*(2*(10*RAE3*ABX2-RAB5)*C2-5*C*RRAB3+4*C3*RRAB5*
  ARX2)-12*HM3*((15*RAE2*AEX2-2*FAB4)*C2+9*C3*RRAB4*ABX2)+8*HM4*
  ((10*RRAB3*ABX2-RAB5)*C3+4*C4*RRAB5*ABX2)-16*HM5*C4*RRAB4*ABX2)+
  HMI2*C*RRAB5-4*RRAB6*HM3*C2+8*RRAB6*HM3*C3*ABX2+6*HMI*C*RRAB4*ABX2
  +15*HMI*RRAB2*ABX2-3*HMI*RRAB4-30*HM2*C*RRAB3*ABX2+6*HM2*C*RRAB5-
  12*HM2*C2*RRAB5*AEX2+24*HM3*C2*FAB4*AEX2-8*HM4*C3*RRAB5*ABX2))
  / (8*RAD9*EXP0*EXP5*CE)
  QINT=Q8*FXPREF*S03
  RETURN
0309
0310 QINT=2.*PI*HMI/15.*S03
0311 RETURN
0312 END

```

```

0001 REAL FUNCTION DS1*(R)
0002 IMPLICIT REAL*(A-H,O-Z)
0003 COMMON/INT/C,CK,RAB,DKC
0004 COMMON/POT/POTCK(15),IPOT
0005 DATA PEACH,DALGAR/ 5HPEACH,8H+DALGARND/
0006 IF(R.EQ.0.0D0) GO TO 100
C*** TAKE OUT GO TO 98 FOR PEACH'S CUTOFF
C
C*** PEACH'S CUTOFF FUNCTION ***
0007 CUT=DK*R
0008 CUT=1.D0-DEXP(-CUT)*(1.D0+CUT*(1.D0+.5D0*CUT))
0009 POTCK(1)=PEACH
0010 GO TO 99
0011 CUT=(DK*R)**3
0012 POTCK(1)=DALGAR
0013 IF(CUT.GT.1.D-10) CUT=1.D0-DEXP(-CUT)
0014 IF(RAB.LT.1.D-10) GO TO 200
0015 TGRAB=2.*C*RAB*R
0016 IF(TGRAB.LT.1.D0) GO TO 199
0017 EXPR1=DEXP(-C*(RAB-R)**2)
0018 EXPR2=DEXP(-C*(RAE+R)**2)
0019 DS1=CUT*(EXPR1-EXPR2)/(F**2.)
0020 RETURN
0021 DS1=CLT*DSINH(TGRAB)*DEXP(-C*(R*R+RAB*R))
U/(R*R)
0022 RETURN
0023 DS1=CLT*R*DEXP(-C*R*R)
0024 RETURN
0025 DS1=0.0D0
0026 RETURN
0027 END

```

FORTRAN IV G LEVEL 21

DS2

```

0001 REAL FUNCTION DS2*(R)
0002 IMPLICIT REAL*(A-H,O-Z)
0003 COMMON/INT/C,CK,RAB,DNG
0004 COM/IN/POT/POTCK(15),IPCT
0005 DATA PEACH,DALGAR/ 5*PEACH,8*DALGARND/
0006 IF(R.EQ.0.0DC) GC TC 100
0007 TGPAB=2.*C*RAB*R
C*** TAKE OUT GC TC 98 FOR PEACH'S CUTOFF
C
0008 GO TO 98
C*** PEACH'S CUTOFF FUNCTION **
97 CUT=D*K*R
CUT=1.00-DEXP(-CUT)*(1.00+CUT*(1.00+.500*CUT))
POTCK(2)=PEACH
GO TO 99
98 CUT=(CK*R)**2
PCTCK(2)=DALGAR
IF(CUT.GT.1.0-10) CUT=1.0C-DEXP(-CUT)
99 IF(TGRAB.LT.1.00) GC TC 199
EXPRM=DEXP(-C*(RAB-R)**2)
EXPRD=DEXP(-C*(RAB+R)**2)
DS2=CUT*(EXPRM+EXPRD)/(R**2.)
RETURN
199 DS2=CUT*DCOSH(TGRAB)*DEXP(-C*(R*R+RAB*RAB))/R
RETURN
100 DS2=0.000
RETURN
0023 END
0024

```

```

0001 REAL FUNCTION DS3*(R)
0002 IMPLICIT REAL*(A-H,O-Z)
0003 COMMON/INT/C,DK,RAB,OKG
0004 COMMON/FUT/POTCK(15),IPCT
0005 DATA PEACH,DALGAR/5HFPEACH,RMDALGARND/
0006 IF(R.EQ.0.0D0) GO TO 100
0007 TGRADE=2.*C*RAB*R
      C
      GC TO 99
C*** TAKE OUT GO TC 98 FOR PEACH'S CUTOFF
0008 PEACH'S CUTOFF FUNCTION **
0009 CUT=DK*R
0010 CUT=1.00-DEXP(-CUT)*(1.00+CUT*(1.00+.5D0*CUT))
0011 POTCK(1)=PEACH
0012 GO TO 99
0013 CUT=(CK*R)**3
0014 POTCK(1)=DALGAR
0015 IF(CUT.GT.1.D-10) CUT=1.00-DEXP(-CUT)
0016 IF(TGRAD.LT.1.00) GO TC 199
0017 EXPRM=DEXP(-C*(RAB-R)**2)
0018 DST=CLT*(EXPRM-EXPRM)/2.
0019 RETURN
0020 DS3=CUT*DSINH(TGRAB)*CEXP(-C*(R*R+RAB*RAB))
0021 RETURN
0022 DS3=0.0D0
0023 RETURN
0024 END

```

```

0001 REAL FUNCTION DS4*(R)
0002 IMPLICIT REAL*(A-M,O-Z)
0003 COMMON/INT/C,DK,RAB,DKG
0004 COMMON/POT/POTCK(15),IPCT
0005 DATA PEACH,DALGAR/ SHFFACH,8HICALGARND/
0006 IF(R.EQ.0.000) GO TO 100
0007 TGRAB=2.*C*RAB*R
      C*** TAKE OUT GO TC 98 FOR PEACH'S CUTOFF
      GO TO 98
0008 C*** PEACH'S CUTOFF FUNCTION ***
0009 CUT=DK*R
0010 POTCK(4)=PEACH
0011 GO TO 99
0012 CUT=(DK*R)**3
0013 POTCK(4)=DALGAR
0014 IF(CUT.GT.1.0-10) CUT=1.00-DEXP(-CUT)
0015 IF(TGRAB.LT.1.00) GO TC 199
0016 EXPRM=DEXP(-C*(RAB-R)**2)
0017 EXPRP=DEXP(-C*(RAB+R)**2)
0018 DSA=CLT*(EXPRM+EXPRP)**R/2.
0019 RETURN
0020 DSA=CUT*DCOSH(TGRAB)*[EXP(-C*(R+RAB)*R)]*R
0021 RETURN
0022 DSA=0.000
0023 RETURN
0024 END

```

```

0001 REAL FUNCTION DSS*(P)
0002 IMPLICIT REAL*8(A-H,O-Z)
0003 COMMON/INT/C,DK,RAB,DKQ
0004 COMMON/FACT/PTCK(15),IPCT
0005 DATA PEACH,DALGAR,SHPEACH,8MDALGARNC/
0006 IF(R.EQ.0.0D0) GC TO 100
C*** TAKE OUT GO TO 98 FOR PEACH'S CUTOFF
C
C*** PEACH'S CUTOFF FUNCTION **
0007 CUT=DKQ*R
0008 PTCK(5)=DALGAR
0009 IF(CJT.GT.1.D-10) CUT=1.D0-DEXP(-CUT)*(1.D0+CUT*(.5D0+CUT/6.D0))
0010 GO TO 99
0011 CUT=(DK*R)**4
0012 PTCK(5)=DALGAR
0013 IF(CJT.GT.1.D-10) CUT=1.D0-DEXP(-CUT)
0014 IF(RAB.LT.1.D-10) GO TO 200
0015 TGRAB=2.*C*RAB*R
0016 IF(TGRAB.LT.1.D0) GO TO 199
0017 EXPR4=DEXP(-C*(RAB-R)**2)
0018 EXPRP=DEXP(-C*(RAB+R)**2)
0019 DSS=CUT*(EXPRM-EXPRP)/(R**4*2.)
0020 RETURN
0021 U R***
C55=CUT*DS INH(TGRAB)*DEXP(-C*(R*R+RAB**2))/
0022 RETURN
0023 D55=CUT*R*DEXP(-C*R*R)
0024 RETURN
0025 DSS=0.0D0
0026 RETURN
0027 END

```

```

0001 REAL FUNCTION DS6*(R)
0002 IMPLICIT REAL*(A-H,O-Z)
0003 COMMON/INT/C,DK,RAB,DKQ
0004 COMMON/PUT/PCTCK(15),IFCT
0005 DATA PEACH,DALGAR, SHPEACH,8FDALGARND/
0006 IF(R.EQ.0.0D0) GO TO 100
0007 TGRAB=2.*C*RAB*R
      C*** TAKE OUT GO TO 98 FOR PEACH'S CUTOFF
      C
0008 C*** PEACH'S CUTOFF FUNCTION ***
0009 CUT=DKQ*R
0010 CUT=1.0D0-DEXP(-CUT)*(1.0D0+CUT*(1.0D0+CUT*(.5D0+CUT/6.0D0)))
0011 PCTCK(6)=PEACH
0012 GC TO 99
0013 CUT=(DK*R)**4
0014 IF(CJT.GT.1.D-10) CUT=1.0D0-DEXP(-CUT)
0015 PCTCK(6)=DALGAR
0016 IF(TGRAB.LT.1.0D0) GO TO 159
0017 EXPRM=DEXP(-C*(RAB-R)**2)
0018 EXPRP=DEXP(-C*(RAB+R)**2)
0019 DS6=CUT*(EXPRM+EXPRP)/(R**3*2.)
0020 RETURN
      U/R**3
0021 DS6=CUT*DCOSH(TGRAB)*DEXP(-C*(R*R+RAB*RAB))
0022 RETURN
0023 DS6=0.0D0
0024 END

```

FORTRAN IV 5 LEVEL 21

DS7

```

0001 REAL FUNCTION DS7*(R,P)
0002 IMPLICIT REAL*(A-H,C-Z)
0003 COMMON/INT/C,DK,RAB,DKG
0004 DATA PFACH,DALGAR/ SHFEACH,8,FDALGARNC/
0005 IF(R.EQ.0.0D0) GO TO 100
0006 TGRAB=2.*C*RAB*R
0007
C*** TAKE OUT GO TC 98 FOR PEACH'S CUTOFF
C
0009 C*** PEACH'S CUTOFF FUNCTION ***
0010 CUT=DKG*R
0011 CUT=1.00-DEXP(-CUT)*(1.00+CUT*(1.00+CUT*(.500+CUT/6.0D0)))
0012 POTCK(7)=PEACH
0013 GO TO 99
0014 CUT=(DK*R)**4
0015 POTCK(7)=DALGAR
0016 IF(CUT.GT.1.0D-10) CUT=1.00-DEXP(-CUT)
0017 IF(TGRAB.LT.1.0D) GO TC 199
0018 EXPRM=DEXP(-C*(RAB-R)**2)
0019 EXPRP=DEXP(-C*(RAB+R)**2)
0020 DS7=CLT*(EXPRM-EXPRP)/(R**2.)
RETURN
U / (R**R)
0021 DS7=CUT*DSINH(TGRAB)*CEXP(-C*(R*R+RAB*R))
0022 RETURN
0023 DS7=0.0D0
0024 END

```



```

0001 REAL FUNCTION D58*(R)
0002 IMPLICIT REAL*(A-H,O-Z)
0003 COMMON/INT/C,CK,FAB,DKG
0004 COMMON/POT/PCTCK(15),IPCT
0005 DATA PEACH,DALGAR,SHPFACH,8FDALGARNO/
0006 IF(R.EQ.0.000) GO TO 100
0007 TGRAB=2.*C*RAB*R
      C*** TAKE OUT GO TO 93 FOR PEACH'S CUTOFF
      GO TO 98
C*** PEACH'S CUTOFF FUNCTION ***
97 CUT=DKG*R
  CUT=1.00-DEXP(-CUT)*(1.00+CUT*(1.00+CUT*(.500+CUT/6.00)))
  POTCK(8)=PEACH
  GO TO 99
98 CUT=(DK*R)**4
  POTCK(8)=DALGAR
  IF(CUT.GT.1.0-10) CUT=1.00-DEXP(-CUT)
  IF(TGRAB.LT.1.00) GO TO 155
  EXPRM=DEXP(-C*(RAB-R)**2)
  EXPRP=DEXP(-C*(RAB+R)**2)
  D58=CUT*(EXPRM+EXPRP)/(R**2.)
  RETURN
199 D58=CUT*DCOSH(TGRAB)*DEXP(-C*(R*R+RAB**2))/R
100 D58=0.000
      RETURN
      END

```

```

0001 REAL FUNCTION DS9*(R)
0002 IMPLICIT REAL*8(A-H,D-Z)
0003 COMMON/INT/C,CK,RAB,CKC
0004 COMMON/POT/PCTCK(15),IPCT
0005 DATA PEACH,DALGAR,5*PEACH,8HDALGARND/
0006 IF(R,E0.0,000) GO TC 100
0007 TGRAB=2.*C*RAB*R
      C*** TAKE OUT GO TO 98 FOR PEACH'S CUTOFF
      C
      C*** PEACH'S CUTOFF FUNCTION ***
0008   97 CUT=DKG*R
0009   CUT=1.00-DEXP(-CUT)*(1.00+CUT*(1.00+CUT*(.500+CUT/6.00)))
0010   POTCK(9)=PEACH
0011   GC TO 99
0012   CUT=(DK*R)**4
0013   POTCK(9)=DALGAR
0014   IF(CUT.GT.1.0-10) CUT=1.00-DEXP(-CUT)
0015   IF(TGRAB.LT.1.00) GO TO 159
0016   EXPRM=DEXP(-C*(RAB-R)**2)
0017   EXPRP=DEXP(-C*(RAB+R)**2)
0018   DS9=CUT*(EXPRM-EXPRP)/2.
0019   RETURN
0020   DS9=CLT*D SINH(TGRAB)*DEXP(-C*(R*R+RAB*RAB))
0021   RETURN
0022   DS9=0.000
0023   RETURN
0024   END

```

```

0001 SUBROUTINE ITROMB(FCN,HIN,ERT,NAPP,VINT,IERR,X0)
0002 IMPLICIT REAL*8 (A-H,O-Z)
0003 DIMENSION AUX(10)
0004 COMMON/ERR/NERR
C REQUIRES EXTERNAL STATEMENT FOR FCN
C EVALUATES INT FORM XO TO INF CF (FCN(X) DX)
C BY TRAPEZOIDAL RULE WITH ROMBERG EXTRAPOLATION
C PROG MAY RESULT IN FRROR IN LANDS ON SUCCESSIVE NODES OF FCN(X)
C HIN IN INTERVAL AT WHICH 1ST INTEGRATION DONE
C ERT IS MAX ERROR DESIRED
C NAPP IS MAX NC TIMES INTEGRAL EVALUATED BY TRAP. MUST BE .LE.10
0005 IERR=0
0006 NERR=0
0007 RO=0.0D0
0008 V=0.0D0
0009 HS=HIN
0010 H=HS
0011 X=XO
0012 A=.5D0*FCN(X)
0013 DO 250 N=1,NAPP
0014 NINT=0
0015 X=X+HS
0016 NINT=NINT+1
0017 T=FCN(X)
0018 IF(NERR.NE.0) GC TO 400
0019 IF(DABS(T).LE.ERT*DABS(A/NINT)) GO TO 100
0020 A=A+T
0021 GC TO 50
0022 A=A+T
0023 IF(RO.NE.0.0D0) GC TO 150
0024 NINT=NINT+1
0025 X=X+HS
0026 T=FCN(X)
0027 IF(NERR.NE.0) GO TO 400
0028 IF(DABS(T).LE.ERT*DABS(A/NINT)) GO TO 101
0029 A=A+T
0030 GC TO 50
0031 IF(X.LT.RO) GC TO 50
0032 AUX(N)=H*A+0.5D0*V
0033 FCRMAT(1H,2FNE,15,5X,7H-AUX(N)=D27.16)
0034 IF(DABS(AUX(N)-V).LE.ERT*CABS(V)) GO TO 251
0035 V=AUX(N)
0036 IF(RO.EQ.0.0D0) RO=X
0037 IF(N.EQ.NAPP) GO TO 250
0038 HS=H
0039 H=.5D0*H
0040 X=XO+H
0041 A=FCN(X)
0042 CONTINUE
0043 FCRMAT(1H,12HMAX VALUE X=D13.6)
0044 D=1.0D0
0045 NK=NAPP-1
0046 DC 300 K=1,NK
0047 D=A.*C
0048 NJ=NAPP-K
0049 Y=AUX(NJ+1)
0050 DO 300 J=1,NJ
0051 NA=NAPP-(K+J)+1
0052 AN=AUX(NA)

```

```

0053 AUX(NA)=Y+(Y-AN)/(O-1.)
0054 IF(DABS(AUX(NA)-Y).LE.ERI*DABS(Y)) GC TO 301
0055 Y=AN
0056 CCONTINJE
0057
300
C
0058 IMPLIES NAPP NOT LARGE ENOUGH
0059 SFPR=AUX(NA)-AUX(NA+1)
0060 WRITE(6,500) SFPR,AUX(NA)
0061 FCRMAT(1H,5X,6HEXOR=,C27.16,5X,5HVINT=,D27.16)
0062 VINT=AUX(NA)
0063 FCRMAT(1H,10X,19FITRCMB CONV WITH K=,I5,5X,3HNK=,I5)
0064 RETURN
0065 VINT=AUX(N)
0066 RETURN
0067 IERR=NERR
0068 IF(NERR.NE.3) GO TO 4C1
0069 TR0=FCN(X-HS)
0070 NERR=C
0071 FCRMAT(1H,10HFCN AT R0=,D27.16)
0072 A=AT
0073 GO TO 101
0074 VINT=H*A+.5*V
0075 WRITE(6,602) NERR
0076 FCRMAT(1H0,13FITRCMB ERROR=,I5//)
0077 RETURN
END

```

```

0001 SUBROUTINE NDGG32(XMIN,XMAX,FCN,VINT,N)
0002 IMPLICIT REAL*8(A-H,C-Z)
0003 EXTERNAL FCN
0004 DCES 32 POINT GAUSSIAN QUADRATURE N TIMES ON INTERVAL
0005 XMIN TO XMAX IN EQUAL SUBINTERVALS
0006 VINT=0.000
0007 STEP=(XMAX-XMIN)/N
0008 XMINI=XMIN
0009 DC 100 IN=1,N
0010 XMAXI=XMINI+STEP
0011 CALL DGG32(XMINI,XMAXI,FCN,VINTI)
0012 VINT=VINT+VINTI
0013 XMINI=XMAXI
0014 RETURN
600 FORMAT(1H ,10X,6HVINTI=,E27.16)
END

```

```

0001 REAL FUNCTION RINT*(IDUM)
0002 IMPLICIT REAL*8(A-H,C-Z)
0003 P*AL*8 K,K2,K3,K4,K5,K6
0004 REAL*4 SEC
0005 LOGICAL INTC,LA
0006 EXTERNAL GS1,GS2,CS3,CS4,GS5,GS6
0007 COMMON/INT/C,DK,RAB,DRG,I,ITYPE
0008 COMMON/SCLR/EXI,FXJ,I,ITYPE,J,ITYPE,ICNTR,R,K,CUT2,CUT3,
0009 U,ALPHA,ALPHAC,AP(4),LA(6),RINTG(6)
0010 COMMON/POY/PCTCK(15),IPCT
0011 DATA PI,RTPI/3.14159265358979D0,1.7724538E090551D0/
0012 DATA NAPP,STEMP/3,1000.00/
0013 C*****WARNING: INTERVALS FOR GAUSSIAN QUAD DECREASED*****
0014 PHI(X)=DFRF(X)
0015 SINH(X)=DSINH(X)
0016 COSH(X)=DCCSH(X)
0017 C PPROGRAM USES INTEGRAL EXPRESSIONS OBTAINED FROM REDUCE
0018 C IITYPE=1,5
0019 C 2,PX
0020 C 3,PY
0021 C 4,PZ: Z ASSUMED TO BE ALONG DIRECTION OF BOND
0022 ICNTR=1 FOR A, THE CLOSEST SHELL ATOM ON WHICH EFFECTIVE POTENTIAL
0023 IS CENTERED
0024 C 2 FOR ATOM B, NON-CLOSED SPELL
0025 IITYPE=ITYPE
0026 DO 99 I=1,6
0027 RINTG(I)=0.0D0
0028 R1=0.0D0
0029 R2=0.0D0
0030 R3=0.0D0
0031 R4=0.0D0
0032 R5=0.0D0
0033 R6=0.0D0
0034 IF(IPBT.EQ.0) GO TC 100
0035 DK=0.0D0
0036 DK=CUT2
0037 GO TO 99
0038 DK=K
0039 RINT=C.0D0
0040 IF(ITYPE.LE.4.AND.JTYPE.LE.4) GC TO 101
0041 WRITE(6,600) IITYPE,JTYPE
0042 FORMAT(1H,25H*****EFCF***** /
0043 U 1H,6H IITYPE=15,5X,6H JTYPE=15 /
0044 U 1H,24H ONLY TYPE .LE.4 ALLOWED /
0045 U 1H,20H***** /
0046 RETURN
0047 IF(ITYPE.FQ.JTYPE.OR.(ITYPE.EQ.1.AND.JTYPE.EQ.4).OR.(ITYPE.EQ.4
0048 .AND.JTYPE.EQ.1)) GO TO 102
0049 RETURN
0050 C=EXI+EXJ
0051 EXPO=1.00
0052 IF(ICNTR.EQ.JCNTR) GC TC 110
0053 EXPREF=DEXP(-EXI*EXJ**2/C)
0054 IF(EXPREF.EQ.0.0D0) RETURN
0055 IF(ICNTR.EQ.1) GC TC 105
0056 PAB=EXI*R/C
0057 GC TO 150

```

```

0045 RAB=EXJ*R/C
0046 GO TO 150
0047 EXPREF=1.D0
0048 IF(ICNTR.EQ.1) GO TO 115
0049 RAB=R
0050 GC TO 150
0051 WAB=0.0D0
0052 PTC=DSORT(C)
0053 IF(IITYPE.NE.1.OR.JTYFE.NF.1).AND.IITYPE.NE.JTYFE.AND
      U RAB.LT.1.D-10) GO TO 200
C DEF
0054 EXP1 = DEXP(K**2/(4*C))
0055 EXP2 = DEXP(K*RAB)
0056 EXP5M=DEXP(-C*RAB**2)
0057 RAM = RAB - K/(2*C)
0058 RAP = RAB + K/(2*C)
0059 IF(LA(1)) GC TO 114
0060 PHIMC=DERFC(-RTC*RAM)
0061 PHIPC=DERFC(RTC*RAP)
0062 PHIOC=PHIPC
0063 EXP22=EXP 2**2
0064 C2=C*C
0065 C4=C2*C2
0066 C5=C4*C
0067 C6=C5*C
0068 RAB2=RAB*RAB
0069 RAP3=RAB*RAP2
0070 K2=K*K
0071 K3=K2*K
0072 K4=K2**2
0073 RAP2=RAP**2
0074 RAP3=RAP2*RAP
0075 RAM2=RAM**2
0076 RAM3=RAM2*RAM
0077 REXP=DSORT(-DLGG(1.D-10)/C)
0078 RMIN=DVAX1(RAB-REXP,C.0C0)
0079 RMAX=FAB+HEXP
0080 I NTC=(C.LT..2D0.CF.(C.LE..2D0.AND.RAE.GT.10.D0)
      U .OR.(C.GE.1.D3.AND.PAB.LT..1D0))
C
C*****WARNING: ALL INTEGRALS DONE BY DGG32
C*****REMOVE C TO GET ITROME*****
P3=3.
P5=5.
IF(RAB.GT.1.D-10) GO TO 116
P3=2.
P5=4.
0081 RMAX1=DMINI(RMAX,1.D10**(1./P3))
0082 RMAX2=DMINI(RMAX,1.D10**(1./P5))
0083 IF(.NOT.LA(1)) CALL NCG32(RMIN,RMAX1,GS1,HM1,NGC)
0084 IF(.NOT.LA(2)) CALL NCG32(RMIN,RMAX2,GS2,HM2,NGC)
0085 GO TO 120
0086 F=EXP(RAB+REXP-RMIN)/STEM
0087 H=ENI=(1.D8)**(1./3.)/STEM
0088 HMIN2=1.D8**-.2/STEM
0089 HINI=DMINI(HEXP,PCEN1)*2**(NAPP-1)
0090 HIN2=DMINI(HEXP,HEN2)*2**(NAPP-1)
0091 IF(.NOT.LA(1)) CALL ITROME(GS1,HINI,1.D-8,NAPP,HM1,IERR,RMIN)
0092 IF(.NOT.LA(2)) CALL ITROME(GS2,HIN2,1.D-8,NAPP,HM2,IERR,RMIN)

```

```

0094 CONTINUE
0095 FORMAT(1H , 4HMMU=.E15.6,5X,SHM21=.E15.6)
0100 IF(IJTYPE.NE.1.CR.JTYPE.NE.1) GO TO 200
C < S / R / S > INTEGRALS
0101 IF(RAE.LT.1.D-10) GO TO 160
C DEF R1 ETC
0102 IF(.NOT.LA(1)) R1=(2*PI*EXPREF*HM1)/(RAB*C)
0103 IF(.NOT.LA(2)) R2=(2*PI*EXPREF*HM2)/(RAB*C)
0104 IF(LA(3)) GO TO 131
0105 R3=(RTPI*PI*(K*(PHIPC*EXP22-PHIMC)+2*RAB*(PHIPC*EXP22+PHIMC)*
C)*EXPI)/(4*FAB*RTC*EXP2*C2)*EXPREF
0106 IF(LA(4)) GO TO 122
0107 RA=(-PI*(4*K*RAB*RTC*RTPI*EXP1*(PHIPC*EXP22+PHIMC)*C-8*RAB*
C*EXP2*EXPSM*C2+PHIPC*FTC*RTPI*EXPI*(4*C2*RAB2*K2+2*C)*EXP22-
C*RTC*RTPI*EXPI*PHIMC*(4*C2*RAB2*K2+2*C)))/(8*RAB*EXP2*C4)*EXPREF
0108 IF(LA(5)) GC TC 133
0109 R5=(-DI*(2*K*(8*FAB*EXP2*EXPSM*C2-3*EXPI*RTC*RTPI*(2*C2*RAB2+
C)*(PHIPC*EXP22-PHIMC))-6*RAB*EXPI*RTC*RTPI*(2*C2+K2*C))*
C*PHIPC*FXP22+PHIMC)-EXPI*FTC*RTPI*(PHIPC*EXP22*(8*C3*RAB3*K3)+
C*PHIMC*(8*C3*RAB3-K3)))/(16*RAB*EXP2*C5)*EXPREF
0110 IF(LA(6)) GC TO 500
0111 R6=(-RTPI*PI*EXPI*(PHIPC*EXP22-PHIMC))/(2*RAB*RTC*EXP0*EXP2*C
C)
C R6=R5*EXPREF
0112 GO TO 500
0113 IF(.NOT.LA(1)) R1=(2*PI*HM1)/( EXP0*C)
0114 IF(.NOT.LA(2)) R2=(2*PI*HM2)/( EXP0*C)
C DEF P3 ETC
0116 IF(LA(3)) GC TC 161
0117 R3=(-PI*(2*K*RTC*RTPI*(K2+2*C)*EXPI*PHI0C))/(2*RTC*C2)
0118 IF(LA(4)) GO TO 162
0119 R4=(-PI*(6*K*RTC*RTPI*EXFI*PHI0C*(FTC*RTPI*EXPI*PHI0C*K3-8*
C2-2*K2*C)))/(4*C4)
0120 IF(LA(5)) GO TO 163
0121 R5=(-PI*(20*K*C2-RTC*EXFI*RTPI*PHI0C*(12*C2+12*K2*C+K4)+2*K3*
C))/(8*C5)
0122 IF(LA(6)) GC TC 500
0123 R6=(-PI*(K*RTPI*EXPI*PHI0C-2*RTC))/(RTC*C)
0124 GC TO 500
0125 IF(RAB.NE.0.CR.IJTYPE.EG.JTYPE) GO TO 201
0126 RINT=C.0D0
0127 RETURN
0128 CC=C3*C3
0129 RAD4=RAB2*RAB2
0130 RAB5=FAB4*RAE
0131 IF(RAB.LT.1.D-10) GO TO 300
C IF(INTC) GO TO 170
0132 RMAX1=DMINI(RMAX,1.D10**.5)
0133 RMAX2=DMINI(RMAX,1.D1C**.25)
0134 IF(.NOT.LA(1)) CALL NCG32(RMIN,RMAX1,GS3,HM2,NGQ)
0135 IF(.NOT.LA(2)) CALL NCG32(RMIN,RMAX2,GS4,HM2,NGQ)
0136 GC TO 171
0137 HDEN1=1.D4/STEPM
0138 HDEN2=1.D2/STEPM
0139 FMIN=DMINI(HEXP,HDEN1)*2*(NAPP-1)
0140 HMIN2=DMINI(HEXP,HDEN2)*2*(NAPP-1)
0141 IF(.NOT.LA(1)) CALL ITROVB(GS3,HINI,1.D-8,NAPP,HM2,IERR,RMIN)
0142 IF(.NOT.LA(2)) CALL ITREME(GS4,FIN2,1.D-8, NAPP, HM22, IERR,RMIN)
0143 CONTINUE

```





```

0174      1/( RAB3*C2)
0175      IF(LA(3)) GO TO 211
          R3=(PI*ABX*(K*(PHIPC*RTPI*EXP1*(2*RAB2*C-1))*EXP22-RTPI*EXP1*
          PHIMC*(2*RAB2*C-1))-4*EXP2*RAB*RTC*EXP5M)+PHIPC*RTPI*EXP1*RAB*
          K2*EXP22*RTPI*EXP1*AB*PHIMC*K2)/(8*EXP2*RTC*C3*RAB3)
0176      IF(LA(4)) GO TO 212
0177      RA=(-PI*ARX*(2*K*RTIC*RTPI*EXF1*(RAB*(PHIPC*EXP22+PHIMC))*C+2*
          PHIPC*C2*RAB3*EXP22+2*PHIMC*C2*RAB3)+RAB*(PHIPC*RTIC*RTPI*EXP1
          *K3*EXP22+(RTIC*RTPI*EXF1*PHIMC*K3-4*EXP2*(2*C2+K2*C))*EXP5M))+
          PHIPC*RTIC*RTPI*EXF1*((4*RAB2*C-1)*K2+4*C2*RAB2-2*C)*EXP22-RTIC
          *RTPI*EXF1*PHIMC*((4*RAB2*C-1)*K2+4*C2*RAB2-2*C))/(16*EXP2*
          C5*RAB3)
0178      IF(LA(5)) GO TO 213
0179      RF=(-PI*ARX*(2*K*(12*RAB*EXP2*EXP5M*C2-EXP1*RTC*RTPI*(PHIPC*
          EXP22-PHIMC))*(12*C2*RAE2+4*C3*RAE4-3*C)+8*EXP2*EXP5M*C3*RAB3)
          -RAB*(EXF1*RTIC*RTPI*(PHIPC*EXP22+PHIMC))*(6*K2*C+K4)-4*EXP2*
          EXP5M*K3*C)-EXF1*RTIC*RTPI*(PHIPC*EXP22*(12*C2*K2*RAB3+16*C3*
          RAB3+K3*(6*RAB2*C-1))+PHIMC*(12*C2*K2*RAB3+16*C3*RAB3-K3*(6*
          RAB2*C-1)))/(32*EXP2*C6*RAB3)
0180      IF(LA(6)) GO TO 500
0181      R6=(-PI*ABX*(K*RTPI*EXF1*RAB*(PHIPC*EXP22+PHIMC)-PHIPC*RTPI*
          EXP1*EXP22*RTPI*EXF1*PHIMC-4*EXP2*RAB*RTC*EXP5M))/(4*EXP2*RTC
          *C2*RAB3)
          GC TO 500
0182      C7=C5*C
0183      RAB6=RAB3*PAR3
0184      RAB7=RAB5*RAB
0185      K5=K4*K
0186      K6=K5*K
0187      IF(RAE.LT.1.D-10) GO TO 309
0188      IF(ITYPE.NE.4) GC TO 302
0189      IF(INTC) GO TO 301
          RMAX1=DMINI(RMAX,1.D10)
          RMAX2=DMINI(RMAX,1.D1C*(1./3.))
          IF(.NOT.LA(1)) CALL NDCG32(RMIN,RMAX1,G55,HM3,NGQ)
          IF(.NOT.LA(2)) CALL NDCG32(RMIN,RMAX2,G56,HM6,NGQ)
          GO TO 302
0190      HDEN1=1.D8/STEPM
0191      HDEN2=(1.D8)**(1./3.)/STEPM
0192      HINI=DMINI(HEXP,HDEN1)*2*(NAPP-1)
0193      HIN2=DMINI(HEXP,HDEN2)*2*(NAPP-1)
0194      IF(.NOT.LA(1)) CALL ITRCME(G56,HIN1,1.D-8,NAPP,HM3,IERR,RMIN)
0195      IF(.NOT.LA(2)) CALL ITRCME(G56,HIN2,1.D-8,NAPP,HM6,IERR,RMIN)
          CONTINUE
0200      FORMAT(1H ,4FHM3=E15.6,5X,4HHM6=E15.6)
0201      C < P / R / P > INTEGRALS
0202      I+23=HM6
          ABX=0.0D0
          EFY=0.0D0
          IF(ITYPE.NE.4) GO TO 310
          ARX=RAB
          IF(ICNTR.NE.JCNTR) EFY=R
          APX2=ABX*ABX
          EFY2=EFY*EFY
          IF(ICNTR.NE.2) GO TO 311
          R=FXJ
          GC TO 312
0203      A=FXJ
0204      GC TO 311
0205
0206
0207
0208
0209
0210
0211
0212
0213
0214
0215

```

0216

DEFI  
312 IF(RAR\*LT\*.1D-19) GO TO 350  
IF(ICNTR\*EQ\*JCNTR) GO TO 320

0217

C DEF

0219 IF(.NOT.LA(1)) R1=(PI\*(4  
\*ARX2\*HM2-2\*AA\*(2\*F\*RAEA\*EFX2\*FM1-2\*CARX\*EFX\*(  
RAB3\*HM2-RAB4\*HM1)+RAB2\*AHX\*EFX\*HM1)-2\*ABX\*EFX\*(  
(2\*C\*(RAB3\*HM2-RAB4\*FM1)-RAB2\*HM1)+2\*C\*(2\*  
RAB2\*ARX2\*FM1+RAB3\*HM2)-RAB2\*HM1-8\*RAB3\*C2\*ABX2\*FM2  
+4\*RAB4\*C2\*ABX2\*HM1+3\*ARX2\*HM1))/(2\*  
\*PAB5\*C3)  
P1=R1\*EXPREF  
FM1=HM21  
HM2=HM22  
HM3=HM23

0220

C DEF

0224 IF(.NOT.LA(2)) R2=(FI\*(4  
\*ARX2\*HM2-2\*AA\*(2\*P\*RARAB4\*EFX2\*HM1-2\*CAHX\*EFX\*(  
RAB3\*HM2-RAB4\*HM1)+RAB2\*ABX\*EFX\*FM1)-2\*ABX\*EFX\*(  
(2\*C\*(RAB3\*HM2-RAB4\*HM1)-RAB2\*HM1)+2\*C\*(2\*  
RAP2\*ARX2\*FM1+RAB3\*HM2)-RAB2\*HM1-8\*RAB3\*C2\*ABX2\*HM2  
+4\*RARAB4\*C2\*ABX2\*HM1+3\*ABX2\*HM1))/(2\*  
\*PAB5\*C3)  
R2=R2\*EXPREF

0225

IF(LA(3)) GO TO 313

R3=(PI\*(PHIPC\*RTPI\*EXPI\*(2\*AB\*(ABX\*EFX\*(RAB2-2\*RAB4\*C)-2\*  
RAB4\*EFX2\*AA)-2\*ABX\*EFX\*(RAB2-2\*RAB4\*C)\*A-(2\*ABX2\*C+1)\*RAB2+4\*  
RAB4\*C+3\*ABX2)\*EXP22-RTPI\*EXPI\*PHIMC\*(2\*E\*(AEX\*FFX\*(HAB2-2\*  
RAB4\*C)-2\*ARAB4\*EFX2\*AA)-2\*ABX\*EFX\*(RAB2-2\*RAB4\*C)\*A-(2\*ABX2\*C+  
1)\*RAB2+4\*ARAB4\*C+3\*ABX2)+4\*EXP22\*RTC\*(3\*ARAB4\*EFX2+2\*ABX\*FFX\*  
RAB3-(2\*ARX\*EFX\*AA+1)\*RAB2)\*EXP5M)-PHIPC\*RTPI\*EXPI\*(3\*RAB\*  
ARX2+2\*AR\*(ARX\*EFX\*AA+1)\*RAB3+4\*ARAB5\*EFX2\*AA)-2\*ABX\*EFX\*  
A-(2\*ABX2\*C+1)\*RAB2+4\*ARAB5\*EFX2\*AA)-2\*ABX\*EFX\*  
EXPI\*PHIMC\*(3\*ARAB5\*EFX2\*AA+1)\*RAB2+4\*ARAB5\*EFX2\*AA)-2\*ABX\*EFX\*  
AA)-2\*ABX\*EFX\*AA+1)\*RAB2+4\*ARAB5\*EFX2\*AA)-2\*ABX\*EFX\*  
RAB2\*ABX2))/(16\*EXP2\*RTC\*C4\*ARAB5)\*EXPREF

0228

313

ANS3=(RTC\*RTPI\*EXPI\*PHIMC\*(2\*AB\*(ABX\*EFX\*(RAB2-4\*PAB4\*C)\*K2-4\*  
C\*PAB4\*K3\*ARAB3+2\*ARAB2\*C)-8\*C2\*EFX2\*ARAB4\*AA-2\*K2\*PAB4\*EFX2\*AA-4\*  
\*PAB4\*EFX2\*C\*AA)-2\*ABX\*EFX\*(RAE2-4\*ARAB4\*C)\*K2-4\*C2\*ARAB4\*K3\*  
PAB3+2\*PAB2\*C)\*AA+4\*(K2\*ARAB4\*ABX2-RAB2\*ABX2+2\*RAA4)\*C2-((2\*  
APX2\*C+1)\*RAB2-6\*RAE4\*C-3\*ARAB4\*C)\*K2-(4\*ABX2\*C+1)\*K3\*ARAB3\*P\*  
RAB6\*K\*PAB2\*ABX2-2\*PAB2\*C+6\*ABX2\*C)-4\*EXP22\*(2\*E\*(ARX\*EFX\*(2\*  
C+K2\*C)\*RAB3+1)\*C2\*PAB5\*EFX2\*AA)-2\*ABX\*EFX\*(2\*C2\*PAB3\*C)\*  
(2\*(K2\*ABX2+1)\*C2\*RAE3+4\*C3\*RAE5+K2\*PAB3\*C)\*EXP5M)  
ANS2=2\*K\*RTC\*RTPI\*EXPI\*(3\*ARAB\*(PHIPC\*EXP22\*PHIMC)\*ARX2\*C+PHIPC  
\*(2\*F\*(APX\*EFX\*(2\*C2\*RAE5\*RAE3\*C)+4\*ARAB5\*EFX2\*AA)+2\*ABX\*EFX\*  
(2\*C2\*ARAB5\*ARAB3\*C)\*A-2\*(PAB3\*ARX2+3\*RAA5)\*C2-PAB3\*C)\*EXP22+  
PHIMC\*(2\*C2\*ARAB5\*ARAB3\*C)\*AA-2\*(RAB3\*ARX2+3\*RAA5)\*C2-PAB3\*C)\*  
RAB\*(PHIPC\*RTC\*RTPI\*EXPI\*PHIMC\*(2\*E\*(ARX\*EFX\*(2\*ARAB5\*EFX2\*AA)+3\*  
EXP22\*(2\*C2+K2\*C)\*EXP5M))\*ABX2-PHIPC\*RTC\*RTPI\*EXPI\*PHIMC\*(2\*E\*(ARX\*  
EFX\*(RAB2-4\*ARAB4\*C)\*K2-4\*ARAB4\*EFX2\*AA)-2\*ABX\*EFX\*(RAB2-4\*  
PAB6\*AA-2\*K2\*ARAB4\*EFX2\*AA-4\*ARAB4\*EFX2\*AA)-2\*ABX\*EFX\*(RAB2-4\*  
RAB4\*C)\*K2-4\*C2\*PAB4-K3\*ARAB3+2\*ARAB2\*C)\*AA+4\*(K2\*PAB4\*ARX2-RAB2  
\*ARX2+2\*ARAB4)\*C2-((2\*ARX2\*C+1)\*PAB2-(PAP4\*C-3\*AEX2+4\*  
APX2\*C+1)\*K3\*ARAB3+8\*C3\*ARAB4\*K4\*PAB2\*ABX2-2\*ARAB2\*C+6\*ARX2\*C)  
EXP22+ANS3  
ANS1=FI\*ANS2

0231

```

0210 C DEF ANS1/(16*EXP2+C6*HAB5)*EXPREF
0211 IF(LA(5)) GO TO 315
0212 C RAB5+K3*HAB3+C-K3*(RAB2-6*HAB4+C)*K4*HAB3)+A+12*C2*(2*K2*
0213 (RAB3*ABX2+PAD5+K2*HAF4*AEK2)+H3*C3*HAB5)*K4*AEK2+5)+16*C4*
0214 (RAB7+K2*HAB3+C-K3*(RAB2-6*HAB4+C)-3*HAB5)+K4*HAB3*(6*HAB2+C+
0215 1)+K5*HAB2*ABX2)*PHIMC*(2*HAB5*EFX*(12*C2*HAB2*PAR5+16*C3*HAB5+6
0216 *H2*HAB3*HAB2*HAB3)+K4*HAB5)*K4*HAB3*(6*HAB2+C+1)+K5*HAB2*
0217 (RAB2-6*HAB4+C)-3*HAB5)+K4*HAB3*(6*HAB2+C+1)+K5*HAB2*
0218 (RAB2-6*HAB4+C)-3*HAB5)+K4*HAB3*(6*HAB2+C+1)+K5*HAB2*
0219 (RAB2-6*HAB4+C)-3*HAB5)+K4*HAB3*(6*HAB2+C+1)+K5*HAB2*
0220 (RAB2-6*HAB4+C)-3*HAB5)+K4*HAB3*(6*HAB2+C+1)+K5*HAB2*
0221 (RAB2-6*HAB4+C)-3*HAB5)+K4*HAB3*(6*HAB2+C+1)+K5*HAB2*
0222 (RAB2-6*HAB4+C)-3*HAB5)+K4*HAB3*(6*HAB2+C+1)+K5*HAB2*
0223 (RAB2-6*HAB4+C)-3*HAB5)+K4*HAB3*(6*HAB2+C+1)+K5*HAB2*
0224 (RAB2-6*HAB4+C)-3*HAB5)+K4*HAB3*(6*HAB2+C+1)+K5*HAB2*
0225 (RAB2-6*HAB4+C)-3*HAB5)+K4*HAB3*(6*HAB2+C+1)+K5*HAB2*
0226 (RAB2-6*HAB4+C)-3*HAB5)+K4*HAB3*(6*HAB2+C+1)+K5*HAB2*
0227 (RAB2-6*HAB4+C)-3*HAB5)+K4*HAB3*(6*HAB2+C+1)+K5*HAB2*
0228 (RAB2-6*HAB4+C)-3*HAB5)+K4*HAB3*(6*HAB2+C+1)+K5*HAB2*
0229 (RAB2-6*HAB4+C)-3*HAB5)+K4*HAB3*(6*HAB2+C+1)+K5*HAB2*
0230 (RAB2-6*HAB4+C)-3*HAB5)+K4*HAB3*(6*HAB2+C+1)+K5*HAB2*
0231 (RAB2-6*HAB4+C)-3*HAB5)+K4*HAB3*(6*HAB2+C+1)+K5*HAB2*
0232 (RAB2-6*HAB4+C)-3*HAB5)+K4*HAB3*(6*HAB2+C+1)+K5*HAB2*
0233 (RAB2-6*HAB4+C)-3*HAB5)+K4*HAB3*(6*HAB2+C+1)+K5*HAB2*
0234 (RAB2-6*HAB4+C)-3*HAB5)+K4*HAB3*(6*HAB2+C+1)+K5*HAB2*
0235 (RAB2-6*HAB4+C)-3*HAB5)+K4*HAB3*(6*HAB2+C+1)+K5*HAB2*
0236 (RAB2-6*HAB4+C)-3*HAB5)+K4*HAB3*(6*HAB2+C+1)+K5*HAB2*
0237 (RAB2-6*HAB4+C)-3*HAB5)+K4*HAB3*(6*HAB2+C+1)+K5*HAB2*
0238 (RAB2-6*HAB4+C)-3*HAB5)+K4*HAB3*(6*HAB2+C+1)+K5*HAB2*
0239 (RAB2-6*HAB4+C)-3*HAB5)+K4*HAB3*(6*HAB2+C+1)+K5*HAB2*
0240 (RAB2-6*HAB4+C)-3*HAB5)+K4*HAB3*(6*HAB2+C+1)+K5*HAB2*
0241 (RAB2-6*HAB4+C)-3*HAB5)+K4*HAB3*(6*HAB2+C+1)+K5*HAB2*
0242 (RAB2-6*HAB4+C)-3*HAB5)+K4*HAB3*(6*HAB2+C+1)+K5*HAB2*
0243 (RAB2-6*HAB4+C)-3*HAB5)+K4*HAB3*(6*HAB2+C+1)+K5*HAB2*
0244 (RAB2-6*HAB4+C)-3*HAB5)+K4*HAB3*(6*HAB2+C+1)+K5*HAB2*
0245 (RAB2-6*HAB4+C)-3*HAB5)+K4*HAB3*(6*HAB2+C+1)+K5*HAB2*
0246 (RAB2-6*HAB4+C)-3*HAB5)+K4*HAB3*(6*HAB2+C+1)+K5*HAB2*
0247 (RAB2-6*HAB4+C)-3*HAB5)+K4*HAB3*(6*HAB2+C+1)+K5*HAB2*
0248 (RAB2-6*HAB4+C)-3*HAB5)+K4*HAB3*(6*HAB2+C+1)+K5*HAB2*

```

```

0249 RA= (PI*(2*K*NTC*RTPI*EXPI*(3*RAB*(PHIPC*EXP22+PHIMC)*ABX2*C-
    PHIPC*(2*(RAB3*ABX2+3*AB5)*C2*RAB3*C)*EXP22-PHIMC*(2*(RAB3*
    ABX2+3*AB5)*C2+RAB3*C))+3*RAB*(PHIPC*RTPI*EXPI*(K3*EXP22+
    (RTC*RTPI*EXPI*PHIYC*K3-4*EXP22*(2*C2+K2*C)*EXPM))*ABX2-PHIPC
    *RTPI*EXPI*(4*(K2*RAE4*APX2-RAB2*ABX2+2*RAB4)*C2-(2*ABX2
    *C+1)*RAB2-6*RAB4*C-3*ABX2)*K2+(4*ABX2*C+1)*K3*FA93+3*C3*RAB6
    *K4*RAB2*ABX2-2*RAB2*C+6*ABX2)*EXP22+(RTC*RTPI*EXPI*PHIMC*(
    *(K2*RAE4*ABX2-RAB2*AE2+2*RAB4)*C2-(2*ABX2*C+1)*RAB2-6*
    *RAB4*C-3*ABX2)*K2-(4*ABX2*C+1)*K3*RAB3+8*C3*RAB6+K4*RAB2*ABX2
    -2*RAB2*C+6*ABX2*C)+4*EXP22*(2*(K2*ABX2+1)*C2*RAB3+4*C3*RAB5+
    *K2*RAB3*C)*EXPM))/ (32*EXP22*C6*RAE5)
322 IF(LA(5)) GO TO 323
0250 R5= (PI*(2*K*(36*FAB4*EXP22*EXP5M*C2*ABX2-EXP1*RTC*RTPI*(12*C2*
0251 *RAB2*ARX2-18*C2*RAB4-12*C3*RAR4*ABX2-16*C3*RAB6+3*RAB2*C-9*
    *ARX2*C)*(PHIPC*EXP22-PHIMC)-12*EXP22*EXP5M*(C2*RAB3+2*C3*(RAH3
    *ABX2+RAB5)))-3*RAB*ABX2*(EXPI*RTPI*RTPI*(PHIPC*EXP22+PHIMC))*(
    *K2*C*K4)-4*EXP22*EXP5M*K3*C)+EXPI*RTC*RTPI*(PHIPC*EXP22*(12*
    *C2*(2*K2*(RAE3*ABX2+RAE5)*K3*RAE4*ABX2)+8*C3*RAB5*(K2*ABX2+5)
    +16*C4*RAE7+6*K2*PAB3*C-K3*(RAB2-8*RAB4*C-3*ABX2)+K4*RAB3*(6*
    *ABX2*C+1)*K5*RAB2*ABX2)+PHIMC*(12*C2*(2*K2*(RAB3*ABX2+RAB5)-
    *K3*RAE4*ABX2)+8*C3*RAE5*(K2*ABX2+5)+16*C4*RAE7+6*K2*RAE3*C+K3
    *(RAB2-8*RAE4*C-3*ABX2)+K4*RAE3*(6*ABX2*C+1))-K5*RAE2*ABX2))-4
    *EXP22*EXP5M*K3*RAE3*(4*C2*AE2*C))/ (64*EXP22*C7*RAB5)
323 IF(LA(6)) GO TO 500
0252 R6= (PI*(K*RTPI*EXPI*(3*RAB*ABX2-RAB3)*(PHIPC*EXP22+PHIMC)-
0253 *PHIPC*RTPI*EXPI*(K2*RAE2*ABX2-RAB2+2*RAB4*C+3*ABX2)*EXP22+
    *RTPI*EXPI*PHIMC*(K2*RAB2*ABX2-RAB2+2*RAB4*C+3*ABX2))-4*EXP22*
    *RTC*((2*ABX2*C-1)*RAE3+3*RAE*ABX2)*EXPM))/ (9*EXP22*RTC*C3*
    *RAB5)
GC TO 500
0254 IF(.NOT.LA(1)) R1=4*PI/3*PI
0255 IF(.NOT.LA(2)) R2=4*PI/3*PI
0256 C DEF
0257 IF(LA(7)) GC TO 351
0258 P3= (-PI*(20*K*RTC*C-RTPI*EXPI*PHI0C*(12*C2+12*K2*C+K4))+2*RTC*
    *K3))/(P4*RTC*C4)
0259 IF(LA(4)) GO TO 352
0260 R4= (-PI*(60*K*RTC*RTPI*EXPI*PHI0C*C2+(RTC*RTPI*EXPI*PHI0C*(20
    *K3*C+K5)-36*C2*K2-64*C3-2*K4*C)))/(48*C6)
0261 IF(LA(5)) GO TO 353
0262 R5= (-PI*(264*K*C3-RTC*EXPI*RTPI*PHI0C*(180*C2*K2+120*C3+30*K4
    *C+K6))+2*(24*C2*K3+K5*C)))/(96*C7)
0263 IF(LA(6)) GO TO 500
0264 R6= (-PI*(6*K*RTPI*EXPI*PHI0C*C+RTPI*K3*EXPI*PHI0C-2*RTC*(K2+4
    *C)))/(12*RTC*C3)
0265 RINT=R1
0266 RINTG(2)=R2
0267 RINTG(3)=R3
0268 RINTG(4)=R4
0269 RINTG(5)=R5
0270 RINTG(6)=R6
0271 FORMAT(1H ,2X,1H1,4X,2HF1/6(1H ,3X,E20.12/),1H ,5SHRINT=E20.12)
0272 RETURN
0273 END

```

```

0001 REAL FUNCTION GS1*(R)
0002 IMPLICIT REAL*(A-H,O-Z)
0003 COMMON/INT/GAM,DK,RAB,DKG, ITYPE
0004 COMMON/PUT/PCTCK(15),IPC1
0005 DATA PEACH,DALGAR, 5*PEACH, 9+DALGARND /
0006 IF(R.LT.1.D-10) GC TC 100
0007 R2=R*R
0008 R3=R2*R
0009 C*** TAKE OUT GO TC 99 FOR PEACH'S CUTOFF
0010 C
0011 C*** PEACH'S CUTOFF FUNCTION ***
0012 97 CUT=DK*R
0013 CUT=1.00-DEXP(-CUT)*(1.00+CUT*(1.00+CUT*.500))
0014 CUT=CLT*CUT
0015 PCTCK(10)=PEACH
0016 GC TO 99
0017 9A CUT=DK**6*R3**2
0018 PCTCK(10)=DALGAR
0019 IF(CUT.GT.1.D-10) CUT=1.00-DEXP(-CUT)
0020 IF(RAB.LT.1.D-10) GO TO 110
0021 GS1=CUT*(DEXP(-GAM*(R-RAB)**2)/(R3*2.)
0022 U -DEXP(-GAM*(R+RAB)**2))/(R3*2.)
0023 RETURN
0024 110 IF(ITYPE.NE.1) GC TC 120
0025 GS1=CUT*DEXP(-GAM*R2)*2.*GAM/R2
0026 RETURN
0027 100 GS1=0.000
0028 RETURN
0029 120 GS1=CUT*DEXP(-GAM*R2)
0030 C CHECK THIS EQU
0031 RETURN
0032 END

```

```

0001 REAL FUNCTION GS2*(R)
0002 IMPLICIT REAL*8(A-H,C-Z)
0003 COMMON/INT/GAM,DK,RAB,DKG,ITYPE
0004 COMMON/POT/POTCK(15),IPOT
0005 DATA PEACH,DALGAR/ 5FFACH,8FDALGARND/
0006 IF(P.LT.1.0-10) GC TO 100
0007 R2=R*R
0008 R4=R2*R2
0009 C*** TAKE OUT GO TO 98 FOR PEACH'S CUTOFF
0010 GC TO 98
0011 C*** PEACH'S CUTOFF FUNCTION ***
0012 CUT=DKQ*R
0013 CUT=CUT*CUT
0014 PCTCK(11)=PEACH
0015 GO TO 99
0016 CUT=DK**R**R**2
0017 PCTCK(11)=DALGAR
0018 IF(CUT.GT.1.0-10) CUT=1.0C-DEXP(-CUT)
0019 IF(RAB.LT.1.0-10) GC TO 110
0020 GS2=CUT*(DEXP(-GAM*(R-RAE)**2)-
0021 U*DEXP(-GAM*(R+RAB)**2))/(R4*R2.)
0022 RETURN
0023 IF(ITYPE.NE.1) GC TO 120
0024 GS2=CUT*DEXP(-GAM*R2)*2.*GAM/R4
0025 RETURN
0026 GS2=0.000
0027 RETURN
0028 G52=CUT/R2*DEXP(-GAM*R2)
0029 CHECK THIS EQU
0030 RETURN
0031 END

```

```

0001 REAL FUNCTION GS3*(R)
0002 IMPLICIT REAL*(A-H,C-Z)
0003 COMMON/INT/GAM,DK,RAB,OKQ,ITYPE
0004 COMMON/FACT/PCTCK(15),JPCT
0005 DATA PEACH,DALGAR,SHFEACH,8HDALGARNC/
0006 IF(R.LT.1.D-10.OR.RAB.LT.1.D-10) GO TO 100
0007 R2=R*R
C*** TAKE OUT GO TO 98 FOR FEACH'S CUTOFF
C
C
C*** PEACH'S CUTOFF FUNCTION ***
0008 CUT=OK*R
0009 CUT=1.DD-DEXP(-CUT)*(1.D0+CUT*(1.D0+CUT*.5D0))
0010 CUT=CUT*CUT
0011 PCTCK(12)=PEACH
0012 GO TO 99
0013 CUT=DK**6*D2**3
0014 PCTCK(12)=DALGAR
0015 IF(CUT.GT.1.D-10) CUT=1.D0-DEXP(-CUT)
0016 GS3=CUT*(DEXP(-GAM*(R-RAB)**2)
U +DEXP(-GAM*(R+RAE)**2))/(R2*2.)
RETURN
0017 GS3=0.DD
0018 RETURN
0019 END
0020

```



```

0001 REAL FUNCTION GS4*(R)
0002 IMPLICIT REAL*8(A-H,O-Z)
0003 COMMON/INT/GAM,DK,RAE,DKG,ITYPE
0004 COMMON/POY/POYCK(15),IPOT
0005 DATA PEACH,CALGAR,SPFEACH,8*FCALGARND/
0006 1*(R,LT,1.0-10.0R,RAE,LT,1.0-10) GO TC 100
0007 R2=R**E
0008 R4=R2**R2
C*** TAKE OUT GO TO 98 FOR FEACH'S CUTOFF
C
C GC TO 98
C*** PEACH'S CUTOFF FUNCTION ***
0009 97 CUT=DKG*R
0010 CUT=1.00-DEXP(-CUT)*(1.00+CUT*(1.00+CUT*(.500+CUT/6.00)))
0011 CUT=CUT*CUT
0012 FCTCK(I3)=PEACH
0013 GC TO 99
0014 98 CUT=DKG**9*R4**2
0015 FCTCK(I3)=DALGAR
0016 IF(CUT.GT.1.0-10) CUT=1.00-DEXP(-CUT)
0017 99 GS4=CUT*(DEXP(-GAM*(R-RAE)**2)
U *DEXP(-GAM*(R+RAE)**2))/(R4*2.)
RETURN
0018 GSA=0.0D0
0019 RETURN
0020 END
0021

```

```

0001 REAL FUNCTION G55*(R)
0002 IMPLICIT REAL*8(A-H,C-Z)
0003 COMMON/INT/GAM,DK,RAB,DKQ,ITYPE
0004 CCYMON/FCT/PCTCK(15),IPCT
0005 DATA PEACH,DALGAR/ SHFEACH,8HDALGARNC/
0006 IF(R,LT,1.0-10) GO TO 100
0007 R2=R*R
0008
0009 C*** TAKE CUT GO TO 98 FOR PEACH'S CUTOFF
0010 GC TC 98
0011 C*** PEACH'S CUTOFF FUNCTION ***
0012 CUT=DK*R
0013 CUT=1.00-DEXP(-CUT)*(1.00+CUT*(1.00+CUT*.500))
0014 CUT=CLT*CUT
0015 PCTCK(14)=PEACH
0016 GO TO 99
0017 CUT=DK**6*R2**3
0018 PCTCK(14)=DALGAR
0019 IF(CUT.GT.1.0-10) CUT=1.00-DEXP(-CUT)
0020 IF(RAE,LT,1.0-10) GO TO 110
0021 G55=CLT*(DEXP(-GAM*(R-RAB)**2))/(R**2)
0022 U -DEXP(-GAM*(R+RAB)**2))/(R**2.)
0023 RETURN
0024
0025 110 G55=CLT*DEXP(-GAM*R2)*R2
0026 RETURN
0027 100 G55=0.000
0028 RRETURN
0029 END

```

```

0001 REAL FUNCTION GSG*(R)
0002 I=PLICIT REAL*(A-H,C-Z)
0003 COMMON/INT/GAM,DK,RAB,DKQ,I,TYPE
0004 COMMON/POT/POTCK(15),IPCT
0005 DATA PEACH,DALGAR,SHFFACH,8+FCALGARNQ/
0006 IF(R.LT.1.D-10) GO TO 100
0007 F2=R*F
0008 R3=R2*R
0009 C*** TAKE OUT GO TO 98 FOR PEACH'S CUTOFF
0010 C
0011 C*** PEACH'S CUTOFF FUNCTION ***
0012 97 CUT=DKQ*R
0013 CUT=1.DD-DEXP(-CUT)*(1.D0+CUT*(1.D0+CUT*(.5D0+CUT/6.D0)))
0014 CUT=CUT*CUT
0015 POTCK(15)=PEACH
0016 GO TO 95
0017 98 CUT=DK**3*R2**4
0018 POTCK(15)=DALGAR
0019 IF(CUT.GT.1.D-10) CUT=1.DC-DEXP(-CUT)
0020 IF(RAB.LT.1.D-10) GO TO 110
0021 GS6=CUT*(DEXP(-GAM*(R-RAB)**2)
0022 -DEXP(-GAM*(R+RAB)**2))/(R3*2.)
0023 U RETURN
0024 110 GS6=CLT*DEXP(-GAM*R2)
0025 RETURN
0026 100 GS6=0.DD0
0027 RETURN
0028 END

```

APPENDIX D

```

0001 IMPLICIT REAL*8(A-H,C-Z)
0002 LOGICAL RESTRT, LAA
0003 DIMENSION F(10), X(10), W(470)
0004 COMMON/FCN/INCUT,K,TIMLIM,DELM(10),LAA(6)
0005 COMMON/FIT/IS,IC,DD,FMIN,TINC,MAXFUN,IPRINT,DSTEP,
    * DMAX,ACC,W,RESTRT,MAXW
0006 EXTERNAL EFFIT
0007 READ(5,600)K,TIMLIM
0008 CALL STIME
0009 FORMAT(15,E10.5)
600 READ(5,601)NVEXP,NVAR,MAXFUN,IPRINT,DSTEP,DMAX,ACC
601 FCORMAT(4I5,3E15.6)
0012 INOUT=1
0013 IF(K.LT.0) WRITE(6,620)
0014 IF(K.GE.0) WRITE(6,621)
0015 FCORMAT(IH1,'FITTING PROGRAM -- INITIAL RUN'//)
620 FCORMAT(IH1,'FITTING PROGRAM -- RESTARTY RUN')
621 WRITE(6,622) TIMLIM,NVEXP,NVAR,MAXFUN,IPRINT,DSTEP,DMAX,ACC
622 FCORMAT(IH,'TIMLIM=',F10.2/IH,'NVEXP=',I5,5X,'NVAR=',I5/
    * IH,'MAXFUN=',I5,5X,'IPRINT=',I5/
    * IH,'DSTEP=',E15.6,5X,'DMAX=',E15.6,5X,'ACC=',E15.6)
    * RESTRT=K.GE.0
0019 IF(.NOT.RESTRT) GC TC 200
0020 READ(5,610) IS,IC,MAXW,DD,FMIN,TINC,(F(I),I=1,NVEXP)
0021 FCORMAT(3I5,3E15.6/(4E20.14))
0022 READ(5,611)(W(I),I=1,MAXW)
0023 FCORMAT(4E20.14)
0024 CALL VA05AD(EFFIT,NVEXP,NVAR,F,X,DSTEP,DMAX,ACC,MAXFUN,
0025 * IPRINT,W)
0026 INOUT=-1
0027 CALL EFFIT(NVEXP,NVAR,F,X)
0028 STOP
0029 END

```

FORTRAN IV C LEVEL

21

BLK DATA

DATE = 79229

09/13/29

PAGE 00

0001  
0002  
0003  
0004  
0005  
0006

BLCK DATA  
IMPLICIT REAL\*8(A-H,C-Z)  
REAL\*4 TIME  
COMMON/TEST/FEA,FEQ,TIMEL(8)  
DATA ERA,ER0/C.000C.0.C00/  
END

(200)







```

0079      GO TO 95
C  RESET PARMO
0080      DC 203 I=1,10
0081      PARMO(I)=PARM(I)
C  CALCULATE NUCLEAR TERMS
      DO 220 N=1,NVEXP
0082      NRC=N.LT.NVRST .OR.INCUT.EO.0
0083      R=RVEXP(N)
0084      IF(.NOT.RECALC(3).AND.NRC) GC TC 205
0085      VNO(N)=X12(CUT2*R)/R**2
0086      VNO(N)=VNO(N)*VNO(N)/2.C0
0087      IF(.NOT.RECALC(2).AND.NRC) GC TC 206
0088      VNO(N)=X13(CUT3*R)/R**2
0089      VNO(N)=VNO(N)*VNO(N)/2.C0
0090      IF(.NOT.RECALC(1).AND.NRC) GOTO 220
0091      FXPR=DEXP(-CUT*R)
0092      VNM1(N)=EXPR
0093      VNM2(N)=R*VNM1(N)
0094      VNM3(N)=R*VNM2(N)
0095      VNM4(N)=EXPR/R
0096      VNM4(N)=EXPR/R
0097      CCNTINUE
C *** DEBUG *****
0098      WRITE(6,660)(RVEXP(I),VND(I),VNO(I),VNO(I),VNO(I),VNM1(I),
0099      * VNM2(I),VNM3(I),VNM4(I),I=1,NVEXP)
660      FORMAT(1H0,2X,1HR,7X,3HVND,12X,4HVNO,12X,4HVNOG,
* 11X,4HVNM1,11X,4HVNM2,11X,4HVNM3,11X,4HVNM4/(1H ,F8.2,8E15.6))
* *****
C  CALCULATE Q TERMS
C  CALL FCTO(RECALC)
C  SET UP RINT CALCULATION
0100      LAA(1)=.NOT.RECALC(3)
0101      LAA(2)=.NOT.RECALC(2)
0102      LAA(3)=.NOT.RECALC(1)
0103      DC 230 I=4,6
0104      LAA(I)=LAA(3)
0105      LAP=.TRUE.
0106      DC 235 I=1,6
0107      IF(.NOT.LAA(I)) GO TO 240
0108      CCNTINUE
0109      LAR=.FALSE.
0110      IF(NVRST.LE.NVEXP) GO TO 240
0111      GC TO 245
0112      C  CALC R INTEGRALS
C  CALL FCTR
C  CALC EFFECTIVE POTENTIALS AND THE SUM OF DIFFERENCES
0113      VPOT=C.000
0114      INOUT=0
0115      ZB2=ZB*ZB
0116      DO 300 N=1,NVEXP
0117      VNOA=-ZB2*ALPHAD*VNO(N)
0118      VNOA=-ZB2*ALPHAQ*VNO(N)
0119      VNM1=ZB2*AP(1)*VNM1(N)
0120      VNM2=ZB2*AP(2)*VNM1(N)
0121      VNM3=ZB2*AP(3)*VNM3(N)
0122      VNM4=ZB2*AP(4)*VNM4(N)
0123      VNOA=ZB*ALPHAD*VNO(N)
0124      VNOA=ZB*ALPHAQ*VNO(N)
0125      VEODA=-ALPHAD*VEQC(N)
0126      VEMAI=-ALPHAD*VEM(1,N)/2.D0
0127

```



FORTRAN IV G LEVEL 21

EFFIT

DATE = 79229

09/13/29

PAGE 0001

```

0176      320  IF(IPERT.EQ.0) RETURN
0177      FRAT=VEFF(I)+ERO
0178      WRITE(6,601) EBAT
0179      601  FORMAT(1H ' TOTAL ENERGY FOR R= ',E20.12)
0180      RETURN
0181      END

```

```

0001 SUBROUTINE OUTR(ICUT,NVAR,NMAX,F,PAR)
0002 IMPLICIT REAL*9(A-H,O-Z)
0003 LOGICAL RESTRT,FCNB,CLCSEC
0004 INTEGER*2 ISNX
0005 DIMENSION F(1),PAR(1)
0006 COMON/INDUT/VNH(10),VABN(10),VND(10),VNG(10),VNDQ(10),VNOQ(10),
* VNM1(10),VNM2(10),VNM3(10),VNM4(10),VEQD(10),VECG(10),VEM(6,10),
* NIRST(50),NLA(50),NCTR(50),NTYPE(50),EX(100),CO(100),
* PARX(10),PARM(10),PARMC(10),ZA,ZB,NVRST,NVEXP,IVAR(10)
0007 COMON/FCN/INDUT,K,TIMLIM,DELM(10)
0008 COMON/FLT/IS,IC,CD,FMIN,TINC,MAXFUN,IPRINT,DSTEP,DMAX,ACC,
* A(470),RESTRT,MAXW
0009 COMON/INTITLE(18),NBF,NCRPA,NOR3B,NSYM,DA(1275),DBA(1275),
* DRAD(1275),
* ALPHAQ,BETA1,FCNB(50),RVEXP(10),VEXP(10),ISNX(50),CLCSED,IPERT
0010 COMON/TEST/ERA,EP?
0011 WRITE(7,699)K,TIMLIM
0012 FCNMAT(15,5)
0013 WRITE(7,673)NVEXF,NVAR,MAXFUN,IPRINT,DSTEP,DMAX,ACC
0014 FCNMAT(415,3E15.6)
0015 WRITE(7,670)IS,IC,MAXW,CC,FMIN,TINC,(F(I),I=1,NVEXP)
0016 FCNMAT(315,3E15.6/(4E20.14))
0017 WRITE(7,671)(W(I),I=1,MAXW)
0018 FCNMAT(4E20.14)
0019 WRITE(10UT,600)IVAR,(PARM(I),PARMO(I),I=1,NMAX),
* (PAR(I),I=1,NVAR)
0020 FCNMAT(1015/(2E20.12))
0021 WRITE(6,610)NVEXP,NVAR,IVAR,(PARM(I),PARMO(I),I=1,NMAX)
0022 FORMAT(1H0,***** CUTOUT VALUES FOR RESTART *****/
* 1H,6HNVEXP=,15,EX,5HNVAR=,15/
* 1H,5HIVAR:,1015/
* 1H,4X,4HPARM,16X,5HPARMC/(1H,2E20.12))
0023 WRITE(6,609)(PAR(I),I=1,NVAR)
0024 FORMAT(1H,4X,3HPAR/(1H,E20.12))
0025 WRITE(10UT,601)EBA,EB0
0026 WRITE(10UT,600)NVEXF
0027 WRITE(10UT,601)(RVEXP(I),I=1,NVEXP)
0028 WRITE(10UT,601)(VNH(I),I=1,NVEXP)
0029 WRITE(10UT,601)(VABN(I),I=1,NVEXP)
0030 WRITE(10UT,601)(VND(I),I=1,NVEXP)
0031 WRITE(10UT,601)(VNG(I),I=1,NVEXP)
0032 WRITE(10UT,601)(VNDQ(I),I=1,NVEXP)
0033 WRITE(10UT,601)(VNM1(I),I=1,NVEXP)
0034 WRITE(10UT,601)(VNM2(I),I=1,NVEXP)
0035 WRITE(10UT,601)(VNM3(I),I=1,NVEXP)
0036 WRITE(10UT,601)(VNM4(I),I=1,NVEXP)
0037 WRITE(10UT,601)(VEQD(I),I=1,NVEXP)
0038 WRITE(10UT,601)(VECG(I),I=1,NVEXP)
0039 WRITE(10UT,601)(VEM(I),I=1,NVEXP)
0040 FCNMAT(4E20.12)
0041 WRITE(6,611)
0042 FORMAT(1H0,***** RESTART OUTPUT COMPLETED ***** )
0043 RETURN
0044 END
0045

```



```

0044 DC 106 I=1,NBF
0045 VAL=H(I)*F
0046 DO 107 J=1,I
0047 IJ=IJ+1
0048 DO(IJ)=DBA(IJ)+VAL*H(J)
0049 CONTINUE
0050 CONTINUE
0051 READ(5,600)ITITLE
0052 WRITE(6,623)ITITLE
0053 FORMAT(1H,'UNDISTORTED ATOM E:','1H,18A4)
0054 CLOSED=.TRUE.
0055 DO 100 K=1,NORRB
0056 READ(5,602) KX,SYM,NX,E,F,(H(I),I=1,NBF)
0057 WRITE(6,622) KX,SYM,NX,E,F,(H(I),I=1,NBF)
0058 IJ=0
0059 IF(.LT.1.00) CLOSED=.FALSE.
0060 DC 116 I=1,NBF
0061 VAL=H(I)*F
0062 DO 117 J=1,I
0063 IJ=IJ+1
0064 IF(.NOT.CLOSED) DBO(IJ)=DEC(IJ)+VAL*H(J)
0065 DB(IJ)=DB(IJ)+VAL*H(J)
0066 CONTINUE
0067 CONTINUE
0068 IF(IPERT.EQ.1) GO TO 122
0069 DC 121 I=1,NSYM
0070 DBA(I)=DBO(I)
0071 DEAO(I)=DBO(I)
0072 WRITE(6,662)
0073 FORMAT(1H0,'FUNCTION FOR DISTORTED ATOM B = UNDISTORTED FUNCTION')
0074 GC TO 123
0075 READ(5,600)ITITLE
0076 WRITE(6,670)ITITLE
0077 FCPMAT(1H,'FUNCTION FOR DISTORTED ATOM E:','18A4)
0078 DO 300 K=1,NORRB
0079 READ(5,602) KX,SYM,NX,E,F,(H(I),I=1,NBF)
0080 WRITE(6,622) KX,SYM,NX,E,F,(H(I),I=1,NBF)
0081 IJ=0
0082 DC 306 I=1,NBF
0083 VAL=H(I)*F
0084 DO 307 J=1,I
0085 IJ=IJ+1
0086 IF(.LT.1.00) DBAO(IJ)=DBAC(IJ)+VAL*H(J)
0087 DBA(IJ)=DBA(IJ)+VAL*H(J)
0088 CONTINUE
0089 CONTINUE
C READ POTENTIAL PARAMETERS
0090 READ(5,603)ALPHA,BETA1,CUT,CUT2,CUT3,AP
0091 READ(5,603)CUT,CUT2,CUT3
0092 READ(5,603)AP
0093 FORMAT(4D15,E)
0094 WRITE(6,624)ALPHA,BETA1,CUT,CUT2,CUT3,AP
0095 FORMATT(1H0/5X,'*** FEACH'S CUTOFF FUNCTIONS *****/
    . 5X,'DIPOLE PARAMETER.....',D15.8/
    . 5X,'QUADRUPOLE PARAMETER.....',D15.8/
    . 5X,'BETA1.....',D15.8/
    . 5X,'CUTOFF PARAMETERS.....',3D15.8/
    . 5X,'MONOPOLE PARAMETERS.....',4D15.8/
    READ(5,631)DELM

```

```

0097 FORMAT(5E15.6)
0098 WRITE(6,632) DELM
0099 FORMAT(1H0,' LIMITS ON VARIATION OF PARM(I)'/
      (1H,5F15.6))
0100 HEAD(5,626) IVAR
0101 FORMAT(10I5)
0102 WRITE(6,627)
0103 FORMAT(1H,' PARAMETERS VARIED IN THIS RUN'/
      1H,' ORDER',5X,'PARAMETER')
0104 PARM(10)=ALPHA
0105 PARM(5)=ALPHA
0106 PARM(8)=BETA
0107 DO 115 I=1,4
0108 PARM(8-I)=AP(I)
0109 PARM(3)=CUT2
0110 PARM(2)=CUT3
0111 PARM(1)=CUT
0112 NV=0
0113 DO 130 I=1,10
0114 IV=IVAR(I)
0115 IF(IV.EQ.0) GC TC 130
0116 IF(DABS(DELM(I)).LT.1.0-10) GO TO 131
0117 NV=NV+1
0118 IF(I.EQ.10) GO TO 129
0119 II=I+1
0120 DO 125 J=1,10
0121 IF(IV.EQ.IVAR(J)) GO TO 131
0122 CONTINUE
0123 WRITE(6,628) IV,FM(I)
0124 FORMAT(1H,5X,15.5X,A8)
0125 CONTINUE
0126 GO TO 132
0127 WRITE(6,630) IV,IVAR,DELM
0128 FORMAT(1H0,'***** ERROR IN PARAMETER VARIATION ORDER *****'/
      1H,' IV=',15/1H,' IVAR:',10I5/
      1H,' DELM:',1H,5E15.6))
0129 STOP
0130 CC 118 I=1,10
0131 PAR(I)=0.000
0132 PARM(I)=PARM(I)
0133 DELM(I)=DELM(I)/PI2
0134 PARM(I)=0.000
0135 IF(NV.EQ.NVAR) GO TO 14C
0136 WRITE(6,640) NV,NVAR
0137 FORMAT(1H0,'***** ERROR *****'/
      1H,' INCORRECT NUMBER OF PARAMETERS VARIED'/
      1H,' NV=',15.5X,' SHOULD = NVAR=',15/
      1H)
0138 STOP
C READ POTENTIAL POINTS TO BE FIT
0139 READ(5,604)(RVEXP(I),VEXP(I),I=1,NVEXF)
0140 FORMAT(2D15.8)
0141 WRITE(6,625)(RVEXF(I),VEXF(I),I=1,NVEXF)
0142 FORMAT(1H0,' POTENTIAL POINTS TO BE FIT'/
      15X,1HR,16X,4HV(R)/(1X,C15.8,2X,D15.8))
C DETERMINE WHICH BASIS FCNS USED FOR ATCM B
      II=0
0143 DO 210 I=1,NDF
0144 II=II+1
0145 FCNB(I)=.TRUE.
0146

```

09/13/29

DATE = 79229

SLTLP

FORTPAN IV G LEVFL 21

```

0147 IF(DRA(II).EQ.0.0C0) FCNP(I)=.FALSE.
0148 RETURN
0149 END

```



```

0001 SUBROUTINE POTHF(IOUT)
0002 IMPLICIT REAL*8(A-H,C-Z)
0003 LOGICAL FCNR,CLOSED
0004 INTEGER*2 IA,IR,IC,IO,IMU,IF,ISNX
0005 COMMON/INTS/NINTS,IAST,IA(500),IC(500),IC(500),IMU(500),
    IF(500),V(500),VO(500)
    COMMON/INCUT/VNHF(10),VAFN(10),VND(10),VNDQ(10),VNDQ(10),VNQC(10),
    VNMI(10),VNMA(10),VNMA(10),VNMA(10),VECC(10),VECC(10),VEM(6,10),
    NFIRST(50),NLAST(50),NCNTR(50),NTYPE(50),EX(100),CO(100),
    PARM(10),PARM(10),FARMO(10),ZA,ZB,NVRST,NVEXP,IVAR(10)
    COMMON/IN/TITLE(18),NBF,NORBA,NCRBB,NSYM,DA(1275),DRA(1275),
    CRAO(1275)
    ALPHAG,BETA1,FCNE(50),FVEXF(10),VEXP(10),ISNX(50),CLOSED,IPERT
    COMMON/QMAT/DB(1275),DBO(1275),DA1(1275),DA2(1275),H(1275),
    HC(1275),DKO(1275),DKAC(1275)
    COMMON/TEST/EBA,EB0
    DATA IJLK/4HIJLK/

```

C CALCULATE HARTREE-FECK TERMS  
C DIVIDE DIAG DA,DB,ELEMENTS BY 2, CALC ISNX ARRAY, AND FORM  
C DENSITY MATRICES FOR ATOM A 2J-K POTENTIAL

```

129 II=0
    DC 129 I=1,NSYM
    IF(.NOT.CLOSED) DKO(I)=-DEC(I)
    DA1(I)=DA(I)*2.00
    CA2(I)=-DA(I)
    II=0
    CC 129 I=1,NBF
    ISNX(I)=1
    II=II+1
    DA(I)=DA(I)*0.5D0
    IF(.NOT.CLOSED) DBG(II)=DEC(II)*0.5D0
    DBA(II)=DRA(II)*0.5D0
    IF(.NOT.CLOSED) CBAC(II)=DEAO(II)*0.5D0
    DR(II)=DB(II)*0.5D0

```

C CALCULATE ELECTRONIC HF TERMS AND < B | ZA/RA + ZB/RB | B >

```

0025 VAR(N)=0.0D0
0026 VAR=0.0D0
0027 READ(I) ITITLE
0028 WRITE(6,626) ITITLE
0029 FCNTRAT(5X,'FILE #1 TITLE = ',18A4)
0030 IF(ITITLE(18).NE.IJLK) GO TO 121
0031 IF(N.NE.1) GO TO 125
0032

```

C READ BASIS SET INFORMATION AND OUTPUT FOR RESTART

```

0033 READ(1)II,(NFIRST(I),NLAST(I),NCNTR(I),NTYPE(I),I=1,II)
0034 IF(II.EQ.NBF) GO TO 122
0035 WRITE(6,627)
0036 FCNTRAT(//5X,***** INPUT FILE ERROR *****
0037 STOP
0038 WRITE(IOUT,600)II,(NFIRST(I),NLAST(I),NCNTR(I),NTYPE(I),I=1,II)
0039 FCNTRAT(5/(4I5))
0040 READ(1) II,(VAL,VAL,EX(I),CC(I),I=1,II),(V(I),I=1,II)
0041 WRITE(IOUT,601)II,(EX(I),CO(I),I=1,II),(V(I),I=1,II)
0042 FCNTRAT(5/(4E20,12))
0043 READ(1)II,X1,Y1,Z1,ZA,X2,Y2,Z2,ZB
0044 IF(II.NE.2) GC TC 121
0045 WRITE(IOUT,602) ZA,ZE
0046 FORMAT(2E20,12)
0047 WRITE(6,630)X1,Y1,Z1,ZA,X2,Y2,Z2,ZB

```

```

0008      630  FCRMAT(1H0,10X,1HX,9X,1FY,9X,1HZ,9X,10HNUC CHARGE/
0049      1H,7HATOM A:,4F10.3/1H,7HATOM B:,4F10.3//)
0050      IF(Z2.NE.RVEXP(N)) GO TO 121
0051      GO TO 130
0052      READ(1) I1
0053      IF(I1.NE.NBF) GO TO 121
0054      READ(1) I1, X1, Y1, Z1, ZZA, X2, Y2, Z2, ZZB
0055      IF(I1.NE.2.OR.ZZA.NE.ZA.OR.ZZB.NE.ZB.CR.Z2.NE.RVEXP(N))
0056      . GO TO 121
0057      READ(1) I1
0058      READ(1) I1
0059      DC 124 I=1, NSYM
0060      H(I)=0.0D0
0061      III=2
0062      IF(IPERT.EQ.0) III=1
0063      DC 132 I=1, III
0064      READ(1) NINTS, LAST
0065      IF(LAST.EQ.0) GC TO 131
0066      READ(1) I1
0067      IF(IPERT.EQ.0) GO TO 133
0068      TBA=0.0D0
0069      TBA=0.0D0
0070      READ(1) NINTS, LAST, IA, IB, IC, V
0071      IF(NINTS.EQ.0) GC TO 335
0072      DO 334 I=1, NINTS
0073      TBA=TRA+V(I)*DBA(ISNX(IA(I))+IB(I))
0074      TBA=TRA+V(I)*DBA(ISNX(IA(I))+IB(I))
0075      WRITE(6,620) IB, TBA
0076      FORMAT(1H, 'KINETIC ENERGY TERMS: ',
0077      1H, 'TBA=', E20.12/1H, 'TBA=', E20.12)
0078      READ(1) I1
0079      READ(1) NINTS, LAST, IA, IB, IC, V
0080      IF(NINTS.EQ.0) GC TO 135
0081      DO 134 I=1, NINTS
0082      V-(ISNX(IA(I))+IB(I))=V(I)
0083      IF(LAST.EQ.0) GO TO 133
0084      C CALCULATE ATOM A 2J-K POTENTIAL FROM UNIT 1 2E INTS AND ADD TO H
0085      READ(1) I1
0086      WRITE(6,680) I1
0087      FORMAT(1H, 'A')
0088      CALL JKPT(H, DAI, DA2, ISNX, I, HC, DKC, 'TRUE.')
0089      IF(IPERT.EQ.0) READ(1, END=136)
0090      IJ=0
0091      DO 137 I=1, NBF
0092      DO 137 J=1, I
0093      IJ=IJ+1
0094      VAB=VAB+H(IJ)*DBA(IJ)
0095      VABN(N)=4.*DO*VAB
0096      CONTINUE
0097      C ***
0098      WRITE(6,650) (VABN(I), I=1, NVEXP)
0099      FORMAT(1H, '2X,4HVABN/(1H, E20.12) )
0100      C ***
0101      CEPIG
0102      IF(IPERT.EQ.0) GC TC 360
0103      REWIND 1
0104      CC 331 I=1,6
0105      READ(1)

```

\*\*\*\*\*

\*\*\*\*\*

```

0101 DO 312 I=1,3
0102 READ(I) NINTS, LAST
0103 IF (LAST.EQ.0) GO TO 336
0104 READ(I) I
0105 II=I
0106 DO 340 I=1, NSYM
0107 HC(I)=0.000
0108 DA2(I)=0.000
0109 IF (I.NE.ISNX(I+1)) GC TO 340
0110 II=II+1
0111 DA2(I)=2.*DA2(I)
0112 CA1(I)=-2.*DO*CA2(I)
0113 CALL JKPTH(H,DA1,CA2,ISNX,1,HC,DKC,CLCSEC)
0114 VJKB=0.000
0115 IJ=0
0116 DO 337 I=1,NRF
0117 DC 337 J=1, I
0118 IJ=IJ+1
0119 VJKB=VJKB+H(IJ)*DB(IJ)+HO(IJ)*DBO(IJ)
0120 REWIND I
0121 DO 341 I=1,6
0122 READ(I) I
0123 DC 342 I=1,3
0124 READ(I) NINTS, LAST
0125 IF (LAST.EQ.0) GO TO 343
0126 READ(I) I
0127 II=I
0128 DC 350 I=1, NSYM
0129 H(I)=C.000
0130 HC(I)=0.000
0131 DA2(I)=-DBA(I)
0132 IF (.NOT.CLOSED) DKAO(I)=-DBAC(I)
0133 IF (I.NE.ISNX(I+1)) GC TO 350
0134 II=II+1
0135 IF (.NOT.CLOSED) DKAO(I)=2.*DKAO(I)
0136 DA2(I)=2.*DA2(I)
0137 DA1(I)=-2.*DO*DA2(I)
0138 CALL JKPTH(H,DA1,CA2,ISNX,1,HO,DKAO,CLOSED)
0139 VJKRA=0.000
0140 IJ=0
0141 DC 347 I=1,NBF
0142 DO 347 J=1, I
0143 IJ=IJ+1
0144 VJKBA=VJKBA+H(IJ)*DBA(IJ)+FO(IJ)*CRAC(IJ)
0145 WRITE(6,621) VJKB, VJKBA
0146 FCRMAT(1H, 'CCULCMB TERMS: ',
0147 'H ', VJKB=, 'E20.12/1H ', VJKBA=, 'E20.12)
0148 EBA=4.*DO*TRA+2.*DO*VJKEA+VABN(I)
0149 C CALCULATE NUCLEAR TERMS ANC < B0 | ZB/RE | B0 >
0150 DO 160 N=NVRST,NVEXP
0151 VNH(N)=0.000
0152 VNF=0.000
0153 VAB=0.000
0154 READ(2) ITITLE
0155 WRITE(6,631) ITITLE
0156 FORMAT(/5X, 'FILE #2 TITLE = ',18A4)
0157 IF (ITITLE(18).NE.IJLK) GC TO 121
0158 READ(2) I

```



```

0001 SUBROUTINE INR(IIN,ICUT,NVAR,NMAX,PAR)
0002 IMPLICIT REAL*8(A-H,C-Z)
0003 INTEGER*2 ISNX
0004 LOGICAL FCNR,RESTRY,CLOSED
0005 DIMENSION RREST(10),PAR(1),IVRR(10)
0006 COMMON/IT/IS,IC,CD,FMIN,TINC,MAXFUN,IPRINT,DSTEP,DMAX,ACC,
    * W(470),RFRSTY,MAXW
    * COMMON/INTS/V(100)
    * COMMON/INOUT/VNHF(10),VARN(10),VND(10),VNO(10),VNOQ(10),VNOQQ(10),
    * VNM1(10),VNM2(10),VNM3(10),VNM4(10),VEOD(10),VECG(10),VEM(6,10),
    * NFIRST(50),NLA(50),NCNTR(50),NTYPE(50),EX(100),CO(100),
    * PARM(10),PARM(10),ZA,ZB,NVRST,NVEXP,IVAR(10)
    * COMMON/IN/TITLE(19),NDF,NORBA,NORBU,NSYM,DA(1275),DBA(1275),
    * DBAD(1275),
    * ALPHA0,BETA1,FCNB(50),RVEXP(10),VEXP(10),ISNX(50),CLOSED
    * COMMON/TEST/EBA,EB0
0007 WRITE(6,660)
0008 FORMAT(1H0, '***** RESTART PARAMETERS READ IN *****')
0009 READ(IIN,600) II,(NFIRST(I),NLA(I),NCNTR(I),NTYPE(I),I=1,II)
0010 WRITE(IOUT,600)II,(NFIRST(I),NLA(I),NCNTR(I),NTYPE(I),I=1,II)
0011 FCNTR(15/(4*IS))
0012 READ(IIN,601)II,(EX(I),CO(I),I=1,II),(V(I),I=1,II)
0013 WRITE(IOUT,601)II,(EX(I),CO(I),I=1,II),(V(I),I=1,II)
0014 FCNTR(15/(4*F20,12))
0015 READ(IIN,602) ZA,ZB
0016 WRITE(IOUT,602) ZA,ZB
0017 FCNTR(15/(4*F20,12))
0018 READ(IIN,610)IVRR,(PARM(I),PARM(I),I=1,NMAX),
0019 (PAR(I),I=1,NVAR)
0020 FORMAT(10I5/(2E20,12))
0021 READ(IIN,611)EBA,EB0
0022 READ(IIN,610)NVRST
0023 WRITE(6,605)ZA,ZB,NVRST
0024 FCNTR(1H, 'ZA=',E15.6, 'ZB=',E15.6/
0025 1H, 'NVRST=',I5)
0026 READ(IIN,611)(RREST(I),I=1,NVRST)
0027 READ(IIN,611)(VNH(I),I=1,NVRST)
0028 READ(IIN,611)(VARN(I),I=1,NVRST)
0029 READ(IIN,611)(VNM1(I),I=1,NVRST)
0030 READ(IIN,611)(VNM2(I),I=1,NVRST)
0031 READ(IIN,611)(VNM3(I),I=1,NVRST)
0032 READ(IIN,611)(VNM4(I),I=1,NVRST)
0033 READ(IIN,611)(VEOD(I),I=1,NVRST)
0034 READ(IIN,611)(VNO(I),I=1,NVRST)
0035 READ(IIN,611)(VNOQ(I),I=1,NVRST)
0036 WRITE(6,606)VEQO
0037 FCNTR(1H, 'SE15.6)
0038 READ(IIN,611)(VEM(I),I=1,NVRST)
0039 READ(IIN,611)(VEM(1),I=1,NVRST)
0040 READ(IIN,611)(VEM(2),I=1,NVRST)
0041 READ(IIN,611)(VEM(3),I=1,NVRST)
0042 READ(IIN,611)(VEM(4),I=1,NVRST)
0043 READ(IIN,611)(VEM(5),I=1,NVRST)
0044 WRITE(6,606)VEQO
0045 READ(IIN,611)((VEM(I),J),J=1,NVRST),I=1,6)
0046 FORMAT(4E20,12)
0047 IF(NVRST.LT.NVEXP) GO TO 152
0048 II=0
0049 DO 100 I=1,NBF
0050 ISNX(I)=II
0051 II=II+I
    DA(II)=DA(I)+0.500

```

```

0052 IF(.NOT.CLOSED) DBAO(II)=DBAC(II)*0.5D0
0053 CBA(II)=DBA(II)*0.5D0
0054 DO 150 I=1,NVRST
0055 IF(DABS(RVEXP(I))-RREST(I)).GT.1.D-10) GO TO 151
0056 CCNTINUE
0057 NVPST=NVPST+1
0058 DO 160 I=1,10
0059 IF(IVRR(I).NE.IVAR(I)) GC TO 170
0060 RETURN
0061
0062 FMIN=-1.D0
0063 CC=0.000
0064 IS=4
0065 IC=0
0066 TINC=1.0D0
0067 DO 171 I=1,MAXN
0068 W(I)=0.000
0069 RETURN
0070 WRITE(6,661)(RREST(I),I=1,NVRST)
0071 FORMAT(1H0,'*****' ERROR *****'/
. 1H 'ORDER OF RESTART DATA DOES NOT AGREE'/
. 1H 'EX.'RREST'/(1H ,E20.12))
. STCP
END
0072
0073

```

```

0001 SURROUPTIME PCTR
0002 IMPLICIT REAL*8(A-H,O-Z)
0003 LOGICAL FCNB,LA,LAR,LFA
0004 INTEGER*2 ISNX
0005 DIMENSION VALR(6)
0006 COMMON/SCMAT/RI(6,1275)
0007 COMMON/SLR/EXI,EXJ,I TYPE,JTYPE,ICNTR,JCNTR,R,CUT,C,CUT3,
0008 ALPHA,ALPHAB,AP(4),LA(6),RINTG(6),LAR
0009 COMMON/INDUT/VNH(10),VAEN(10),VND(10),VNG(10),VNGO(10),VNGO(10),
0010 VNM1(10),VNM2(10),VNM3(10),VNM4(10),VNM5(10),VNGO(10),VEM(6,10),
0011 VNFIRST(50),NLAST(50),NCNTR(50),NTYPE(50),FX(100),CD(100),
0012 PARM(10),PARM(10),PARM(10),ZAZB,NVRST,NVFXP,IVAR(10)
0013 COMMON/IN/ITITLE(18),ABF,NOREA,NORBB,NSYM,DA(1275),D9A(1275),
0014 ALPHAQ,BETA1,FCNB(50),RVEXP(10),VFXP(10),ISNX(50)
0015 COMMON/FCM/INDUT,K,TIMLIM,DELM(10),LAA(6)
0016 C INITIALIZE R
0017 CC 100 J=1,NSYM
0018 DC 100 I=1,6
0019 RI(I,J)=0.0D0
0020 C CALCULATE NEEDED NEW R INTEGRALS
0021 DO 400 N=1,NVEXP
0022 IF(N*GE*NVRST) GO TO 102
0023 IF(LAR) GC TC 105
0024 GO TO 400
0025 IF(INCJT.EQ.0) GO TO 101
0026 DC 103 I=1,6
0027 LA(I)=.FALSE.
0028 GO TO 110
0029 DC 106 I=1,6
0030 LA(I)=LAA(I)
0031 R=RVEXP(N)
0032 IJ=0
0033 DC 350 I=1,NRF
0034 IJST=NFIRST(I)
0035 ILST=NLAST(I)
0036 ITYPE=NTYPE(I)
0037 ICNTR=NCNTR(I)
0038 DN 349 J=1,I
0039 IJ=IJ+1
0040 IF(.NOT.FCNB(I).OR..NCT.FCNB(J)) GO TO 349
0041 JI=NFIRST(J)
0042 JI=NLAST(J)
0043 JTYPE=NTYPE(J)
0044 JCNTR=NCNTR(J)
0045 DO 310 IR=1,6
0046 VALR(IR)=0.0D0
0047 DC 346 II=JI,ILST
0048 EXI=EX(II)
0049 TEMPE=CO(II)
0050 DC 346 JJ=JI,JI,II
0051 EXJ=EX(JJ)
0052 TCO=TEMP*CO(JJ)
0053 VALR(I)=VALR(I)+TCO*RIINT(ICUM)
0054 DO 345 IR=2,6
0055 VALR(IR)=VALR(IR)+TCO*RIINTG(IR)
0056 CONTINUE
0057 DC 348 IR=1,6
0058 IF(LA(IR)) GO TO 348

```

```

0052 RI(IP,IJ)=VALR(IR)
0053 CONTINUE
0054 CONTINUE
0055 CONTINUE
0056 DD 355 IR=1.6
0057 VALR(IP)=0.000
0058 IJ=0
0059 DT 360 I=1,NRF
0060 DC 360 J=1,I
0061 IJ=IJ+1
0062 DD 358 IR=1.6
0063 VALR(IR)=VALR(IR)+RI(IR,IJ)*CBA(IJ)
0064 CONTINUE
0065 DC 361 IR=1.6
0066 IF(LA(IR)) GC TC 361
0067 VEM(IR,N)=VALR(IR)*4.00
0068 CONTINUE
0069 CONTINUE
0070 WRITE(6,601)((VEM(I,J),I=1,6),J=1,NVE XP)
0071 FCRMAT(1H ,3HVEV/1H ,6E15.6)
0072 RETURN
0073 END

```



```

0001 SUBROUTINE PUTQ(RECALC)
0002 IMPLICIT REAL*8(A-F,C-Z)
0003 LOGICAL RFCALC(10),FCNB,LA,CLOSED
0004 INTEGER*2 IA,IB,IC,IC,IMU,IF,ISNX,JV(4),ISET(14),IVAL
0005 DIMENSION DB2(1275),HG(1275),HGC(1275),DRC2(1275)
0006 COMMON/OMAT/C(1275,8),H(1275),HO(1275)
0007 COMMON/INTS/INTS,IA(500),IB(500),IC(500),IMU(500),
    * IF(500),V(500),VG(500)
0008 COMMON/SLR/EXI,EXJ,IJTYPE,JTYPE,ICNTR,JCNTR,R,CUT,CUT2,CUT3,
    * ALPHA,ALPHOB,AP(4),LA(6),RINTG(6)
0009 COMMON/INOUT/VNHF(10),VAEN(10),VND(10),VNO(10),VNOQ(10),VNOQ(10),
    * VNM1(10),VNM2(10),VNM3(10),VNM4(10),VEQC(10),VEQQ(10),VEM(6,10),
    * NFIRST(50),NLA(50),NCNTR(50),NTYPE(50),EX(100),CO(100),
    * PARM(10),PARM(10),PARM(10),ZA,ZB,NVRST,NVEXP,IVAR(10)
0010 COMMON/IN/ITITLE(18),NDF,NORBA,NCRBB,NSYM,DA(1275),DBA(1275),
    * CEAD(1275),
    * ALPHAQ,BETA,FCNB(50),FVEXP(10),VEXP(10),ISNX(50),CLOSED
0011 COMMON/FCN/INOUT
0012 EQUIVALENCE (VAL,JV),(IVAL,JV(4))
0013 DATA ISET/9,6,4,1,12,7,5,3,14,8,11,2,13,10/
    * ZERC/1,D-14/
C INITIALIZE Q AND SET UP C CALC
0014 NI=1
0015 IF(RECALC(3)) GO TO 212
0016 IF(RECALC(2)) GO TO 214
0017 GO TO 301
0018 KI=1
0019 KF=3
0020 IF(RECALC(2)) GO TO 215
0021 GC TO 216
0022 KI=4
0023 KF=8
0024 DO 217 K=1,9
0025 DO 217 I=1,NSYM
0026 G(I,K)=0.000
C SET UP DP2
0027 CC 204 I=1,NSYM
0028 IF(.NCT.CLOSED) DE02(I)=-DEAC(I)
0029 DR2(I)=-DBA(I)
0030 II=0
0031 DO 205 I=1,NBF
0032 II=II+1
0033 IF(.NCT.CLOSED) DEC2(II)=2.00*DE02(II)
0034 DR2(II)=DR2(II)+DR2(II)
0035 CC 300 N=NI,NVEX
0036 IF(N.LT.NVRST) GC TO 206
0037 KI=1
0038 KF=R
0039 IJ=0
0040 R=RVEXP(N)
C CALCULATE NEEDED NEW Q INTS
0041 DO 230 I=1,NBF
0042 IIST=NFIRST(I)
0043 ILST=NLA(1)
0044 IJTYPE=NTYPE(I)
0045 ICNTR=NCNTR(I)
0046 DO 225 J=1,I
0047 IJ=IJ+1
0048 IF(.NCT.FCNB(I).CF..NCT.FCNB(J)) GO TO 225

```

```

0040 JIST=NFIRST(J)
0050 JLAST=NLAST(J)
0051 JTYPE=NTYPE(J)
0052 JCNTR=NCNTR(J)
0053 DO 220 K=KI,KF
0054 VAL=0.0D0
0055 DO 215 II=IIST,ILST
0056 TEMP=CN(II)
0057 FXI=EX(II)
0058 DO 218 JJ=JIST,JLST
0059 EXJ=FX(JJ)
0060 VAL=VAL+TEMP*CO(JJ)*OINT(K)
0061 CONTINUE
0062 G(IJ,K)=VAL
0063 CONTINUE
0064 CONTINUE
C***** DEBUG
605 WRITE(6,605)((O(I,J),J=1,8),I=1,NSYM)
0066 FORMAT(1H,0 INTS)/(1H,RE15.6)
C***** DEBUG
IJ=0
VAR=0.0D0
VAR4=C.0D0
DC 235 I=1,NRF
DC 235 J=1,I
IJ=IJ+1
VAB=VAB+Q(IJ,I)*CEA(IJ)
235 VAB4=VAB4+Q(IJ,4)*DBA(IJ)
IF(KI.EQ.1) VNOC(N)=VNOC(N)*VAB*4.D0
IF(KF.EQ.8) VACQ(N)=VACQ(N)*VAB4*4.D0
C***** DEBUG
610 WRITE(6,610)VAB,VAB4
0078 FORMAT(1H,0 INT: VAE=, E15.6,5X,VAB4=,E15.6)
C***** DEBUG
NINTS=0
LAST=C
IJ=0
C FORM 2 EL 0 INTS
DO 290 I=1,NRF
150J=0
LSTOP=I-1
DO 275 J=1,I
IJ=IJ+1
IF(I.NE.J) GC TC 236
LSTOP=I
150J=2
236 KSTOP=I
DC 237 K=1,IJ
HQ(K)=0.0D0
H(K)=0.0D0
237 IF(KI.NE.1) GC TC 242
DO 240 K=1,3
DC 239 KL=1,IJ
H(KL)=H(KL)+G(KL,K)*O(IJ,K)
239 CONTINUE
240 IF(KF.NE.8) GO TO 243
242 DO 241 K=4,8
0099 DO 241 KL=1,IJ
0101 HQ(KL)=HQ(KL)+G(KL,K)*O(IJ,K)
0102

```



```

0152 CC 241 I=1,NSYM
0153 H(I)=C.000
0154 HQ(I)=0.000
0155 HC(I)=0.000
0156 HD(I)=0.000
0157 DEAI(I)=-2.00+DB2(I)
0158 REWIND 10
0159 REWIND 11
0160 IF(KI.EQ.1) CALL JKPCCT(P,CEA,CB2,ISNX,10,HO,DR02,
* .CLOSED)
0161 IF(KF.EQ.8) CALL JKPCCT(HQ,DBA,DB2,ISNX,11,HOO,DR02
* .CLOSED)
C***** DEBUG *****
0162 WRITE(6,507)(HQ(I),I=1,NSYM)
0163 FORMAT(1H,5HC*/(1H,5E15.6))
C***** DEBUG *****
0164 REWIND 10
0165 REWIND 11
C CHANGE DB BACK
0166 DO 282 I=1,NSYM
0167 DBA(I)=DBA(I)/2.00
0168 I1=0
0169 DO 283 I=1,NDF
0170 I1=I1+1
0171 DBA(I)=DBA(I)/2.00
C CALC < B B | 2J0-K0 | B B >
VAR=0.000
VAB=C.000
VAB4=C.000
IJ=0
0172 DO 285 I=1,NBF
0173 DO 285 J=1,I
0174 IJ=IJ+1
0175 VAB=VAB+H(IJ)*DBA(IJ)+HC(IJ)*DEAC(IJ)
0176 VAB4=VAB4+HQ(IJ)*DBA(IJ)+HOO(IJ)*DBAD(IJ)
0177 IF(KI.EQ.1) VEGD(N)=VAB+2.C0
0178 IF(KF.EQ.8) VEQD(N)=VAB+2.D0
C***** DEBUG *****
0179 WRITE(6,610)VAB,VAB4
C***** DEBUG *****
0180 CCNTINUE
0181 WRITE(6,601)(VNOQ(I),VNOQ(I),VEGD(I),VEGD(I),I=1,NVEXP)
0182 FORMAT(1H,50 INTEGRAL TERMS,
* 1H,4X,4HVNOQ,16X,4HVEGD,16X,4HVEQD,16X,4HVEQD/(1H,4E20.12))
0183 RETURN
0184 IF(NVST.GT.NVEXP)JR=INCUT.EQ.0) RETURN
0185 NI=NVST
0186 GO TO 210
0187 FND
0188
0189
0190

```

```

0001 SUBROUTINE MBIID(M,N,A,IA,W)
0002 IMPLICIT REAL*8(A-P,O-Z)
0003 DIMENSION A(IA,1),W(1)
0004 C PARTITION THE WORKING SPACE ARRAY W
0005 C THE FIRST PARTITION FOLDS THE FIRST COMPONENTS OF THE VECTORS OF
0006 C THE ELEMENTARY TRANSFORMATIONS
0007 C THE SECOND PARTITION RECORDS ROW INTERCHANGES
0008 C THE THIRD PARTITION RECORDS COLUMN INTERCHANGES
0009 C SET THE INITIAL RECORDS OF ROW AND COLUMN INTERCHANGES
0010 DO 1 I=1,M
0011 W(NRW+I)=0.500+DFLOAT(I)
0012 C CONTINUE
0013 DO 2 I=1,N
0014 W(NCW+I)=0.500+DFLOAT(I)
0015 C CONTINUE
0016 *KK: COUNTS THE SEPARATE ELEMENTARY TRANSFORMATIONS
0017 KK=1
0018 C FIND LARGEST ROW AND MAKE ROW INTERCHANGES
0019 RMAX=C.0D0
0020 DO 4 I=KK,M
0021 SUM=0.0D0
0022 DO 5 J=KK,N
0023 SUM=SUM+A(I,J)**2
0024 IF (RMAX-SUM) 6,4,4
0025 RMAX=SUM
0026 IR=I
0027 C CONTINUE
0028 IF (IR-KK) 7,7,8
0029 SUM=W(NRW+KK)
0030 W(NRW+IR)=SUM
0031 W(NRW+KK)=SUM
0032 A(KK,J)=A(IR,J)
0033 A(IR,J)=SUM
0034 C CONTINUE
0035 C FIND LARGEST ELEMENT OF PIVOTAL ROW, AND MAKE COLUMN INTERCHANGES
0036 RMAX=0.0D0
0037 DO 10 J=KK,N
0038 SUM=SUM+A(KK,J)**2
0039 IF (RMAX-SUM) 11,10,10
0040 RMAX=SUM
0041 IR=J
0042 C CONTINUE
0043 IF (IR-KK) 12,12,13
0044 RMAX=W(NCW+KK)
0045 W(NCW+IR)=W(NCW+IR)
0046 W(NCW+KK)=W(NCW+IR)
0047 DO 14 I=1,M
0048 WMAX=A(I,IR)
0049 A(I,IR)=A(I,IR)
0050 A(I,IR)=WMAX
0051 C CONTINUE
0052 C REPLACE THE PIVOTAL ROW BY THE VECTOR OF THE TRANSFORMATION
0053
0054
0055
0056
0057
0058
0059

```

```

0049 12 SIGMA=DSQRT(SUM)
0050 BSO=DSQRT(SUM+SIGMA*DABS(A(KK,KK)))
0051 W(KK)=DSIGN(SIGMA*DABS(A(KK,KK)),A(KK,KK))/BSQ
0052 A(KK,KK)=-DSIGN(SIGMA,A(KK,KK))
0053 KP=KK+1
0054 IF (KP-N) 15,15,16
0055 DO 17 J=KP,N
0056 A(KK,J)=A(KK,J)/BSQ
0057 CCNTINUE
C
0058 17 APPLY THE TRANSFORMATION TO THE REMAINING ROWS OF A
0059 IF (KP-M) 18,18,16
0060 DO 19 I=KP,M
0061 SUM=W(KK)*A(I,KK)
0062 DC 20 J=KP,N
0063 SUM=SUM+A(KK,J)*A(I,J)
0064 CONTINUE
0065 A(I,KK)=A(I,KK)-SUM*W(KK)
0066 DO 21 J=KP,N
0067 A(I,J)=A(I,J)-SUM*A(KK,J)
0068 CONTINUE
0069 19 CONTINUE
0070 KK=KP
C
0071 GO TO 3
C
0072 AT THIS STAGE THE REDUCTION OF A IS COMPLETE
0073 NOW WE BUILD UP THE GENERALIZED INVERSE
0074 APPLY THE FIRST ELEMENTARY TRANSFORMATION
0075
0076 16 KK=M
0077 KP=M+1
0078 SUM=W(M)/A(M,M)
0079 IF (N-M) 33,33,34
0080 DO 35 J=KP,N
0081 A(M,J)=-SUM*A(M,J)
0082 CCNTINUE
0083 35 A(M,M)=1.000/A(M,M)-SUM*W(M)
0084 NOW APPLY THE OTHER (M-1) TRANSFORMATIONS
0085 KP=KK
0086 IF (KK) 37,37,38
0087 FIRST TRANSFORM THE LAST (M-KK) ROWS
0088 DO 39 I=KP,M
0089 SUM=0.000
0090 DO 40 J=KP,N
0091 SUM=SUM+A(KK,J)*A(I,J)
0092 CCNTINUE
0093 DO 41 J=KP,N
0094 A(I,J)=A(I,J)-SUM*A(KK,J)
0095 CONTINUE
0096 W(I)=-SUM*W(KK)
0097 CCNTINUE
C
0098 THEN CALCULATE THE NEW ROW IN POSITION KK
0099 DO 42 J=KP,N
0100 SUM=-W(KK)*A(KK,J)
0101 DO 43 I=KP,M
0102 SUM=SUM-A(I,KK)*A(I,J)
0103 CONTINUE
0104 A(KK,J)=SUM/A(KK,KK)
0105 CCNTINUE
C
0106 AND REVISE THE COLUMN IN POSITION KK
0107 SUM=1.000-W(KK)*2
0108
0109
0110
0111
0112
0113
0114
0115
0116
0117
0118

```

```

0100      CC 44 I=K+M
0101      SUM=SUM-A(I, KK)*W(I)
0102      A(I, KK)=W(I)
0103      44 CONTINUE
0104      A(KK, KK)=SUM/A(KK, KK)
0105      GO TO 36
0106      C
0107      RESTORE THE ROW INTERCHANGES
0108      DO 45 I=1, M
0109      46 IR=IDINT(W(NRW+I))
0110      47 SUM=W(NRW+I)
0111      W(NRW+I)=W(NRW+IR)
0112      W(NRW+IR)=SUM
0113      DO 48 J=1, N
0114      SUM=A(I, J)
0115      A(I, J)=A(IR, J)
0116      A(IR, J)=SUM
0117      48 CONTINUE
0118      GO TO 46
0119      C
0120      RESTORE THE COLUMN INTERCHANGES
0121      DO 49 J=1, N
0122      50 IR=IDINT(W(NCW+J))
0123      IF (J-IR) 51, 49, 45
0124      51 SUM=W(NCW+J)
0125      W(NCW+J)=W(NCW+IR)
0126      W(NCW+IR)=SUM
0127      CC 52 I=1, M
0128      SUM=A(I, J)
0129      A(I, J)=A(I, IR)
0130      A(I, IR)=SUM
0131      52 CONTINUE
0132      GO TO 50
0133      49 CONTINUE
0134      RETURN
0135      END

```

```

0001 SUBROUTINE VA05AC(CALFUN,M,N,F,X,DSTEP,DMAX,ACC,MAXFUN,IPRINT,b)
0002 IMPLICIT REAL*8(A-H,O-Z)
0003 LOGICAL RESTRT
0004 C NOTE THAT THE INSTRUCTION CALLING SUBROUTINE 'MBL11A',
0005 C CN LINE NUMBER '138', IS NOT STANDARD FORTRAN
0006 C DIMENSION F(1),X(1),*(1)
0007 C COMMON/FIT/IS,IC,DD,FMIN,TINC,EXX(474),RESTRT,MAXM
0008 C SFT VARIOUS PARAMETERS
0009 C MAXC=C
0010 C *MAXC: COUNTS THE NUMBER OF CALLS OF CALFUN
0011 C NPA=M+N
0012 C NTEN=2
0013 C NTEST=0
0014 C *NT: AND *NTEST: CAUSE AN ERRCR RETURN IF F(X) DOES NOT DECREASE
0015 C DTEST=FLOAT(N+N)-C.5
0016 C *DTEST: IS USED IN A TEST TO MAINTAIN LINEAR INDEPENDENCE
0017 C PARTITION THE WORKING SPACE ARRAY W
0018 C THE FIRST PARTITION HOLDS THE JACOBIAN APPROXIMATION
0019 C *WI=M*N
0020 C THE NEXT PARTITION HOLDS THE GENERALIZED INVERSE
0021 C *NWX=NWI*MPN*N
0022 C THE NEXT PARTITION HOLDS THE BEST VECTOR X
0023 C *NWF=NWX+N
0024 C THE NEXT PARTITION HOLDS THE BEST VECTOR F
0025 C *NWC=NWF+W
0026 C THE NEXT PARTITION HOLDS THE COUNTS OF THE INDEPENDENT DIRECTIONS
0027 C *NWD=NWC+N
0028 C THE NEXT PARTITION HOLDS THE INDEPENDENT DIRECTIONS
0029 C *NWX=NWD+N*N
0030 C THE REMAINDER OF W IS USED FOR SCRATCH VECTORS
0031 C *NWT=NWX+W
0032 C *NWU=NWT+N
0033 C *MAXW=2*(N*(M+N)+M)+S*N
0034 C USUALLY *FMIN: IS THE LEAST CALCULATED VALUE OF F(X)
0035 C *DSS=DSTEP*DSTEP
0036 C *DM=DVAX*DMAX
0037 C *PARM=DSORT(ACC)/DMAX
0038 C *PARM: IS THE LEAST VALUE OF THE MARQUARDT PARAMETER
0039 C *DPAR=10.0D0*DM
0040 C *IS: AND *NTPAR: ARE USED TO REGULATE THE MARQUARDT PARAMETER
0041 C *TINC: CONTROLS A GOTO STATEMENT FOLLOWING A CALL OF CALFUN
0042 C *TINC: IS USED IN THE CRITERION TO INCREASE THE STEP LENGTH
0043 C START A NEW PAGE FOR PRINTING
0044 C IF(RESTRT) GOTO 200
0045 C FMIN=-1.D0
0046 C DD=0.0D0
0047 C IS=4
0048 C IC=0
0049 C TINC=1.D0
0050 C IF (IPRINT) 1,3,1
0051 C 200 1 PRINT 2
0052 C 2 FORMAT (IHI,4X,'THE FOLLOWING OUTPUT IS PROVIDED BY SUBROUTINE',
0053 C 1,VA05AC,/)
0054 C IFC=0
0055 C GOTO 3
0056 C TEST WHETHER THERE HAVE BEEN MAXFUN CALLS OF CALFUN

```

2 3 4 5 6 7 8 9 10 11 12 13 14 15 16 17 18 19 20 21 22 23 24 25 26 27 28 29 30 31 32 34 36 37 38 39 40 41 42 44 47 48 49 50 51 52 53 54 55



```

0076      4 IF (MAXFUN-MAXC) 5,5,2
0077      5 IF (IPRINT) 139,140,139
0078      140 IPRINT=2
0079      GC TO 19
0080      139 PRINT 6,MAXC
0081      6 FCRMAT (//5X,'ERROR RETURN FROM VA05A BECAUSE THERE HAVE BEEN',
0082      115,' CALLS OF CALFUN')
0083      GO TO 7
0084      C CALL THE SUBROUTINE CALFUN
0085      3 MAXC=MAXC+1
0086      CALL CALFUN (M,N,F,X)
0087      C CALCULATE THE SUM OF SQUARES
0088      FSO=0.000
0089      DC 8 I=1,M
0090      FSO=FSO+F(I)*F(I)
0091      8 CONTINUE
0092      C TEST FOR ACC
0093      IF(FSO-ACC) 180,180,181
0094      180 WRITE(6,780)
0095      780 FCRMAT(//1H,'FSC .LT. ACC//')
0096      GO TO 7
0097      C TEST FOR ERROR RETURN BECAUSE F(X) DOES NOT DECREASE
0098      181 GO TO (9,10,9,10),IS
0099      9 IF (FSO-FMIN) 11,12,12
0100      12 IF (DC-DSS) 13,13,10
0101      13 NTEST=NTEST-1
0102      14 IF (NTEST) 14,14,10
0103      17 IPRINT=1
0104      GC TO 19
0105      15 PRINT 16
0106      16 FORMAT (//5X,'ERROR RETURN FROM VA05A BECAUSE F(X) NO LONGER',
0107      1,' DECREASES',//5X,'THIS MAY BE DUE TO THE VALUES OF DSTEP',
0108      2,' AND ACC, OR TO LOSS OF RANK IN THE JACCOBIAN MATRIX')
0109      PROVIDE PRINTING CF FINAL SOLUTION IF REQUESTED
0110      C
0111      7 IF (IPRINT) 18,19,18
0112      18 PRINT 20,MAXC
0113      20 FCRMAT (//5X,'THE FINAL SOLUTION CALCULATED BY VA05A REQUIRED',
0114      115,' CALLS OF CALFUN, AND IS')
0115      PRINT 21,(I,W(NWX+1),I=1,N)
0116      21 FORMAT (//4X,'I',7X,'X(I)',10X,'I',7X,'X(I)',10X,'I',7X,'X(I)',
0117      110X,'I',7X,'X(I)',10X,'I',7X,'X(I)//5(I5,D17.8)')
0118      PRINT 22,(I,W(NWF+1),I=1,M)
0119      22 FORMAT (//4X,'I',7X,'F(I)',10X,'I',7X,'F(I)',10X,'I',7X,'F(I)',
0120      110X,'I',7X,'F(I)',10X,'I',7X,'F(I)//5(I5,D17.8)')
0121      PRINT 23,FMIN
0122      23 FORMAT (//5X,'THE SUM CF SQUARES IS',D17.8)
0123      C RESTORE THE BEST VALUES CF X AND F
0124      19 DD 135 I=1,N
0125      X(I)=W(NWX+1)
0126      135 CCNTINUE
0127      DD 136 I=1,M
0128      F(I)=W(NWF+1)
0129      136 CONTINUE
0130      RETURN
0131      11 NTEST=NT
0132      C PROVIDE ORDINARY PRINTING IF REQUESTED
0133      10 IF(IAES(IPRINT)-1) 35,36,4C
0134      38 PRINT 41,MAXC

```

56  
57  
58  
59  
60  
61  
62  
63  
64  
65  
66  
67  
68  
69  
70  
71  
  
72  
73  
74  
75  
76  
77  
78  
79  
80  
81  
82  
83  
84  
85  
86  
87  
88  
89  
90  
91  
92  
93  
94  
95  
96  
97  
98  
99  
100  
101  
102  
103  
104  
105  
106  
107  
108  
109

09/13/79

DATE = 79229

VAD5AC

FORTRAN IV G LEVEL 21

```

0082 41 FORMAT (//5X,'AT THE',IS,' TH CALL OF CALFUN WE HAVE')
0083 42 PRINT 21,(I,X(I),I=1,N)
0084 PRINT 23,F50
0085 IF (I PRINT) 39,39,142
0086 PRINT 22,(I,F(I),I=1,M)
0087 GO TO 39
0088 40 IPC=IPC-1
0089 IF (IPC) 43,43,39
0090 43 PRINT 44,MAXC
0091 44 FORMAT (//5X,'THE BEST ESTIMATE AFTER',IS,' CALLS OF CALFUN IS')
0092 IPC=IABS(IPRINT)
0093 IF (FMIN) 42,46,46
0094 IF (F50-FMIN) 42,45,45
0095 PRINT 21,(I,W(NWX+I),I=1,N)
0096 PRINT 23,FMIN
0097 IF (I PRINT) 35,39,143
0098 PRINT 22,(I,W(NWF+I),I=1,M)
0099 GC TO (49,47,47,48),IS
C STORE THE INITIAL VECTORS X AND F
0100 48 IF (I) 50,50,51
0101 50 DO 52 I=1,N
0102 W(NWX+I)=X(I)
0103 CCNTINJE
0104 GO TO 54
C CALCULATE THE INITIAL JACCOBIAN APPROXIMATION
0105 51 K=IC
0106 DO 55 I=1,M
0107 W(K)=(F(I)-W(NWF+I))/DSTEP
0108 K=K+N
0109 55 CCNTINJE
C TEST WHETHER THE MOST RECENT X IS BEST
0110 56 X(IC)=W(NWX+IC)
0111 IF (FMIN-F50) 56,56,57
0112 GO TO 58
0113 57 W(NWX+IC)=X(IC)
0114 DO 53 I=1,M
0115 W(NWF+I)=F(I)
0116 CCNTINJE
0117 FMIN=F50
C SET X FOR THE NEXT CALL OF CALFUN
0118 IC=IC+1
0119 IF (IC-N) 59,59,60
0120 X(IC)=W(NWX+IC)+DSTEP
0121 GC TO 3
C SET THE DIRECTION MATRIX
0122 60 K=NWD
0123 DO 61 I=1,N
0124 DO 62 J=1,N
0125 K=K+1
0126 W(K)=G.000
0127 CCNTINJE
0128 W(K+I-N)=1.00
0129 W(NWC+I)=1.00+DFLOAT(N-I)
0130 61 CCNTINJE
C SET THE MARQUARDT PARAMETER TO ITS LEAST VALUE
0131 24 PAR=PARM
C COPY THE JACCOBIAN AND APPEND THE MARQUARDT MATRIX
0132 25 PPAR=PAR*PAR
0133 NTPAR=0

```

```

110
111
112
113
114
115
116
117
118
119
120
121
122
123
124
125
126
127
128
129
130
131
132
133
134
135
136
137
138
139
140
141
142
143
144
145
146
147
148
149
150
151
152
153
154
155
156
157
158
159
160
161
162
163
164
165
166
167
168

```

00/13/29

DATE = 79229

VAOSAC

FORTRAN IV G LEVEL 21

```

0134      KK=0
0135      K=NWI+1
0136      DO 26 I=1,N
0137      DC 141 J=1,M
0138      KK=KK+1
0139      W(KK+NWI)=W(KK)
0140      CONTINUE
0141      DO 27 J=1,N
0142      K=K+1
0143      W(K)=0.000
0144      CONTINUE
0145      W(K+1-N)=PAR
0146      CONTINUE
0147      C
0148      C CALCULATE THE GENERALIZED INVERSE OF J
0149      C CALL MRLAD(N,MPN,W(NWI+1),N,W(NWI+1))
0150      C NOTE THAT THE THIRD AND FIFTH ENTRIES OF THIS ARGUMENT LIST
0151      C START FOR ONE-DIMENSIONAL ARRAYS.
0152      C START THE ITERATION BY TESTING FMIN
0153      C IF (FMIN-ACC) 7,7.65
0154      C NEXT PREDICT THE DESCENT AND MARQUARDT MINIMA
0155      DS=0.000
0156      DN=0.000
0157      SP=0.000
0158      DO 66 I=1,N
0159      X(I)=0.000
0160      F(I)=C.000
0161      K=I
0162      DO 67 J=1,M
0163      X(I)=X(I)-W(K)*W(NWF+J)
0164      F(I)=F(I)-W(NWI+K)*W(NWF+J)
0165      K=K+N
0166      CONTINUE
0167      DS=DS+X(I)*X(I)
0168      DN=DN+F(I)*F(I)
0169      SP=SP+X(I)*F(I)
0170      CONTINUE
0171      C PREDICT THE REDUCTION IN F(X) DUE TO THE MARQUARDT STEP
0172      C AND ALSO PREDICT THE LENGTH OF THE STEEPEST DESCENT STEP
0173      PRD=SP+SP
0174      DMULT=0.000
0175      K=0
0176      DO 68 I=1,M
0177      AD=0.000
0178      DO 69 J=1,N
0179      K=K+1
0180      AF=AP+W(K)*F(J)
0181      AD=AD+W(K)*X(J)
0182      CONTINUE
0183      PRD=PRD-AP*AP
0184      DMULT=DMULT+AD*AD
0185      CONTINUE
0186      C TEST FOR CONVERGENCE
0187      IF (DN-DM) 28,28.29
0188      AP=DS CRT(DN)
0189      IF (PRD+2.000*PPAF*AP*(CMAX-AP)-ACC) 770,770.70
0190      IF (PRD+PPAR*(DM-DN)-ACC) 770,770.70
0191      WRITE(6,771)
0192      FORMAT(1H,' PREDICTED REDUCTION IN F(X) IS LESS THAN ACC')
0193
0194
0195
0196
0197
0198
0199
0200
0201
0202
0203
0204
0205
0206
0207
0208
0209
0210
0211
0212
0213
0214
0215
0216
0217
0218
0219
0220
0221
0222
0223

```

```

0185      GO TO 7
0186      TEST WHETHER TO APPLY THE FULL MARQUARDT CORRECTION
0187      DMULT=DS/DMULT
0188      CS=DS*DMULT*DMULT
0189      IS=2
0190      IF (DN-DD) 72,72,73
0191      TEST THAT THE MARQUARDT PARAMETER HAS ITS LEAST VALUE
0192      IF (PAR-PARM) 30,30,24
0193      DD=DMAX1(DN,DSS)
0194      DS=0.2500*DN
0195      YNCE=1.000
0196      IF (DN-DSS) 74,132,132
0197      GO TO 103
0198      TEST WHETHER TO INCREASE THE MARQUARDT PARAMETER
0199      IF (DN-DPAR) 31,31,32
0200      NTPAR=0
0201      GC TO 33
0202      IF (NTPAR) 34,34,35
0203      NTPAR=1
0204      GO TO 33
0205      NTPAR=NTPAR+1
0206      PTM=DMINI(PTM,DN)
0207      IF (NTPAR-NI) 33,26,36
0208      SET THE LARGEN VALUE OF THE MARQUARDT PARAMETER
0209      PAR=PAR*(PTM/DM)**0.2500
0210      IF (6.00*DD-DM)137,25,25
0211      AP=DSQRT(PRE=0/DN)
0212      IF (AP-PAR) 25,25,138
0213      PAR=DMINI(AP,PAR*(DM/(6.00*CC))**0.2500)
0214      GO TO 25
0215      TEST WHETHER TO USE THE STEEPEST DESCENT DIRECTION
0216      IF (DS-DD) 75,76,76
0217      TEST WHETHER THE INITIAL VALUE OF DD HAS BEEN SET
0218      IF (DC) 77,77,78
0219      DD=DMINI(DM,DS)
0220      IF (DC-DSS) 75,78,78
0221      GO TO 71
0222      SET THE MULTIPLIER OF THE STEEPEST DESCENT DIRECTION
0223      ANMUL=0.00
0224      DMULT=DMULT*DSQRT(DD/DS)
0225      GO TO 80
0226      INTERPOLATE BETWEEN THE STEEPEST DESCENT AND MARQUARDT DIRECTIONS
0227      SP=SP*DMULT
0228      ANMUL=((DD-DS)/((SP-DS)+DSQRT((SP-DC)**2+(DN-CC)*(DD-DS)))
0229      DMULT=DMULT*(1.00C-ANMUL)
0230      CALCULATE THE CORRECTION TO X, AND ITS ANGLE WITH THE FIRST
0231      DIRECTION
0232      DN=0.000
0233      SP=0.000
0234      DO RI I=1,N
0235      F(I)=DMULT*X(I)+ANMUL*F(I)
0236      DN=DN+F(I)*F(I)
0237      SP=SP+F(I)*F(NWD+I)
0238      CCNT=I
0239      DS=0.2500*DN
0240      TEST WHETHER AN EXTRA STEP IS NEEDED FOR INDEPENDENCE

```

```

0233 IF (W(NWC+1)-DTEST) 122,132,82
0234 IF (SP*SP-DS) 93,132,132
C TAKE THE EXTRA STEP AND UPDATE THE DIRECTION MATRIX
0235 DC 94 I=1,N
0236 X(I)=W(NWC+1)+DSTEP*W(NWC+1)
0237 W(NWC+1)=W(NWC+1)+1.00
0238 CONTINUE
0239 W(NWD)=1.00
0240 IF(N.LE.1)GO TO 4
0241 DC 95 I=1,N
0242 K=NWD+1
0243 SP=W(K)
0244 DO 86 J=2,N
0245 W(K)=W(K+N)
0246 K=K+N
0247 CONTINUE
0248 W(K)=SP
0249 GO TO 4
0250 CONTINUE
C EXPRESS THE NEW DIRECTION IN TERMS OF THOSE OF THE DIRECTION
C MATRIX X, AND UPDATE THE COUNTS IN W(NWC+1) ETC.
132 IF(N.CE.2)GO TO 153
151 IS=1
152 GO TO 152
153 SP=0.00
154 K=NWD
DO 87 I=1,N
X(I)=DW
DW=0.000
DO 88 J=1,N
K=K+1
DW=DW+F(J)*W(K)
88 CONTINUE
GO TO (89,90),IS
90 W(NWC+1)=W(NWC+1)+1.00
SP=SP+DW*DW
91 IS=1
IF (SP-DS) 87,87,91
92 KK=1
X(I)=DW
GO TO 92
93 X(I)=DW
94 W(NWC+1)=W(NWC+1)+1.00
97 CONTINUE
W(NWD)=1.00
REORDER THE DIRECTIONS SO THAT KK IS FIRST
IF (KK-1) 93,93,94
94 K=NWC+KK*N
K=K+1
SP=W(K)
DC 95 J=2,KN
W(K)=W(K-N)
K=K-N
96 CONTINUE
W(K)=SP
97 CONTINUE
GENERATE THE NEW CRITICAL DIRECTION MATRIX
C 93 DO 97 I=1,N
0251
0252
0253
0254
0255
0256
0257
0258
0259
0260
0261
0262
0263
0264
0265
0266
0267
0268
0269
0270
0271
0272
0273
0274
0275
0276
0277
0278
0279
0280
0281
0282
0283
0284
0285
0286
0287
0288
0289
0290
0291
0292
0293
0294
0295
0296
0297
0298
0299
0300
0301
0302
0303
0304
0305
0306
0307
0308
0309
0310
0311
0312
0313
0314
0315
0316
0317
0318
0319
0320
0321
0322
0323
0324
0325
0326
0327
0328
0329
0330
0331
0332
0333
0334
0335
0336
0337
0338
0339
0340
0341
0342

```

```

0307 W(NMW+I)=0.000
0308 CONTINUE
0309 SP=X(I)*X(I)
0310 K=NWD
0311 DC 08 I=2,N
0312 CS=SQRT(SP*(SP+X(I)*X(I)))
0313 CW=SP/DS
0314 DS=X(I)/DS
0315 SP=SP+X(I)*X(I)
0316 DC 09 J=1,N
0317 K=K+1
0318 W(NMW+J)=W(NMW+J)+X(I-1)*W(K)
0319 W(K)=DW*(K+N)-DS*(NMW+J)
0320 CONTINUE
0321 99 100 I=1,N
0322 SP=1.000/DSQRT(DN)
0323 K=K+1
0324 W(K)=SP*F(I)
0325 CONTINUE
0326 100 CONTINUE
0327 C 152 PREDICT THE NEW RIGHT HAND SIDES
0328 FV=0.000
0329 K=0
0330 DC 101 I=1,M
0331 W(NMW+I)=W(NMF+I)
0332 DC 102 J=1,N
0333 K=K+1
0334 W(NMW+I)=W(NMW+I)+W(K)*F(J)
0335 FNF=FN+W(NMW+I)**2
0336 CONTINUE
0337 101 CONTINUE
0338 C CALCULATE THE NEXT VECTOR X, AND THEN CALL CALFUN
0339 DO 104 I=1,N
0340 X(I)=W(NWX+I)+F(I)
0341 CONTINUE
0342 GO TO 4
0343 C UPDATE THE STEP SIZE
0344 DMULT=0.900*FMIN+0.100*FNF-FSC
0345 IF (DMULT) 105,106,106
0346 DD=DMAXI(DSS,0.2500*DD)
0347 TINC=1.000
0348 IF (FSC-FMIN) 106,107,107
0349 TRY THE TEST TO DECIDE WHETHER TO INCREASE THE STEP LENGTH
0350 SP=0.000
0351 SS=0.000
0352 DO 105 I=1,M
0353 SP=SP+DABS(F(I)*(F(I)-W(NMW+I)))
0354 SC=SS+(F(I)-W(NMW+I))**2
0355 CONTINUE
0356 PJ=1.000+DMULT/(SP+DSQRT(SP*SP+DMULT*SS))
0357 SP=DMINI(A,000,TINC,PJ)
0358 TINC=PJ/SP
0359 DD=DMINI(DM,SP*DD)
0360 GO TO 106
0361 IF F(X) IMPROVES STORE THE NEW VALUE OF X
0362 IF (FSC-FMIN) 106,110,110
0363 FMIN=FSC
0364 DO 111 I=1,N
0365 SP=X(I)

```

343  
344  
345  
346  
347  
348  
349  
350  
351  
352  
353  
354  
355  
356  
357  
358  
359  
360  
361  
362  
363  
364  
365  
366  
367  
368  
369  
370  
371  
372  
373  
374  
375  
376  
377  
378  
379  
380  
381  
382  
383  
384  
385  
386  
387  
388  
389  
390  
391  
392  
393  
394  
395  
396  
397  
398  
399  
400  
401

```

0341 X(I)=W(NWX+I)
0342 W(NWX+I)=SP
0343 CONTINUE
0344 DO 112 I=1,M
0345 SP=F(I)
0346 F(I)=W(NWF+I)
0347 W(NWF+I)=SP
0348 CONTINUE
0349 DO 110 J=1,N
0350 IS=2
0351 IF (FMIN-ACC) 7,7,93
C CALCULATE THE CHANGES IN X AND IN F
0352 DO 107 I=1,N
0353 X(I)=X(I)-W(NWX+I)
0354 DS=DS+X(I)*X(I)
0355 CONTINUE
0356 DO 114 I=1,M
0357 F(I)=F(I)-W(NWF+I)
0358 CONTINUE
0359 K=NI
C CALCULATE THE GENERALIZED INVERSE TIMES THE CHANGE IN X
0360 SS=0.0D0
0361 DO 116 I=1,M
0362 SP=0.0D0
0363 DC 117 J=1,N
0364 K=K+1
0365 SP=SP+W(K)*X(J)
0366 CONTINUE
0367 W(NWV+I)=SP
0368 SS=SS+SP*SP
0369 CONTINUE
0370 C CALCULATE J TIMES THE CHANGE IN F
C ALSO APPLY PROJECTION TO THE GENERALIZED INVERSE
0371 DO 118 I=1,N
0372 ST=0.0D0
0373 K=NI+1
0374 DO 119 J=1,M
0375 ST=ST+W(K)*W(J+NWV)
0376 K=K+1
0377 CONTINUE
0378 ST=ST/SS
0379 K=NI+1
0380 DO 120 J=1,M
0381 W(K)=W(K)-ST*W(J+NWV)
0382 K=K+1
0383 CONTINUE
0384 ST=PPAR*X(I)
0385 K=I
0386 DO 121 J=1,M
0387 ST=ST+W(K)*F(J)
0388 K=K+1
0389 CONTINUE
0390 W(NW+I)=ST
0391 CONTINUE
0392 REVISE J AND CALCULATE ROW VECTOR FOR CORRECTION TO INVERSE
0393 IC=0
0394 K=NI
0395 KK=NI+1

```

```

0405 SPO=0.000
0406 SPP=0.000
0407 DO 122 I=1,M
0408 SS=F(I)
0409 ST=F(I)
0410 DO 123 J=1,N
0411 IC=IC+1
0412 KK=KK+1
0413 SS=SS-W(IC)*X(J)
0414 ST=ST-W(KK)*W(NMW+J)
0415 CONTINUE
0416 SS=SS/D5
0417 W(NMW+1)=ST
0418 SP=SP+F(I)*ST
0419 SPP=SPP+ST*ST
0420 DO 124 J=1,N
0421 K=K+1
0422 W(K)=W(K)+SS*X(J)
0423 CONTINUE
0424 124 CONTINUE
0425 122 CONTINUE
0426 ST=DAP*X(I)
0427 DO 126 J=1,N
0428 KK=KK+1
0429 ST=ST-W(KK)*W(NMW+J)
0430 CONTINUE
0431 W(NWT+1)=ST
0432 SPP=SP+PAR*X(I)*ST
0433 SPP=SPP+ST*ST
0434 CONTINUE
0435 C TEST THAT THE SCALAR PRODUCT IS SUFFICIENTLY ACCURATE
0436 C IF(0.0100*SPP-DABS(SP-SPP))63.63,127
0437 C CALCULATE THE NEW GENERALIZED INVERSE
0438 DO 128 I=1,N
0439 KENWI+1
0440 STEX(I)
0441 DO 129 J=1,M
0442 ST=ST-W(K)*F(J)
0443 K=K+N
0444 CONTINUE
0445 SS=0.000
0446 DO 130 J=1,N
0447 SS=SS+W(K)*X(J)
0448 K=K+N
0449 ST=(ST-PAR*SS)/SP
0450 KENWI+1
0451 DO 131 J=1,M,N
0452 W(K)=W(K)+ST*W(NMW+J)
0453 K=K+N
0454 131 CONTINUE
0455 128 CONTINUE
0456 GO TO 64
0457 END

```

461  
462  
463  
464  
465  
466  
467  
468  
469  
470  
471  
472  
473  
474  
475  
476  
477  
478  
479  
480  
481  
482  
483  
484  
485  
486  
487  
488  
489  
490  
491  
492  
493  
494  
495  
496  
497  
498  
499  
500  
501  
502  
503  
504  
505  
506  
507  
508  
509  
510  
511  
512  
513  
514



APPENDIX E

ON THE POSSIBILITY OF EXPERIMENTAL SEPARATION OF  
RESONANCES AND CUSPS FROM BACKGROUND IN ELECTRON SCATTERING

C.Jung\* and H.S.Taylor

Department of Chemistry, University of Southern California,  
Los Angeles, Calif. 90007 , USA

Subject index: 34.80

\* Present address : Fachbereich Physik, Universität,  
6750 Kaiserslautern , West Germany

### Abstract

It is demonstrated with the help of model calculations that a laser field can be used to suppress the background in electron scattering cross sections and to pick out only those parts which are rapidly varying as function of the incoming electron energy. Therefore it becomes possible to measure the pure Breit-Wigner peaks and threshold effects independent of the fact that interference between the resonances and the background in radiationless electron scattering is strong. The results are interpreted within the low frequency limit for free-free transitions. The AC Stark shift of the resonance is also observed.

## 1. Introduction

Some of the most spectacular physics in electron-atom scattering is in the appearance of resonances and threshold effects. Unfortunately, in many cases these effects are small structures buried in a big background and their shape is usually modified by interference with the background. Sometimes it is difficult to be sure if a measured structure is real or noise and sometimes it is hard to pull the interesting physical parameters out of the measured data. For a review of these effects and their experimental difficulties see ref.1. If on the other hand, an experimentalist were able, by some method, to suppress all the background in the neighborhood of a resonance, then a pure Breit-Wigner peak would be observed and it would be straightforward to determine the position  $E_R$  and the width  $\Gamma$  of this resonance. The purpose of this paper is to explain a method of performing an electron scattering experiment in such a way that only those parts of the scattering amplitude lead to a signal, which vary rapidly as function of the incoming electron energy. Thereby we pick resonances and cusps out of the total scattering amplitude and get rid of all background influences.

The basic idea is to perform the electron scattering process within a strong laser field and to collect only those scattered electrons which have emitted or absorbed a certain number of photons. This method has been suggested first in ref.2 in a treatment of free-free transitions in first order perturbation theory and low frequency limit.

It will become clear in this paper that the idea works under much more general circumstances. Processes in which an electron scatters off an atom or molecule and emits or absorbs photons at the same time are known under the name free-free transitions. (For a review of these processes see ref.3). In these processes three systems ( electron, target, laser field ) interact with each other and this makes a theoretical treatment so complicated that up to now only special cases and approximations have been investigated. If the photon energy is far away from all transition energies of the target states involved in the process then the interaction between the laser and the target can to a high degree of approximation be neglected and the problem reduces to the description of electrons under the simultaneous influence of the target potential and the laser field. To check this the

influence of the laser-target interaction on the processes considered here can be estimated by the following considerations: The external field induces an electric dipole moment in the target atom and this dipole field can be felt by the scattered electron and can thereby modify the electron-target interaction potential  $V$ . Next let us estimate the order of magnitude of this effect. In most of our calculations a photon energy of 0.005 a.u. is used which is close to the  $\text{CO}_2$  laser photon energy of 117meV. Because this photon energy is smaller by a factor 10 to 100 compared to the first excitation energy of the

atomic ground states we use the static polarizability to calculate the induced dipole moment ( Thereby we overestimate the effect ). For atoms the polarizability is between  $2 \cdot 10^{-25} \text{ cm}^3$  ( in e.s. units ) for such a small closed shell atom like Helium and  $400 \cdot 10^{-25} \text{ cm}^3$  for such a big alkali atom like Cesium.

To see strong signals in free-free transitions we need laser power fluxes in the order of  $10^8 \text{ Watt/cm}^2$  and for a  $\text{CO}_2$  laser this corresponds to an electric field amplitude of 270000 V/cm or 900 e.s.u.. Therefore the induced dipole moment is between  $1.8 \cdot 10^{-22} \text{ e.s.u.}$  and  $3.6 \cdot 10^{-20} \text{ e.s.u.}$  for the various atoms. A scattering electron at a distance of  $10^{-8} \text{ cm}$ , which is in the order of magnitude of the average distance of an electron in a resonance state from the atomic center, will feel a potential energy  $E_d$  of a magnitude between  $10^{-3} \text{ eV}$  and  $10^{-1} \text{ eV}$ . In electron scattering dipole effects are usually of importance only at very low energy where the electron-dipole interaction energy  $E_d$  is of the same order of magnitude as the kinetic energy  $E_i$  of the electron. In the case considered here  $E_d/E_i \approx 0.01$  in the worst case. Therefore it seems to be justified to neglect the laser-atom interaction.

This neglect of the laser-target interaction does not of course apply at all to molecules which have vibrational transition energies close to the photon energy. In general, the laser frequency must be far out of resonance with the target system.

In addition the laser field strength considered here is small compared to the internal field in the atoms and therefore it is not necessary to worry about the ionization of the target.

Now even this simplified problem without laser-target interaction has not yet been solved in general. Various treatments have either treated the laser field in perturbation expansion or have used the low frequency approximation. The method used here to suppress the background can be interpreted theoretically in the low frequency limit. The relevant ideas of this approximation will be given later in section 3 ( For some additional information about more general aspects of the low frequency approximation see refs. 4-7 ).

To fully appreciate the method it is perhaps better to forget about formal theories and instead to make some simple model calculations in the spirit of a numerical experiment. In section 2 we investigate in this way what may happen in an experiment since up to now the new method has not yet been realized in the laboratory. As such we construct a simple 1-dimensional model, which can be solved in terms of known functions. We do not use the low frequency approximation and we do not make a perturbation expansion of the electron-laser interaction. The approximations we must make are the neglect of the laser-target interaction, mentioned above, the dipole approximation and a cut off of the photon Fock space due to the inability to numerically

handle more than a finite number of photon number states. In practice this is not a problem as all reported results, upon inclusion of further photon states in the model, do not significantly change.

In section 3 we present a theoretical interpretation of our numerical results. Section 4 contains conclusions and final remarks and some suggestions onto how to optimise possible experiments. In the appendix we explain our model in detail and show how we calculate all transition amplitudes in terms of known functions.

We use atomic units for all numbers throughout the whole rest of the paper.



## 2. Results of the numerical experiments

We take a scattering problem in 1 dimension and represent the target by a 2-state system with an excitation energy  $E_{12}=0.6$ . We assume that this target provides a 2-channel square well potential  $V$  to the incoming electron ( see fig.1). In each figure below we have indicated the special choice of  $V$  used. We always start the process with the target in its lower state. If the laser is switched off and the incoming kinetic energy  $E_i$  of the electron is below 0.6 then the electron may either be transmitted or reflected without energy change. We denote this probability for transmission by  $T_{rl}$  and the probability for reflexion by  $R_{rl}$  (  $rl$  is an abbreviation for "radiationless" ). If  $E_i$  is above 0.6 the electron may excite the target and leave it in its upper state. We denote the probability for excitation in radiationless transmission by  $S_{rl}$  and the probability for excitation in radiationless reflexion by  $Q_{rl}$ .  $S_{rl}$  and  $Q_{rl}$  exist only for  $E_i > 0.6$  .

If we switch on the laser field, then the electron can, in addition to the above, exchange energy with the field in integer multiples of the photon energy  $\omega$ . We denote the probabilities for processes in which the electron gains (loses) the energy  $N\omega$  from the field by  $Q_N, R_N, S_N, T_N$  respectively.  $R_N(E_i)$  is the probability that an electron comes in with initial kinetic energy  $E_i$ , hits the target, is reflected leaving the target behind in its lower state and flies away with a final kinetic energy  $E_f = E_i + N\omega$  .

Similarly,  $Q_N(E_i)$  is the probability that the electron comes in with energy  $E_i$ , hits the target, is reflected leaving the target behind in its upper state and flies away with final energy  $E_f = E_i - E_{12} + N\omega$ .  $T_N(E_i)$  and  $S_N(E_i)$  are the probabilities for the corresponding processes in transmission. Of course,  $Q_N(E_i)$  and  $S_N(E_i)$  only exist for  $E_f > 0$  i.e.  $E_i + N\omega > E_{12}$ . The quantities  $Q, R, S, T$  are the 1-dimensional analogs to the differential cross sections in 3 dimensions.

In fig.2 we have chosen a potential  $V$  which causes an elastic scattering resonance at an incoming energy of  $E_R \approx 0.233$  with a width of  $\Gamma \approx 0.0002$ . This  $\Gamma$  is in the same order as the natural width of electron-rare gas atom resonances. The energy  $E_R$  is far below the threshold at  $E_T = 0.6$  and therefore no excitation of the target is possible near this energy. In the top line of fig.2 we show the quantities  $T_{r1}(E_i)$  on the left and  $R_{r1}(E_i)$  on the right as functions of  $E_i$ . Below we show the quantities  $T_N(E_i)$  and  $R_N(E_i)$  as functions of  $E_i$  for several values of  $N$ . The photon energy is always  $\omega = 0.005$  which is close to the photon energy of a  $CO_2$  laser. The power density of the field is so big that the quantity  $\alpha = eA / mc \hbar \omega$  has a magnitude of exactly 1. ( $e$  is the electron charge,  $m$  is the electron mass,  $c$  is the speed of light,  $A$  is the amplitude of the vector potential). This is still a moderate power density and therefore only one photon processes give a strong signal. Two photon transitions can just be seen. In fig.3 we show the results for a calculation in which we have increased the laser

power so that  $\alpha = 2$  but left all other parameters unchanged.

The important results of these figures are: The elastic resonance causes a whole series of resonances in each  $R_N$  and  $T_N$  but only a few ones are strong enough so that we can observe them immediately. The distance between two adjacent structures is exactly  $\omega$ . The strength of the individual structures depends on the laser power. In general we see more resonances if we increase the laser power. The most striking observation is, that in  $T_N, N \neq 0$  there is no background at all and the resonances appear as pure Breit-Wigner peaks. In all other cases ( i.e. for  $T_0$  and all  $R_N$  ) the interference of the resonances with the background is either similar to the corresponding radiationless case only with the difference that the relative resonance effect is smaller or the resonance shape is reflected compared to the radiationless case. The best examples for this reflection are in  $R_{+1}$  in fig.3. We see that it is easier to determine  $E_R$  and  $\Gamma$  out of  $T_{+1}$  or  $T_{-1}$  than out of  $T_{r1}$  or  $R_{r1}$ . In fig.2 note that  $T_N$  and  $T_{-N}$  or  $R_N$  and  $R_{-N}$  look similar in shape but are shifted by  $N\omega$ .

In fig.4 we have changed the offdiagonal elements of  $V$  so that the width  $\Gamma$  of the elastic resonance is now 0.0012 which is in the order of the resolution of common electron spectrometers. This change in  $V$  causes also a small shift in the position  $E_R$  of the resonance ( see the top line in fig.4 ). All other parameters are the same as in fig.2. The width  $\Gamma$  is now so big that there are overlaps of the

various resonance structures in  $R_N$  and  $T_N$  which influence the resonance shapes in general. For  $T_N, N \neq 0$  the wings of two adjacent resonance peaks simply add without any visible interference. Again  $T_N$  and  $T_{-N}$  or  $R_N$  and  $R_{-N}$  look similar in shape but shifted by  $N\omega$ . In fig.5 we show the resonance curves for  $\alpha=3$  and otherwise the same parameters as in fig.4. We did not make calculations with another value of  $\omega$  because the interesting quantity is the ratio between  $\omega$  and  $\Gamma$  and a increase of  $\omega$  would cause similar effects as a decrease of  $\Gamma$ .

The only threshold of our 2-channel model is at  $E_T=0.6$  and it is interesting to compare radiationless scattering and free-free transitions close to this energy. Fig.6 shows radiationless scattering in the top line and free-free transitions below. In the drawings T and R are represented by solid lines and S and Q are represented by dotted lines. First we see that in free-free transitions the threshold for  $S_N$  and  $Q_N$  lies at  $E_i = E_T - N\omega$ . This is easy to understand because the energy which the electron gains/losses from the laser field goes into the energy balance for the excitation of the target by the electron impact and the new channel opens as soon as the final kinetic energy of the electron is above zero i.e. as soon as  $E_i + N\omega - E_T > 0$ , or  $E_i > E_T - N\omega$ . In  $T_{-1}$  we see a plateau between  $E_T$  and  $E_T + \omega$  and in  $T_{+1}$  a plateau between  $E_T - \omega$  and  $E_T$  with a sharp drop on both sides. In addition there are smaller threshold effects shifted by  $\omega$  away from the sharp drops. In  $T_{-2}$  and  $T_{+2}$  we see a sharp peak at  $E_T + \omega$  or  $E_T - \omega$

respectively and again smaller effects shifted away by  $\omega$ . In the other cases (  $T_0$  and all  $R_N$  ) the threshold effects occur at various  $E_i = E_T + n\omega$  and their shape is either of the same type as in the corresponding radiationless scattering or it is just turned upside down. In  $S_N$  and  $Q_N$  there are only very weak structures, too weak to be seen clearly in fig.6.

In fig.7 we see results for  $\alpha = 2$  and otherwise the same parameters as in fig.6. Now the threshold effects are distributed over more energy values and for example in  $T_{-1}$  the main drop on both sides of the plateau is shifted outwards by  $\omega$  on both sides compared to fig.6. In the picture for  $Q_0$  we see an "accidental" zero near  $E_i = 0.607$  which will be explained below. In fig.8 we see results for  $\omega = 0.002$  and otherwise the same parameters as in fig.6. All curves look nearly the same as in fig.6 only the energy scale is changed by a factor 2.5 which is the ratio between the photon energies in the two examples.

The most important results for the thresholds are in summary: A sudden drop ( or increase ) in the radiationless scattering as function of the incoming energy produces in the free-free probabilities  $T_{+1}$  and  $T_{-1}$  a plateau near the threshold energy and zero signal otherwise. At moderate laser power the length of the main structure is exactly  $\omega$ . Thereby the presense or absense of a threshold makes a 100% change in the relative signal strength but the absolute signal strength is always very low. Depending on

the values of  $\omega$  and  $\alpha$  the strong contributions to the threshold effects in  $T_N$  appear at different energies.

### 3. Interpretation of the numerical results

A theoretical explanation of the results of section 2 can be given most easily within the low frequency approximation and therefore let us first explain its basic idea. In order to be more general we give all formulas for the 3-dimensional case and consider the numerical results from section 2 as the special cases of the scattering angles 0 and  $\pi$ . If the laser wavelength is very long compared to atomic distances, then we can separate the free-free transition into three steps. First a free electron moves within the laser field and can virtually emit and absorb photons. Let us assume that the laser field is single mode and in the pure number state  $|N\rangle$  in absence of the electron. We denote the state of a free electron moving with momentum  $\vec{p}$  by  $|\vec{p}\rangle$ . If we neglect photon depletion effects and use the dipole approximation, then the exact state of the electron in the field is given by ( see appendix )

$$|\phi_{\vec{p}, N}\rangle = \sum_n J_n(\vec{\alpha} \cdot \vec{p}) |\vec{p}\rangle |N+n\rangle \quad (1)$$

$J_n$  is the Bessel function of first kind and order  $n$ .  
 $\vec{\alpha} = eA \vec{E} / mc \hbar \omega$  where  $\vec{E}$  is the polarization vector of the laser field. This  $\vec{\alpha}$  is the 3-dimensional generalization of the  $\alpha$  given above in section 2.

The Bessel functions  $J_n(\vec{\alpha} \cdot \vec{p})$  can be viewed as interaction coefficients for virtual  $n$  photon absorption/emission at absence of a target.

In dipole approximation there is no recoil of the electron during emission or absorption of a photon and therefore the electron momentum does not depend on how many photons the electron has absorbed or emitted i.e.  $|\vec{p}\rangle$  in (1) is independent of  $n$ . The energy of the electron is different in its various states and the electron wave connected with the photon number state  $|N+n\rangle$  is at energy  $E = p^2/2m - n\omega$ . Only the  $n=0$  term is on the energy shell and all other terms are off shell.

Then in the second step of the free-free transition this mixture of electron waves hits the target and is scattered. The main idea of the low frequency approximation is to neglect the laser-electron interaction during this second step and therefore the electron-target scattering is described by a radiationless scattering amplitude. But according to what was said above each term of the sum in (1) is scattered at its particular intermediate energy  $E_i - n\omega$  and its scattering is therefore described by a scattering amplitude at this shifted energy.

In the third step the scattered electron waves interact again with the laser and evolve into their final states.

Along these lines the following formula (3) has been derived first in ref.8 and confirmed later in ref.9 by another derivation. This formula gives the scattering

amplitude  $f_N(E_i, \vartheta)$  for an electron to come in with kinetic energy  $E_i$ , be scattered by an angle  $\vartheta$  and to have a final kinetic energy  $E_f$  of

$$E_f = E_i + N \omega \quad (2)$$

$$f_N(E_i, \vartheta) = \sum_k J_{N-k}(\vec{\alpha} \vec{p}_f) f_{rl}(E_i + k\omega, \vartheta) J_k(-\vec{\alpha} \vec{p}_i) \quad (3)$$

$f_{rl}$  is the corresponding amplitude for radiationless electron-target scattering. The three factors correspond to the three physical stages above. An analogous formula holds for scattering with excitation of the target if we take on the r.h.s. of (3) the corresponding scattering amplitude for radiationless excitation of the target and take the excitation energy into the energy balance (2).

Now let us decompose  $f_{rl}$  in (3) into a resonance part and a background part

$$f_{rl}(E_i + k\omega, \vartheta) = f_{rl}^R(E_i + k\omega, \vartheta) + f_{rl}^{BG}(E_i + k\omega, \vartheta) \quad (4)$$

The Bessel functions decrease rapidly for increasing order and fixed argument as soon as the absolute value of the order becomes larger than the absolute value of the argument. Therefore only a few  $k$  give a strong contribution to the  $k$  sum in (3). <sup>Since</sup>  $f_{rl}^{BG}$  depends only weakly on its energy argument then we can neglect this dependence, take all  $f_{rl}^{BG}$  at the energy  $E_i$ , pull  $f_{rl}^{BG}$  out of the  $k$  sum and apply the addition theorem of the Bessel functions and find

$$f_N(E_i, \vartheta) = J_N(\vec{\alpha}(\vec{p}_f - \vec{p}_i)) f_{rl}^{BG}(E_i, \vartheta) + \sum_k J_{N-k}(\vec{\alpha} \vec{p}_f) f_{rl}^R(E_i + k\omega, \vartheta) J_k(-\vec{\alpha} \vec{p}_i) \quad (5)$$

Our model calculation is independent of the low frequency



approximation and so a comparison between the exact numerical results of sec.2 and (5) can be viewed as test of (5).

The present state of the experimental verification of (5) is as follows: In ref.10  $|f_N|^2$  has been measured as function of N for several values of  $\vartheta, E_1, \vec{\epsilon}$ . All results are in qualitative agreement with (5). It has not been possible to check for quantitative agreement because the exact laser power distribution in space and time has not been known. For quantitative calculations its knowledge would be absolutely necessary since multiphoton transitions are a nonlinear effect and depend essentially on the exact power distribution in space and time and not only on the average power ( For these problems see also ref.11 ). In ref.10 resonances did not play any role and therefore only the first term in (5) has been measured. From such a measurement we cannot, in contrast to the present work, learn anything new about electron-atom scattering because the result is essentially the product of the elastic background cross section and a Bessel function - both well known quantities.

In refs.12,13  $|f_{-1}|^2$  has been measured as function of  $E_1$  near the argon resonances at 11eV but unfortunately only in backward direction for the one scattering angle  $\vartheta = 160^\circ$ . Since a weak laser has been used only the resonance structures at  $E_R$  and  $E_R + \omega$  could be seen. Their shape and strength is in full agreement with (5).

For scattering without excitation of the target  $|p_i| \approx |p_f|$  since  $\omega \ll E_1$  and therefore in forward direction we find

$\vec{\alpha}(\vec{p}_f - \vec{p}_i) \approx 0$ . The background term in (5) disappears in forward direction for  $N \neq 0$  because  $J_N(0) = \delta_{N,0}$ . This is the explanation why we did not see a background contribution for  $T_N, N \neq 0$  in the model calculations.  $f_{r1}^R$  produces a resonance structure when its energy argument is at  $E_R$  and therefore we get a resonance structure in the k-sum in (5) every time when  $E_i + k\omega = E_R$  for a  $k \in \mathbb{Z}$ . The magnitude of the resonance effect at  $E_i = E_R - k\omega$  depends on the exact value of the two Bessel functions in the corresponding term in (5). If  $\Gamma \ll \omega$  we get a series of well separated resonances with an energy spacing  $\omega$  between adjacent peaks. This is exactly what we saw in figs. 2-5.

In backward direction  $\vec{p}_f \approx -\vec{p}_i$  and in general  $J_N(\vec{\alpha}(\vec{p}_f - \vec{p}_i))$  is not near a zero and the background does not disappear. Depending on the relative signs of the various Bessel functions the relative phase between the resonance term and the background term is either the same as in the radiationless case or it is just shifted by  $\pi$ . Therefore the resonance shape is either the same as in the radiationless case or it is just reflected. The magnitude of the relative resonance effects depends again on the exact values of the corresponding Bessel functions and thereby on the parameters  $E_i, \alpha$ . We saw that  $T_N$  and  $T_{-N}$  or  $R_N$  and  $R_{-N}$  look nearly the same in shape but are only shifted by  $N\omega$ . This can be explained by the fact that  $J_N = (-1)^N J_{-N}$ .

One effect which is not contained in (5) is the AC Stark shift of the resonances. Let us look at fig. 9.

In this figure we show resonance structures in  $T_N$  and  $R_N$  at various initial energies  $E_i = E_R + k\omega$  and for various values of  $\omega$ ,  $\alpha$  and  $N$ . The potential  $V$  is the same as in figs. 2 and 3. In each picture we show the low frequency approximation of (3) as broken line and the exact numerical result as solid line. We see a shift of the resonance structures which does not depend on  $E_i$ ,  $N$  and  $\mathcal{V}$  but depends on  $\omega$  and  $\alpha$ . Besides this shift the low frequency limit gives the correct shape and height for all resonance peaks. The fact that the shift does not depend on the particular peak at which we look i.e. does not depend on  $E_i$ ,  $N$  and  $\mathcal{V}$  is an indication that the resonance itself is shifted and not only its appearance in the free-free transitions. The Stark shift goes quadratically with  $\omega$  and quadratically with  $\alpha$ . This is in exact agreement with the results of ref. 9. In our examples in fig. 9 the shift  $\Delta E_R \approx -0.25 \omega^2 \alpha^2$ . According to ref. 9 the proportionality constant between  $\Delta E_R$  and  $\omega^2 \alpha^2$  is a measure of the laser induced coupling between the resonance wave function  $\varphi_2$  in channel 2 and the continuum wave function  $\varphi_1$  in channel 1. Therefore a measurement of  $\Delta E_R / \omega^2 \alpha^2$  could give experimental information about the dipole matrix element  $\langle \varphi_1 | \vec{\epsilon} \vec{p} | \varphi_2 \rangle$ .

We could not see a change of  $\Gamma$  with increasing laser power. For this extra width caused by the Stark decay to become important much higher laser powers would be necessary.

Now let us try to explain the threshold effects in figs.6-8 by making a quite crude model for a threshold effect in radiationless scattering and representing the amplitude for scattering without target excitation by

$$f_{r1}(E_i, \mathcal{V}) = c(\mathcal{V}) + \Theta(E_i - E_T) d(\mathcal{V}) \quad (6)$$

where  $c$  and  $d$  do not depend on  $E_i$  and  $\Theta$  is the unit step function. If we insert (6) into (5) we get

$$f_N(E_i, \mathcal{V}) = c(\mathcal{V}) J_N(\alpha(\vec{p}_f - \vec{p}_i)) + d(\mathcal{V}) \sum_k J_{N-k}(\alpha \vec{p}_f) \Theta(E_i + k\omega - E_T) J_k(-\alpha \vec{p}_i) \quad (7)$$

For  $\vec{p}_f \approx \vec{p}_i$  and  $N \neq 0$  the first term drops. The second term produces a step at each  $E_i = E_T - k\omega, k \in \mathbb{Z}$ . The relative strength of the various steps depends on the exact values of the Bessel functions and thereby on the values of the parameters  $E_i$  and  $\alpha$ .

If we set  $\mathcal{V} = 0$  in (7) and assume a moderate laser power for which only first order contributions are important, we obtain

$$f_{-1}(E_i, 0) = \frac{1}{2} \alpha |p| d(0) \left\{ \Theta(E_i - E_T) - \Theta(E_i - \omega - E_T) \right\}$$

This is just a plateau between  $E_T$  and  $E_T + \omega$  and it is zero otherwise. An analogous calculation applies to  $T_{+1}$  and gives a plateau between  $E_T - \omega$  and  $E_T$ .  $T_{r1}$  in fig.6 does not have a sharp step at  $E_T$  but a rounded one and therefore also  $T_{+1}$  and  $T_{-1}$  have a rounded drop off on both sides of the plateau.

We see additional smaller threshold effects at other  $E_i$  which come from higher order contributions. For higher laser powers as e.g. in fig.7 higher order contributions

may become more important than first order contributions and therefore the steps at other  $E_i$  become more important.

If we look at  $T_{-2}$  and take only second order contributions of (7) we get

$$f_{-2}(E_i, 0) = d(0) \frac{1}{8} \alpha^2 p^2 \left\{ \theta(E_i - E_T) - 2\theta(E_i - E_T - \omega) + \theta(E_i - E_T - 2\omega) \right\}$$

This is a positive plateau between  $E_T$  and  $E_T + \omega$  and a negative plateau of the same absolute value between  $E_T + \omega$  and  $E_T + 2\omega$  and it is 0 otherwise.  $T_{-2} = \frac{p_f}{p_i} |f_{-2}(E_i, 0)|^2$  is then just a plateau between  $E_T$  and  $E_T + 2\omega$ . The step in  $T_{r1}$  in fig.6 is rounded and therefore a wedge remains at  $E_T + \omega$  in  $T_{-2}$  in fig.6. This wedge is a left over between two rounded cut offs on both sides. For higher power density in fig.7 again additional threshold effects at other  $E_i$  become important in  $T_{-2}$ . An analogous reasoning applies to  $T_{+2}$ .

For  $T_0$  and  $R_N$  both terms in (7) contribute and the relative phase between both terms is either the same as in the radiationless scattering or it is shifted by  $\pi$ . Therefore the shape of the threshold structures is either the same as in the radiationless case or it is just turned upside down as e.g. in  $R_0$  in fig.6 at  $E_T \pm \omega$ .

For  $E_i = 0.607$ ,  $\alpha = 2$ ,  $N = 0$ ,  $\vartheta = \pi$  and excitation of the target the quantity  $\vec{\alpha}(\vec{p}_f - \vec{p}_i)$  is just at the first zero of the Bessel function  $J_0(\vec{\alpha}(\vec{p}_f - \vec{p}_i))$  and this explains the accidental zero of  $Q_0$  in fig.7.

#### 4. Discussions and conclusions

We have seen that the low frequency approximation given in (3) explains all qualitative features of resonances and thresholds in free-free transitions except the AC Stark shift. The quantitative error of the low frequency approximation - corrected for the AC Stark shift - has always been below a few percent ( see fig.9 ). But the dependence of this error on the various parameters will probably depend on the dimension of the space. Therefore it would not be of general interest to add here a detailed investigation of the numerical error of the low frequency approximation in our 1-dimensional model.

What advice can we give to an experimentalist, who wants to utilize free-free transitions in order to look for resonances and cusps in electron-atom scattering?

The most interesting property of free-free transitions shown in this paper is that only rapidly varying parts of the radiationless scattering causes any free-free signal in forward direction. This fact may be used in an experiment to project out resonances and threshold effects. The price

to pay for this removal of the background is a reduction of the number of electrons which contribute to the signal. As shown in figs. 2-5 the ratio between the resonance height in  $T_N, N \neq 0$  and in  $T_{r1}$  is 0.1 in the most

favorable cases.

In an experiment it is not possible to measure at an angle of exactly  $\vartheta=0$ . By proper adjustment of the laser polarization vector  $\vec{\epsilon}$  it is possible to fulfil the relation

$$\vec{\epsilon} \cdot (\vec{p}_f - \vec{p}_i) = 0 \quad (8)$$

for any choice of  $\vec{p}_i$  and  $\vec{p}_f$ , just turn  $\vec{\epsilon}$  perpendicular to the momentum transfer  $\vec{q} = \vec{p}_f - \vec{p}_i$ . At the same time we want to see a strong resonance signal and according to (5)  $\vec{\epsilon} \cdot \vec{p}_f$  and  $\vec{\epsilon} \cdot \vec{p}_i$  should be big enough to give a big value for the Bessel functions. Therefore,  $\vec{\epsilon}$  should be as parallel to  $\vec{p}_f$  and  $\vec{p}_i$  as possible. All these conditions can be met best if  $\vec{p}_f$  and  $\vec{p}_i$  are as parallel to each other as the construction of the electron spectrometer allows and if  $\vec{\epsilon}$  is in the direction exactly in between  $\vec{p}_f$  and  $\vec{p}_i$ .

As indicated by the figs. 2-5 resonance signals are biggest and clearest in  $T_{+2}$  or  $T_{-2}$  at  $E_i = E_R - \omega$  or  $E_i = E_R + \omega$  respectively if the laser power density is so big that  $\vec{\alpha} \cdot \vec{p}_f$  and  $\vec{\alpha} \cdot \vec{p}_i$  are in between 1.5 and 2.2 i.e. if  $J_1(\vec{\alpha} \cdot \vec{p})$  is near its first maximum. In this case the resonance signal comes from the term  $J_{\pm 1}(\vec{\alpha} \cdot \vec{p}_f) f_{r1}(E_i \pm \omega, \vartheta) J_{\pm 1}(\vec{\alpha} \cdot \vec{p}_i)$  in (5). This means: The electron comes in shifted by one photons energy away from the resonance energy. Then it absorbs/emits one photon and can go into the resonance state. The resonance decays and the outgoing electron absorbs/emits another photon on its way out. For this choice of the parameters the resonance signal in  $T_{\pm 2}$  is about 10% of the resonance signal in the radiationless scattering, which is the best one

can hope for. In addition, for these values of the parameters the other resonance structures in  $T_{\pm 2}$  ( i.e. the ones at  $E_R, E_R \pm 2\omega, E_R \pm 3\omega$ , etc.) are quite small and this decreases the sources of confusion if several elastic resonances occur close together.

For the investigation of thresholds choose a moderate power density of the laser so that only first order contributions give a strong signal to the free-free amplitudes and look at  $T_{+1}$  or  $T_{-1}$  for structures of the length  $\omega$ . Two sharp drops in  $T_{+1}$  at  $E_a - \omega$  and  $E_a$  and a smooth behavior in between indicate a threshold at  $E_a$ . A similar structure in  $T_{-1}$  between  $E_a$  and  $E_a + \omega$  indicates the same threshold at  $E_a$ .

As indicated in figs. 6-8 the absolute signal in  $T_{N, N \neq 0}$  is extremely weak but the relative threshold effect is 1 and can therefore be seen clearly. This is in sharp contrast to elastic scattering where the relative threshold effects are generally small. Usually these effects are observed in electron impact excitation, where their relative effect is bigger than in the elastic channel. Our idea is unusual in so far that it filters out threshold effects in a process which is elastic with respect to the electron-target interaction. The big disadvantage of our method is the extremely small absolute size of the signal and there is the possibility that in a real experiment machine noise will bury the weak threshold signal and make it impossible to utilize our idea in the laboratory.



In any case for resonances or thresholds the photon energy should be chosen larger than the energy interval over which the radiationless scattering varies rapidly in order to avoid confusing overlaps of the structures in free-free transitions.

Can "accidental" zeros like the one in  $Q_0$  shown in fig.7 ( i.e. those values of parameters for which  $\vec{\alpha}(\vec{p}_f - \vec{p}_i)$  is at a zero of some Bessel function ) used for anything? We don't think so, because their position depends strongly on the exact laser power and in an experiment the laser power varies in time and space and the electrons, collected in the detector, have experienced quite different laser powers during their scattering process. Therefore, such an accidental zero would be completely smeared out in any real experiment.

There is also the interesting possibility that a free-free experiment might be used to probe the laser field strength. In ref.11 it has been shown how the results of a measurement of  $|f_N(E_i, \vartheta)|^2$  as function of  $N$  can be used to calculate the average power density of the laser field in which the experiment has been performed. It is probably possible to generalize the results of ref.11 and to work backwards to even more detailed information about the laser field.

Appendix

In this section we explain our model in detail and show how we calculate the amplitudes for all processes.

We work in a 1-dimensional space and choose  $x$  as space coordinate. We describe the electron-target interaction by a 2-channel square well potential of the form

$$\mathbf{V}(x) = \begin{pmatrix} V_{11} & V_{12} \\ V_{21} & V_{22} \end{pmatrix} \cdot \Theta(R - |x|) \quad (\text{A1})$$

$V_{12} = V_{21} \in \mathbb{R}$  so that  $\mathbf{V}$  is a self adjoint operator.

$\Theta$  is the unit step function. The matrix of excitation energies is

$$\mathbf{B} = \begin{pmatrix} 0 & 0 \\ 0 & E_{12} \end{pmatrix} \quad (\text{A2})$$

We cut the  $x$ -axis into the three intervals

$$I_1 = (+R, \infty), \quad I_2 = (-R, +R), \quad I_3 = (-\infty, -R)$$

The target is in its ground state initially and the electron comes in with momentum  $k_{in}$ . Then the matrix of the electron momentum in intervals  $I_1$  and  $I_3$  is

$$\mathbf{K} = \begin{pmatrix} k_0 & 0 \\ 0 & k_0 \end{pmatrix} = \begin{pmatrix} k_{in} & 0 \\ 0 & \sqrt{k_{in}^2 - 2mE_{12}} \end{pmatrix} \quad (\text{A3})$$

In  $I_2$  we set  $\mathbf{M} = \mathbf{B} + \mathbf{V}$  and construct the orthogonal matrix  $\mathbf{U}$  which diagonalizes  $\mathbf{M}$  according to

$$\mathbf{U}^+ \mathbf{M} \mathbf{U} = \mathbf{\Sigma} \quad \text{with} \quad \mathbf{\Sigma} = \begin{pmatrix} \sigma_1 & 0 \\ 0 & \sigma_2 \end{pmatrix} \quad (\text{A4})$$

$[\mathbf{k}_{in}^2 \mathbf{1} - 2m \mathbf{\Sigma}]^{\frac{1}{2}}$  is the diagonalized momentum matrix in  $I_2$ .

We assume a single mode laser field and use the dipole approximation.

The total Hamiltonian  $\mathbb{H}$  for the motion of the electron under the simultaneous influence of the target and the laser field is

$$\mathbb{H} = \left\{ \frac{p^2}{2m} + \hbar\omega a^+ a - \frac{ep}{mc} \beta (a^+ + a) \right\} \mathbb{1} + \mathbb{B} + \mathbb{V}(x) \quad (\text{A5})$$

$\beta$  is an abbreviation for  $\beta = (2\pi c^2 / \omega L^3)^{\frac{1}{2}}$  where  $L^3$  is the quantization volume of the electromagnetic field.  $p$  is the electron momentum operator,  $a$  and  $a^+$  are the annihilation and creation operators for a laser photon. We write  $|N\rangle$  for an eigenstate of  $a^+ a$  with eigenvalue  $N \in \mathbb{N}$ .

First let us look at eigenfunctions of  $\mathbb{H}$  in the intervalls  $I_1$  and  $I_3$ . There  $\mathbb{H}$  is diagonal with respect to the target states. We neglect photon depletion effects in the sense that we set  $\sqrt{N+n} = \sqrt{N}$  in the coupling strength between various photon number states, where  $N$  is the initial number of photons in the laser beam and  $N+n$  is the number of photons in intermediate or final states. Using the recursion formula of the Bessel functions

$$2n J_n(y) = y \{ J_{n-1}(y) + J_{n+1}(y) \} \quad (\text{A6})$$

we see that functions of the form

$$\varphi(k_0, x, N) = \exp(ik_0 x) \sum_n J_n(\alpha k_0) |N+n\rangle \quad (\text{A7})$$

are eigenfunctions of the operator

$$\frac{p^2}{2m} + \hbar\omega a^+ a - \frac{ep}{mc} \beta (a^+ + a) \quad (\text{A8})$$

with eigenvalue

$$N\omega + k_0^2 / 2m \quad (\text{A9})$$

$\alpha$  is an abbreviation for  $\alpha = e\sqrt{N}2\beta / mc \hbar \omega$ .

The quantity  $2\beta\sqrt{N}$  is the amplitude of the corresponding classical vector potential  $A$  of the laser field. Note that  $k_0$  is independent of  $n$  in (A7) because recoil effects of the electron are neglected in dipole approximation. In order to start from the most general eigenfunctions of  $H$  we must consider that the functions  $\varphi$  in (A7) are degenerate in two ways:

- 1.:  $\varphi$  remains an eigenfunction of operator (A8) to the same energy (A9) if we reverse  $k_0$  i.e. if we replace  $k_0$  by  $-k_0$ .
- 2.: We get an eigenfunction to the same energy if we replace  $N$  by  $N+L$  and simultaneously replace  $k_0$  by  $k_L$  where  $k_L^2 / 2m + L\omega = k_0^2 / 2m$

Therefore the most general eigenfunction of  $H$  with eigenvalue  $E$  in the interval  $I_1$  is the 2 component column vector

$$\Phi_1(E, x) = \sum_L \begin{pmatrix} r_{1,L} \varphi(k_L, x, L+N) + w_{1,L} \varphi(-k_L, x, L+N) \\ r_{2,L} \varphi(h_L, x, L+N) + w_{2,L} \varphi(-h_L, x, L+N) \end{pmatrix} \quad (A10)$$

where all  $k_L$  and  $h_L$  are given by

$$E = k_L^2 / 2m + (N+L)\omega = h_L^2 / 2m + (N+L)\omega + E_{12} \quad (A11)$$

$r_{i,L}$  and  $w_{i,L}$  are arbitrary complex constants to be fixed later by boundary conditions.

In a completely analogous way we find for the most general eigenfunction of  $H$  with eigenvalue  $E$  in interval  $I_3$

$$\Phi_3(E, x) = \sum_L \begin{pmatrix} j_{1,L} \varphi(k_L, x, L+N) + t_{1,L} \varphi(-k_L, x, L+N) \\ j_{2,L} \varphi(h_L, x, L+N) + t_{2,L} \varphi(-h_L, x, L+N) \end{pmatrix} \quad (A12)$$

$j_{i,L}$  and  $t_{i,L}$  are again constants to be fixed later by boundary conditions.

In the interval  $I_2$   $H$  is not diagonal with respect to target states but  $U^+ H U = \tilde{H}$  is and therefore we first construct eigenfunctions to  $\tilde{H}$ . In the same way as before we find for the most general eigenfunction of  $\tilde{H}$  with eigenvalue  $E$

$$\tilde{\Phi}_2(E, x) = \sum_L \begin{pmatrix} a_{1,L} \varphi(\lambda_L, x, L+N) + b_{1,L} \varphi(-\lambda_L, x, L+N) \\ a_{2,L} \varphi(\mu_L, x, L+N) + b_{2,L} \varphi(-\mu_L, x, L+N) \end{pmatrix} \quad (A13)$$

$$\text{where } \lambda_L^2 / 2m(N+L)\omega + \sigma_1 = E = \mu_L^2 / 2m(N+L)\omega + \sigma_2 \quad (A14)$$

with  $\sigma_1$  and  $\sigma_2$  given in (A4).

$a_{i,L}$  and  $b_{i,L}$  are again constants to be fixed later by boundary conditions.

$$\text{Because of } H U \tilde{\Phi}_2 = U \tilde{H} \tilde{\Phi}_2 = E U \tilde{\Phi}_2$$

we see that  $\Phi_2 = U \tilde{\Phi}_2$  is an eigenfunction of  $H$  with eigenvalue  $E$  in interval  $I_2$ .

At  $x=+\infty$  we choose the boundary condition that there is only one incoming wave with the target in state 1 and the laser and electron in state  $\varphi(-k_{in}, x, N)$  i.e.

$$w_{i,L} = \delta_{i,1} \delta_{L,0} \quad (A15)$$

At  $x=-\infty$  we choose the boundary condition that there is no incoming wave at all from the left i.e.

$$j_{i,L} = 0 \text{ for all } i \text{ and all } L \quad (A16)$$

At  $x=+R$  and  $x=-R$  we require that the wavefunction  $\Phi$  is

continuous and has a continuous first derivative. This gives 4 equations for 2-component column functions or 8 equations for linear combinations of photon number states. These equations must be fulfilled for the coefficients of each photon state separately and therefore each photon state gives us 8 equations which connect the constants  $a_{i,L}, b_{i,L}, t_{i,L}, r_{i,L}$  ( $i=1,2$ ). Some of these equations are inhomogeneous.

Al together, we get an infinite inhomogeneous system of linear equations to determine the free constants. In our model calculations we could only handle a finite number of equations with a finite number of unknowns and therefore we had to cut off the system of equations. Out of the coefficient matrix of the system of linear equations we have cut out the  $(2l+1) \cdot 8 \times (2l+1) \cdot 8$  matrix centered at the  $8 \times 8$  block which comes from the  $L=0$  terms in (A10, A12, A13) and the  $n=0$  terms in (A7). Accordingly we have cut out of the inhomogeneity vector a  $(2l+1)8$  component piece centered at the block which comes from the  $n=0$  terms in (A7). Then we have solved these  $(2l+1)8$  coupled linear equations.

We have found rapid convergence of the results with increasing  $l$  values as soon as  $l > |\alpha p|$ . For all calculations shown in figs. 2-9 it has been sufficient to choose a  $l$  value between 5 and 10. The rapid convergence can be understood from the fact that Bessel functions decrease rapidly as soon as the absolute value of the order becomes larger than

the absolute value of the argument. If we take a larger value of  $l$ , then we include coefficients which contain Bessel functions of higher orders.

As a last step we calculate the quantities

$$R_L = \frac{k_L}{k_{in}} |r_{1,L}|^2, \quad Q_L = \frac{h_L}{k_{in}} |r_{2,L}|^2$$

$$T_L = \frac{k_L}{k_{in}} |t_{1,L}|^2, \quad S_L = \frac{h_L}{k_{in}} |t_{2,L}|^2$$

These are the quantities plotted in figs. 2-9 as function of the incoming electron energy  $E_i$ .

All these calculations can also be performed for the case that the target is in state 2 initially. The only change is to replace  $\mathbf{K}$  of (A3) by

$$\mathbf{K} = \begin{pmatrix} k_0 & 0 \\ 0 & h_0 \end{pmatrix} = \begin{pmatrix} \sqrt{k_{in}^2 + 2mE_{12}} & 0 \\ 0 & k_{in} \end{pmatrix}$$

and to replace (A15) by

$$w_{i,L} = \delta_{i,2} \delta_{L,0}$$

#### Acknowledgment

This work has been supported by NSF Grant CHE 76-15656 A02 and ONR Grant N000-14-77-C-0102. We thank Prof. J. Hinze and the Zentrum für interdisziplinäre Forschung of the Universität Bielefeld for their hospitality while this work was being completed.

References

- 1.G.Schulz, Rev.Mod.Phys 45,378 ( 1973 )
- 2.C.Jung and H.Krüger, Z.Physik A287,7 ( 1978 )
- 3.M.Gavrila and M.Van der Wiel, Comments At.Mol.Phys 8,1 ( 1978 )
- 4.F.Low, Phys.Rev. 110,974 ( 1958 )
- 5.L.Heller, Phys.Rev. 174,1580 ( 1968 )
- 6.M.Mittleman, Phys.Rev.A21,79 ( 1980 )
- 7.L.Rosenberg, Phys.Rev.A21,1939 ( 1980 )
- 8.H.Krüger and C.Jung, Phys.Rev.A17,1706 ( 1978 )
- 9.M.Mittleman, Phys.Rev.A20,1965 ( 1979 )
- 10.A.Weingartshofer,E.Clarke,J.Holmes and C.Jung,  
Phys.Rev.A19,2371 ( 1979 )
- 11.C.Jung, Phys.Rev.A21,408 ( 1980 )
- 12.D.Andrick and L.Langhans, J.Phys.B 11,2355 ( 1978 )
- 13.L.Langhans, J.Phys.B 11,2361 ( 1978 )



Figure captions

Fig.1:Plot of the diagonal elements of the model potential for electron-target interaction used in all numerical calculations. The offdiagonal elements  $V_{12}=V_{21}$  ( not plotted in fig.1 ) are of the same shape as  $V_{11}$  but of different depth. Bound states of the 1-channel potential  $V_{22}+E_{12}$  become Feshbach type resonances of the full coupled 2-channel potential. Their width  $\Gamma$  is determined by the magnitude of  $V_{12}$ . For small  $V_{12}$  we find  $\Gamma \propto (V_{12})^2$ . See the two resonances in the upper lines of fig.2 and fig.4. A threshold effect occurs at the rim of the upper well i.e. at  $E=E_{12}$ .

Fig.2:Plots of resonance structures in radiationless scattering and in free-free transitions. For more explanations see main text.

Fig.3:Plots of resonance structures in free-free transitions. For more explanations see main text.

Fig.4:Plots of resonance structures in radiationless scattering and in free-free transitions. For more explanations see main text.

Fig.5:Plots of resonance structures in free-free transitions. For more explanations see main text.

Fig.6:Plots of threshold structures in radiationless scattering and in free-free transitions. For more explanations see main text.

Fig.7:Plots of threshold structures in free-free transitions. For more explanations see main text.

Fig.8:Plots of threshold structures in free-free transitions.For more explanations see main text.

Fig.9:Some examples for the AC Stark shift of resonances in free-free transitions.The solid lines are the results of numerical calculations.The broken lines are the results of eq.(3).For more explanations see main text.

Fig. 1

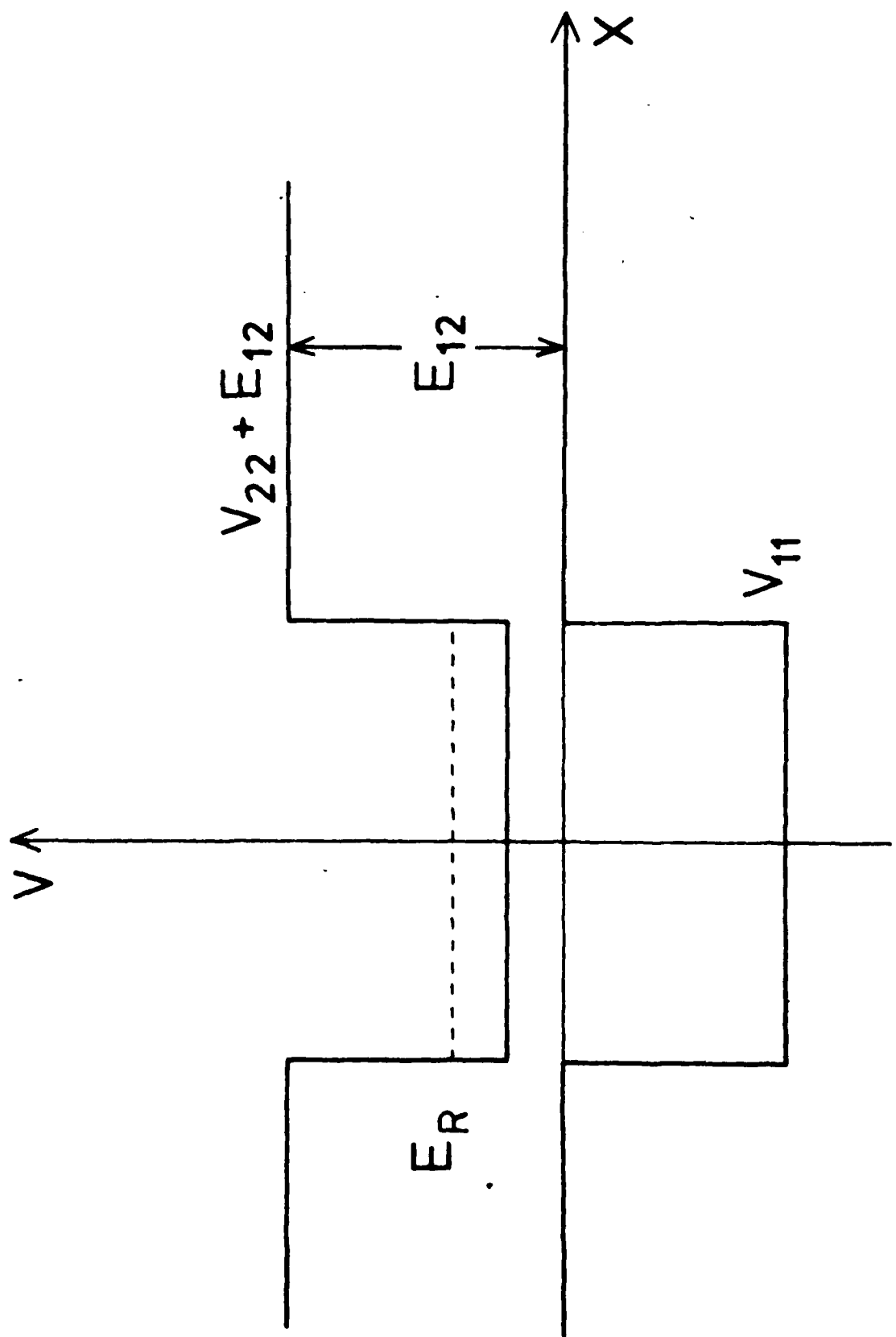


Fig. 2

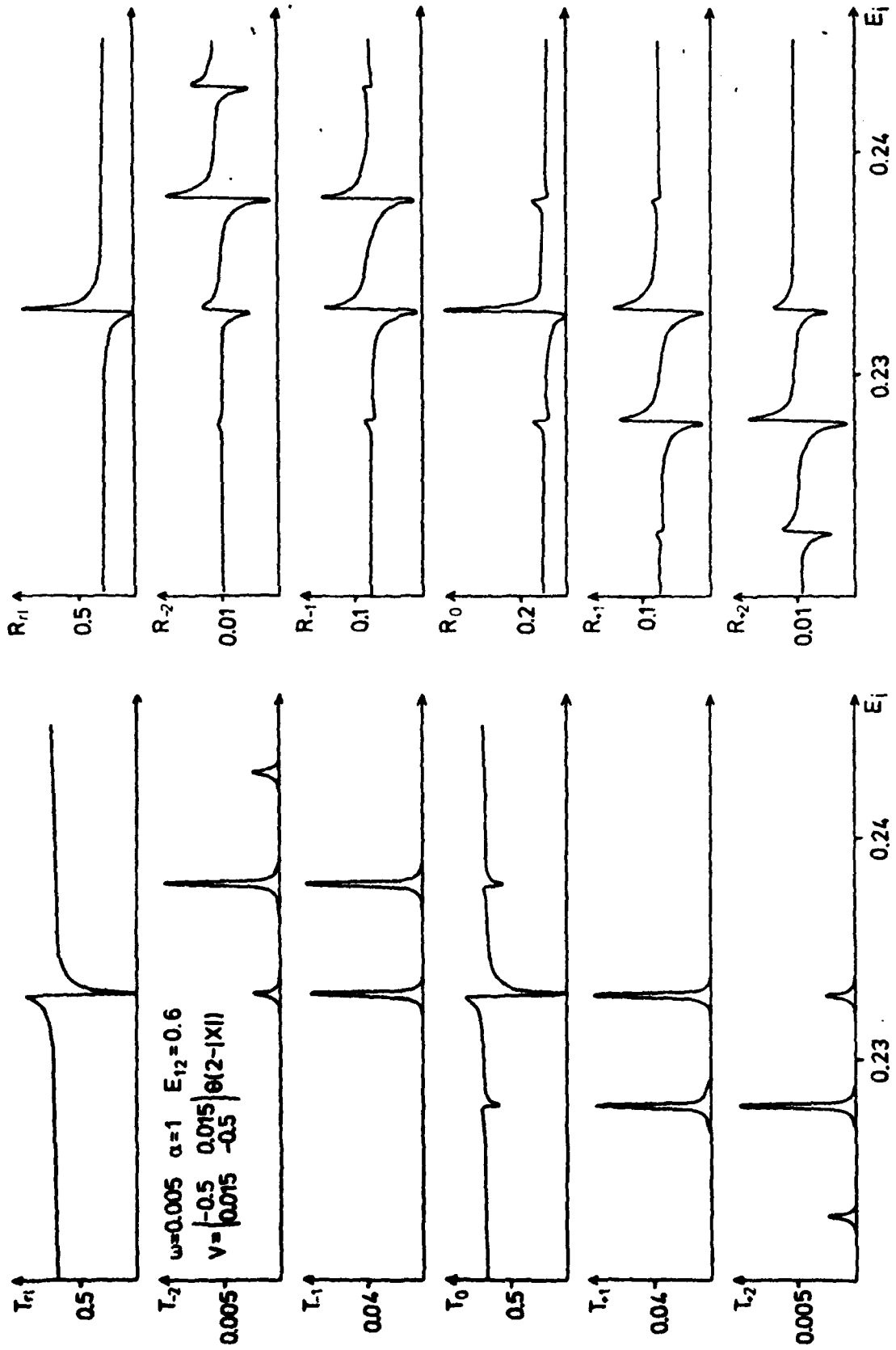


Fig. 3

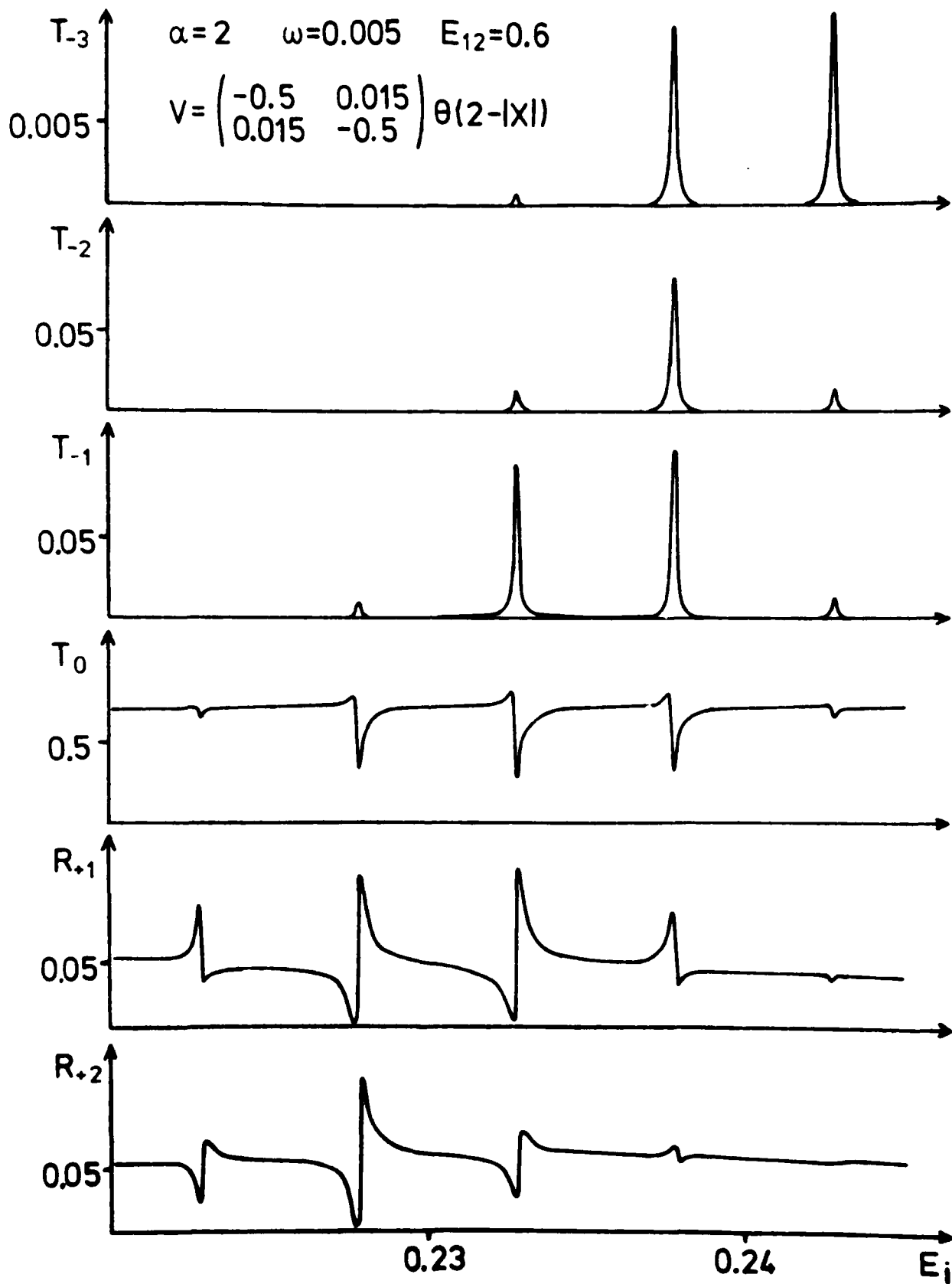


Fig. 4

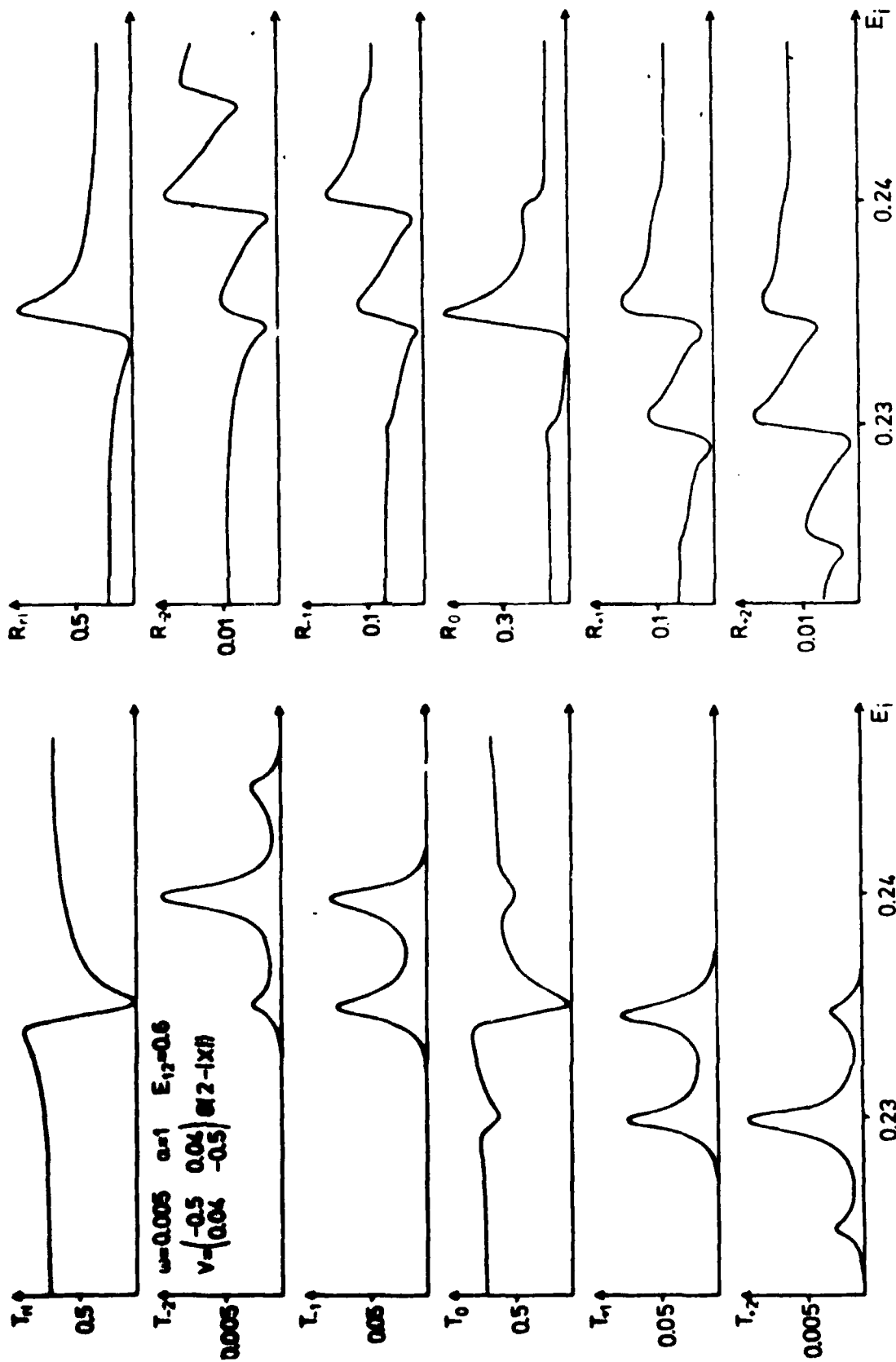


Fig. 5

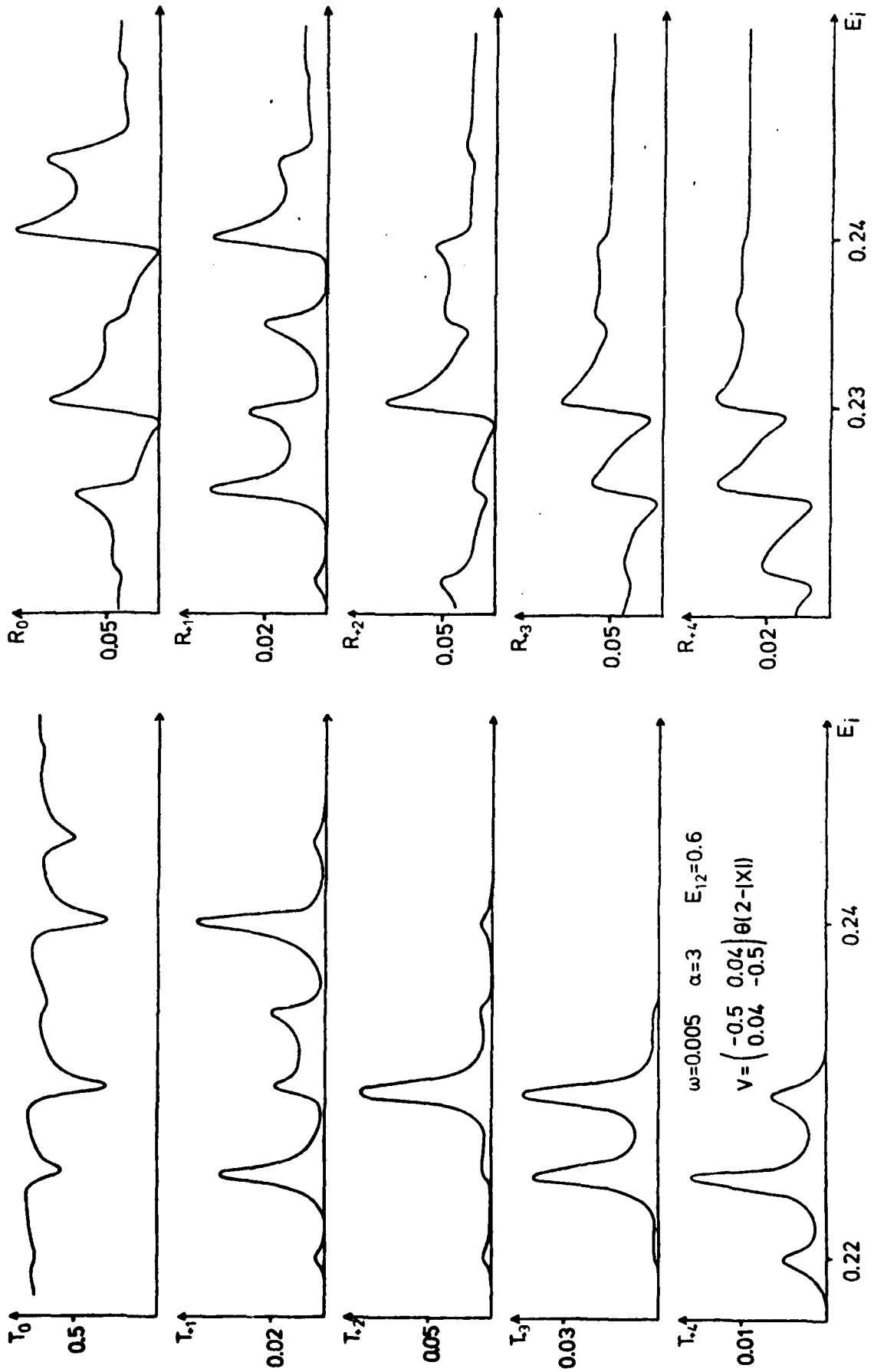


Fig. 6

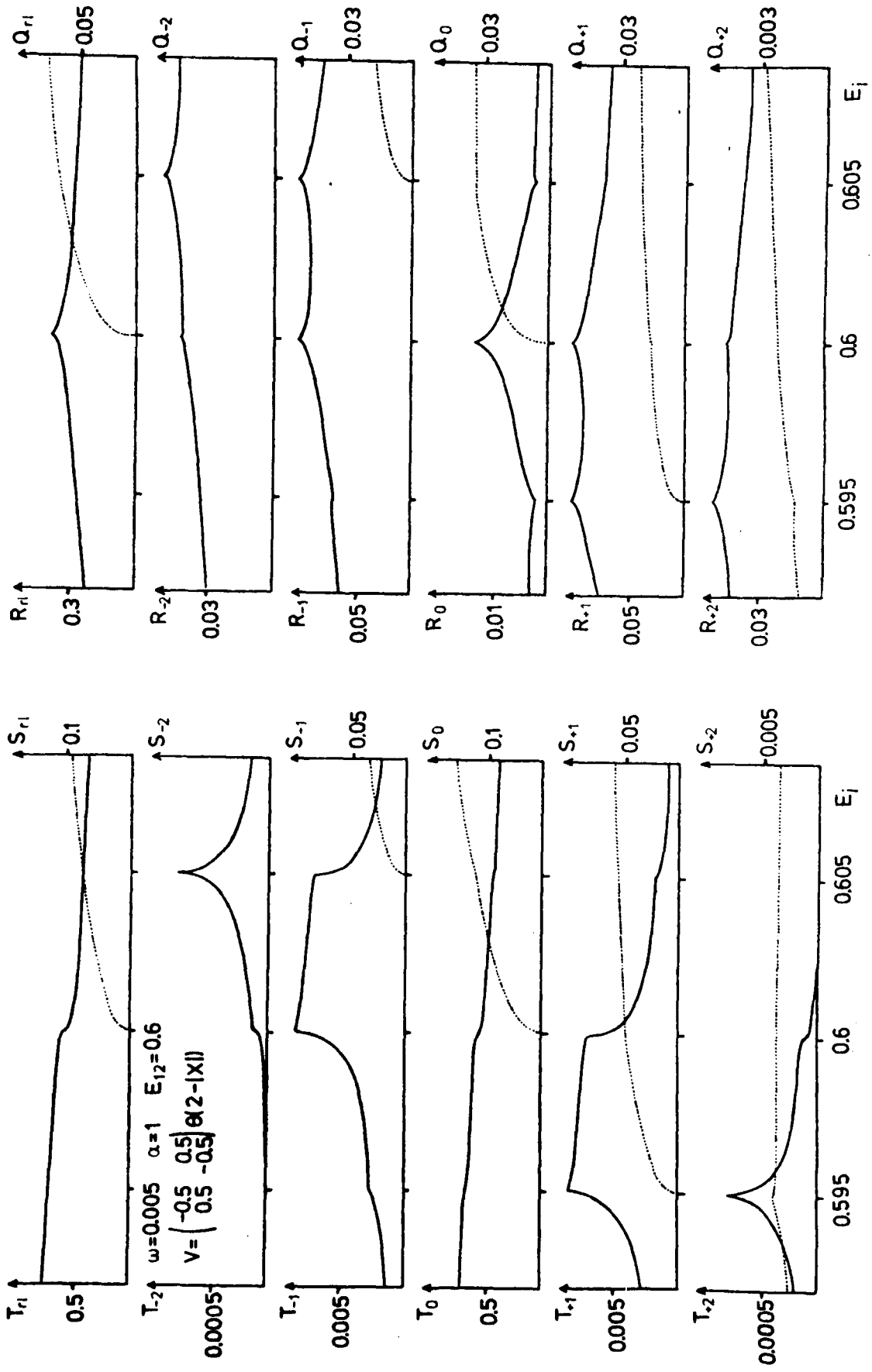




Fig. 7

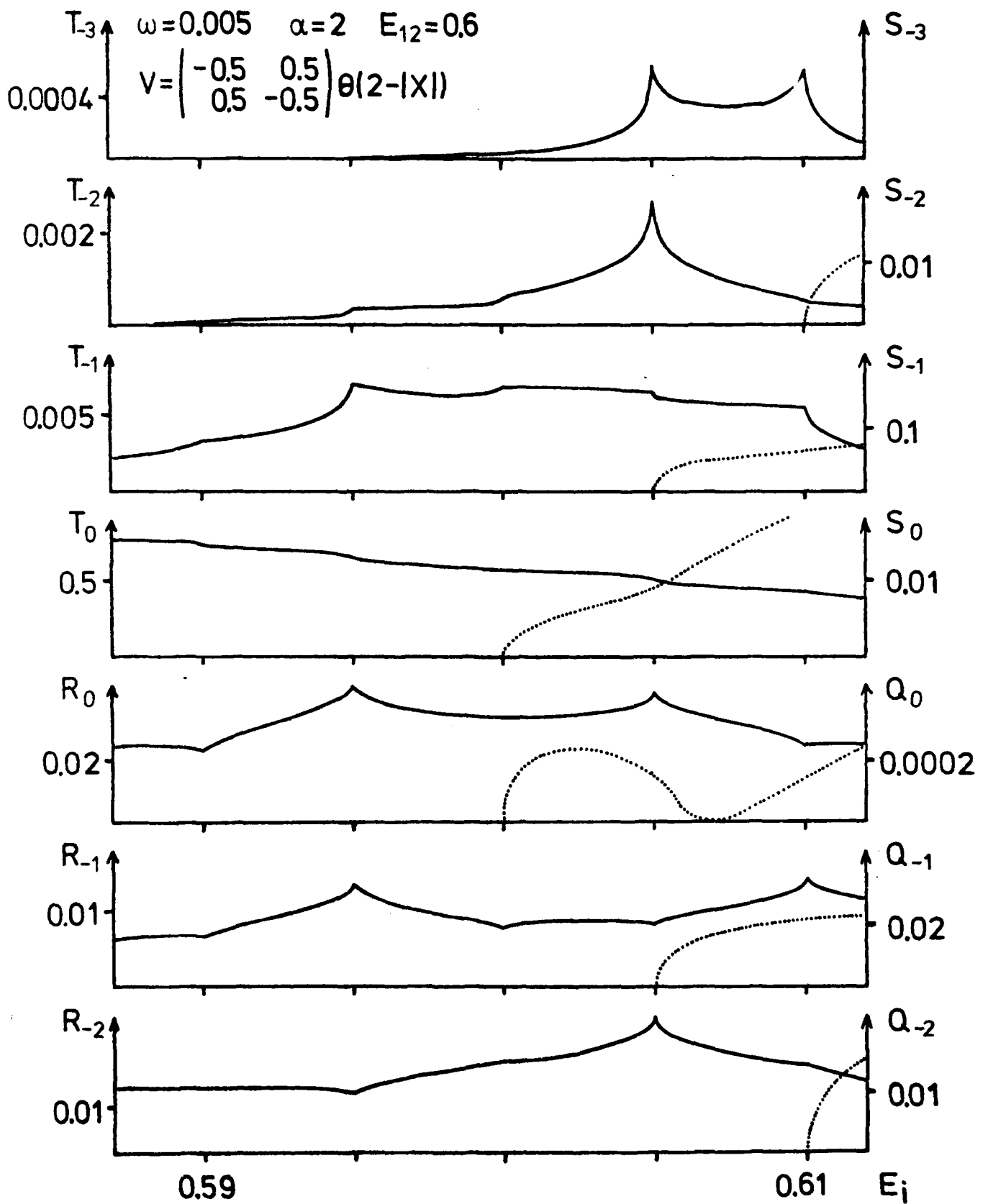


Fig. 8

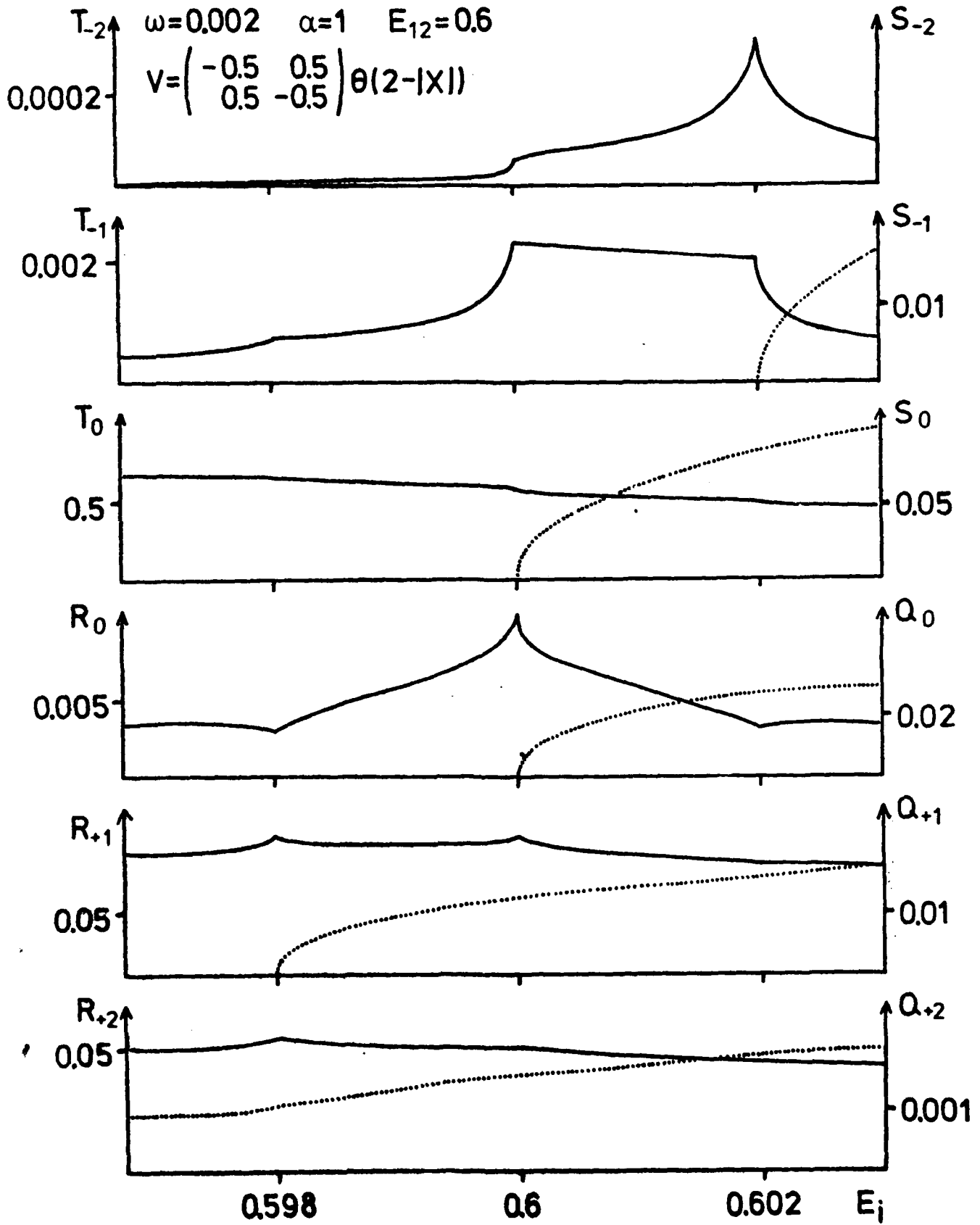


Fig. 9

